

# CLIMATE CHANGE IN THE LA PLATA BASIN



## ■ Editors

Vicente Barros  
Robin Clarke  
Pedro Silva Dias

# CLIMATE CHANGE IN THE LA PLATA BASIN

## ■ Editors

Vicente Barros  
Robin Clarke  
Pedro Silva Días

## Project

SGP II 057: "Trends in the hydrological cycle of the Plata basin:  
Raising awareness and new tools for water management"  
of the INTER AMERICAN INSTITUTE ON GLOBAL CHANGE (IAI)

FOREWORD .....	7
----------------	---

## CHAPTER I

INTRODUCTION .....	8
1.1. Dropping the hypothesis of stationary climate .....	8
1.2. Climatic and hydrological trends in the La Plata basin .....	9
1.3. Climate forcings .....	11
1.4. Global climate models and climate scenarios .....	12
1.5. Extreme value assessment .....	12
1.6. Interdecadal variability .....	13
References .....	14

## CHAPTER II

LA PLATA BASIN CLIMATOLOGY .....	16
2.1. Introduction .....	17
2.2. General precipitation regime .....	20
2.2.1. <i>Satellite estimates</i> .....	20
2.2.2. <i>Annual and seasonal averages</i> .....	21
2.2.3. <i>Mean annual cycle</i> .....	22
2.3. Regions .....	23
2.3.1. <i>Region of the monsoon (Upper Paraguay and High Upper Paraná basins)</i> ..	23
a. <i>Paraguay River upper basin: The Pantanal region.</i> .....	23
b. <i>Upper and septentrional basins of the Upper Paraná.</i> .....	24
2.3.2. <i>Great Chaco Region</i> .....	24
2.3.3. <i>Region centred at the east of Paraguay</i> .....	26
2.3.4. <i>Region of the meridional Planalto and the Rio Grande ridges</i> .....	27
2.3.5. <i>Region of the Argentine Litoral and bordering areas</i> .....	27
2.3.6. <i>Eastern Uruguay and South of Rio Grande do Sul</i> .....	28
2.3.7. <i>West and South borders</i> .....	30
References .....	32

### INTERANNUAL LOW FREQUENCY VARIABILITY:

BACKGROUND .....	35
3.1. Introduction .....	36
3.2. Variability over the La Plata basin .....	39
References .....	40

## CHAPTER IV

	PHYSIOGRAPHY AND HYDROLOGY	44
4.1.	Location of the La Plata basin	45
4.2.	Importance of the basin	46
4.3.	Ecosystems in the basin	46
4.4.	Characteristics of the sub-basins	47
4.4.1.	<i>The Paraná River sub-basin</i>	48
4.4.2.	<i>The Paraguay River sub-basin</i>	51
4.4.3.	<i>The Uruguay River sub-basin</i>	53
4.5.	Slopes in the basin	54
4.6.	Environmental problems	55
	References	59

## CHAPTER V

	REGIONAL PRECIPITATION TRENDS	61
5.1.	Introduction	62
5.2.	Data sets	62
5.3.	Trends	62
5.3.1.	<i>Total Precipitation</i>	63
a.	<i>Annual trends</i>	63
b.	<i>Seasonal trends</i>	65
c.	<i>Trends associated with ENSO</i>	66
5.3.2.	<i>Frequency of intense precipitation</i>	68
5.4.	Rainfall-streamflow relationships	69
5.5.	Summary	71
	References and web addresses	72
	HYDROLOGICAL TRENDS	74
6.1.	General considerations	75
6.2.	River streamflows	75
6.3.	Extreme Hydrological Events (EHE)	81
6.4.	Relationship between precipitations and EHE	85
6.5.	Relationship between El Niño and EHE	85
	References	86
	REAL EVAPORATION TRENDS	87
7.1.	Introduction	88
7.2.	Data	88

7.3.	Methodology	88
7.4.	Results	91
7.4.1.	<i>West of Argentina and Paraguay</i>	91
7.4.2.	<i>Paraguay River and Litoral of Argentina</i>	91
7.4.3.	<i>East of Paraguay</i>	96
7.5.	Discussion and final comments	102
	References	102

## CHAPTER VIII

	THE MAIN SERVICES AND PROBLEMS OF WATER RESOURCE	104
8.1.	Introduction	105
8.2.	Main problems	106
8.2.1.	<i>Floods</i>	106
8.2.2.	<i>Environment and Ecosystem vulnerabilities</i>	108
8.3.	Main services of water resources	109
8.3.1.	<i>Water supply and urban drainage</i>	109
8.3.2.	<i>Agriculture</i>	110
8.3.3.	<i>Energy</i>	112
	<i>a. Hydroelectric dependence</i>	112
	<i>b. Large hydroelectric utilities</i>	113
	<i>c. Dam sedimentation</i>	114
8.3.4.	<i>Fluvial navigation</i>	114
	References	115

## CHAPTER IX

	GLOBAL CLIMATIC CHANGE	117
9.1.	Introduction	118
9.2.	Causes of climatic changes	118
9.3.	Solar and terrestrial radiation	119
9.4.	Greenhouse effect	120
9.5.	Greenhouse gases (GHG)	120
9.6.	Global warming during the industrial period	121
9.7.	The climate in the twenty first century	123
9.8.	The Climatic Change is already unavoidable: mitigation and adaptation	125
	References	126
	BACKGROUND ON OTHER REGIONAL ASPECTS: LAND USE CHANGE, AEROSOLS AND TRACE GASES	127
10.1.	Introduction	128

10.2.	Regional effects of biomass burning	129
10.3.	Land use change	131
10.3.1.	<i>Deforestation</i>	131
10.3.2.	<i>Urban effects</i>	135
	References	136

## CHAPTER XI

	GLOBAL CLIMATE MODELS	140
11.1.	Introduction	141
11.2.	Atmospheric General Circulation models (AGCMs)	142
11.3.	AGCMs uncertainties and their use for Climate Change studies	145
	References	148

## CHAPTER XII

	CLIMATE SCENARIOS	150
12.1.	Introduction	151
12.2.	Criteria for the selection of climatic scenarios	151
12.3.	Techniques for developing climatic scenarios	152
12.3.1.	<i>Synthetic Scenarios</i>	152
12.3.2.	<i>Analogous Scenarios</i>	152
a.	<i>Temporal analogous scenarios</i>	153
b.	<i>Spatial analogous scenarios</i>	153
12.3.3.	<i>Scenarios from global climate models outputs</i>	153
12.4.	Development of other scenarios	154
12.4.1.	<i>Social Economic Scenarios</i>	154
12.4.2.	<i>Sea level raise scenarios</i>	157
12.5	Validation of the GCM for the current period	157
12.6	Climate change scenarios from GCM	158
12.6.1.	<i>Baseline scenarios</i>	159
12.6.2.	<i>Global scenarios</i>	159
	References	165
	REGIONAL CLIMATIC SCENARIOS	166
13.1.	Introduction	167
13.2.	Regional Climatic Scenarios	167
13.2.1.	<i>Direct use of GCM outputs</i>	167
13.2.2.	<i>Interpolation of GCM outputs</i>	167
13.2.3.	<i>Statistical downscaling</i>	168
13.2.4.	<i>High resolution experiments</i>	168

13.3.	Regional validation of GCM for South America	169
13.4.	Regional Scenarios for the La Plata basin	171
13.4.1.	<i>Hadley Centre GCM</i>	171
13.4.2.	<i>Regional features in other Climate Change experiments</i>	174
a.	<i>Pre-industrial period</i>	176
b.	<i>1% increase in CO<sub>2</sub> up to doubling</i>	176
c.	<i>Climate of the twentieth century</i>	177
13.4.3.	<i>Hadley Centre and ECHAM GCM</i>	179
13.5.	Future plans of CPTEC/INPE in Climate Change modeling	179
	References	181

## CHAPTER XIV

	LOW-FREQUENCY VARIABILITY	183
14.1.	Background on low frequency variability	184
14.2.	Data Analysis	185
14.3.	Precipitation Patterns	186
14.4.	SST composites	190
14.5.	SLP composites	192
14.6.	Conclusions	195
	References	197

## CHAPTER XV

	STATISTICAL ANALYSIS OF EXTREME EVENTS IN A NON-STATIONARY CONTEXT	199
15.1.	Introduction	200
15.2.	Parametric and non-parametric methods for detecting trend in hydrological variables	201
15.3.	Example: Testing for trend in annual maximum one-hour rainfall at Porto Alegre, Brazil	202
15.4.	Example: POT procedure applied to fitting daily rainfalls at Ceres, Argentina	204
15.5.	Records with missing values	209
15.6.	Spatial trends	211
15.7.	Methods based on L-moments	212
15.8.	The concept of return period in the presence of time-trends	213
	References	215
	Curricula of the authors	216

This book is the result of the Project "Trends in the Hydrological cycle of the La Plata Basin: Raising awareness and new tools for water management". The project has been funded by the grant SGP II 057 of the Inter-American Institute for Global Change (IAI) in the framework of a programme for the elaboration and publication of Technical Reports.

To a great extent, the Project was the result of a wider initiative funded by the IAI, the Project CRN 055 "PROSUR" with focus on climate variability in the southeast of South America. Part of the knowledge of the impacts of climate variability in the hydrology of the Plata basin was developed in the PROSUR project by researchers who took part of this new initiative. Later, these researchers joined other investigators to develop the SGP II 057 Project.

The object of this book is to raise awareness in the hydrologic community of the important changes that have occurred in the climate and hydrology of the La Plata basin during recent last decades. In a context of global climate change and of great regional changes, the assumption that series of climatological and hydrological observations are stationary must be regarded with suspicion. This book therefore presents an overview of the few available techniques for assessing future climate and hydrology.

## INTRODUCTION

*Vicente Barros<sup>1</sup>*

<sup>1</sup> CIMA/CONICET. University of Buenos Aires.

### 1.1. Dropping the hypothesis of stationary climate

There is climate variability in almost all scales of time. In some of them, climatic variability come from processes of intrinsically random nature or are caused by multiple and complex processes that hamper its prediction. Hence, the use of the climate information is fundamentally based on the statistical analysis of its series.

Up to not long ago, many of the uses of the climatic information, rested on the premise that the climate was stationary, at least at decadal scale, and so future climate would be similar to that of the immediate past. Therefore, the series of climatic elements and their hydrological derivates<sup>1</sup> were statistically treated as stationary.

Nowadays, the hypothesis that climatic series or their derivates are stationary does not seem quite appropriate. Every time there are less doubts that the planet has entered in a rapid climatic change induced by human activities. In consequence the hypothesis almost always implicit that the statistics of the past climate can represent those of the future climate it is no longer valid. The whole methodological arsenal that was based on this simple presumption for the calculation of parameters of design of infrastructures, the planning of the use of the water resources, of the territory, of the forest activity or of the agriculture to medium term should be revised.

In some regions and for certain parameters, the climatic series are already no longer stationary. For the cases that are still stationary, neither is a wise attitude to suppose, a priori and without further analysis, they will continue being so. In consequence, the estimate of some or several features of the future climate for some planning requirement can no longer relay in the comfortable hypothesis that the climate is stationary and therefore new methods are required. In spite of this necessity, there still is not a completely developed and sure methodology to estimate the future climate. Indeed, the great challenge for the world climatology during next years will be to develop the methods to predict the climate of next decades in view of the man induced climatic change.

Meanwhile, the activities where climate is an input for decision making require answers that cannot wait for the development of an impeccable and precise methodology that today is not available. In particular, the main demand is in the estimate of future climate conditions in the next two or three decades, which is the usual time horizon for medium and long term planning. The purpose of this book is to offer a conceptual and critical framework of the few tools available today and of its future evolution. In the last part of this book (chapters 11 at 15), three of these tools are analyzed, climatic scenarios, the use of the low frequency climatic variability and the statistical treatment of extremes for non stationary series. Given the remarkable importance of the climatic and hydrological trends of the last decades in the La Plata basin, the three types of tools are illustrated with examples of this basin.

## **1.2. Climatic and hydrological trends in the La Plata basin**

La Plata basin is an environment of great economic and demographic significance, shared by 5 countries with a population surpassing the 200 millions. It accounts for the generation of most of the electricity, the food and the exports of these countries. In most of this immense basin of 3500000 km<sup>2</sup>, there are clear manifestations of important climatic and hydrological trends that could likely be related with the Global Climate Change. The most direct indication in such a sense is the simultaneity of the beginning of these trends with the last trend of global heating initiated in the 1970 decade, which as will be seen in chapter 9, is attributed to the concentration increase of greenhouse gases.

Amongst sub-continental regions of the world, Southern South America has shown the largest positive trend in precipitation during the last century (Giorgi 2002). This is regardless that the region includes subtropical Chile where there were negative trends (Minetti and Vargas 1998; IPCC 2001). The increase in annual precipitation in the last 40 years has been more than 10% over most of the region, but in some places it has reached 30% or more (Castañeda and Barros, 1994; Minetti et al. 2003). For example, in the West of the Buenos Aires province and in part of the Argentine-Brazilian border, the mean annual precipitation increases more than 200 mm.

In addition to the increase in the mean annual precipitation, episodes of heavy rainfall are becoming more frequent. The frequency of precipitation events exceeding 100 mm in Central and Eastern Argentina three-folded during the last 40 years (Barros 2004). This trend was also observed in Sao Paulo, Brazil, where the frequency of heavy rainfalls has increased significantly (Xavier et al. 1992 and 1994) especially during summertime. Extreme precipitations in Southeastern South America (SESA) usually come from mesoscale convective systems (MCS) (Velasco and Fritsch 1990). Rainfalls from MCS have a large destructive potential

as they pour water over tens of thousands of km<sup>2</sup> with great intensity in relatively short periods of time, often causing severe floods. SESA has been identified as one of the world's regions with more frequency of MCSs (Nesbitt and Zipser 2001). Thus, heavy precipitation is a distinctive feature of the SESA climate, and its positive trends are resulting in more frequent floods.

Increased precipitation has led to increased river discharge (García and Vargas 1998; Genta et al. 1998); since evaporation -controlled by temperature- appears not to have changed too much (Berbery and Barros 2002, see also chapter 7). The percent rate of change of the river discharges was amplified when compared to the corresponding rate of change of La Plata basin average precipitation (Berbery and Barros 2002; Clarke 2003; Collishonn et al. 2001). This feature can be attributed partially to deforestation and land use change that resulted in increased runoff (Tucci and Clark 1998; Collinshon et al. 2001). However, interannual changes in rainfall and river discharge occurs also between consecutive years. Since in this case, the impact of the land use change is irrelevant, this result leads to infer that the amplification in the streamflows is a natural and intrinsic feature of this system (Berbery and Barros 2002). This characteristic increases the vulnerability of the activities that depend on water resources to precipitation changes, which in the current context of Climate Change is a relevant issue.

The most adverse effect of this change is the greater frequency and severity of flooding, both at the river valleys and in extensive flat areas of the Pampas. Despite the better hydro-meteorological forecasts, damages due to intense rainfalls and consequent flooding has been increasing as a result of the regional climate trend and of the increased occupation by settlements and agriculture of areas that until recently had relatively low risk of flooding.

In the alluvial valleys of the Paraná, Uruguay and Paraguay, floods have become more frequent since the middle seventies. During the 20th century, 12 out of the 16 highest monthly discharges of the Paraná River in Corrientes occurred in the last 25 years and four of the five highest monthly discharges have also occurred during this last period (Camilloni and Barros 2003). In the Paraguay River, eleven of the 15 largest floods in Asunción during the last century have also occurred after 1975 (Barros et al. 2003) whilst for the Uruguay River, none of the 16 largest peaks since 1950 occurred before 1970 (Camilloni and Caffera 2003). These examples indicate the severity of impact that regional climate trends have caused in the intensity and frequency of floods.

The cost of coping with these changing conditions is extremely high. As but an example, if losses are measured as a percentage of the Gross Domestic Product (GDP), Argentina is one of the 14 countries most affected by floods, with losses estimated as high as 1.1% of its GDP (World Bank 2001). These and others impacts of the recent trends in the hydrology of the La Plata basin are discussed in chapter 8.

The new climate conditions have rendered obsolete a great part of the infrastructure related to water management, since it was designed for a different climate. Much of this toll could be avoidable in the future, if part of the infrastructure were modified to meet the new conditions, and the new constructions were built according to the new and future hydrometeorological conditions. With few exceptions, none of these things are being done. Specifically, most of the infrastructure was, and still is, designed with the implicit assumption of a stationary climate. The few appropriate methods available to assess future climate under non-stationary climate conditions, some of which are still evolving, are neither known nor used. This attitude reflects the lack of awareness of the technical community about the regional climate trends and their hydrological consequences.

For these reasons, the second purpose of this book is to draw attention on the climate and hydrological trends showing its territorial dimension in order that the local trends not to be misinterpreted as random and unrelated symptoms. The description of these trends is made in chapters 5, 6 and 7 and for its better understanding, in chapters 2, 3 and 4 the most general features of the regional climate and hydrology are previously approached.

### **1.3. Climate forcings**

Carbon dioxide and other greenhouse gases emissions (GGE) are considered responsible for at least part of the global temperature increase during the twentieth century and it will be the main drive for climate change during the twenty first century. The evolution of the GEG emissions in the future will depend on numerous factors whose prediction is quite complex. They are the economic and demographic growth, the technological changes and even the development toward a society with more or less equity; and last, but not less important, on the humanity's collective decision to reduce or at least to diminish the rate of growth of the emissions. Since all this is very difficult to be foreseen, it is only possible to build possible future socioeconomic scenarios. The different scenarios presuppose levels of economic activity that imply in turn different scenarios of emissions. The construction and characteristic of these scenarios are discussed in chapter 12.

The global climate change issue is summarized in chapter 9. Long-term changes in global climate are assessed using global climate models (GCMs), which simulate the responses to the changes in the atmospheric constituents that have been observed in the past or that will be expected in the future. GCMs are also used to simulate other changes that can modify climate, as deforestation and changes of vegetation and in the use of soil. These and other regional forcings are treated in chapter 10.

A better understanding of the observed trends will help to develop and to apply techniques of assessment of the statistics of the near future precipitation scenario under non-stationary conditions. However, it should be pointed out that some questions have not yet a conclusive scientific answer: What is the cause of the regional climate trend? Are these trends related to global Climate Change? What is the impact of land use change and air pollution (from mega cities and biomass burning)? Will these trends continue in the next decades?

#### **1.4. Global climate models and climate scenarios**

At present, there are results from GCM-runs provided by several centres with different models. They simulate the future climate under diverse socio-economic scenarios that result also in different greenhouse gases emissions. Chapter 11 describes GCM, their performance and limitations.

Some of the GCM rainfall outputs for La Plata basin were checked against observational data. This validation analysis, demonstrated that the rainfall simulated by the GCM are not in agreement with observational data and that some adjustments are required to prepare future rainfall scenarios based on GCMs simulations (Bidegain and Camilloni 2002).

The lack of correct representation of the present mean precipitation fields by the GCM creates some doubts on their ability to simulate future climate. However, the incremental method, which will be discussed in chapter 13, may filter some of these errors when they are not very important. On the other hand, it is expected in the upcoming months new experiments with regional models of high resolution nested in the exits of the GCM for the region of the La La Plata Basin. This technique can improve the simulation of the fields of precipitation for the current climate, but there is no certainty about it.

#### **1.5. Extreme value assessment**

GCM scenarios are still far from reproducing the statistical properties of the extreme values of the rain and consequently cannot be used to provide extremes of the river flows, which are required for the design or planning processes. Thus, trends of such properties are almost the only tool available for near future scenarios and, chapter 15 will focus in the statistical analysis for the study of the frequency of occurrence of extreme rainfalls, and the extent to which trends in extreme rainfalls are statistically significant. This will involve the discussion of the fitting of Generalised Extreme Value (GEV) distributions to annual maximum rainfall accumulated over different duration periods and the assessment of the extent to

which parameters of the GEV distributions show statistically-significant evidence of trend, using (for example) statistical methods described by Coles (2001). Other alternatives are statistical analysis of rainfall intensities that exceed some threshold value (POT: “peaks-over-threshold” analysis) along lines described by Clarke (2003) and Coles (2001).

Rainfall records are in general longer than discharge records in rivers, and are free from some of their complications (increased abstraction; impounding by reservoirs; changing relationships between river level and discharge; effects of sediment deposition and removal; etc). However, similar analyses are also required for runoff data. These will require not only a station-by-station analysis of individual runoff records from selected, good-quality sites, but also a spatial analysis to take account of spatial correlation between flood flows. Appropriate statistical tools for such analyses are not well developed (for example, methods for fitting GEV distributions to spatially-correlated flows that also contain time-trends need to be explored).

## **1.6. Interdecadal variability**

Superimposed to the climatic trends forced by changes in the concentrations of greenhouse effect gases, there are variations of interdecadal scale that hinder the climatic projections for the lapse that they are most required, the next 30 years. The MCG that have shown certain ability to simulate the global climatic trends of the last one hundred years, have not been that successful in describing the interdecadal fluctuations for the same period, Thus, it cannot be guaranteed that model simulations will capture the future interdecadal variability. This is because some of these fluctuations are caused by the internal variability of the system, and are unpredictable. In spite of it, in many cases, when these fluctuations reach certain magnitude, their later evolution can be assessed.

In certain cases, regional climate variables as precipitation or temperature can be related to explanatory variables (such as variables derived from sea-surface temperature analysis or large scale or planetary circulation indexes) and when these variables undergo low-frequency (decadal variability), they may have certain potential for developing hydrological scenarios of the next ten to twenty years in La Plata basin. Remarkable results in this sense were reported by Robertson et al. (2001) for the summer season streamflow of the Paraná at Corrientes and for the whole region by Kayano (2003). These methods are based on the low frequency change of the sea surface temperature in regions that are related to La Plata basin precipitation and one example is developed in chapter 14.

## References

- Barros, V. 2004: Tendencias climáticas en la Argentina: precipitación. Proyecto Agenda Ambiental Regional-Mejora de la Gobernabilidad para el Desarrollo Sustentable PNUD Arg. /03/001. Fundación Torcuato Di Tella y Secretaría de Medio Ambiente y Desarrollo Sustentable.
- \_\_\_\_\_, L. Chamorro, G. Coronel and J. Baez 2003: The greatest discharge events in the Paraguay River *J Hydrometeorology* 2004 Vol 5, 1061-1070
- Berberly, E. and V. Barros 2002: The hydrologic cycle of the La Plata basin in South America. *J. of Hydrometeorology*, 3, 630-645.
- Bidegain, M. and I. Camilloni 2002: Regional climate baselines scenarios for the Rio de la Plata basin. AIACC workshop on Climate Change and the Rio de la Plata, Montevideo, November 2002.
- \_\_\_\_\_ and \_\_\_\_\_ 2003: Extreme discharge events in the Paraná River. *J. Hidrology*, 278, 94-106.
- \_\_\_\_\_ and M. Caffera 2003: The largest floods in the Uruguay River and their climate forcing. Submitted to the *J. of Hydrometeorology*.
- Castañeda, E. and V. Barros 1994: Las tendencias de la precipitación en el Cono Sur de América al este de los Andes. *Meteorológica*, 19, 23-32
- Clarke R. T. 2003: Frequencies of Future Extreme Events Under Conditions of Changing Hydrologic Regime. *Geophys. Research Letters*, 30, 3, 24-1 to 24-4. DOI 10.1029/2002GL016214.
- Coles, S. 2001: An Introduction to Statistical Modeling of Extreme Values. Springer Series in Statistics.
- Collinshon, W., C. Tucci and R. Clarke 2001: Further evidences of changes in the hydrological regime of the River Paraguay: a part of a wider phenomena of climate change. *J. of Hydrology*, 245, 218-238.
- García, N. and W. Vargas 1998: The temporal climatic variability in the Rio de la Plata basin displayed by the river discharges. *Climatic Change*, 38, 359-379.
- Genta, J. L., G. Perez Iribarne and C. Mechoso 1998: A recent increasing trend in the streamflow of rivers in Southeastern South America. *J. Climate*, 11, 2858-2862.
- Giorgi, F. 2002: Variability and trends of sub-continental scale surface climate in the twentieth century. Part I: observations. *Climate Dynamics*, 18, 675-691.
- Intergovernmental Panel on Global Change (IPCC) 2001: IPCC WGI Third Assesment Report. The Scientific Basis. Chapter 2. Cambridge University Press.
- Kayano, M.T. 2003: A note on the precipitation anomalies in Southern South America associated with ENSO variability in the Tropical Pacific, *Meteorol. Atmos. Phys.*, 84, 267-274.
- Minetti J. and W. Vargas 1998: Trends and Jumps in the annual Precipitation in South America, South of the 15 S. *Atmósfera*, 11, 205-2221, 1998.
- \_\_\_\_\_, \_\_\_\_\_, A. Poblete, L. Acuña and G. Casagrande 2003: Non-linear trends and low frequency oscillations in annual precipitation over Argentina and Chile. 1931-1999. *Atmósfera*, 16, 119-135.
- Nesbitt, S. and E. Zipser 2000: Census of precipitation features in the tropics using TRMM: radar, ice scattering and lightening observations. *J. Climate*, 13, 4087-4106.

- Robertson, A., C. Mechoso and N. García 2001: Interannual prediction of river flows in south-eastern South America. *Geophys. Res. Let.*
- Tucci, C. and R. Clarke 1998: Environmental issues in the Rio de la Plata basin. *Water Resources Development*, 14,157-175
- Velasco, I. and J. M. Fritsch 1987: Mesoscale convective complexes in the Americas. *J. Geophys. Res.*, 92, D8, 9591-9613.
- World Bank 2001: Argentina, Management of Water Resources. Report 20729 - AR.
- Xavier, T. M. B. S., M. A. F. Silva Dias and A. F. S. Xavier 1992: Tendências da Pluviometria na Grande São Paulo e a Influência dos Processos de Urbanização e Industrialização. *Anais, VII Congresso Brasileiro de Meteorologia*, 1, 220-224.
- \_\_\_\_\_, A. F. S. Xavier and M. A. F. Silva Dias 1994: Evolução da Precipitação Diária num Ambiente urbano: O Caso da Cidade de São Paulo. *Rev. Brasileira de Meteorologia*, 9, 44- 53.

## LA PLATA BASIN CLIMATOLOGY

*Rubén Mario Caffera<sup>1</sup> and Ernesto Hugo Berbery<sup>2</sup>*

<sup>1</sup> Universidad de la República.

<sup>2</sup> Universidad de Maryland.

### ABSTRACT

The hydrologic cycle of the La Plata basin is influenced by the South Atlantic High, which reaches greater intensity near the continent during winter. This system is responsible for the atmospheric moisture flow from the Atlantic Ocean over the coastal ridges of Brazil, and favors the southward flow in the central part of the continent. In this region, there is sometimes low level flow of water vapour from the Amazon region

The other regional atmospheric configurations of importance, the Bolivian High, the Chaco Low, the South Atlantic Convergence Zone, the Low Level Jet, the Meso Convective Systems and the Westerly Circulation, are succinctly described, along with their influences on weather and climate.

The general features of the precipitation field are described using modern data sets. There are two well defined rainfall regimes. One, north of the 20°, with summer rainfall, associated to the monsoon system, and a second with more uniform annual distribution to the south. The overall average of the basin is of 5.5 mm/day during the warm season and it is lower than 2 mm/day in June.

From north to south and from east to west, can be identified seven large climatic areas: the Monsoon Region in the Pantanal and in the north of the Upper Paraná basin, the Great Chaco, the east of Paraguay, the Planalto and the southern Rio Grande ridges, the Argentine Litoral, the eastern part of Uruguay and southern Rio Grande, and the southern and western edge of the La Plata basin. For each one of them, it is described the annual cycle of precipitation and temperature.

## 2.1. Introduction

The atmospheric circulation over the La Plata basin and bordering areas has a noticeable seasonality, which leads to a significant signal in the annual cycle of the determinant climatic elements of the hydrological cycle. The main centre of action on the atmospheric over the basin is the South Atlantic High semi permanent pressure system, with its subsiding and anticyclonic circulation. One of the main characteristics of this system is that it reaches greater intensity in Winter than in Summer (Prohaska 1976), contrary to what happens with most of the maritime subtropical anticyclonic systems in the planet. A branch of the associated circulation is responsible for the humidity advection over the coastal ridge mountains in Brazil (Marengo et al. 2004), where are located the sources of the most important tributaries of La Plata, with the exception of River Paraguay. It is also of first degree the system's displacement to the North and its penetration over the continent during winter so determining the dry season of all the tropical and subtropical regions of the basin.

In the low troposphere, the most important feature of circulation is that the predominant meridional component is from the North all year long, especially in winter (*Fig. 2.1*). In the mid troposphere, the West Circulation dominates over most of the basin, since on one hand during Winter the Anticyclone is more to the North, and on the other it shifts to the South of 35°S in Summer, but its wet border is more to the East over the ocean.

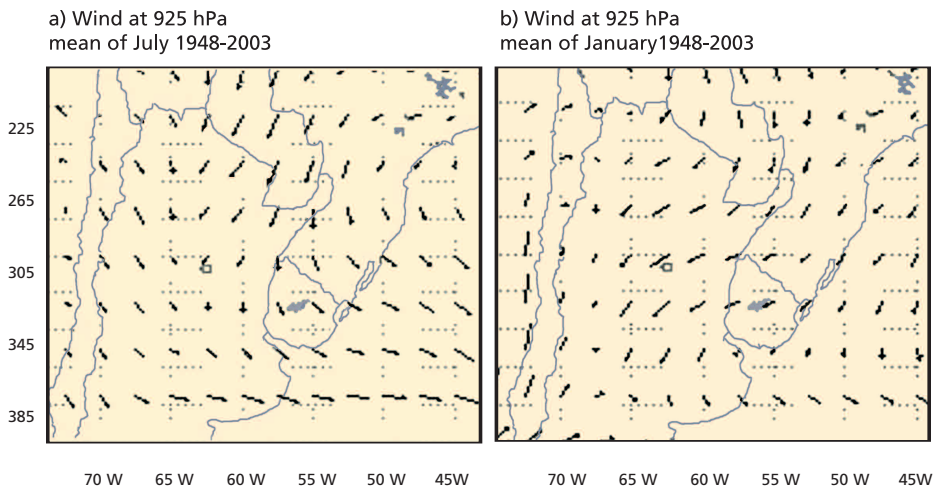


**Fig. 2.1.** Predominant winds in the (a, b) low and (c,d) middle troposphere, for the central months of both warm and cold seasons.

[NCAR/NCEP reanalysis (<http://www.cdc.noaa.gov>)].

Within the aforementioned seasonality, there is the Summer development of the low pressure system of Chaco, the intermittent thermal-ographic depression of the Argentine Northwest, present all along the year but more intense during Summer, as well as the South Atlantic Convergence Zone (Kodama 1992), and the Bolivia High. The last is a circulation pattern that appears in the high troposphere during the warm season. It establishes every year in September, together with the displacement of the nucleus of the tropical continental convection, from the North of South Amazon to the South. Its divergent flux at high levels is linked to abundant rainfall in the Highland (altiplano) itself and in the Northeast region of the La Plata basin, in the counterforts of River Paraguay (Lenters and Cook 1995). It is complemented over the tropical Atlantic by the called zonal wave of monsoon characteristics (Chen et al. 1999; Nogués-Paegle et al. 2002). The Bolivia High is a hot nucleus anticyclone, generated, among other causes by regional forcings: the radioactive heating in the Highlands, and the liberation of latent heat itself in the intense convection of the Amazon. This configuration, pertaining to the summer term, at the core of summer (January) is usually centred just at the West of the Titicaca Lake (Figuroa et al. 1995).

The South Atlantic Convergence Zone (hereinafter referred to as SACZ), is also a summer configuration (October-March). It is a convective complex that extends to the Southeast from the main nucleus of the continent summer convection in the centre of Amazonia. Its mean and characteristic location is around 20°S, continuing over the ocean up to latitudes close to 45°S (Gusmão de Carvalho y Gandu 1996). This system has pulses in intensity and position related shifts (Barros et al. 2000; Barros et al. 2002). The SACZ shows periods (Nogués-Paegle and Mo 1997; Barros et al. 2002; Nogués-Paegle et al. 2002) similar in time scale to the West perturbations, but also has important variations within the season, causing the intensity of rainfall to fluctuate from North to South on the strip that occupies over the continent, most of which belongs to La Plata basin (Díaz et al 1998; Barros et al. 2002). Casarin and Kousky, back in 1986, determined that the drought events in the South region of Brazil are linked to a weakening of the SACZ at an interseasonal scale. Thus, it is possible to distinguish two SACZ leading position patterns, with different behaviours (Barros et al. 2002), which are related with anomalies in the rainfall at the South of its location. These patterns can be considered as extreme positions. In the first pattern the SACZ has a position that cuts the coastal line more to the North than 20°S. It has a very intense convective activity and heavy rainfalls over the SACZ itself (Barros et al. 2002) and likely, due to a subsidence compensating phenomenon it is associated to negative anomalies in the precipitation on the South extreme of Brazil, South of Paraguay, Uruguay and Northeast of Argentina (Robertson y Mechoso 2002). In the second circulation pattern, the SACZ takes a more southerly position, with its intersection with the coast over the State of Sao Paulo. It has a weaker convection over the system, with smaller rainfalls than normal. Rainfall positive anomalies are then located in the same zone where in the other pattern appeared the negative ones.

Deeper inside the continent, over the slope extending from Chaco to Los Andes mountain range, there is a summer low pressure system: the Chaco Low. Due to its thermal nature, its development rarely involves levels higher than 700hPa, and therefore does not causing rainfall in a direct way. Toward the SW of its core, another system develops, intermittent, of thermal-orographic nature that appears as an appendix of the Chaco Low: The Argentine Northwest Summer Low (Lichtenstein 1980; Saulo et al. 2004). Its intensity is higher during summer. Its presence is related with the shift of the SACZ to the West of its usual position (Nogués-Paegle et al. 2002). Thus, its fluctuations in intensity and latitude provoke to its East intermissions in the humidity flux toward the central and southern region of the La Plata basin.

Another inherent characteristic of the central region of the basin is the development of the so called Mesoscale Convective Systems (MCS) (Velasco and Fritsch 1987). These systems are mostly nocturnal, organized in a kind of circular manner and have a minimum lifetime of 6 hours, which results noticeably greater than an isolated convection cell. MCSs are frequently found at leeward of the mountain systems (Figueiredo and Scolar 1996; Nieto Ferreira et al. 2003). During their lifecycle, they may have displacements of several hundred kilometres, in general with East component (Guedes et al. 1994). These Mesosystems are fed by intense humidity flows at low layers. From September to May, they are responsible of most of the rainfall in the whole basin.

In the Southern part of the basin, the circulation of the West with its baroclinic waves leaves its trace in the climate (Vera et al. 2002), with frontal and prefrontal rainfalls, and alternations of air masses from diverse origin. In winter, this circulation of mean latitudes usually penetrates sporadic and deeply toward the tropics, accompanied by intrusions of polar air, with the consequent and important plunges of the air temperature still in the most northern part of the basin (called *friagens* in Brazil).

The general thermal regime in the basin is asymmetric, with higher temperatures in spring than in autumn, except for the northeaster region of the high basin of the Paraná. Some districts of that region, and also the heights of the Southern Planalto (States of Santa Catarina, Paraná and Sao Paulo) are noticeably colder than the rest of the tropical and subtropical territory of the La Plata basin.

This is how diverse conditions both local (*geography, local annual cycle of solar radiation*), as well as remote define the distribution of the climatic elements in the several regions that compose La Plata basin (Prohaska 1976). Its territorial extension so has different climate districts discriminated first by their rains regime and secondly by some characteristics of the thermal regime. Transitions also appear among those climatic regions and subregions, what in turn will be mentioned concisely. Then a general description of the space-temporal distribution of the precipitations of the whole basin at scale is introduced. Next, a description of the climatology of the big units is made. The causal atmospheric dynamics will be mentioned

in this last description, although it is mentioned now the general predominance of winds with East component mainly from the Northeast. It is also important the already mentioned humidity flux at low levels from the Amazonia, bordering The Andes, which many times takes the characteristics of a low level jet in low layers (from now on, LLJ; see Verji 1981; Berbery and Collini 2000). The LLJ is present all over the year (Berbery and Barros 2002). Together with the SACZ constitute the determining elements of the basin's precipitation weather in combinations with the already mentioned South Atlantic High.

## 2.2. General regime of precipitation

### 2.2.1. Satellite estimates

For La Plata basin, a satellite estimated data set has been used for the period 1979-2000, in order to describe the space distribution of the precipitation (*Fig. 2.2a*). The data set includes the called CMAP (Climate Prediction Centre - CPC - Merged Analysis of Precipitation) from the National Oceanic and Atmospheric Administration (NOAA) whose validity was discussed in Xie and Arkin (1997). The precipitation was estimated for a  $2.5^\circ \times 2.5^\circ$  latitude/longitude array, as a result of combining a group of satellite products with local observations, including the GPI (Infrared supported Index of Precipitation of the GOES satellite system), the OPI (The Outgoing Longwave Radiation based Index of Precipitation), and microwave based measurements. The used version of CMAP doesn't include the reanalyses of the NCEP-NCAR precipitation forecasts.

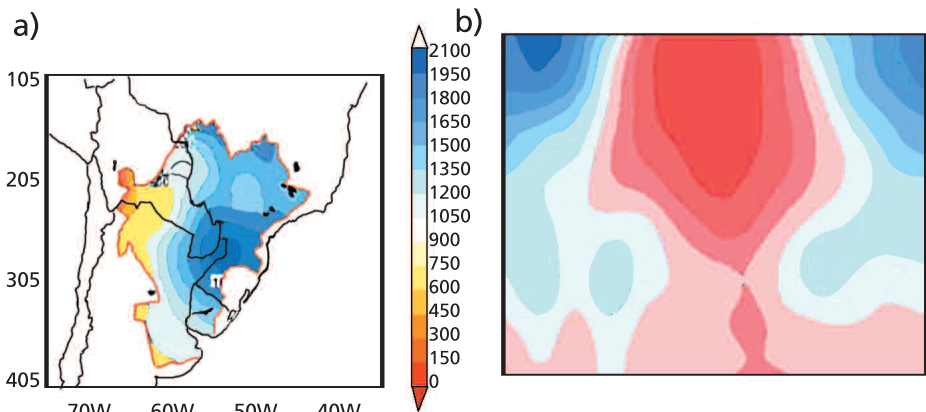


**Fig. 2.2.** a) Accumulated precipitation in the La Plata Basin, b) Distribution according to latitude stripes vs. the months of the year, in mm/day.

### 2.2.2. Annual and seasonal averages

At great scale, two well defined precipitation regimes are observed (e.g., Berbery and Barros 2002): the first one toward the North of the basin and the second over the central portion (*Fig. 2.2a*). The transition between both regimes is clearly illustrated in *figure 2.2b*, which represents the annual cycle of precipitation averaged in bands of longitude between 60 and 50 W, as a function of latitude. The regime of Summer precipitation, associated to the South American monsoon system, can be observed up to the 20°S (*Fig. 2.3b*), while more to the South, the central portion of the basin can reach its maximum at different times of the year, what suggests that there is more than one acting mechanism, not only the monsoon forcing. Therefore, precipitation in the central and southern strips of the basin tends to be more evenly distributed during the whole year (*Fig. 2.3 a, d*). Thus, during the

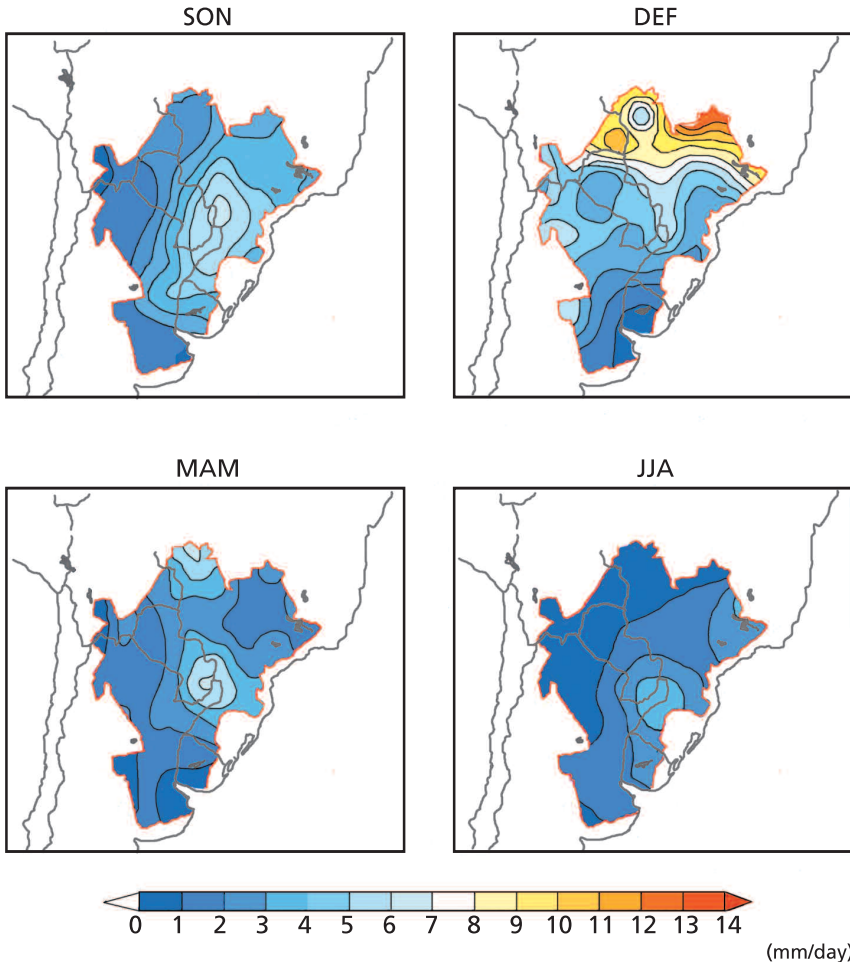


*Fig. 2.3.* Seasonal precipitation of the basin in mm/day.

warm season (October-April), in the central strip are frequent the Mesoscale Convective Systems (CCM), which account for a great deal of the precipitation (Velasco and Fritsch 1987; Laing and Fritsch 2000). In the cold season (May-September), the most important contribution is imposed by the activity at synoptic scale of mean latitudes (Vera et al. 2002). Over the Southern end of the basin, this pre-eminence of the waves of the West circulation covers all of the year seasons except for summer.

### 2.2.3. Mean Annual Cycle

Figure 2.4 presents the annual cycle averaged over the total area of the La Plata basin. The precipitation of the order of 5.5 mm/day during the warm season is a clear indicator of the predominant monsoon region, where maximum close to 9 mm/day are reached, in the average of the region, Fig. 2.4b. This contrasts with what happens toward the central part of the basin (Fig. 2.4c) where a markedly irregular intra annual variation is noticed. This last chart suggests a larger volume by the end of summer, at the beginning of the autumn, and in spring (Sep-Oct).

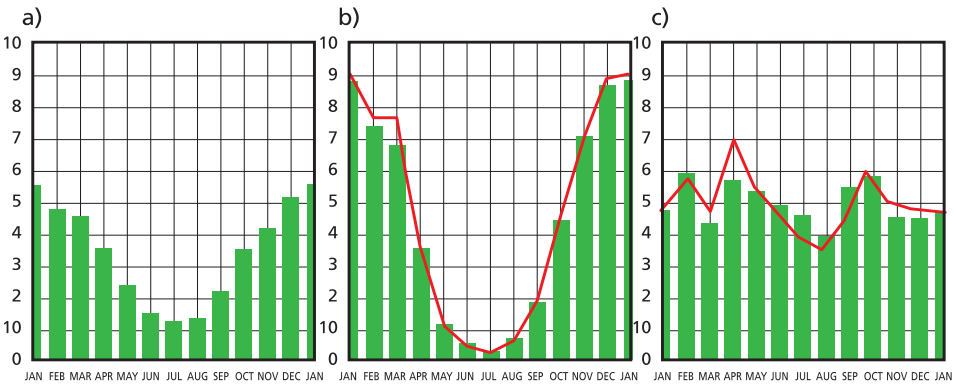


**Fig. 2.4.** a) Average precipitation of the whole La Plata Basin in mm/day, b) Average of the Monsoon region, bars: CMAP analysis (see text) in mm/day, and lines: observations, c) bars: average in mm/day (CMAP) in Misiones, representative of the central region and lines: observations.

The reliability of the "CMAP" data set has been examined comparing them with a new data set of observed precipitation interpolated in a regular  $0.5 \times 0.5^\circ$  of latitude-longitude mesh (Willmott and Matsuura 2001). The annual cycle for two representative points of the main precipitation regimes in the basin (Fig. 2.4b and 2.4c) shows that in both of them the estimate is close and shares the same yearly cycle. However, it is to notice that the CMAP estimate underestimates the precipitation during the warm season, probably due to its low resolution that cannot solve the convective precipitation appropriately. It also has a slight overestimation during the cold season.

## 2.3. Regions

### 2.3.1. Region of the monsoon regime

*(Upper Paraguay and High Upper Paraná basins)*

This is a region of great contrast in the precipitation regime with a marked minimum in winter and an abundant maximum in summer, when the superficial heating together with the vapour advection from the North favours the convection. The difference with the Asian monsoon classic regime is that the longitude of the dry season is slightly shorter, because of this, for similar annual totals, in La Plata "monsoon" region, the rainfall is distributed over more months, lacking both the spectacular summer picks and extremely low humidity at low layers during winter, like in most of the Asian Monsoon. Nevertheless, they are similar in the seasonality type and the dynamic causes of the rain regime: alternation of the anticyclonic presence and subsiding high-pressure in winter, with low pressures during summer, which is because of the thermal contrast of the Tropical Continent with the adjacent Atlantic. Thus, Zhou and Lau (1998) affirm that when removing the mean annual fluxes the same characteristics as in the Asian Monsoon appear and so they reach the conclusion that there is monsoon-like regime in South America. Inside La Plata basin region, it can be distinguished: *a)* the superior basin of River Paraguay in the western territory, including the Pantanal, *b)* the High Paraná valley, separated from the previous region by the Maracayú ridges, together with the region of the Central Planalto, and the corresponding ridge mountains on the East that separate the basin from the coast. In all of them, there is a predominance of winds from the North to Northeast sector, while in summer, in the upper troposphere, the presence of the Bolivian High affects the West of this tropical region and even more the South. The advection of humidity coming from the Amazon basin is an important source for the precipitation. Although this aspect is present the whole year, the winter subsidence almost causes a ceasing of the rain from May to August. The interannual variability is relatively small, although, like as it will be seen later, an important ENSO signal exists, what is extensive to the subtropical regions of the La Plata basin (Barros et al. 2000; Barros et al. 2002).

#### *a. Paraguay River upper basin: El Pantanal region*

By way of example, Corumbá is mentioned, right in the core of El Pantanal, where the precipitation maximum takes place in December, with annual totals superior to 1300 mm. On the counterfort of the slope more to the West, the annual precipitation is even larger. Extensive records of the region are shown to be more profuse in autumn than in spring, although in the last years this situation is reverting. The LLJ presence is the main source of humidity.

### b. Upper and septentrional basins of the Upper Paraná.

The influence of the trade winds is notorious, in spite of being to leeward of the coastal mountains. Thus, the rain period extends a little longer than in the basin of the Paraguay River and in the ridges the annual precipitation is higher. Cuiabá, representative locality of the area, presents maximum precipitation in January, and annual totals superior to 1400 mm being the precipitations more abundant in spring than in autumn. It is remarkable that in spite of the fact those heights over 1300 m separate this sub basin from the coast, the advection of humidity is present not only from the Amazon North, but also from the Atlantic.

In the most oriental heights of the Planalto night temperatures near to 0°C can be registered, as well as in the middle of the Alto Paraná basin valley, upstream of Itaipú. (Bela Vista, see *figure 2.5c*, and in light green in *figure 2.5a*). The charts correspond to points taken from the IRI interactive map. The source of the chart data is the University of East Anglia, its Monthly Climatology in grid points of 0.5° x 0.5°, available in:

[http://iridl.ldeo.columbia.edu/maproom/.Regional/.S\\_America/.Climatologies/Select\\_a\\_Point.html](http://iridl.ldeo.columbia.edu/maproom/.Regional/.S_America/.Climatologies/Select_a_Point.html)

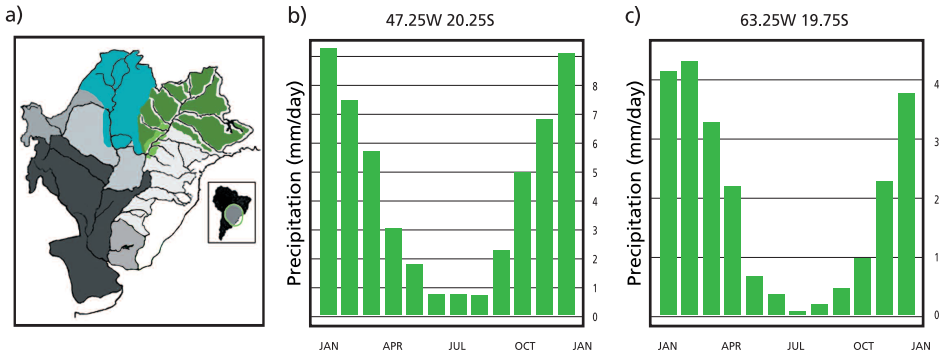


**Fig. 2.5.** Monsoon climate regions. a) Location, b) Precipitation (mm/day, of a representative location in El Pantanal. c) Precipitation (mm/day) of a representative place of the upper basin of the High Paraná.

#### 2.3.2. Great Chaco Region

Although the Tropic of Capricorn is included in this region (*Fig. 2.6a*), from the climatic point of view it is a subtropical area whose nucleus embraces approximately from the 19°S to 25°S and from the 64° to the 58° and 60°W. Approximately along this meridian, a quick transition between the humid subtropical regions and the dry ones takes place. In these last ones, located to the West, most of the precipitation concentrates in 3 to 5 months of the summer period, beginning in spring, while the maximum of precipitation is usually in December. It is the warmest region in the basin, with summer daily maximum temperatures frequently over

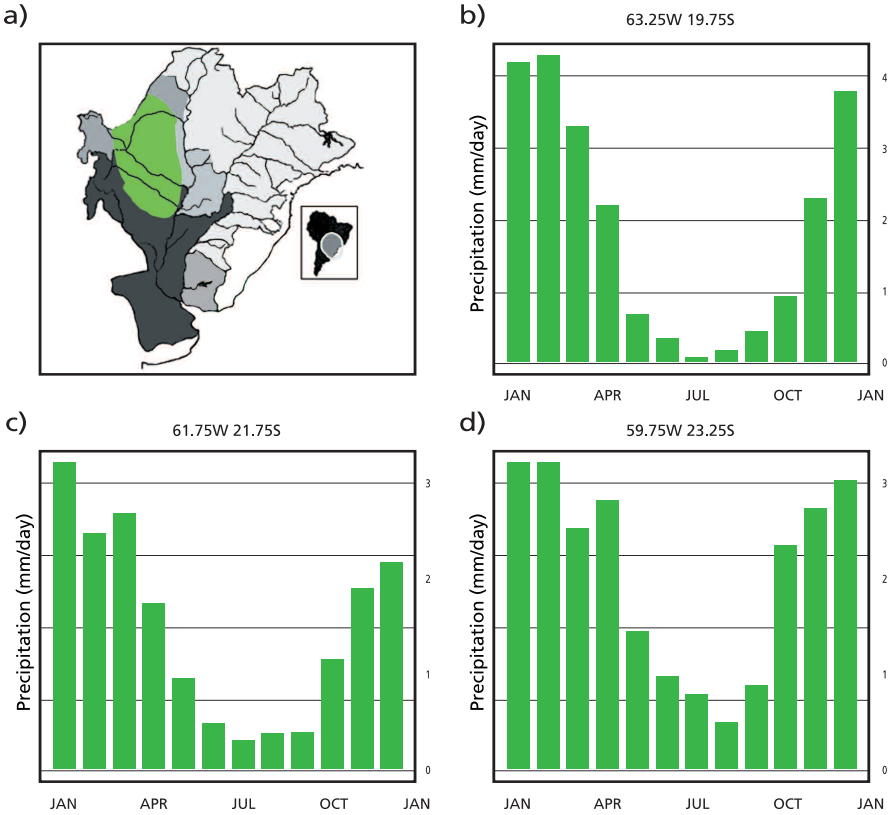


**Fig. 2.6.** The Chaco region. a) Approximated location. Rainfall regime at: b) the Boreal Chaco, c) at  $\sim 62^{\circ}\text{W}$  and d) at  $\sim 60^{\circ}\text{W}$ , Example of the east-west gradient of precipitation in the La Plata Basin.

$45^{\circ}\text{C}$ . In spite of the important flow of humidity at low layers, which somehow continues during the winter, during this season rains are null or almost null because of the presence of a continuous subsidence over the region, when the tropospheric circulation of the West, reaches the Chaco region. The humidity drops from more than  $20\text{ g/kg}$  in summer to less than  $14\text{ g/kg}$  in winter. However, cloudiness continues to be important by this time of the year, close to 40% in the average (Prohaska 1976). In Chaco, the rainy season usually begins in September and ends in March-April, being the flux in low layers from Amazonia, the only effective source of humidity.

The slopes of the Chaco toward the Andes maintain all a semi-arid character, except in the Aconquija Mountains where it rains more than in the plains with the same spatial pattern than in the northern and western borders of the Pantanal. With this exception, the precipitation gradient goes from less than  $300\text{ mm}$  in the West end to close to  $1000\text{ mm}$  in the East, always maintaining the great concentration of the period of rains in summer, though.

### 2.3.3. Region centred at the East of Paraguay

This humid subtropical region, maintains an annual mean precipitation between 1500 and 1900 mm, according to the locations. Precipitation minimums occur in winter, although less marked than in the Chaco, with a transition toward the Southeast with a more constant-like annual regime. The Mesoscale Convective Systems are directly responsible for the abundance of precipitation during the extensive summer period (September-April). Notice (*Fig. 2-7b d*) the maximum during Spring-beginning of the summer.

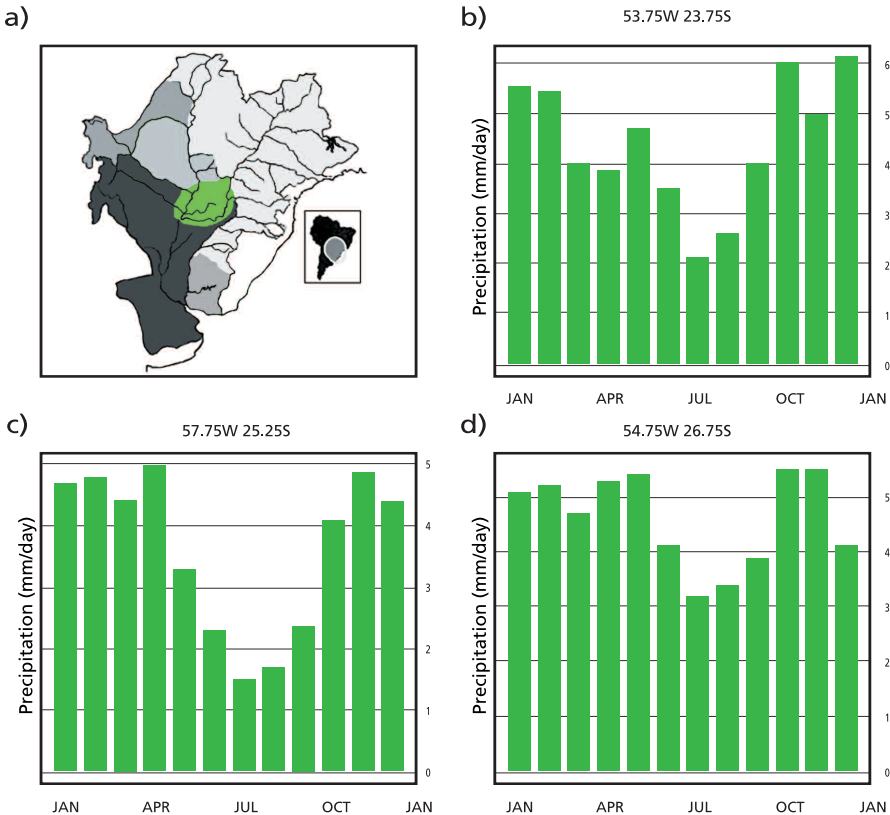


**Fig. 2.7.** Central region. a) Location. Rainfall regime at: b) at the northern part of the region, c) close to the confluence of Pilcomayo and Paraguay rivers, d) in the southeast of the region.

Although there are frequent invasions of polar air during winter in the region, it is common the occurrence of winters without frosts, except for the districts with important topography. A characteristic of this region is the low cloudiness at the end of the winter (August), what brings along a rapid thermal recovery at the beginning of the spring. (González and Barros 1998).

### 2.3.4. Region of the meridional Planalto and the Rio Grande Ridges

This is a region with precipitations during the whole year. It is one of the territories of the La Plata basin under the direct influences of the South Atlantic Convergence Area, which determine the summer and contiguous months' rain regime. In Winter, it is frequent the passage of perturbations from the West circulation, which added to important fluxes of humidity in low layers, from the Northwest on one hand, and from the Northeast on the other, causes precipitations to be considerable also in Winter. The dynamics of the SACZ produces the greatest intraseasonal and interannual variability in this region. It is a transition regime, from the typically tropical one with maximums in summer, more to the North, to one of maximums in winter in the southern part of Rio Grande do Sul and in Southeast of Uruguay. The annual means are higher than 2000 mm. Although the region is at relatively low latitudes, the height of the region makes temperatures to be considerably low, with frequent occurrence of frosts in winter, with the exception of the coast, where the radiative effects are less important than the advective ones. The high over sea level makes that in winter, during some polar air intrusions, the precipitations in some subregions of Southern Planalto to be in form of snow, especially in high places of the State of Santa Catarina, but also in Paraná and Rio Grande do Sul.

For the mentioned mixed regime, the annual cycle of precipitation ends up showing three picks: (Grimm et al. 1998) one at the beginning of Spring, other in the middle of Summer and another in Autumn (*Fig. 2.8b*), being the August-September-October quarter the one with more precipitation (*Fig. 2.8c, d*), in the sub region of the eastern tributaries of the Uruguay River.

### 2.3.5. Region of the Argentine Litoral and bordering areas

The Argentine Mesopotamia is the place of the transition place between the predominance of the zonal flux more to the South, and the prevalence of the meridional flux from the North, which, although still predominant, alternates with the West flow.

The maximum of precipitation is in the intermediate seasons, with a main minimum in winter and other, barely insinuated, in summer. In this season, the Mesoscale Convective Systems alternate with some front passages and produce most of the precipitation. In winter, the circulation of the West is noticeable with its well defined front systems and presence of the jet flow in the upper troposphere and low level flows from the North and the East. The main maximum of rainfall is in autumn. Together with the pampas region more to the South, the Uruguayan territory and the south of Rio Grande do Sul, this region is scenario of frequent but dispersed severe phenomena, especially not during winter: hail, intense winds caused

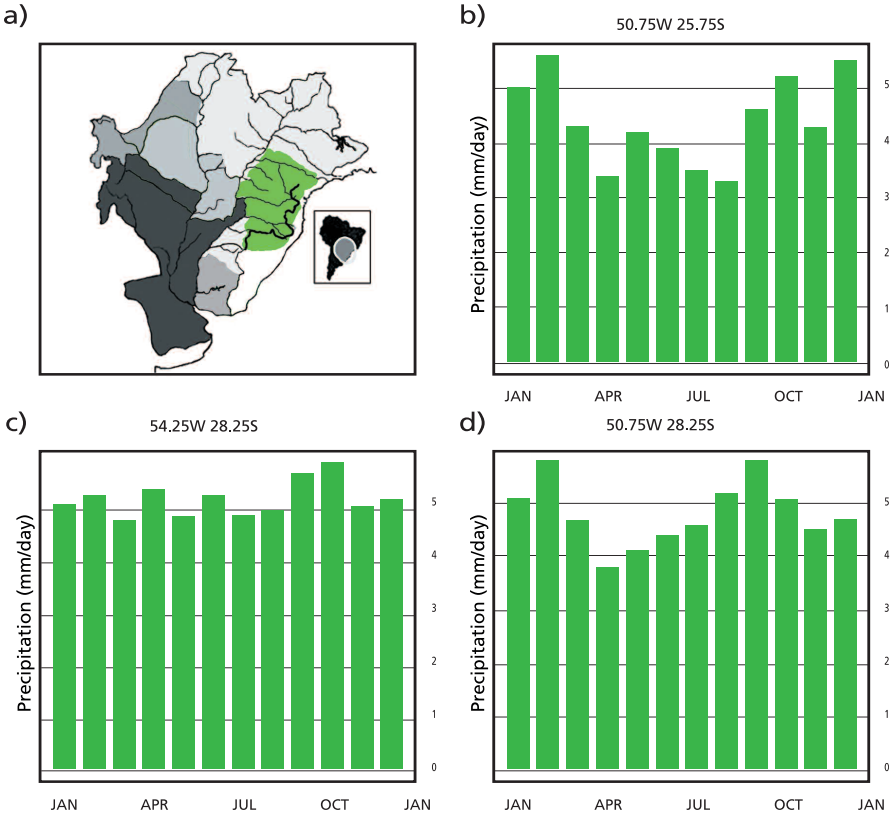


**Fig. 2.8.** Southern Planalto a) Location. Rainfall regime at: b) central-eastern region (River Iguazú basin) c) at the west d) at the south of the Planalto, where a shift of the spring maximum can be noticed by the end of winter.

by descending currents from cumulonimbus, tornados, in general as by-products of the activity of Mesoscale Convective Systems. There is a great interannual and intraseasonal variability and the annual isohyets have a noticeable North-South orientation, slanted toward the Southwest in the most southern region. The general orientation is indicative of the transition regime, between the Great Chaco minimums (<900 mm) and the Southern Planalto maximums (>1400 mm).

### 2.3.6. Eastern Uruguay and South of Rio Grande do Sul

It is a transition region, with a very high variability both intra and interseasonal, and fluctuating monthly rainfall, although in general the intermediate seasons are those with more rain. The annual mean is in the order of 1600 mm in the North and of 1200 mm in the South.

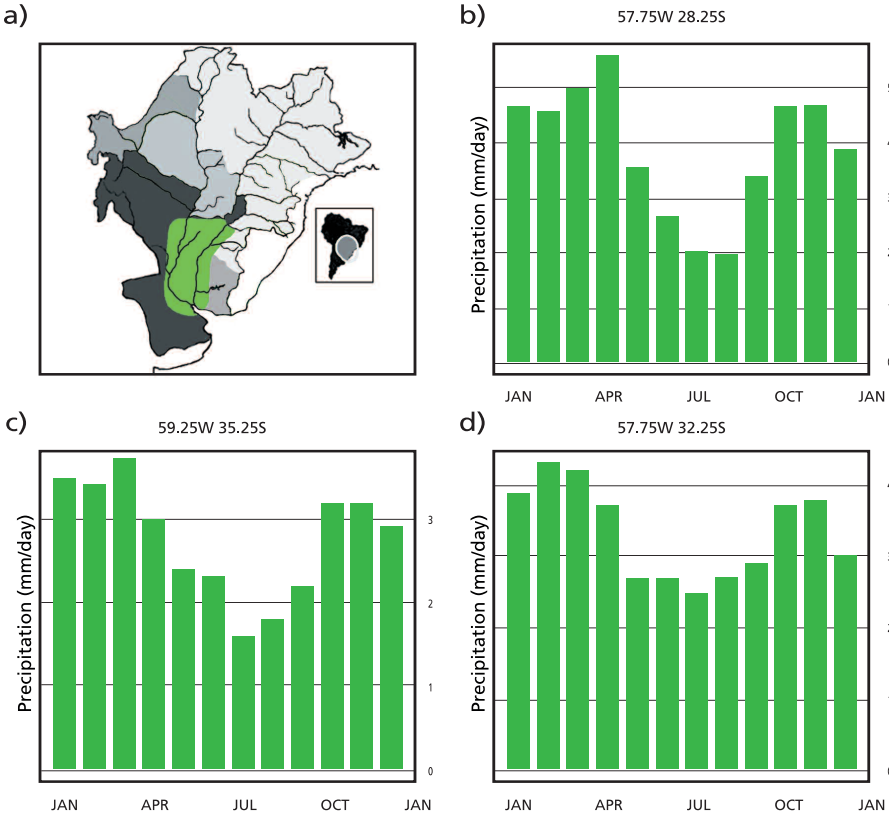
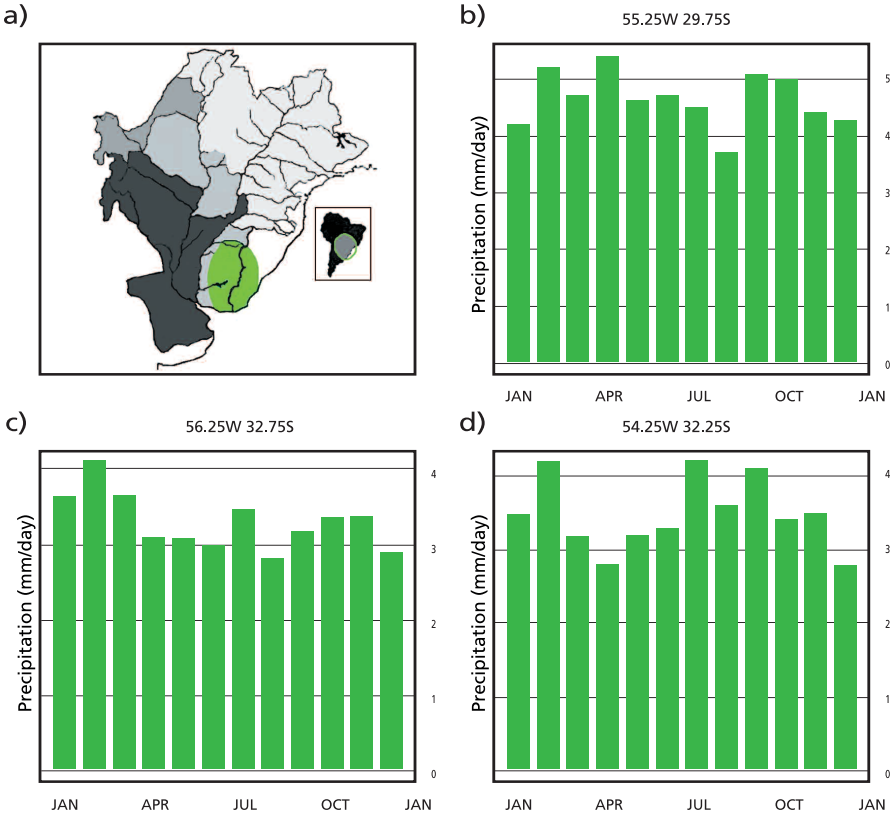


FIG. 2.9. Littoral Region a) Location. Rainfall regime at characteristic sites: b) Center-North c) South region d) Eastern Region.

Here the influence of the circulation of the West is especially important in winter. In this season, the cyclogenesis over either Uruguayan or the Argentine Mesopotamia has a maximum in frequency (Gan and Rao 1991; Vigliarolo 1998). The further displacement toward the Southeast of these recently generated low pressures centres causes a maximum of precipitation by the end of winter, on the southeaster border of the continent, practically entirely outside La Plata basin.

Spite of the relative proximity to the Atlantic Ocean, the region presents features of continental climate as in Winter there is frequent frosts, while in Summer, the daily maximum temperatures usually exceed the 36°C (except near the coast), especially during the second half of December and January.



**Fig. 2.10.** Eastern Uruguay and South of Brazil. a) Location. Rainfall regime at characteristic sites: b) and c) in the middle of the transition zone d) at the Southeast, region of winter maximum.

### 2.3.7. West and South borders

It embraces the whole western and southern fringe of the La Plata basin in Argentine territory, from the 25°S to the Ridge Mountains of Aconquija (Fig. 2.11a). Except for the oriental bands of the ridge mountains, where the precipitation is considerable (Fig. 2.11c, Hoffman, 1982), it has similar characteristic to the Chaco climate, with maximums at the beginning of autumn. The rest is a flat region, with scarce precipitation and mainly very little runoff, contributes very little to La Plata flow.

To the South of 32°S, the circulation of the West prevails, although the polar front during the summer, usually locates more to the South (around Bahía Blanca). Thus, in this season, it is frequent the convective prefrontal activity in the tropical air, which in addition to intense short lasting precipitations, usually bring along, severe phenomena (descending winds, tornados, hail). The intensity of the frontal perturbations depends on the intensity and position of the polar jet in winter, and of the sub-

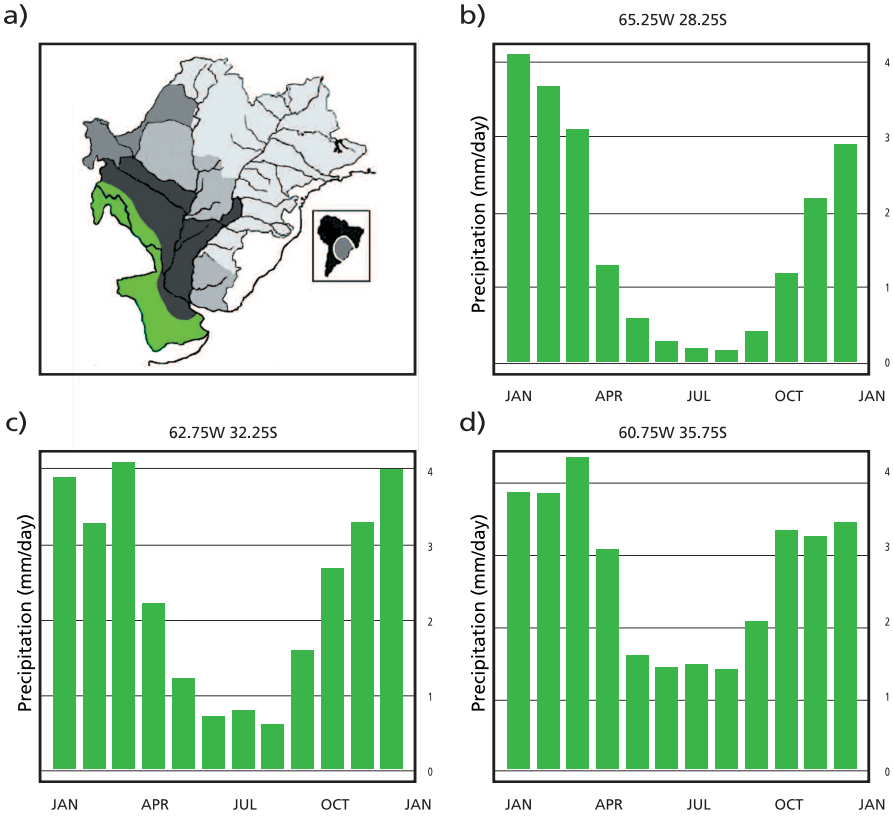


**Fig. 2.11.** Western and southern border of the La Plata basin. Rainfall regime at characteristic sites: b) eastern border of the Aconguija Mountain range c) southwestern corner, d) south border.

tropical jet in summer. Their effectiveness in terms of the occurrence, character and intensity of the rainfalls, will depend in turn on the position and intensity of both the Argentine Northwest Low and the one of the Chaco, which modulate the advection of humidity from the North. During winter, the frosts are a recurrent phenomenon, although it rarely snows. The rainfall minimum appears in winter. There is a gradient of annual isohyets toward the Southwest, registering an average of around 1100 mm in the coast of La Plata River, and less than 800 in the Southeast end.

In this chapter it has been described the main characteristics of the Climate in La Plata basin. The regional features of the La Plata basin climate are summarized in the *table 2.1*. The whole region is subject both to long period fluctuations as well as trends in climate that will be addressed in chapter 5.

**Table 2.1.** Summary of the principal climatic characteristics per region

Region	Main causes of the climatic regime	Characteristics	
		Precipitation	Thermal Regime
Monsoon a) Pantanal b) High Paraná	a) Monsoon, Bolivia High b) Monsoon, ZCAS	Summer maximum and Winter minimum, both marked	Low seasonal variation
Chaco	Monsoon, LLJ, MCS, position of the ANW Low, position of the Jet.	Maximum in Summer, often void in Winter	Very hot in Summer
East of Paraguay and surrounding areas	LLJ, MCS, ZCAS, frontal activity in Winter.	Maximum in Summer, minimum in Winter	Very hot in Summer
Meridional Planalto and Rio Grande ridges	ZCAS, MCS, Frontal activity (indirectly LLJ)	Abundant the whole year. Variable between months	Hot in Summer. Relatively cold Winter in high regions.
Argentine Littoral and surrounding areas	LLJ, MCS, frontal activity, position of the ANW Low, (indirectly ZCAS)	Maximum in intermediate seasons, with a marked minimum in Winter	Hot in Summer, Winter with frosts
Oriental Uruguay and South of Río Grande do Sul	Frontal activity, MCS, (indirectly ZCAS and LLJ)	Maximum in intermediate seasons, abundant in Summer except for the extreme South	Hot in Winter, Winter with frosts
West Borders and South of La Plata basin  a) To the North of 32°S b) To the South of 32°S	a) Position of the currents in jet and of the Chaco and ANW Lows b) Frontal activity, position of the currents in jet and of the ANW Low	a) scarce, greater in Summer b) less scarce, although minor than in the East and North, more distributed throughout the year, Winter minimum	a) Similar to Chaco b) Several days with frosts almost every winter

## References

- Barros, V., M. González, B. Liebmann and I. Camilloni 2000: Influence of the South Atlantic convergence zone and South Atlantic sea surface temperature on interannual Summer rainfall variability in southeastern South America. *Theor. Appl. Meteor.*, 67, 123-133.
- \_\_\_\_\_, M. Doyle, M. González, I. Camilloni, R. Bejarán y R. M. Caffera 2002: Climate Variability over Subtropical South America and the South American Monsoon: a Review. *Meteorológica*, 27, 33-57.
- Berberly, E. H. and E. A. Collini 2000: Springtime precipitation and water vapor flux convergence over southeastern South America. *Mon. Wea. Rev.*, 128, 1328-1346.
- \_\_\_\_\_ and V. R. Barros 2002: The hydrologic cycle of the La Plata Basin in South America. *J. Hydrometeorology*, 3, 630-645.
- Casarin, D. P. and V. Kousky 1986: Precipitation anomalies in Southern Brazil and related changes in the atmospheric circulation. *Revista Brasileira de Meteorologia*, 1, 83-90.

- Chen, T., C. S. and S. Schubert 1999: Maintenance of upper-tropical circulation over tropical South America: the Bolivian high-Nordeste low system. *J. Atmos. Sci.*, 56, 2081-2100.
- Díaz, A. F., C. D. Strudinski and C. R. Mechoso 1998: Relationships between precipitation anomalies in Uruguay and Southern Brazil and sea surface temperature in the Pacific and Atlantic Oceans. *J. Climate*, 11, 251-271.
- Figueiredo, J. C. y E. J. Scolar 1996: Estudo da trajetória dos sistemas convectivos de mesoescala na América do Sul. VII Congreso Argentino y VII Congreso Latinoamericano e Ibérico de Meteorología, Buenos Aires, Setiembre 1996, 165-166.
- Figueroa, S. N., P. Satyamurty and P. L. Silva Dias 1995: Simulations of the Summer circulation over the South American region with an eta coordinate model. *J. Atmos. Sci.*, 52, 1573-1584.
- Gan, G. A. and V. B. Rao 1991: Surface Cyclogenesis over South America. *Mon. Wea. Rev.*, 119, 1293-1302.
- González, M. and V. Barros 1998: The relation between tropical convection in South America and the end of the dry period in subtropical Argentina. *J. Climate*, 18, 1669-1685.
- Grimm, A. M., S. E. T. Ferraz and J. Gomes 1998: Precipitation anomalies in Southern Brazil associated with El Niño and La Niña events. *J. Climate*, 11, 2863-2880.
- Guedes, R. L., L. A. T. Machado, J. M. B. Silveira, M. A. S. Alves and R. C. Waltz 1994: Trajetórias dos sistemas convectivos sobre o continente americano. X Congresso Brasileiro de Meteorologia, 8, 77-80. Belo Horizonte-MG. Anais II.
- Gusmão de Carvalho, A. M. y A. W. Gandu 1996: A Zona de Convergência do Atlântico Sul. Climanálise, Edição especial comemorativa de 10 anos. Cach. Paulista, octubre 1996. <http://www.cptec.inpe.br/products/climanalise/cliesp10a/16.html>
- Hoffmann, J. 1982: Atlas Climático de América del Sur. WHO - UNESCO Cartography.
- Kodama, Y. M. 1992: Large-scale common features of subtropical precipitation zones (the Baiu frontal zone, the SPCZ and SACZ). 1. Characteristics of subtropical frontal zones. *J. Meteor. Soc. Japan*, 70, 813-836.
- Laing, A. G. and J. M. Fritch 2000: The large-scale environments of the global populations of mesoscale convective complexes. *Mon. Wea. Rev.*, 128, 2756-2776.
- Lichtenstein, E. R. 1980: La depresión del Noroeste Argentino. Tesis Doctoral, FCEyN, Universidad de Buenos Aires.
- Lenters, J. D. and K. H. Cook 1997: On the Origin of the Bolivian High and Related Circulation Features of the South American Climate. *J. Atmos. Sci.*, 54, 656-678.
- Marengo, J. A., W. R. Soares, C. Saulo and M. Nicolini 2004: Climatology of the Low-level jet east of the Andes as derived from the NCEP-NCAR reanalyses: characteristics and temporal variability. *J. Climate*, 17, 2261-2280.
- Nieto Ferreira, R., T. M. Rickembach, D. L. Herdies and L. M. V. Carvalho 2003: Variability of South American convective cloud systems and tropospheric circulation during January-March 1998 and 1999. *Mon. Wea. Rev.*, 131, 961-973
- Nogués-Paegle, J. and K. Mo 1997: Alternating wet and dry conditions over South America during Summer. *Mon. Wea. Rev.*, 125, 279-291.
- \_\_\_\_\_, C. R. Mechoso, R. Fu, E. H. Berbery, W. C. Chao, T. C. Chen, K. Cook, A. F. Díaz, D. Enfield, R. Ferreira, A. M. Grimm, V. Kousky, B. Liebmann, J. Marengo, K. Mo, J. D. Neelin, J. Paegle, A. W. Robertson, A. Seth, C. S. Vera and J. Zou 2002: Progress in Pan American CLIVAR Research: Understanding the South American Monsoon. *Meteorologica*, 27, 3-32.

- Robertson, A. W. and C. R. Mechoso 2000: Interannual and interdecadal variability of the South Atlantic Convergence Zone. *Mon. Wea. Rev.*, 128, 2947-2957.
- Prohaska, F. J. 1976: *Climates of Central and South America*. World Survey of Climatology vol. 12. Elsevier Scientific Publishing Company, Amsterdam. 57-69.
- Saulo, C., L. J. Ferreira, J. Mejia and M. Seluchi 2004: A Description of the Thermal Low characteristics using SALLJEX special observations. *CLIVAR Exchanges Contributions*, 29, 1-4.
- Velasco, I. and J. M. Fritsch 1987: Mesoscale convective complex in the Americas. *J. Geophys. Res.*, 92, D8, 157-175.
- Vera, C., P. K. Vigliarolo and E. H. Berbery 2002: Cold season synoptic scale waves over subtropical South America. *Mon. Wea. Rev.*, 130, 684-699.
- Vigliarolo, P. 1998: Ciclogénesis sobre Sudamérica. *Meteorológica*, 23, 73-81.
- Virji, H. 1981: A preliminary study of Summertime tropospheric circulation patterns over South America estimated from cloud winds. *Mon. Wea. Rev.*, 109, 599-610.
- Willmott, C. J. and K. Matsuura 2001: Willmott, Matsuura, and Collaborators' Global Climate Resources Pages: <http://climate.geog.udel.edu/climate/index.shtml>
- Xie and Arkin 1997: Global precipitation: a 17-year monthly analysis based on gauge observations, satellite estimations and numerical model outputs. *Bull. Amer. Meteor. Soc.*, 78, 2539-2558.
- Zhou, J. and K. M. Lau 1998: Does a monsoon climate exist over South America? *J. Climate*, 11, 1020-1040.

## INTERANNUAL LOW FREQUENCY VARIABILITY: BACKGROUND

Tércio Ambrizzi<sup>1</sup>

<sup>1</sup> University of São Paulo, Brasil.

### ABSTRACT

A well known atmospheric low frequency variability is the so-called El Niño-Southern Oscillation - ENSO, which is considered one of the most prominent sources of interannual variations in weather and climate around of the world. The major atmospheric and oceanic features associated with *El Niño* episodes are: predominance of positive anomalies of sea surface temperature (SST), weakness of the trade winds in the surface and low pressure with deep convection on the oriental Pacific and high pressure with subsidence movement on the western Pacific, Indonesia and Australia. *La Niña* events generally feature reversed atmospheric and oceanic patterns. South America is one of the continental areas around the world that is directly influenced by the ENSO cycle where several studies have documented the ENSO impacts (mainly the *El Niño* events) in the South American rainfall. Findings of these works indicate, in general, that the main areas of South America influenced by ENSO are located at the sections West (Peru and Ecuador), North and Northeast (Amazonian and Brazilian Northeast) and South-Southeast (Southern Brazil, Uruguay and Argentina). In analyses focused on southern Brazil and Southern South America (SSA), some results showed that the impact on rainfall in Summer is much weaker than in Spring. Other studies indicate that ENSO may have considerable signal in the interannual variability of the precipitation over La Plata basin. This signal varies along each of the ENSO phases, but is particularly strong during the Spring. Studies focused in the response to ENSO in smaller areas within La Plata basin show no evidence of a signal in rainfall during midsummer, but in late Summer and Autumn there is again a strong correlation between SSTs at *El Niño* regions 3 and 3.4, and Outgoing Longwave Radiation (OLR) over the Upper and Middle Paraná. The goal of this chapter is to offer a general view of the ENSO impact on the South America and particularly over the La Plata basin.

### 3.1. Introduction

Most of the annual total rainfall observed over South America usually occurs during the austral Summer, December to February (DJF) and Autumn, March to May (MAM)...The large and synoptic meteorological systems that modulate the rainfall in the Summer are linked to the performance of the South Atlantic Convergence Zone (SACZ) (Casarin and Kousky, 1986; Figueroa et al., 1995; Nogués-Paegle and Mo, 1997), the Bolivian High and the upper tropospheric cyclonic vortices (Virji 1981; Kousky and Gan 1981; Kayano et al. 1997).

The variability of precipitation in the subtropical plains of South America is also closely tied to the variability of the South American low level jet (SALLJ) that is a long, narrow, low level northerly wind current that flows to the East of the Andes Mountains year-round (Nogues-Paegle and Mo 1997; Saulo et al. 2000). The SALLJ supplies the warm, moist tropical air that fuel convection and precipitation in the subtropical plains of South America, being modulated by the *El Niño-Southern Oscillation* on interannual time-scales (Zhou and Lau 2001), frontal passages and SACZ on submonthly timescales, and boundary layer dynamics on diurnal timescales. In the subsequent period, MAM, the rainy season is located on the centre-East of the Amazonian and Northeast of Brazil, which is modulated by the migration to the South of Equator of Inter Tropical Convergence Zone - ITCZ (Hastenrath and Heller 1977; Moura and Shukla 1981; Nobre and Shukla 1996, Souza et al. 1998a).

The so-called *El Niño-Southern Oscillation* - ENSO, is considered one of the most prominent sources of interannual variations in weather and climate around of the world (Trenberth and Caron 2000). ENSO, a phenomenon of planetary scale related to a strong and complex ocean-atmosphere coupling over the tropical Pacific basin (Cane 1992), has a cycle, with the *El Niño* (warm phase) manifesting in one extreme phase and the *La Niña* (cold phase) in the opposite extreme. The major atmospheric and oceanic features associated with *El Niño* episodes are: predominance of positive anomalies of sea surface temperature (SST), weakness of the trade winds in the surface and low pressure with deep convection on the oriental Pacific and high pressure with subsidence movement on the western Pacific, Indonesia and Australia. *La Niña* events generally feature reversed atmospheric and oceanic patterns (Kousky and Ropelewski 1989). These anomalous patterns occur over the tropical Pacific basin, including an extensive spatial area of the tropics (more than a third of the tropical belt around of the globe). A schematic view of these features is given by *figure 4.1*, where the ocean-atmosphere changes can be observed in a 3-D picture during a typical event of *El Niño* (*Fig.3.1a*), *La Niña* (*Fig.3.1b*) and a normal year (*Fig.3.1c*).

Hence, ENSO triggers off changes in the general circulation of the atmosphere, resulting in climatic impacts in several continental areas located in the trop-

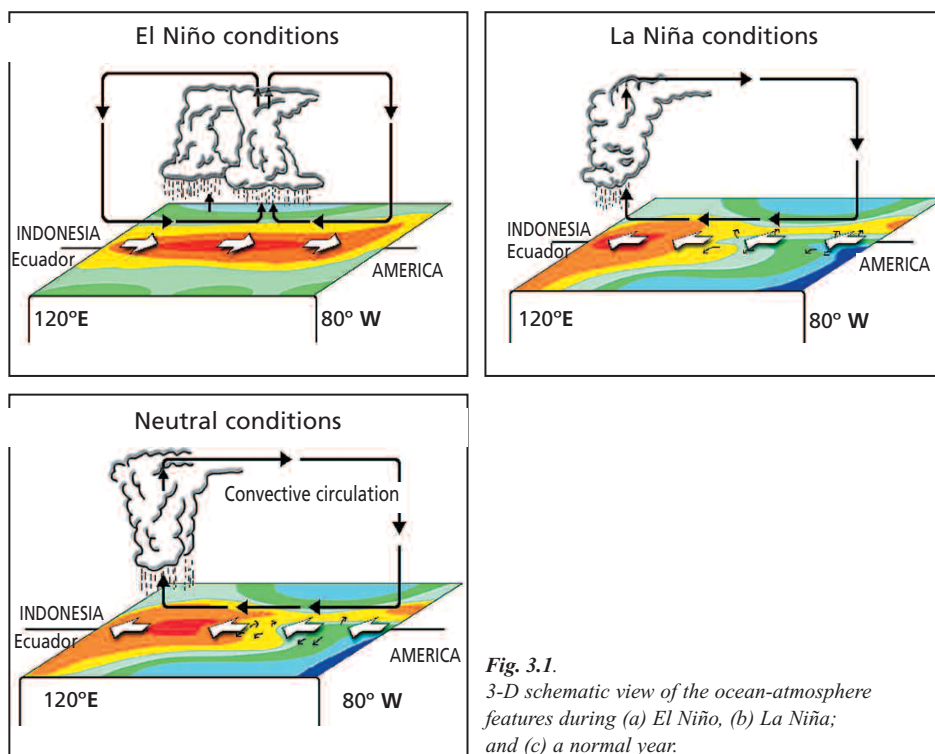


**Fig. 3.1.** 3-D schematic view of the ocean-atmosphere features during (a) El Niño, (b) La Niña; and (c) a normal year.

ics and extratropics. These changes are basically related to the weakness, intensification and/or displacements of the large-scale atmospheric circulation in the meridional and zonal planes, mainly those linked to the Hadley and Walker circulations (Kidson 1975; Kousky et al. 1984, Souza and Ambrizzi 2002) as well as large-scale Rossby waves that propagate into the extratropics producing, for instance, changes in extratropical storm tracks (Trenberth et al. 1998; Ambrizzi and Magaña 1999). Recent studies have indicated that the extratropical response to SST anomalies such as ENSO-related anomalies is less robust and predictable than the tropical response due to the chaotic nature of extratropical circulations such as transient baroclinic waves, fronts, and the SACZ (e.g., Shukla et al. 2000). The Walker circulation is a result of the “see-saw” in surface pressures between the eastern and western hemispheres linking these action centres through an atmospheric circulation in the zonal plan, restricted in the tropical strip, with ascending branch over the western Pacific and descending branch over the eastern Pacific (Bjerknes 1969). On the other hand, the differential heating between tropic-extratropics, results in the formation of a meridional circulation, the Hadley Circulation, with ascending branch over the equatorial areas and sinking over the subtropical latitudes (around 30° of latitude) in both Southern and Northern Hemispheres (Hastenrath 1985). *Figure 3.2* shows a schematic view of the Hadley and Walker circulation during ENSO years. For fur-

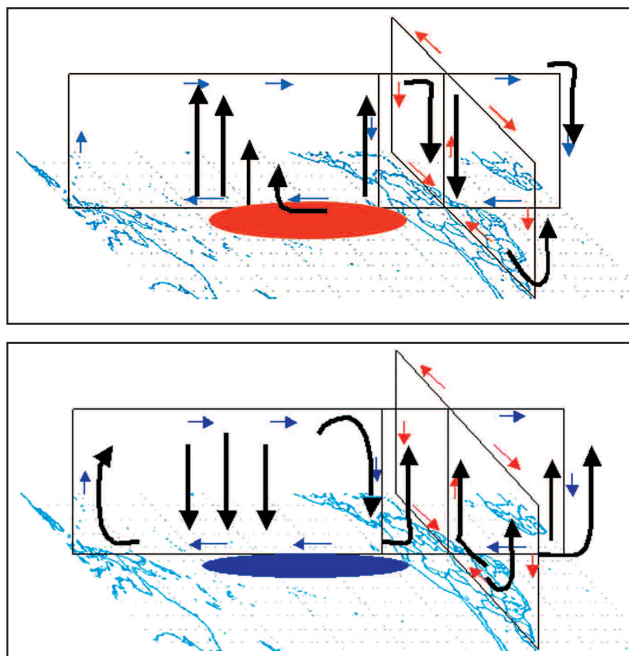


**Fig. 3.2.** Schematic diagrams showing the anomalous regional Walker and Hadley circulation for the (a) *El Niño* and (b) *La Niña* canonical impacts. The blue (red) arrows indicate the regional climatological circulation of the Walker (Hadley) cell and the black thick arrows show the anomalous circulation observed in the ENSO composites.

[Adapted from Ambrizzi et al, 2004]

ther information about the relationship between Hadley and Walker cells and their impact over the South American precipitation patterns during ENSO years see Ambrizzi et al. (2004).

South America is one of the continental areas around the world that is directly influenced by the ENSO cycle (Ropelewski and Halpert 1987). Several studies documented the ENSO impacts (mainly the *El Niño* events) in the South American rainfall (Aceituno, 1988; Kousky et al. 1984; Rao and Hada 1990; Alves and Repelli 1992; Grimm et al. 1998; Uvo et al. 1998; Diaz et al. 1998; Coelho et al. 1998; Souza et al. 1998b; among others). Findings of these works indicate, in general, that the main areas of South America influenced by ENSO are located at the sections West (Peru and Ecuador), North and Northeast (Amazonian and Brazilian Northeast) and South-Southeast (Southern Brazil, Uruguay and Argentina). In analyses focused on southern Brazil and Southern South America (SSA), Grimm et al. (1998, 2000) showed that the impact on rainfall in summer is much weaker than in spring. In terms of surface temperature impacts during ENSO events over the SSA, Barros et al. (2002) found a modest signal in this region, where only during the austral winter prior to the full development of the ENSO event that there were consistent anomalies in the surface temperature field. In most of the subtropical region, these anomalies are positive during *El Niño* and negative during *La Niña* events, with a maximum in northern Argentina. They coincide in time and approximately in space with an enhancement (reduction) of the northern component of the flow, and of the warm advection at low levels in *El Niño* (*La Niña*) events.

Others studies have shown that the tropical Atlantic Ocean also plays an important role in the interannual variability of the rainy season of the Amazon and Northeast region of Brazil (Hastenrath and Heller 1977; Moura and Shukla 1981; Servain 1991; Pulwarty, 1994; Nobre and Shukla 1996; Uvo et al. 1998; Souza et al. 2000 and others). However, for the Uruguay and southern Brazil, Diaz et al. (1998) show that both Pacific and Atlantic SST anomalies influence the rainfall regime in these regions during austral Spring and Summer, although during the fall-Winter period (April-July) only the SST anomalies in the southwestern Atlantic seem to have an influence on rainfall anomalies in this region.

Much of the precipitation during the rainfall season in La Plata basin is produced by large mesoscale precipitation systems. Mesoscale Convective Processes (MCCs; Maddox 1980) are a subset of mesoscale precipitation systems characterized by their large size and longevity. The term MCC is an infrared satellite image-based definition of cloudiness that was named by Maddox (1980) to classify the mesoscale systems that produce great rainfall amount over the North American Great Plains during spring and summer. Most MCCs occur over land regions situated on the lee side of major topographic features and downstream from a low level jet that brings a continuous supply of warm-moist tropical air to feed the convection (Laing and Fritsch 1997; Velasco and Fritsch 1987). In that sense, La Plata basin is a favourable region for the occurrence of MCCs because it is located on the lee side of the Andes Mountains and downstream of the SALLJ, which supplies warm and moist air from the Amazon basin to feed the convection (Marengo et al, 2004). Recently, Nieto Ferreira et al (2003) have presented an observational study of the January-March 1998-99 differences in precipitation, atmospheric circulation, and occurrence of large, long-lived convective cloud systems in South America. They chose this period because of the strongly contrasting Southern Oscillation conditions, where one of the strongest *El Niño* episodes on record was under way in the Pacific Ocean during JFM 1998 and a strong *La Niña* conditions prevailed in the Pacific Ocean during JFM 1999. They found that the SALLJ was about twice as strong during the warm ENSO phase than during the cold one. The stronger SALLJ was accompanied by large, long-lived convective cloud systems and nearly twice as much rainfall in subtropical South America (parts of southern Brazil, Uruguay, and Argentina).

### **3.2. Variability over the La Plata basin**

Studies of precipitation variability have been hampered by the lack of an extensive observational network. Nevertheless, there are some results, mainly in connection with the *El Niño Southern Oscillation* (ENSO) that show that it has a considerable signal in the interannual variability of the precipitation over the La Plata basin (Aceituno 1988; Ropelewski and Halpert 1987, 1989; Kiladis and Diaz

1989). This signal varies along each of the ENSO phases, but is particularly strong during the spring. Studies focused in the response to ENSO in smaller areas within La Plata basin show no evidence of a signal in rainfall during midsummer (Rao and Hada 1990; Grimm et al. 1998; Pisciotano et al. 1994; Grimm et al. 2000), but in late Summer and Autumn there is again a strong correlation between SSTs at *El Niño* regions 3 and 3.4, and Outgoing Longwave Radiation (OLR) over the Upper and Middle Paraná (Camilloni and Barros 2000).

There are also links between SST anomalies in the nearby Atlantic Ocean and precipitation anomalies in La Plata basin. Diaz et al. (1998) found that precipitation in Uruguay and southern Brazil are positively correlated with SST anomalies in the southwestern tropical Atlantic during spring and summer. La Plata basin precipitation south of 25°S is positively correlated to the SSTs near the South Atlantic Convergence Zone (SACZ); on the other hand, precipitation near the Paraná headwaters is negatively correlated with the SSTs in the western South Atlantic (Barros et al. 2000b; see also Nogués-Paegle and Mo 1997, 2002, and Doyle and Barros 2002). Robertson and Mechoso (2000) and Robertson et al. (2003), however, suggest that SST anomalies are driven by atmospheric anomalies, thus questioning the predictive values of these relationships.

Lower frequency variability in annual rainfall has been documented as well. Barros et al. (2000a) observed an important positive trend in precipitation, south of 25°S, while Camilloni and Castañeda (2000) found a positive trend in the autumn precipitation over the Upper and Middle Paraná after 1980. Zhou and Lau (2001) found that the variability in interannual time scales is associated with ENSO, while that in decadal time scales is associated with cross-equatorial SST gradients in the Atlantic and Pacific.

## References

- Aceituno, P. 1988: On the functioning of the Southern Oscillation in the South American sector. Part I: Surface climate. *Mon. Wea. Rev.*, 116, 505-524.
- Alves, J. M. B. and C. A. Repelli 1992: A variabilidade pluviométrica no setor norte do nordeste e os eventos El Niño/Oscilação Sul. *Rev. Bras. Meteo.*, 7(2): 583-592.
- Ambrizzi, T. and V. Magaña 1999: Dynamics of the impacts of El Niño/Southern Oscillation on the Americas Climate: The December- January- February signal. 14th Conference on Hydrology. 79th AMS Annual Meeting, Dallas, 14th. Conference on Hydrology, Dallas, Texas, 1: 307-308.
- \_\_\_\_\_, E. B. Souza and R. S. Pulwarty 2004: The Hadley and Walker regional circulations and associated ENSO impacts on the South American seasonal rainfall. *The Hadley Circulation: Present, Past and Future*. Henry F. Diaz and Raymond S. Bradley Editors, Kluwer Academic Publishers, 7, 203-238.

- Barros, V. and M. Doyle 1996: Precipitation trends in Southern South America to the east of the Andes. Center for Ocean-Land-Atmosphere Studies. Report N° 26. Editors J. L. Kinter III and E. K. Schneider. pp. 76-80
- \_\_\_\_\_, M. E. Castañeda and M. E. Doyle 2000: Recent precipitation trends in Southern South America east of the Andes: an indication of climatic variability. Southern Hemisphere paleo- and neoclimates. Eds.:P. P. Smolka, W. Volkheimer. Springer-Verlag Berlin Heidelberg New York, 187-206.
- \_\_\_\_\_, A. M. Grimm and M. E. Doyle 2002: Relationship between temperature and circulation in Southeastern South America and its influence from El Niño and La Niña events. *J. Meteor. Soc. Japan*, 80, 21-32.
- Bjerknes, J. 1969: Atmospheric teleconnections from the equatorial Pacific. *Mon. Wea. Rev.*, 97, 163-172.
- Camilloni, I. and E. Castañeda 2000: On the change of the annual steamflow cycle of the Paraná River. Preprints, Sixth Int. Conf. on Southern Hemisphere Meteorology and Oceanography, Santiago de Chile, Chile, Amer. Meteor. Soc., 294-295.
- \_\_\_\_\_, and V. Barros 2000: The Paraná river response to El Niño 1982-83 and 1997-1998 events. *J. Hydromet.*, 1, 412-430.
- Cane, M. 1992: Tropical Pacific ENSO modes: ENSO as a mode of coupled system. In: Trenberth, K.E. ed. *Climate System Modeling*. Cambridge University Press, Cambridge, p-583-614.
- Casarin, D. P. and V. E. Kousky 1986: Anomalias de precipitação no sul do Brasil e variações da circulação atmosférica. *Rev. Bras. Meteo.*, 1, 83-90.
- Coelho, C. A. S., A. R. M. Drumond, T. Ambrizzi and G. Sampaio 1998: Estudo climatológico sazonal da precipitação sobre o Brasil em episódios extremos da oscilação sul. *Rev. Bras. Meteo.*, 14(1), 49-65.
- Diaz, A. F., C. D. Studzinski and C. R. Mechoso 1998: Relationship between precipitation anomalies in Uruguay and Southern Brazil and sea surface temperature in the Pacific and Atlantic Oceans. *J. Climate*, 11, 251-271.
- Doyle, M. E. and V. Barros 2002: Midsummer low-level circulation and precipitation in subtropical South America and related sea surface temperature anomalies in the South Atlantic. *J. Climate*, 15, 3394-3410.
- Figueroa, S. N., P. Satyamurty and P. L. Silva Dias 1995: Simulations of the Summer circulation over the South American region with an ETA coordinate model. *J. Atmos. Sci.*, 52, 1573-1584.
- Grimm A. M., S. E. T. Ferraz and J. Gomes 1998: Precipitation anomalies in southern Brazil associated with El Niño and La Niña events. *J. Climate*, 11, 2863-2880.
- \_\_\_\_\_, V. Barros and M. Doyle 2000: Climate variability in southern South America associated with El Niño and La Niña events. *J. Climate*, 13, 35-58.
- Hastenrath, S. and P. Lamb 1977: *Climatic atlas of the tropical Atlantic and eastern Pacific oceans*. University of Wisconsin Press.
- \_\_\_\_\_, and L. Heller 1977: Dynamics of climatic hazards in Northeast Brazil. *Q. J. Roy. Meteor. Soc.*, 103(435), 77-92.
- \_\_\_\_\_, 1985: *Climate and circulation of the tropics*. D.Riedel, Dordrecht. 312 pp.
- Kayano, M. T., N. J. Ferreira and M. C. V. Ramirez 1997: Summer circulation patterns related to the upper tropospheric vortices over the tropical South Atlantic. *Meteorol. Atmos. Phys.*, 64, 203-213.

- Kidson, J. W. 1975: Tropical eigenvector analysis and the Southern Oscillation. *Mon. Wea. Rev.*, 103, 187-196.
- Kiladis, G. N. and H. F. Diaz 1989: Global climatic anomalies associated with extremes in the Southern Oscillation. *J. Climate*, 2, 1069-1090.
- Kousky, V. E. and C. Ropelewski 1989: Extremes in the southern oscillation and their relationship to precipitation with emphasis on the South American region. *Rev. Bras. Meteor.*, 4, 351-363.
- \_\_\_\_ and M. A. Gan 1981: Upper tropospheric cyclonic vortices in the tropical South Atlantic. *Tellus*, 33, 538-551.
- \_\_\_\_, I. F. A. Cavalcanti and M. T. Kayano 1984: A review of the Southern Oscillation: oceanic-atmospheric circulation changes and related rainfall anomalies. *Tellus*, 36A, 490-504.
- Laing, A. G. and J. M. Fritsch 1997: The global population of mesoscale convective complexes. *Quart. J. Roy. Meteor. Soc.*, 123, 389-405.
- Maddox, R. A. 1980: Mesoscale convective complexes. *Bull. Amer. Meteor. Soc.*, 61, 1374-1387.
- Marengo, J. A., W. R. Soares, C. Saulo and M. Nicolini 2004: Climatology of Low-Level Jet East of the Andes as derived from the NCEP-NCAR reanalyses: Characteristics and Temporal Variability. *J. Climate*, 17, 2261-2280.
- Moura, A. D. and J. Shukla 1981: On the dynamics of droughts in northeast Brazil: observations, theory and numerical experiments with a general circulation model. *J. Atmos. Sci.*, 38(7), 2653-2675.
- Nieto Ferreira, R., T. M. Rickenbach, D. L. Herdies and L. M. V. Carvalho 2003: Variability of South American convective cloud systems and tropospheric circulation during January-March 1998 and 1999. *Mon. Wea. Rev.*, 131, 961-973.
- Nobre, P. and J. Shukla 1996: Variations of sea surface temperature, wind stress and rainfall over the tropical Atlantic and South America. *J. Climate*, 10(4), 2664-2479.
- Nogués-Paegle, J. and K. C. Mo 1997: Alternating wet and dry conditions over South America during Summer. *Mon. Wea. Rev.*, 125, 279-291.
- \_\_\_\_ and \_\_\_\_ 2002: Linkages between Summer rainfall variability over South America and sea surface temperature anomalies. *J. Climate*, 15, 1389-1407.
- Pisciottano, G., A. Díaz, G. Cazes and C. R. Mechoso 1994: El Niño-Southern Oscillation impact on rainfall in Uruguay. *J. Climate*, 7, 1286-1302.
- Pulwarty, R. S. 1994: Annual and interannual variability of convection over tropical South America. Ph.D., Program in Atmospheric and Ocean Sciences, University of Colorado, 220 pp.
- Rao, V. B. and K. Hada 1990: Characteristics of rainfall over Brazil - Annual variations and connections with the Southern Oscillation. *Theor. Appl. Climatol.*, 42, 81-91.
- Robertson, A. W. and C. R. Mechoso 2000: Interannual and interdecadal variability of the South Atlantic Convergence Zone. *Mon. Wea. Rev.*, 128, 2947-2957.
- \_\_\_\_, J. D. Farrara and C. R. Mechoso 2003: Simulations of the atmospheric response to South Atlantic sea surface temperature anomalies. *J. Climate*, 16, 2540-2551.
- Ropelewski, C. F. and S. Halpert 1989: Precipitation patterns associated with the high index phase of the Southern Oscillation. *J. Climate*, 2, 268-284.
- \_\_\_\_ and \_\_\_\_ 1987: Global and regional scale precipitation patterns associated with the El Niño-Southern Oscillation. *Mon. Wea. Rev.*, 115, 1606-1626.
- Saulo, A. C., M. Nicolini and S. C. Chou 2000: Model characterization of the South American low level flow during the 1997-1998 Spring-Summer season. *Climate Dyn.*, 16, 867-881.

- Servain, J. 1991: Simple climate indices for the tropical Atlantic Ocean and some applications. *J. Geophys. Res.*, 96, 15137-15146.
- Shukla, J., J. Anderson, D. Baumhefner, C. Brankovic, Y. Chang, E. Kalnay, L. Marx, T. Palmer, D. Paolino, J. Ploshay, S. Schubert, D. Straus, M. Suarez and J. Tribbia 2000: Dynamical seasonal prediction. *Bull. Amer. Meteor. Soc.*, 81, 2593-2606.
- Souza, E. B. and P. Nobre 1998a: Uma revisão sobre o Padrão de Dipolo no Oceano Atlântico tropical. *Rev. Bras. Meteo.*, 13(1), 31-44.
- \_\_\_\_\_, J. M. B. Alves and P. Nobre 1998b: Anomalias de precipitação no norte e leste do Nordeste Brasileiro em associação aos eventos do Padrão de Dipolo observados no Atlântico tropical. *Rev. Bras. Meteo.*, 13(1), 31-44.
- \_\_\_\_\_, M. T. Kayano, J. Tota, L. Pezzi, G. Fisch and C. Nobre 2000: On the influences of the El Niño, La Niña and Atlantic dipole pattern on the Amazonian rainfall during 1960-1998. *Acta Amazonica*, 30(2): 305-318.
- \_\_\_\_\_, and T. Ambrizzi 2002: ENSO impacts on the South American rainfall during 1980s: Hadley and Walker circulation. *Atmósfera*, 15, 105-120.
- Trenberth, K. E. and J. M. Caron 2000: The Southern Oscillation Revisited: Sea level pressures, surface temperatures and precipitation. *J. Climate*, 13, 4358-4365.
- \_\_\_\_\_, G.W. Branstator, D. Karoly, A. Kumar, N. C. Lau and C. Ropelewski 1998: Progress during TOGA in understanding and modeling global teleconnections associated with tropical sea surface temperature. *J. Geophys. Res.*, 103, 14291-14324.
- Uvo, C. R. B., C. A. Repelli, S. Zebiak and Y. Kushnir 1998: The relationships between tropical Pacific and Atlantic SST and northeast Brazil monthly precipitation. *J. Climate*, 11(4), 551-562.
- Velasco, I. and M. Fritsch 1987: Mesoscale convective complexes in Americas. *J. Geophys. Res.*, 92, 9591-9613.
- Virji, H. 1981: A preliminary study of Summer time tropospheric circulation patterns over South America estimated from cloud winds. *Mon. Wea. Rev.*, 109, 599-610.
- Zhou, J. and W. K. Lau 2001: Principal modes of interannual and decadal variability of Summer rainfall over South America. *Int. J. Climatol.*, 21, 1623-1644.

## PHYSIOGRAPHY AND HYDROLOGY

*Genaro Coronel<sup>1</sup> and Ángel Menéndez<sup>2</sup>. Colaboración: Lucas Chamorro<sup>1</sup>*

<sup>1</sup> Universidad de Asunción.

<sup>2</sup> Instituto Nacional del Agua (INA). Universidad de Buenos Aires.

### ABSTRACT

The main physiographic and hydrologic features of the Plata basin are introduced. Also its location and economic importance are explained. The main ecosystems are described, including *the Pantanal*, one of the most important wetland of the world. The main features of the three most important sub basins, namely those of the Paraná, Paraguay and Uruguay rivers are addressed. Finally, the main problems like floods and its human dimensions, and the deforestation from the environmental point of view are addressed.

#### 4.1. Location of the La Plata basin

La Plata basin is located in South America, between latitudes 16° and 34°S, i.e., between the subtropic and mid-latitudes (*Fig. 4.1*). It is bounded to the West by the Pampean ridges and the pre-mountain range of the Andes and to the Northeast and the East by the Brazilian Plateaus and the Serra do Mar respectively.



*Fig. 4.1. La Plata Basin.*

With an extension of around 3.1 million km<sup>2</sup>, the basin is second in drainage area in South America and fifth in the world. Notice that its area is approximately a third of the total surface of the U.S.A. and almost similar to that of all the countries that integrate the European Union.

It stretches over five countries and includes 50% of their population. The distribution of the surface of the basin is approximately the following: 46% is in Brazil, 30% in Argentina, 13% in Paraguay, 7% in Bolivia and 5% in the Uruguay (*Table 4.1*).

**Table 4.1.** Distribution of the La Plata basin and sub-basins

SUB-BASIN COUNTRY	Paraná	Paraguay	Uruguay	Surface covered by the basin in each country (**)
Argentina	565.000 km <sup>2</sup> 37,5%	165.000 km <sup>2</sup> 15,0%	60.000 km <sup>2</sup> 16,4%	920.000 km <sup>2</sup> 29,7%
Bolivia	*	205.000 km <sup>2</sup> 18,7%	*	205.000 km <sup>2</sup> 6,6%
Brazil	890.000 km <sup>2</sup> 59,0%	370.000 km <sup>2</sup> 33,9%	155.000 km <sup>2</sup> 42,5%	1.415.000 km <sup>2</sup> 45,7%
Paraguay	55.000 km <sup>2</sup> 3,5%	355.000 km <sup>2</sup> 32,4%	*	410.000 km <sup>2</sup> 13,2%
Uruguay	*	*	150.000 km <sup>2</sup> 41,1%	150.000 km <sup>2</sup> 4,8%
Total	1.510.000 km <sup>2</sup> 48,7%	1.095.000 km <sup>2</sup> 35,3%	365.000 km <sup>2</sup> 11,8%	3.100.000 km <sup>2</sup> 100%

(\*\*) The areas in this column do not include La Plata River estuary, of 130.000 km<sup>2</sup>, which is shared by Argentina and Uruguay.

## 4.2. Importance of the basin

La Plata basin is the settlement of most of the agriculture of the Mercosur countries. Grain production surpasses 100 million tons, which not only constitutes the alimentary base of the countries of the region, but also an important share of their exports.

From the perspective of the regional economy, its importance lays on the fact that in the area is produced close to 70% of the total Gross Domestic Product (GDP) of the five countries. From the hydrological point of view, the first place in importance corresponds to agriculture and cattle rising. Other important activity is navigation along the rivers that are natural channels, which have increased their transported volume greatly due to the integration of the regional economies in recent years. The hydroelectric power utilities are also very important, as they provide energy to the region; in fact, in Brazil 92% of the produced energy depends on the hydroelectric resources. Finally, the rivers of the basin provide the water for the consumption of the inhabitants of the region, which is the most populated of South America.

## 4.3. Ecosystems in the basin

La Plata basin contains key ecosystems. *The wetland of the Pantanal*, located in the upper part of the basin of the Paraguay River and shared by Brazil, Bolivia and Paraguay, is a reservoir of enormous biological wealth that also works as regulator of the hydrological system of the La Plata basin.

*The Chaco* is the second biome in extension of South America. It corresponds to an alluvial area that is located East from the Andes mountain range, formed by the deposit of sediments, mainly from the Bermejo and Pilcomayo rivers. Since the Bermejo is the only river whose waters starts at the Andes and reaches the Paraguay River, it constitutes a natural ecological corridor among the puna ecosystems in the mountain, the yungas forest and the dry and humid areas of El Chaco plains.

*The Pampas's plain*, due to their dimensions, is the third ecosystem of global importance. The most fertile soils in the La Plata basin are located in these plains and since long ago the agricultural production has settled in the area.

The territory of the basin is completed by other key ecosystems of South America: *the Cerrado*, to the North, of a wide biological diversity and the *Mata Atlantica*, to the Northeast, at present characterized mainly by a strong deforestation of their original forests that have been reduced to 4% of its primary state.

These data indicate the abundance and quality of the natural resources and the natural productivity, goods and services that these ecosystems provide. They also show how significant it has been and it's still being the availability, both in quality and quantity, of their water resources for the sustainability of the development process of the region.

#### 4.4. Characteristics of the sub-basins

La Plata basin is basically composed by three big sub-basins, corresponding to the Paraná, Paraguay and Uruguay rivers. *Table 4.2* identifies and characterizes

*Table 4.2. Physical features of the three main rivers.*

River	Stretch	Distance to the source (km)	Basin area (10 <sup>3</sup> km <sup>2</sup> )	Annual mean volume (m <sup>3</sup> /s)
Paraná	Confluence Paranaíba-Grande	1200 (Paranaíba) 1000 (Grande)	376	4370
	River Paraguay outlet	2540	975	12480
	Outlet at La Plata River	3780	1510	17700
Paraguay	Up to Cáceres	420	33,8	345
	Up to Puerto Bermejo	2620	1095	3840
Uruguay	Concordia		294	4640
	Outlet at La Plata River	1600	365	5500

[Internave 1990, Ministerio del Interior-Argentina 1994]

the most important stretches of these three main components. In the confluence of Paraguay and Paraná rivers, the contribution of the first one is 18.6% of the total flow. In relation to the relative contribution of the Uruguay and Paraná rivers to the La Plata River, the second contributes 76.3% of the mean flow.

The altitudes in the La Plata basin vary from 1500 masl in the Sea Ridge and between 1000 and 4000 masl in the Andes, up to less than 2 masl in the low basin. On the other hand, the annual precipitation vary from more than 2000 mm in the Northeast of Argentina and in the Serra do Mar, up to less than 200 mm in the pre-mountain range of the Andes.

#### *4.4.1. Sub-basin of the Paraná River*

The Sub-basin of the Paraná River, with a surface of 1.51 million km<sup>2</sup> (without including the basin of the Paraguay River), occupies close to half of the area of the La Plata River.

The following nomenclature will be used for the subdivision of the Paraná River:

- Upper Paraná: from its source up to the city of Corrientes
- Low Paraná: from Corrientes up to its outlet in the La Plata River

In turn, the Upper Paraná is subdivided in:

- Upper North Paraná: from its origin up to Jupiá Dam.
- Upper Central Paraná: from Jupiá up to Itaipu Dam
- Upper Paraná South: from Itaipu up to the city of Corrientes

While the Low Paraná is subdivided in:

- Middle Paraná: from Corrientes up to the city of Rosario
- Lower Paraná: from Rosario up to the city of San Pedro
- Paraná Delta: from San Pedro up to the outlet at La Plata River.

The Paraná River has its source at the confluence of the Paranaíba and Grande Rivers to the North of 20°S. In the Upper sub-basin, characterized by a quick run off, it receives the contribution of numerous tributaries, among which the Paranapanema and the Iguazu rivers. In it, the Paraná and its tributaries are much regulated by various dams, most of which were built after 1980. On the main course of the river are located the dams of Jupiá, Ilha Solteira, Porto Primavera, Itaipu and Yacyretá.

Near the city of Corrientes, it receives the contribution of Paraguay River. From there on develops the Low Paraná which course extends with a very slight decline to the La Plata River. This sector presents very low coasts, especially on its

right bank, for what the very high discharges cause severe floods. Because of the scarce contributions from Paraguay River, these floods are generally product of the climatic forcings in the Upper sub-basin of the Paraná River.

As shown in *Figure 4.2*, up to the Itaipu Dam, the Paraná River presents marked seasonality, accompanying the Brazil Southeasterly climate regime. The streamflows at Posadas indicate a reduction in the annual range due to the different hydrological regime of the Iguazu. In Corrientes, the Paraná receives the contribution of the Paraguay River, significantly increasing its flow, mainly in June-July, when the Paraguay River presents the largest volumes.

*Table 4.3* presents some characteristics of the main tributaries of the Paraná River, with the exception of the Paraguay River that is approached independently hereinafter.

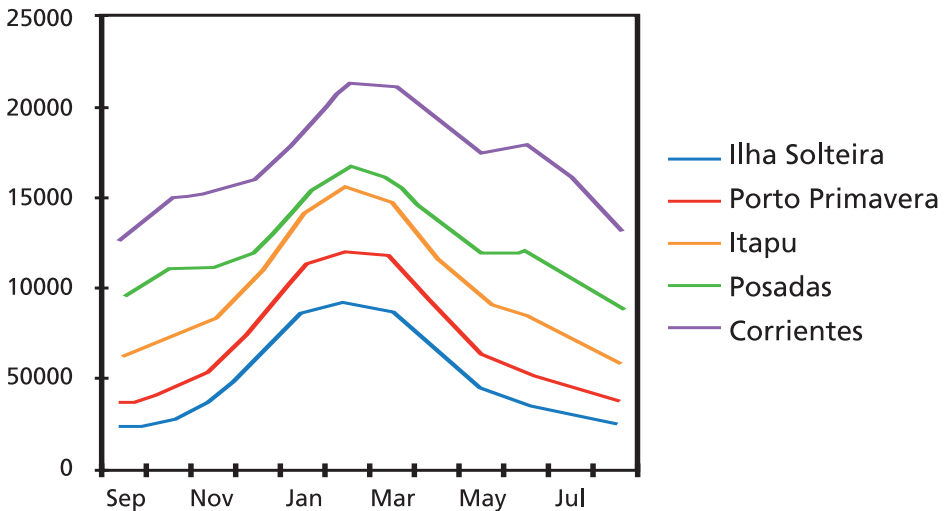


*Fig. 4.2.* Mean monthly flows of the Paraná River at different stations along the main course.

[National Operator of the System-Brazil WWWeb, ANA WWWeb, Mining of the Argentine Republic, WWWeb]

*Table 4.3.* Features of the main tributaries of the Paraná River.

River	Station	Drainage Area (km <sup>2</sup> )	Annual mean volume (m <sup>3</sup> /seg)
Paranaíba	São Simão	181040	2347
Grande	Água Vermelha	139900	2069
Tietê	Três Irmãos	71510	788
Paranapanema	Rosana	99000	1278
Iguazú	Salto Caxias	57974	1320

[Operador Nacional do Sistema-Brasil WWWeb, ANA WWWeb]

The *Paranaíba* River (ANEEL/IBAMA/ANA 2001) has its source in the "da Mata da Corda" mountain, in the state of Minas Gerais, at an altitude of 1140 masl, and it crosses an extension of 1120 km up to its confluence with the Grande River. The river presents three differentiated sections with different topography: more pronounced in the High Paranaíba, and diminishing toward the outlet.

The *Grande* River (Comitê of bacia hidrográfica do Grande WWWeb) has its source in the state of Minas Gerais at altitudes over 1250masl, in the western slopes of the Serra da Mantiqueira. The main course extends for 1300 km up to its encounter with the Paranaíba River, at 300masl. The great slope in the water courses, added to the abundant rainfall occurrence, transforms the river and their diverse tributaries in important resources for electric power generation.

The sub-basin of the *Tietê* River (Comitê of bacia hidrográfica do Tietê WWWeb) is located in the state of São Paulo. The Upper Tietê basin has its source in the Serra do Mar, to the East of the state, running West toward the Paraná River. The Upper Tietê basin presents a hydrological regime extremely complex due to the alterations produced by the urbanization in the last century that covers approximately 37% of the high basin. It is the most important area in the production of industrial goods of Brazil, with a GDP of 147 billion dollars, corresponding to 18% of the Brazilian total. The impermeabilization of urban areas resulted in the worsening of floods. This problem is enhanced by the occupation of the flood plain of the river.

The *Paranapanema* River (Comitê de bacia hidrográfica do Rio Paranapanema WWWeb) has its source in the mountain of Paranapiacaba, in the State of São Paulo, and ends in the Paraná River after more than 900 km.

The *Iguazu* River (Plano Director de la Cuenca del Río Iguazu WWWeb) has its source in the Serra do Mar, at an altitude of more than 1000 mosl, and drains in a West-East direction, an area of 55024 km<sup>2</sup>. Its importance is related to its capacity to generate exceptional discharges with direct impact in the whole basin below.

The *Middle Paraná* sub-basin (Minería de la República Argentina WWWeb) extends from the convergence of the Paraná River with the Paraguay River up to the city of Rosario (Argentina), running along a distance of approximately 1000 km. In this sector, the river runs through an alluvial plain whose width varies between 6 and 40 km. This stretch receives not very significant contributions. The middle course is very different of the upper due to the important sedimentary load contribution of the Paraguay River, especially the Bermejo River. After the confluence with the Paraguay River, in the middle of the Argentine territory and up to its outlet, the slope of the riverbed is around 4 cm/km. Its width goes from 4200 meters at Corrientes to 2000 meters at Rosario; but, on the other hand, its flood valley gets progressively wider between Corrientes (13 km) and Rosario (56 km) and extends almost totally on the right riverbank. The major problem in this sub-basin is the flooding during the extraordinary discharges of the Paraná River.

The distinction of the *Lower Paraná* regarding the Middle, from the hydraulic point of view, is that the first one is influenced by tides. The main problem of the *Lower Paraná* (Minería de la República Argentina WWWeb) is the flooding caused by the extraordinary discharges of the Paraná River. The riverside area, in general terms, is of scarce height. The periodic floods take place, on the average, every two or three years. These can happen at any time of the year, prevailing during February and March with eventual worsening in June.

In the last section (Minería de la República Argentina WWWeb) the river is divided in a series of branches of a complex conformation (*Paraná Delta*) that consists on an undifferentiated set of islands associated to an intricate group of courses of natural channels. The sediments of the Paraná River are deposited due to the increase in the width of the riverbed at its outlet with the La Plata River. As a result, the delta is in a continuous advance process toward the La Plata River, growing at an approximate mean speed of 70 m/year. The delta has a width that varies between 18 and 61 km, covering a surface of 17500 km<sup>2</sup>. The low areas of the delta are affected by the floods of the La Plata River caused by "sudestadas". This phenomenon blocks the natural drainage of superficial waters, streams, channels and rain-fall waters, causing serious floods.

#### **4.4.2. The Paraguay River sub-basin**

The Paraguay River has its source in the central region of the Brazilian State of Mato Grosso, in the oriental slope of the "Chapada do Parecis" and ends in the Paraná River, running along 2550 km. Its basin area is of 1095000 km<sup>2</sup>.

The sub-basin of the Paraguay River is mainly in a great plain and, with few exceptions, has a small and uniform slope (Tossini 1959). The elevation of the Paraguay basin rarely exceeds the 70m over the sea level, and its gradient is typically lower than 1.5 cm per kilometer.

The sub-basin can be subdivided in four areas:

- Pantanal
- High Paraguay
- Middle Paraguay
- Low Paraguay

The landscape in the area of the Pantanal includes low and periodically flooded lands and plateaus, ridges and depressions that are not flooded. From a hydrological point of view, this zone presents two areas: Plateau ("Planalto") and Pantanal. The first one corresponds to the upstream part of the basin which has a similar behavior to the High Paraná with a rapid runoff.

The Pantanal itself is the downstream part of this sub basin, an area of 138000 km<sup>2</sup>. 50-60% of the water volume and sediments from the tributaries are retained in the flood plain, which reduces hugely the volume downstream. Since precipitation is smaller than evaporation, in the Pantanal there is a mixture of swamp vegetation proper of the rainy station and of savannah at the dry season.

From the Pantanal exit up to the outlet of the Paraguay, the river flows along a plain with low coasts, which facilitates the floods in both the Paraguayan and Argentine territories. In the Low Paraguay the river receives an important tributary, the Bermejo River. From the outlet of the Bermejo River, the riverbed of the Paraguay River is characterized by its lack of stability, due to the solid discharge of this tributary. The decrease of the capacity of discharge of the Paraguay River is associated to the hydrodynamic linger produced by the Paraná River, causing a reduction of speed from the confluence area up to more than 340 km upstream.

The Paraguay River presents the major discharges in Autumn-Winter and low waters in Spring-Summer, with regular regime and slow variations. In this behavior it is important the influence of the Pantanal, diminishing the propagation of the large discharges and the length of the low water. But it is also a consequence that in the Low Paraguay basin the evaporation balances the rainfall in Summer, while it is very inferior to it in Autumn (Barros et al. 2004).

Figure 4.3 illustrates the annual hydrological cycle of the Paraguay River in some sections. It can be observed the retard effect in the freshet wave with regard to the one at the North of the Pantanal. The Cáceres section in the Pantanal plateau registers the largest flows in March, while in Porto Murtinho and Puerto Bermejo they take place in June.

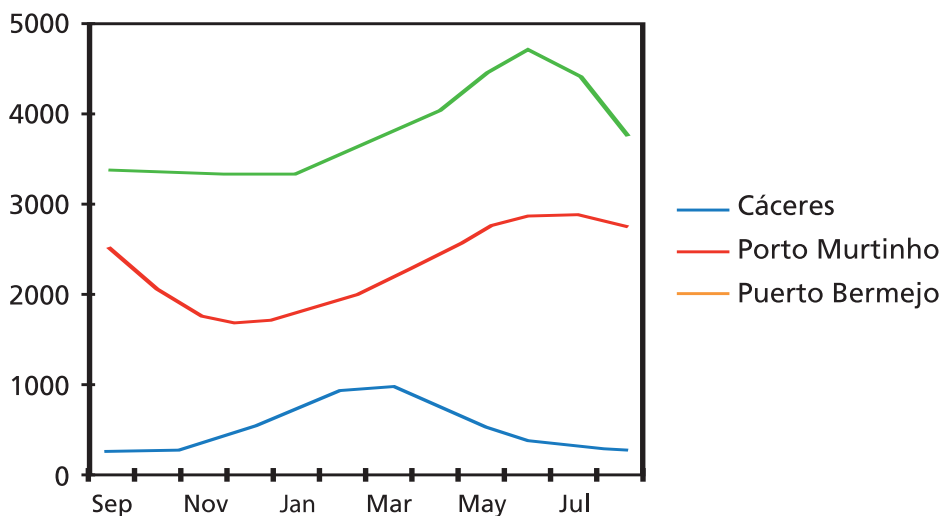


Fig. 4.3. Mean flows of the Paraguay River at different sections.

[ANA WWWeb, Mining of the Argentine Republic, WWWeb]

Table 4.4 shows the characteristics of some tributaries of the Paraguay River.

**Table 4.4.** Characteristics of main tributaries of the Paraguay River

Sub-basin	Station	Drainage Area (km <sup>2</sup> )	Mean Annual Volume (m <sup>3</sup> /seg)
Pilcomayo	Fortín Nuevo Pilcomayo	130.000	153
Bermejo	El Colorado	65.735	396

[Comisión Binacional para el Desarrollo de la Alta Cuenca del Río Bermejo y el Río Grande de Tarija WWWeb, Comisión Trinacional para el desarrollo de la cuenca del Río Pilcomayo WWWeb]

The *Pilcomayo* River sub-basin (Comisión Trinacional para el desarrollo de la cuenca del Río Pilcomayo WWWeb) is shared by Argentina, Bolivia and Paraguay. Its sources are in the Bolivian plateau, in a mountainous area that extends from Sucre (to the North) up to La Quiaca (to the South), and runs toward the Southeast through a series of plains up to its outlet at the Paraguay River. This basin is characterized by its topographical as well as lithological, edaphic, hydrological, climatic, physiographical and population contrasts.

The *Bermejo* River sub-basin (Comisión Binacional para el Desarrollo de la Alta Cuenca del Río Bermejo y el Río Grande de Tarija WWWeb) is located in the southern end of Bolivia and in the North of Argentina has 123000 km<sup>2</sup> of surface, with more than 1300 km. The basin of the Bermejo River is divided in two well differentiated areas: the high basin, where the climatic conditions determine a great variability in vegetation, and the low basin extremely plane topography and with dry forests in the West and the prevalence of humid lands and forests in gallery to the East.

The rivers of the basin present a rainfall control with a season variability very well defined, reaching 85% of runoff during Summer and low waters between April and September.

#### 4.4.3. The Uruguay River Sub-basin

The sub-basin of the Uruguay River has an area of total drainage of 365000 km<sup>2</sup> and has its source in the convergence of the Pelotas and Peixe rivers, which have their origin in the Serra do Mar and Geral, at almost 2000 masl. The Uruguay River ends in the La Plata River, 2200 km. The hydrological regime of the Uruguay River is very irregular. The Uruguay River is the only big river of the La Plata system that is not tributary of the Paraná. Although its basin is bigger than that of the Iguazu, both share the same features that their large discharges can be caused by

forcings of synoptic scale. Due of its small longitudinal gradient and with a basin that has a comparatively narrow transverse section, the delay between the precipitation and the discharge of the river is short (Tossini 1959).

The climatic characteristics of the basin determine the possibility of occurrence of floods in any time of the year. As the slope is pronounced, floods caused as consequence of intense rains are rapid and concentrated on small areas.

Figure 4.4 shows mean flows of the Uruguay River at different sections. The hydrological regime presents large discharges in Winter and lower waters in Summer.

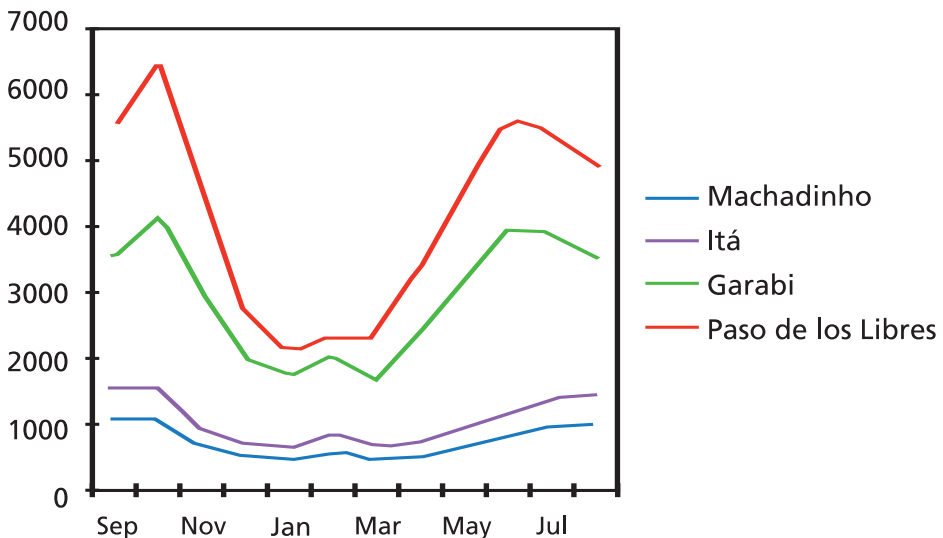


Fig. 4.4. Mean flows of the Uruguay River at different sections.

[Mining of the Argentine RepublicWWWeb, National Operator of the System-Brazil. WWWeb]

#### 4.5. Slopes in the basin

In Table 4.5 mean slopes in the main rivers of the La Plata basin are presented.

Table 4.5. Slopes in the main systems of the La Plata basin

Basins	Terrain slope (m/km)	Fluvial slope (m/km)
Alto Paraná	0,284	0,232
Paraguay	0,055	0,037
Bajo Paraná	0,036	0,042
Uruguay	0,103	0,086

The sub-basin of the Paraná River can be divided in two parts according to its characteristics of height: upper and lower. The upper basin extends from the sources of Paranaíba and Grande rivers up to the tributaries of the oriental region of the Paraguay and Northwest of Misiones; it occupies a higher plane and its slope is more significant that facilitates the water runoff. The lower basin, except for the hilly region of the left riverbank, between the Corrientes and Gualeguay rivers, is a continuation (due to its topography and geology) of the right part of the basin of the Paraguay that is an immense plain of very scarce and uniform slope.

The sub-basin of the Paraguay River is an immense alluvial plain of very scarce and uniform slope, except for the southern part of the left riverbank between the Apa and Confluencia Rivers that presents a hilly landscape with valleys of regular slope, and excluding as well the regions where are located the sources of Pilcomayo and Bermejo rivers.

The sub-basin of the Uruguay River presents very different characteristic. The terrain's landscape is complex, with numerous valleys and a branched fluvial system, formed by water courses of short range and marked slope. Actually, this sub-basin lacks of expansion area, therefore can be considered as both, reception and discharge basin.

As a resume, La Plata basin presents two well differentiated large regions. The human relation with these two regions is also different. In the oriental part with larger slopes, there is an important source of hydropower while in the occidental part, large and long floods are the major concern.

#### **4.6. Environmental problems**

The major concerns in the region are the *floods*, due to the damage they cause in almost the whole basin (losses of human lives and considerable damages to infrastructures and economy), mainly in the urban areas. This is the result of a complex human interaction with the environment, where it is not absent the lack of planning and the poverty problem, since most of those damaged by this phenomenon are the poorest sectors of the society that, at a large extent, occupy precarious settlements in easily floodable areas. Provinces of the Northeaster Argentine periodically have floods as a result of the overflow of the three main rivers of the La Plata basin (Paraná, Uruguay and Paraguay).

The extensive deforested areas, the acceleration of flood frequency and the disordered riverside population's growth that occupy the flood plains, increase the problem. The existent scientific literature indicates that the biggest events in floods of disastrous characteristics are associated to the El Niño phenomenon, but they would also be influenced by regional forcings of the climate.

It is noticeable that the anthropic development in the hydrographical basin has been intense and has had major consequences for the environment, with emergent trans-boundary problems that constitute a challenge for the countries that share the basin.

The severe floods with losses of life and big damages to infrastructures and economic production happen very frequently, especially in the sub-basins of the Paraná and Uruguay rivers. The Paraná and its tributaries have many cities on their banks that are repeatedly flooded, especially since 1970. The Argentine cities of Resistencia, Corrientes, Rosario and Santa Fé suffer a lot with the strong floods. On the Iguazu River alone, damages due to floods among 1983-93 have been estimated in more than U\$S 110 millions.

The floods also cause large damage in cities of the sub-basin of the Uruguay River, mainly in São Borja, Itaqui, Uruguayana and cities on the tributary Alegrete. During El Niño 1982-83 events more than 40000 people were affected in more than 70 cities in the riverside of the Uruguay in the Brazilian state of Rio Grande do Sul. In the entire La Plata basin losses related to that El Niño event reached more than a billion dollars. In the Middle Paraná the four registered largest discharges followed El Niño events in 1983, 1905, 1992 and 1998.

Only in Argentina direct and indirect damages of these floods were assessed in 2640 million dollars and 235000 persons were evacuated. Floods of the period 1991-92 meant for this country a loss of 513 million dollars, more than 3 million flooded hectares and 122000 evacuated people. In Santa Catalina's state, in Brazil, the same floods of the Paraná meant equivalent losses to 8% of the annual DGP of this state. Floods also cause serious damages to the coastal cities and the economic activities in the basin of the Uruguay River. During the 1982-83 El Niño event, in the middle Uruguay more than 40000 people were affected, in more than 70 cities.

The *quality of water* is an important factor for an effective environmental administration in the La Plata basin, affected mainly by the development reached in the region, namely by the loss of the vegetable cover, urban concentrations, the intensive agricultural practices with high dependence of agrochemicals, the construction of dams with its reservoirs, and by the river navigation.

The situation of the river navigation and the increasing deposition of sediments appear to be a relevant issue at present, with the addition of pollution cases increased by mining activities. The Pilcomayo River, shared by Argentina, Bolivia and Paraguay recedes annually in its bed and doesn't reach to pour its waters in the Paraguay due to the enormous load of sediments.

*Deforestation and agriculture* are intensive in the three sub-basins of the Paraguay, Paraná and Uruguay rivers. The agricultural expansion as from 1960 particularly in Brazil has left some areas with only 5% of its original forest covering.

In the Brazilian state of São Paulo the area of primary forest has fallen from 58% to near 8% at the end of the twentieth century. In the state of Paraná, the forest covering fell from 83% in 1890 to 5% in 1990. In 1945 55% of the East side of the Paraguay was forest; in 1990 it was only the 15% (Fig. 4.5).

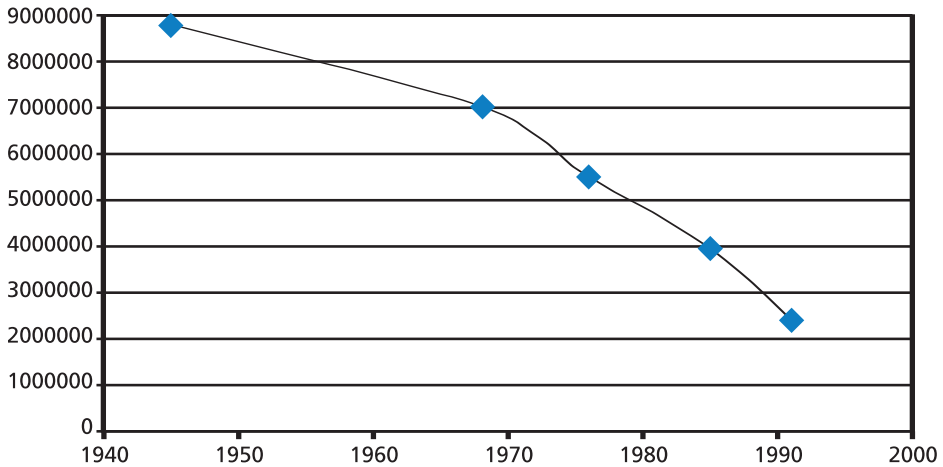


Fig. 4.5. Wooded area in the Eastern Paraguay in hectares.

[Source MAG-GTZ]

In Brazil, in the basin of the Ibicuí River, a tributary of the Uruguay where rice is produced with irrigation, the conflict is among the rice' farmers and the cities of the region that need water for the domestic consumption. In Argentina, the cereals and oleaginous sowed areas increased from 20 to 26 million hectares in the last decade. The areas of cereal production have increased in order to include the areas that are marginal to cereals, where the intensive production introduces high risks of degradation of the soil. This is a matter of concern since the organic content of the floor has fallen in 50% from its value at the beginning of the twentieth century, reducing the soil capacity to assimilate water. The introduction of the direct sowing in the cultivations is growing quickly, driving to certain restoration of the arable area, and being another factor of change in the hydrological cycle.

The economy of Paraguay which is totally inside the La Plata basin, is highly dependent on agriculture, 90% of which is cattle production; however its grain production, at the moment around 10 million tons, is increasing as a result of new technologies.

Deforestation and deterioration of the ecosystems are critical factors as a consequence of the expansion of the agriculture in the last decades. It has meant the disappearance of the forest coverings that were a decisive part of the functioning of the ecosystems and of the hydrology. One of the acute cases has been the deforesta-

tion of the Mata Atlantica, ecosystem that covers the basin of the High Paraná, the area with the largest and most intense precipitation. In this ecosystem, its forest-like covering decreased from 58% to 8% in Sao Paulo' state in the last century, and in the state of Paraná it went from 85% of its covered surface to current 5%. Something similar happens in Paraguay, with a quicker process by the end of the century but with the same path. Soils are uncovered and are incorporated to agriculture, leaving soil more compacted and increasing the water erosion whose consequences are both the increase and acceleration of the superficial runoffs toward the courses of water, the rise of peak flows, its occurrence in shorter periods, the increment of the sedimentation of the rivers and reservoirs, affecting its navigability and accelerating the turbidity of the reservoirs (with the consequent loss of its potential energy) and less feeding to the aquifers.

In the Pampas, due to economic conditions the pastures are being replaced by cultivations due to their more favorable prices compared to the cattle rising. For example, in the Province of Buenos Aires the areas under cultivation were increased in 40% between 1988 and 1993. These changes have pressed the opening of the agricultural frontier toward marginal soils of the Pampas ecosystem itself as well as the Chaco, which implies larger deforestation required by an escalation of the production systems and raw material, increasing the risk of degradation in areas with desertification processes.

Deforestation of the natural forests of the Paraguay has accelerated, going from 200 to 400 thousand annual hectares during the last 50 years; thus, the probability of maintaining areas with forest-like coverings is small. With the loss of the forests biodiversity is suffering, with the consequent disappearance of important genetic resources. In the Oriental Region between 1945 to 1991, the forest covering went from 8805000 to 2403000 hectares. It has to be highlighted that most of the reduction of the forest surface was verified in the last 20 years. To this situation contributed the combined actions of the following main factors: the expansion of the agricultural border, the lack of policies on use of the land, the scarce appraisalment of the forests, and the loan policy that has fomented the expansion of the agricultural frontier in detriment of the forests.

The affectation of the *aquatic ecosystems* deserves special attention in the whole La Plata basin, characterized as one of the basins of larger continental aquatic diversity of the world, in particular the sub-basins of the Paraná and Paraguay rivers (Pantanal) and of its marine front. At the moment these ecosystems are constantly and mainly affected by: I) the increments of sediments, II) the modifications in the contribution of nutrients to the waters, III) the obstruction that present the dams and the proliferation of reservoir constructions that are particularly important in the High Paraná and in the Uruguay River, IV) the punctual and diffuse pollution of certain water courses, added to the lack of an appropriate handling of the difficulties associated to the trans-boundary character of the issue, V) the handling of

the biodiversity of these ecosystems, particularly of their ichthyologic resources conditioned by different fishing situations, which require a complete knowledge of the operation and a common regulatory framework, beyond existing bi-national agreements in place.

There is an environmental degradation caused by the intensive *urbanization*. Population at La Plata basin is highly concentrated in cities. The capital cities of the five countries, with the exception of Bolivia, are within La Plata basin, and these urban concentrations need water for the domestic use. The incomplete treatment of urban waste waters causes a deterioration of the quality of the water. The population of the basin has grown from 61 millions in 1968 to 116 millions in 1994. The most concentrated part is in small or medium size cities lacking the basic both social and economic infrastructure. The possibility of a better life in the cities attracts poor people from rural areas, where sometimes they can only find a place to live on the margins of the rivers that are frequently flooded and degraded by debris.

Besides the effects of urbanization, the damage to the water resources can also result from *industrial* waste waters and toxic spills in areas of intensive industrialization.

## References

- ANA (Agência Nacional de Águas) 2001: *Bacias Brasileiras do Rio da Prata: avaliações e propostas*. Brasília. 102 pp.
- ANA (Agência Nacional de Águas). WWWeb. Sistema de Informações hidrológicas. <http://hidroweb.ana.gov.br/hidroweb/>.
- ANEEL/IBAMA/ANA 2001: *Diagnóstico do Monitoramento da Qualidade de água na Bacia do Prata em território brasileiro*. Brasília. 88 pp.
- Barros, V., L. Chamorro, G. Coronel and J. Báez 2004: The major discharge events in the Paraguay River: Magnitudes, source regions, and climate forcings. Accepted in *J. of Hydrometeorology*.
- Comisión Binacional para el Desarrollo de la Alta Cuenca del Río Bermejo y el Río Grande de Tarija. WWWeb. <http://www.cbbermejo.org.ar/>.
- Comisión Trinacional para el desarrollo de la cuenca del Río Pilcomayo. WWWeb. <http://www.pilcomayo.org.py/>.
- Comitê de bacia hidrográfica do Rio Grande. WWWeb. Secretaria de Energia e Recursos Hídricos do Estado de São Paulo. [http://www.sigrh.sp.gov.br/cgi-bin/sigrh\\_index.exe](http://www.sigrh.sp.gov.br/cgi-bin/sigrh_index.exe).
- Comitê de bacia hidrográfica do Rio Paranapanema. WWWeb. Secretaria de Energia e Recursos Hídricos do Estado de São Paulo. [http://www.sigrh.sp.gov.br/cgi-bin/sigrh\\_index.exe](http://www.sigrh.sp.gov.br/cgi-bin/sigrh_index.exe).
- Comitê de bacia hidrográfica do Tietê. WWWeb. Secretaria de Energia e Recursos Hídricos do Estado de São Paulo. [http://www.sigrh.sp.gov.br/cgi-bin/sigrh\\_index.exe](http://www.sigrh.sp.gov.br/cgi-bin/sigrh_index.exe)
- Cooperación Técnica Nacional para la Protección de los Recursos Naturales 1995: Documento base sobre el sector agrícola y su impacto ambiental. Enaprena /Geosurvey S.R.L.

- INTERNAVE 1990: Hidrovia Paraguai-Paraná. Estudio de viabilidade econômica. Relatório final. Internave Engenharia. São Paulo, Brasil.
- Minería de la República Argentina. WWWeb. Inventario de Recursos Naturales. <http://www.mineria.gov.ar/ambiente/estudios/inicio.asp>.
- Ministerio del Interior-Argentina 1994: Subunidad Central de Coordinación para la Emergencia. Estudio de regulación del valle aluvial de los ríos Paraná, Paraguay y Uruguay para el control de las inundaciones. Buenos Aires.
- Operador Nacional do Sistema-Brasil. WWWeb. Acompanhamento Diário da Operação Hidroenergética. [http://www.ons.com.br/ons/planejamento/index\\_ophen.htm](http://www.ons.com.br/ons/planejamento/index_ophen.htm).
- Plano Director de la Cuenca del Río Iguazu. WWWeb. Gobierno del Estado de Paraná. <http://www.hidricos.mg.gov.br/ufparana/relprin2/indice1.htm>.
- Tossini, L. 1959: Sistema hidrográfico y Cuenca del Río de la Plata. Anales de la Sociedad Científica Argentina.
- Cooperación Técnica Nacional para la Protección de los Recursos Naturales. 1995. "Documento base sobre el sector agrícola y su impacto ambiental". Enaprena /Geosurvey S.R.L.
- INTERNAVE 1990: Hidrovia Paraguai-Paraná. Estudio de viabilidade econômica. Relatório final. Internave Engenharia. São Paulo, Brasil.
- Minería de la República Argentina. WWWeb. Inventario de Recursos Naturales. <http://www.mineria.gov.ar/ambiente/estudios/inicio.asp>.
- Ministerio del Interior-Argentina 1994: Subunidad Central de Coordinación para la Emergencia. Estudio de regulación del valle aluvial de los ríos Paraná, Paraguay y Uruguay para el control de las inundaciones. Buenos Aires.
- Operador Nacional do Sistema-Brasil. WWWeb. Acompanhamento Diário da Operação Hidroenergética. [http://www.ons.com.br/ons/planejamento/index\\_ophen.htm](http://www.ons.com.br/ons/planejamento/index_ophen.htm).
- Plano Director de la Cuenca del Río Iguazu. WWWeb. Gobierno del Estado de Paraná. <http://www.hidricos.mg.gov.br/ufparana/relprin2/indice1.htm>.
- Tossini, L. 1959: Sistema hidrográfico y Cuenca del Río de la Plata. Anales de la Sociedad Científica Argentina.

## REGIONAL PRECIPITATION TRENDS

*Ernesto Hugo Berbery<sup>1</sup>, Moira Doyle<sup>2</sup> and Vicente Barros<sup>2</sup>*

<sup>1</sup> Universidad de Maryland.

<sup>2</sup> CIMA/CONICET. Universidad de Buenos Aires.

### ABSTRACT

During approximately the last century southeastern South America has experienced important changes in its precipitation regime, consequently affecting the hydrologic balance of the region, and particularly of the La Plata basin. Changes have been observed in many other regions of the world, but South America is probably one where largest change magnitudes are found. Moreover, the trends have intensified in the last 30 to 40 years due to changes in changes in the atmospheric circulation and likely due to land use changes.

As a consequence of the increased precipitation in semiarid regions of Argentina, the agricultural land extent has increased, which has been beneficial for increased revenues, but at the same time this has created new ecological problems. Consequently, although semiarid regions have benefited from the increased precipitation, other regions are flooding more frequently, and in certain cases some areas have been left permanently under water

Changes in precipitation correspond with a doubling of changes in river discharge, so that by each 1% increase precipitation, the streamflow increases by 2% or more. This indicates that activities dependent on the streamflows are highly vulnerable to possible regional trends related to the global Climate Change.

## **5.1. Introduction**

Precipitation and other land surface water cycle variables have undergone very large decadal scale changes over the last century in much of the southern part of South America, and within La Plata basin in particular.

Understanding the nature and cause of these trends has important scientific implications for prediction of the interaction of local (land-based) and remote (largely oceanic) climate forcings, but also has important practical implications given the critical role of the basin's hydropower generating capacity. Hydropower produces about 70% of the electric energy consumed within La Plata basin. The water resources of the basin are also critical for metropolitan, industrial, and agricultural water supply in one of the most densely populated regions of South America; and are essential for harvests and livestock, which are among the region's most important assets. The changes in the hydrologic cycle of the basin are therefore a subject of interest not only for physical reasons but also for practical ones.

## **5.2. Data sets**

The estimates produced in this chapter are based on raingauge observations obtained from the Argentine National Meteorological Service and the National Direction of Meteorology of Paraguay. Most of the series for Brazil were obtained from the Institute of Agricultural Research of Rio Grande do Sul and from Brazil's National Agency of Electricity. Additional records for Brazil and Uruguay were obtained from the Climate Data Centre (CDC) in Boulder, Colorado.

## **5.3. Trends**

Rainfall variability in most of southern South America has important interdecadal components (see chapter 14). The strongest interdecadal variability in the annual cycle of precipitation occurs in regions of transition between precipitation regimes, especially in the Paraná River basin (Rusticucci and Penalba 1997). Collischonn et al. (2001) also found changes in the hydrologic regime of the Paraguay basin. The changes, although appearing as a positive trend, in fact were rather abrupt, with the latest increase occurring after 1970. Precipitation trends in Argentina have generally been positive since 1916 with a pronounced increase after the late fifties (Castañeda and Barros 1994). Barros et al. (2000a) observed an important positive trend in precipitation, South of 25°S. Precipitation increased by up to 30% between 1956 and 1991 East of the Andes in several locations between 20° and 35°S.

In a large part of this region, most of the increase occurred during the 1960s, and it seems to have been associated with a reduction of the meridional gradient of surface temperature, which probably caused a southward shift of the regional circulation. Consistently, the leading principal component of annual precipitation correlates with the meridional gradient of temperature at interannual as well as interdecadal timescales (Barros and Doyle 1996). Another strong precipitation increase was observed during the late 1970s. This correlates with an increase in the subtropical temperature of the Southern Hemisphere and a decrease of the Southern Oscillation Index (Barros and Doyle 1996).

### 5.3.1. Total Precipitation

#### a. Annual trends

Southern South America is the region of the World with greatest increase of annual precipitation during the 20th Century (Giorgi 2003). However, West of the Andes Mountains the precipitation trend was markedly negative (Fig. 5.1). Each continent depicts the opposite precipitation trend (negative to the West and positive to the East) at subtropical latitudes. The only exception is South Africa, where the land extent at subtropical latitudes is small. On the other hand, South America is the continent with the largest contrast. Barros (2004) has suggested that the reason for these changes may be related to the poleward shift of the subtropical anticyclones observed in the last few decades (Gillet et al. 2003; Escobar et al. 2003).

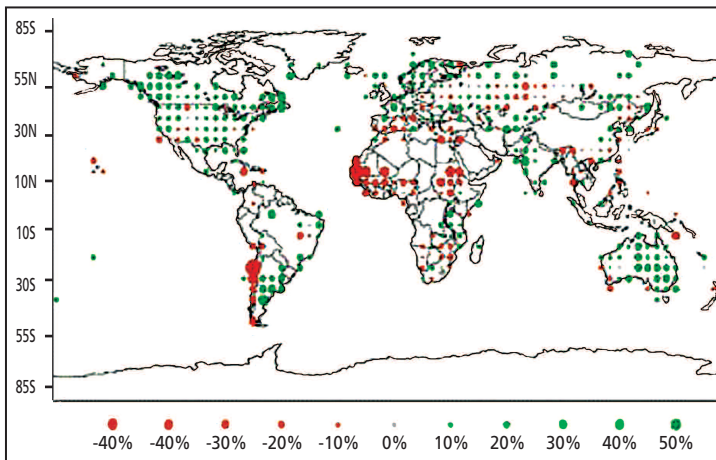


**Fig. 5.1.** Annual global precipitation trends (%) in the twentieth.

[Source: IPCC 2001]

From 1956 to 1991, in most of the Argentine territory North of 40 ° S, the annual precipitation increase was larger than 10%, and even in some regions larger than 40% (Castañeda and Barros 1994). Largest increases have occurred in western Buenos Aires Province, East of La Pampa and East of Corrientes. In both, precipitation increased by more than 200 mm between 1960 and 2000 . The increase of almost 35% in the West of Buenos Aires case explains the more frequent floods, and even lands that have become almost permanent lagoons. In Corrientes the marshes and lakes of the Iberá System have expanded notably their surfaces, except for a recent drought period when values went back to those of the 1960s.

In subtropical Argentina, the mean precipitation diminishes from West to East and therefore the isohyets run approximately in a North-South direction. Thus, the changes in precipitation have resulted in a westward shift of the isohyets. The 600 mm isohyet, which is the approximate western boundary of the agriculture in the South of the Humid Pampa, shifted more than 200 km toward the West of the region, while the 800 mm isohyet that is the agriculture boundary in the North shifted more than 100 km over the Chaco region (Fig. 5.2). For this reason, the land with aptitude for crop cultivation increased in 100000 km<sup>2</sup>, which together with new technologies favoured the expansion of the crop farming (Barros et al. 2000b). On the other hand, the undesired result of the increased precipitation is that some areas of Buenos Aires, Santa Fe and Corrientes Provinces have seen an increase in floods and consequently a diminished value of their agricultural activities.

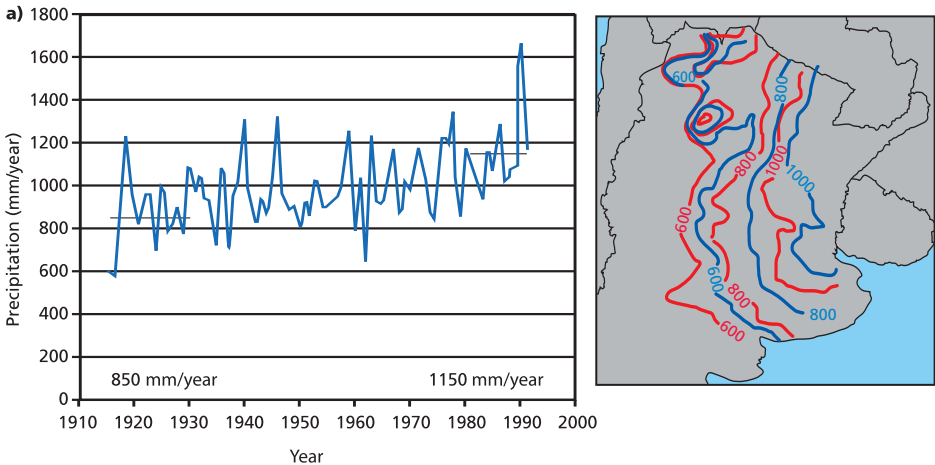


**Fig. 5.2.**

(a) Mean annual precipitation in the wet Pampa.

[adapted from Barros et al 2000a]

(b) Changes in isohyets since 1950/1969 (black contour) up to 1980/1999.

The precipitation changes have not occurred simultaneously over the entire region. Positive trends in southern Brazil and northeastern Argentina started sometime around the middle of the 1970 decade (Fig. 5.3a, b), apparently related to stronger intensity El Niño (Barros and Doyle 1996; Barros et al. 2000). In the southern and central portions of subtropical Argentina (Provinces of Buenos Aires, Córdoba and La Pampa), the strong positive trend started at the end of the 1960s decade (Fig. 5.3c, d). This occurred simultaneously with the notable warming of the western hemisphere Antarctic coastland and islands, and probably is related to the southward displacement of the South Atlantic Anticyclone (Barros and Doyle 1996; Barros et al. 2000). However, it is also likely that warming of the western South Atlantic Ocean is also related (Liebmann et al. 2004).

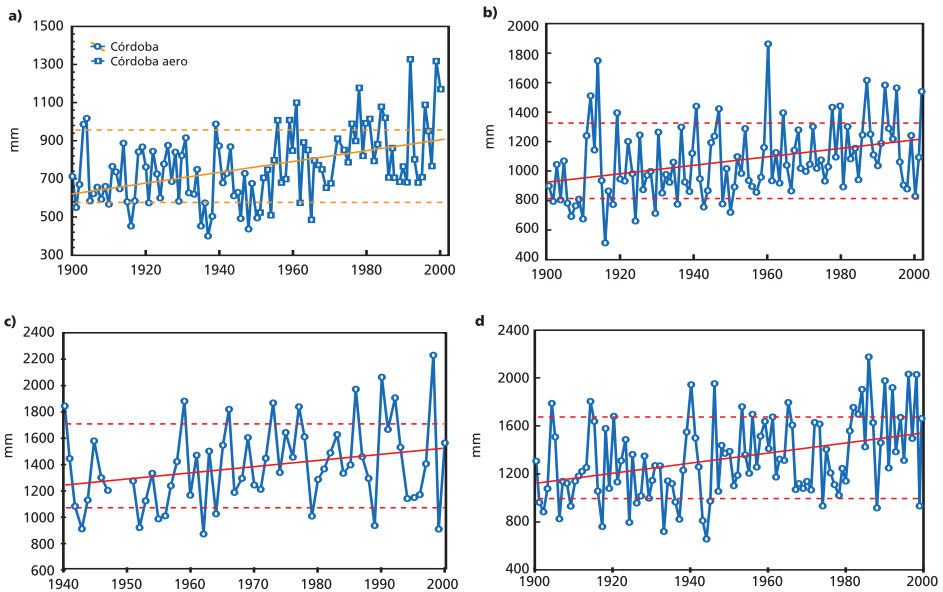


**Fig. 5.3.** Time series of annual precipitation and their linear trends for: (a) Córdoba, (b) Buenos Aires, (c) Monte Caseros, and (d) Corrientes.

### b. Seasonal trends

We have just discussed the annual precipitation trends. However, the precipitation increase is not evenly distributed along the year (Castañeda and Barros 2001). According to figure 5.4, the largest positive trends are found during Summer and Autumn while negative trends of smaller magnitude are found during Spring over Brazil and during Winter over Uruguay, southern Brazil, and Buenos Aires. The positive precipitation trend during Autumn affects the Upper Paraná basins after 1980.

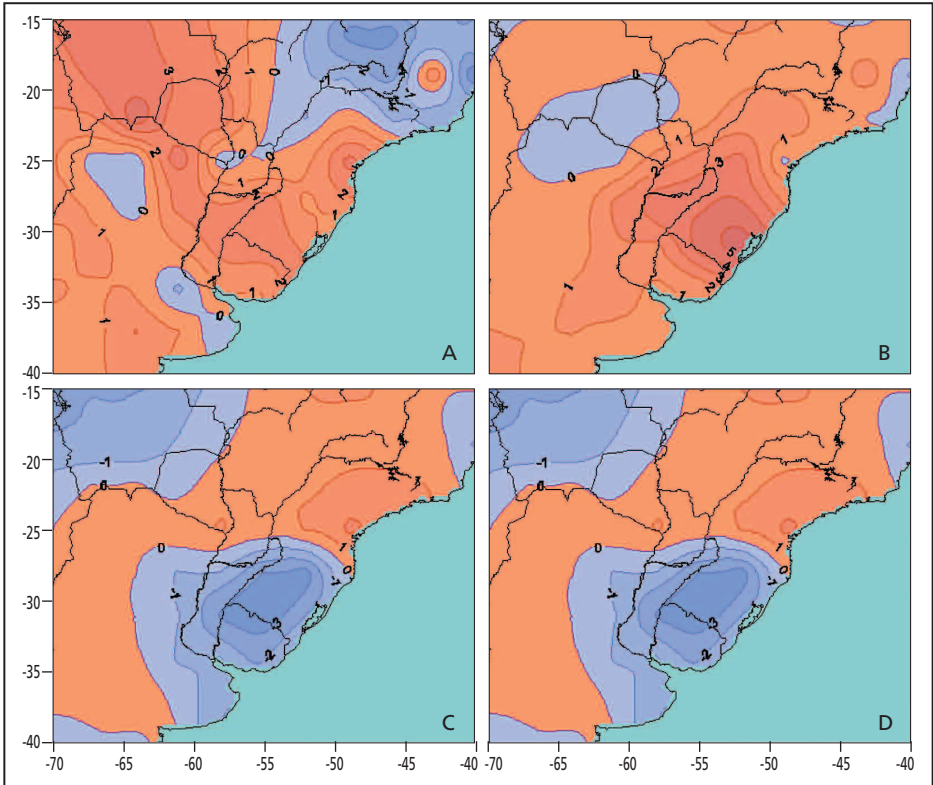


**Fig. 5.4.** Trends of the seasonal precipitation for 1961-2000 in mm/yr. (a) summer, (b) autumn, (c) winter, and (d) spring.

### c. Trends associated with ENSO

In the same way that the precipitation trends are not uniformly distributed throughout the year, they also depict differences with respect to the ENSO phase. The ENSO cycle is the main source of interannual variability in southern South America. Given that El Niño events have gained in intensity during recent decades, the trend analysis is performed separately over the El Niño, La Niña and Neutral years, Fig. 5.5. The largest trends over Paraguay appear associated with El Niño, while those over Buenos Aires and La Pampa provinces appear linked to neutral years, while in the provinces of northeaster Argentina were caused during both phases.

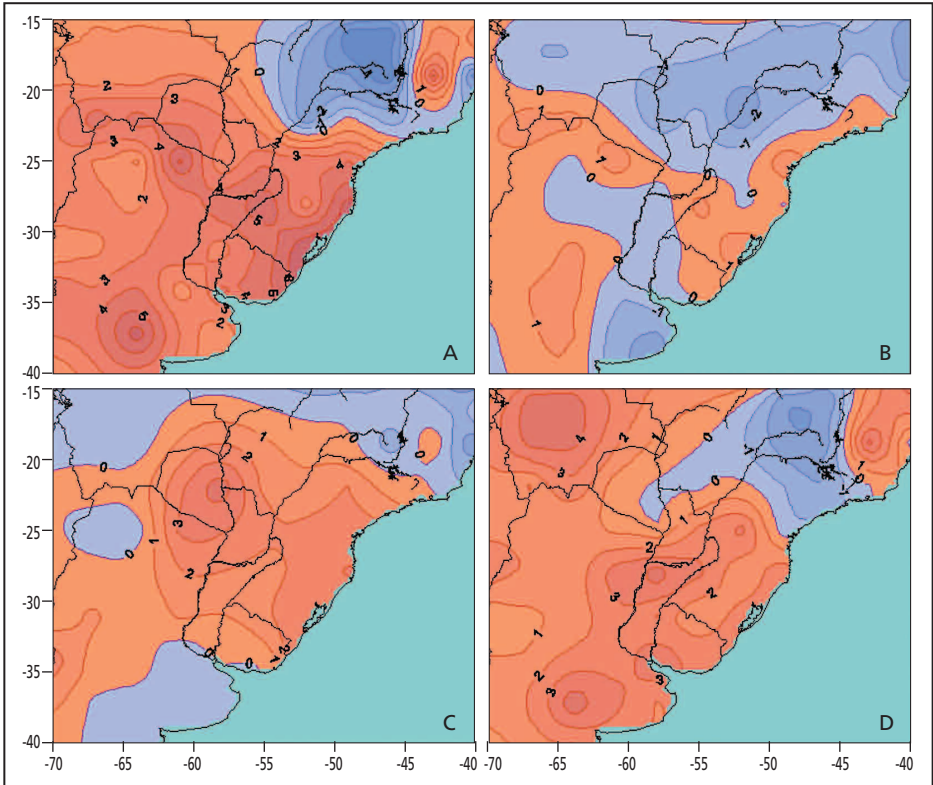


**Fig. 5.5.** Precipitation trends for 1961-2000 in mm/yr. (a) annual precipitation, (b) La Niña contribution, (c) El Niño contribution, and (d) Neutral years contribution.

The positive trend is in the band between 20° and 40°S East of the Andes Mountains. El Niño contribution to the trend is noticeable for the region that goes from Paraguay, through Northeastern Argentina up to Rio Grande in Brazil. To the South, El Niño contribution to the trend is close to zero, while the Neutral years appear to be the ones that carry most of the trend signal. Neutral years also contribute to the maximum in the region of the triple boundary of Paraguay, Brazil and Argentina. It can also be noticed that during La Niña periods the trend is close to zero everywhere. In other words, largest contributions to precipitation trends are found during El Niño or Neutral years, but not during La Niña years.

These results are relevant when preparing future scenarios of climate change, because they provide important information about the mechanisms behind the trends observed in the last few decades.

### 5.3.2. Frequency of extreme precipitation

Frequency of heavy precipitations in Argentina has increased notably since the late 1970s (Fig. 5.6). Since that time, the number of recorded cases with precipitations over 100 mm in less than 48 hours has been three folded in the Centre and East of Argentina and the same happens with the thresholds of 50 and 1590 mm (Barros 2004).

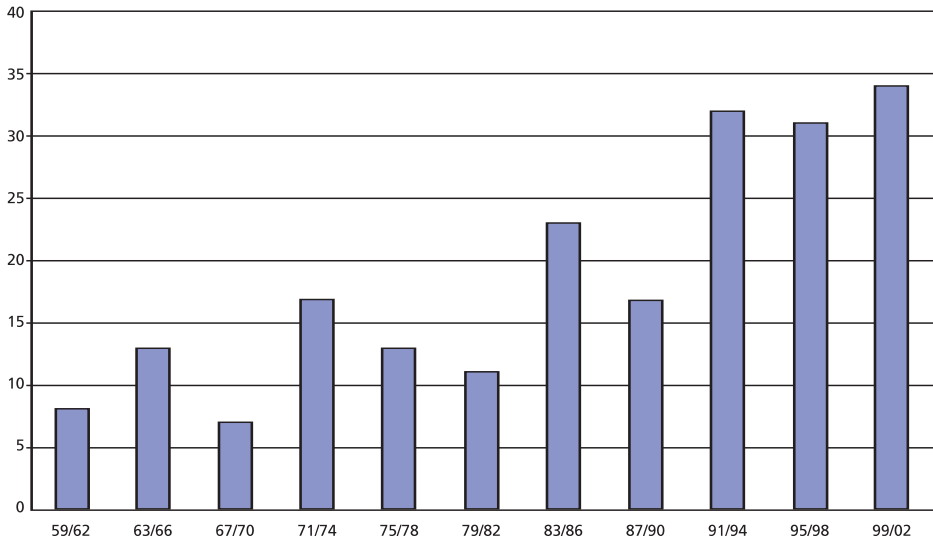


Fig. 5.6. Number of cases with precipitation larger than 100 mm.

It should be noted that cases as those documented in *figure 5.6* are the ones that lead to floods, particularly if the terrain favours surface runoff that concentrates the water in certain areas

Increased frequency of extreme rainfalls has been observed also in southern Brazil (Xavier et al. 1992 y 1994), especially in summertime. This seems part of a global trend, which on the other hand should be expected because of the increased concentration of the greenhouse gasses. This increment would lead to the warming of the low level troposphere favouring larger water vapour content and a vertical gradient more unstable as a consequence of the stratospheric cooling. Both changes, more vertical instability and greater water vapour content favours the development of the intense rainfall processes

## 5.4. Rainfall-streamflow relationships

The streamflow of the main rivers of the La Plata basin, and La Plata River itself, have strong interannual and interdecadal variability forced by the climatic variability (Robertson and Mechoso 1998; Camilloni and Barros 2000). Of particular interest for this chapter, is that trends in precipitation have given place to simultaneous trends in the river streamflows.

Streamflow variability of the La Plata basin rivers is addressed in the next chapter. However, in this section it will be discussed the relationship between the variability of precipitation and river streamflows in the La Plata basin. In particular it will be discussed the increase in the sum of the streamflows in the three tributaries of the La Plata River.

*Table 5.1* (from Berbery and Barros 2002) shows that percent changes in precipitation over the La Plata basin, upstream of Corrientes in the Paraná River and Paso de los Libres in the Uruguay River are amplified in respective changes in the streamflow. In the case studied, the sensitivity of streamflow to basin-averaged precipitation changes, expressed as elasticity (fractional change in streamflow per fractional change in precipitation) was about two, that is, for every one percent change in precipitation there was a two percent change in streamflow. Three cases (one case study and two “climatological” cases) corresponding to different time scale variability are presented in *table 5.1*. The first case is an example of extreme year-to-year variability of the hydrologic cycle focused in 1998 and 1999. The second case is a generalization of the first example, as it contrasts composites of El Niño

*Table 5.1. Basin averaged rainfall rates and river discharges of La Plata River corresponding to different timescale variability.*

	Rainfall rate ( $\text{m}^3 \text{s}^{-1}$ )	Streamflow ( $\text{m}^3 \text{s}^{-1}$ )	Evap+Infiltr ( $\text{m}^3 \text{s}^{-1}$ )
1998	107000	36600	70400
1999	81600	20440	61600
Difference	23%	44%	13%
El Niño	76000	25250	50750
La Niña	71000	21640	49360
Difference	7%	17%	3%
1951-1970	72000	19300	52700
1980-1999	83500	26000	56500
Difference	16%	35%	9%

and La Niña for 1951-1999. El Niño and La Niña periods until 1996 are defined following Trenberth (1997) and the Climate Diagnostics Centre afterwards. The third case assesses the changes in the hydrologic cycle between two 20-year periods (1951/1970 and 1980/1999) that are illustrative of a low frequency variability or trend. Precipitation for 1951-1990 was taken from the raingauge network, and CMAP was used for 1991-1999. The table also includes an estimate of evaporation plus infiltration rate, which was calculated as the difference between rainfall and streamflow.

*First case.* In 1997, an El Niño event begun and continued during the first part of 1998; it was accompanied by large streamflow in the Paraná River during 1998 (this happened in all El Niño cases that persisted into the Autumn of the following year). El Niño was followed by La Niña conditions during 1999, which were accompanied by negative rainfall anomalies over most of the basin, resulting in a precipitation difference of about 23% (Table 5.1). Changes in streamflow were also observed in association with the changes in precipitation. The mean streamflow of the Uruguay River at Paso de Los Libres in 1998 was 9533 m<sup>3</sup>/s and only 3305 m<sup>3</sup>/s in 1999 (about one third the value during 1998). The Paraná River at Corrientes registered, in those same years, mean flows of 27127 m<sup>3</sup>/s and 17137 m<sup>3</sup>/s respectively, which implies a difference of about 36%. The overall combined effect resulted in a 44% change of the La Plata River discharge.

*Second case.* The composite of El Niño events shows larger precipitation and streamflow than the composite of La Niña events (precipitation is 7% larger; streamfunction is 17% larger; evaporation and infiltration are the least affected, with changes of only 3%). Although the magnitude of the changes is smaller compared to the other cases, still the amplification of the streamflow signal is noticed. Notably, cold events (La Niña) are not associated with droughts or even with a significant reduction of the streamflow. The reason is that the reduced precipitation occurs toward the South of the basin and outside the areas that feed the streamflow of the main rivers (Grimm et al. 2000).

*Third case.* According to table 5.1, from 1951/1970 to 1981/1999, the precipitation increased by about 16%. As in the case of the year-to-year variability, the interdecadal variability of streamflow is also large (a 35% increase between 1951/1970 and 1981/1999). This increase is found in each of the major rivers: the Uruguay experienced an increase of 32%; the Paraná (excluding the contribution of the Paraguay River) had an increase of 31%; and finally the Paraguay's increase in river discharge was about 45%. The mean annual river flows of the two 20-year periods are believed to have little impact from the increment of the dams' storage, as changes in the evaporation rate over the basin are relatively small due to the comparatively limited surface of the reservoirs. On the other hand, since 1950 there was a considerable change in the use of land all over the considered basins, with a notorious increment of agriculture at the expense of natural vegetation (Tucci and

Clarke 1998). This aspect may have contributed to the observed streamflow changes in addition to the effect of rainfall variation. However, the amplification of the precipitation change in the streamflow in the first case, where a significant use of land change can be discarded and the persistence of approximately the same factor of amplification in the different time scales indicate that without dismissing a possible effect of the use of land change, the major part of the change in the streamflows between 1951/1970 and 1981/1999 was caused by the change in precipitation

As stated, in all cases the variability in precipitation is considerably amplified in the corresponding river streamflow. In any given year (or long period) a significant amount of the water precipitated over the basin is either evaporated or infiltrated in a way that does not runoff to the rivers. In the examples of *table 5.1*, the evaporated plus infiltrated fraction accounts approximately for 70% of the precipitated water, but this fraction is larger during relatively dry years and smaller during the rainy ones. On the other hand, although the streamflow accounts only for approximately 30% of the precipitated water, its interannual or interdecadal variability is larger (in absolute values) than the evaporation plus infiltrated water, and consequently, its relative variability is even larger. This implies that in the La Plata basin the balance between precipitation, streamflow, evaporation and infiltration are such that the interannual variability in precipitation is mostly translated to the river discharge while only a smaller fraction of it is converted in evaporation or infiltration (see also chapter 7).

The relative changes in streamflow in all examples are considerably large, about 17% as the average in the El Niño/La Niña composites, but as large as 44% for the 1998/1999 case, and 35% between the two 20-year periods. These relative changes are more impressive when they refer to the streamflow of one of the largest rivers of the world. At the same time, these examples show the great sensitivity of the streamflows of the major rivers within La Plata basin to the rainfall variability. This sensitivity transforms into vulnerability for the activities that depend on river water supply and become a matter of concern since during the last half of the past century, the region showed a great interannual and interdecadal variability in the precipitation that can be repeated in the future.

## 5.5. Summary

The rainfall positive trend in subtropical Argentina seems part of a global pattern found during the 20th Century. It has been stronger than in other parts of the world, and has been intensified in the last 30 to 40 years due to changes in the atmospheric circulation.

As a consequence of the increased precipitation in semiarid regions of Argentina, the agricultural frontier has been extended towards the West. By con-

trast, other regions suffer flooding more frequently, and in certain cases have been left permanently under water. This happens in regions of southern Santa Fe, West of Buenos Aires, and East of Corrientes.

Larger precipitation has been observed in Paraguay and Brazil, therefore the river discharges have also increased notably. Moreover, it has been found that increases in precipitation tend to be doubled in river discharge, so that by each 1% increase precipitation, the streamflow increases by 2% or more.

Positive trends in central and South-western portions of Argentina are related to neutral ENSO years, while in Paraguay and in a vast region around the triple frontier between this country, Brazil and Argentina the positive trends are mostly due to the El Niño phase.

The increase in the frequency of intense precipitations has become important since the late 1970s, but the trend has become even more marked after 1990, with the consequent damages to infrastructure, personal property and life.

The features of the precipitation trends of the last decades implies that the region is under the new climate conditions that need to be considered for the planning and administration of the water resources.

## References

- Barros, V. 2004: Segundo informe al proyecto de la Agenda Ambiental de Argentina, componente Cambio Climático. Fundación Torcuato Di Tella, 25 pp.
- \_\_\_\_\_ and M. Doyle 1996: Precipitation trends in Southern South America to the East of the Andes. Center for Ocean-Land-Atmosphere Studies. Report N° 26. Editors J. L. Kinter III and E. K. Schneider. pp. 76-80.
- \_\_\_\_\_, M. E. Castañeda and M. E. Doyle 2000a: Recent precipitation trends in Southern South America East of the Andes: an indication of climatic variability. Southern Hemisphere paleo- and neoclimates. Eds.:P. P. Smolka, W. Volkheimer. Springer-Verlag Berlin Heidelberg New York, 187-206.
- \_\_\_\_\_, M. González, B. Liebmann and I. Camilloni 2000b: Influence of the South Atlantic convergence zone and South Atlantic sea surface temperature on the interannual Summer rainfall variability in southern South America. *Theor. Appl. Climatol.*, 67, 123-183.
- Berbery, E. H. and V. R. Barros 2002: The hydrologic cycle of the La Plata basin in South America. *J. Hydrometeor.*, 3, 630-645.
- Camilloni, I. and V. Barros 2000: The Paraná river response to El Niño 1982-83 and 1997-1998 events. *J. Hydrometeor.*, 1, 412-430.
- Castañeda, M. E. and V. Barros 1994: Las tendencias de la precipitación en el cono Sur de America al este de los Andes. *Meteorológica*, 19(1-2), 23-32.
- and \_\_\_\_\_ 2001: Tendencias de la precipitación en el oeste de Argentina. *Meteorológica*, 26, 5-23.

- Collischonn, W., C. E. M. Tucci and R. T. Clarke 2001: Further evidence of changes in the hydrological regime of the River Paraguay: part of a wider phenomenon of climate change? *J. Hydrology*, 245, 218-238.
- Escobar, G., V. Barros and I. Camilloni 2003: Desplazamiento del anticiclón subtropical del Atlántico Sur y su relación con el cambio de vientos sobre el Estuario del Río de la Plata. X Congreso Latinoamericano e Ibérico de Meteorología. La Habana.
- Gillet, N., F. Zwiers, A. Weave and P. Scott 2003: Detection of human influence on sea-level pressure. *Letters to Nature*, 422, 292-294
- Giorgi, F. 2003: Variability and trends of sub-continental scale surface climate in the twentieth century. Part I: Observations. *Clim. Dyn.*, 18, 675-691.
- Grimm, A. M., V. Barros and M. Doyle 2000: Climate variability in southern South America associated with El Niño and La Niña events. *J. Climate*, 13, 35-58.
- Liebmann, B., C. Vera, L. Carvalho, I. Camilloni, V. Barros, M. Hoerling and D. Allured 2004: An Observed Trend in Central South American Precipitation. *J. Climate*, 17, 4357-4367.
- Robertson, A. W. and C. R. Mechoso 1998: Interannual and decadal cycles in river flows of southeastern South America. *J. Climate*, 11, 2570-2581.
- Rusticucci, M. and O. Penalba 1997: Relationship between monthly precipitation and warm/cold periods in Southern South America. Preprints: Fifth Int. Conf. on Southern Hem. Met. and Ocean., 298-299.
- Trenberth, K. E. 1997: The definition of El Niño. *Bull. Amer. Meteor. Soc.*, 78, 2771-2777.
- Tucci, C. E. M. and R. T. Clarke 1998: Environmental issues in the La Plata Basin. *Water Resources Development*, 14, 157-174.
- Xavier, T. M. B. S., M. A. F. Silva Dias and A. F. S. Xavier 1992: Tendências da Pluviometria na Grande São Paulo e a Influência dos Processos de Urbanização e Industrialização. *Anais, VII Congresso Brasileiro de Meteorologia*, 1, 220-224.
- \_\_\_\_\_, A. F. S. Xavier and M. A. F. Silva Dias 1994: Evolução da Precipitação Diária num Ambiente urbano: O Caso da Cidade de São Paulo. *Rev. Brasileira de Meteorologia*, 9, 44- 53.

#### **web addresses**

Intergovernmental Panel on Climate Change (IPCC): <http://www.ipcc.ch/>

Southern Oscillation Index (SOI):<http://www.cgd.ucar.edu/cas/catalog/climind/soi.html>

## HYDROLOGICAL TRENDS

*Ángel Menéndez<sup>1</sup>. Collaborator: Ernesto Hugo Berbery<sup>2</sup>*

<sup>1</sup> Instituto Nacional del Agua (INA). Universidad de Buenos Aires.

<sup>2</sup> Universidad de Maryland.

### ABSTRACT

The main hydrological trends observed in the La Plata basin are addressed through the analysis of the streamflows series of the main rivers, namely the Paraguay, Paraná y Uruguay, as well as of other important tributaries. Extreme hydrological events such as large discharges and extreme ebbs causing the major perturbations in the human and natural system are also analyzed. The relationship between precipitations and streamflow is also addressed. Finally, the relation between El Niño events and extreme hydrological extremes is discussed.

## 6.1. General considerations

Climate trends discussed in chapter 5 transform in even more pronounced hydrological trends. This implies that the hydrological regime cannot longer be consider stationary Data and cases that illustrate this situation are presented and analyzed in this chapter that was particularly noticeable in the last decades of the twentieth century.

## 6.2. River streamflows

In *figure 6.1* are shown the annual maximum, minimum and mean daily flows of the Paraná River in the section Paraná-Santa Fe for a period little longer than one century, namely 1902-2004 (for the last year are only available data until August at the moment of this writing), based on the data provided by Sistema de Información y Alerta Hidrológico del INA-Argentina (System of Information and Hydrological Alert of the INA-Argentina). The figure suggests that the 1970 decade constitutes a transition stage between two different states of relative statistical stability: one in the period 1902-1970 that will be denominated "old stage" and another one, the second, during the 1980 and 1990 decades (1980-2000) that will be called "modern stage". Additionally, it can be distinguished a behaviour a bit different in the first years of the present century that will be named "current situation" since it still cannot be assigned any statistical relevance.

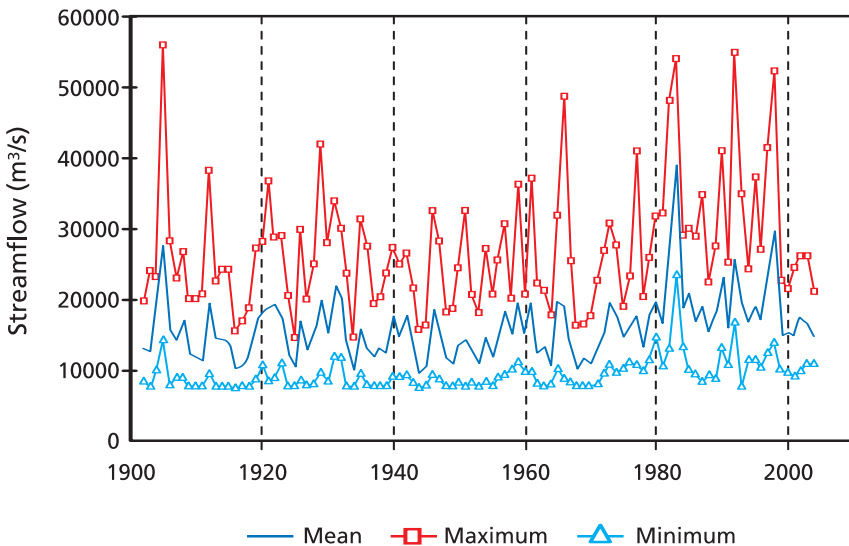


*Fig. 6.1.* Annual maximums, minimums and mean of the daily flows of the Paraná River in the section Paraná-Santa Fe for period 1902-2004.

Following are the observed changes:

- Mean flow in the modern stage is 37% superior to in the old stage.
- Annual maximums of the modern stage have also increased regarding the old one. Also, the frequency of extraordinary discharges has increased: Out of the 4 discharges with peak flows higher than 50.000 m<sup>3</sup>/s (1905, 1983, 1992, and 1998), 3 took place in the modern stage.
- Annual minimums also show an increment when passing from the old stage to the modern one.
- The current situation indicates a sequence of annual mean and maximum values smaller than those of the modern stage. In particular, mean values are similar to those of the 1970 decade (transition stage), the maximums to those of the old stage and the minimums to those of the modern stage.

The trend change from the 1970 decade was rigorously established by García and Vargas (1998), by means of statistical techniques, based on data of monthly mean flows in stations located upstream from Corrientes, analyzing the period 1901-1992. This was corroborated later by Jaime and Menéndez (2002) using monthly mean flows in the period 1931-2001 for the section Paraná-Santa Fe.

The increase of mean flows means that there is a larger runoff in the high basin of the Paraná, where precipitations that feed the river take place. This increase of the runoff should be bound to the increment of mean precipitations and to the change in the use of the land.

The increase in frequency of the large discharges indicates changes in the climatic conditions that favour the generation of extraordinary storms. The increase of minimum flows is strongly linked to the regulation imposed by the chain of Brazilian reservoirs developed since the 1960 decade.

The current situation is still uncertain in terms of determining if it is a new tendency change or if it simply responds to climatic variability matters. Eventually, the permanence of minimum levels similar to those of the modern stage confirms that it is due to the regulation imposed by the chain of reservoirs.

*Figures 6.2 and 6.3* show annual minimums and maximums of the Paraná River monthly mean flows, in the section Paraná-Santa Fe, and of the Uruguay River, in Concordia, for the period 1931-2001, based on the data provided by the Sistema de Información y Alerta Hidrológico del INA (System of Information and Alert Hydrological of the INA). Trends observed in the first one are, obviously, compatible with the ones discussed in relation to *figure 6.1*. For the Uruguay River (*Fig. 6.3*) the increase of mean flow is similar to the one of the Paraná (Jaime and Menéndez 2002); although due to the variability of its regime this tendency is less noticeable at first sight.

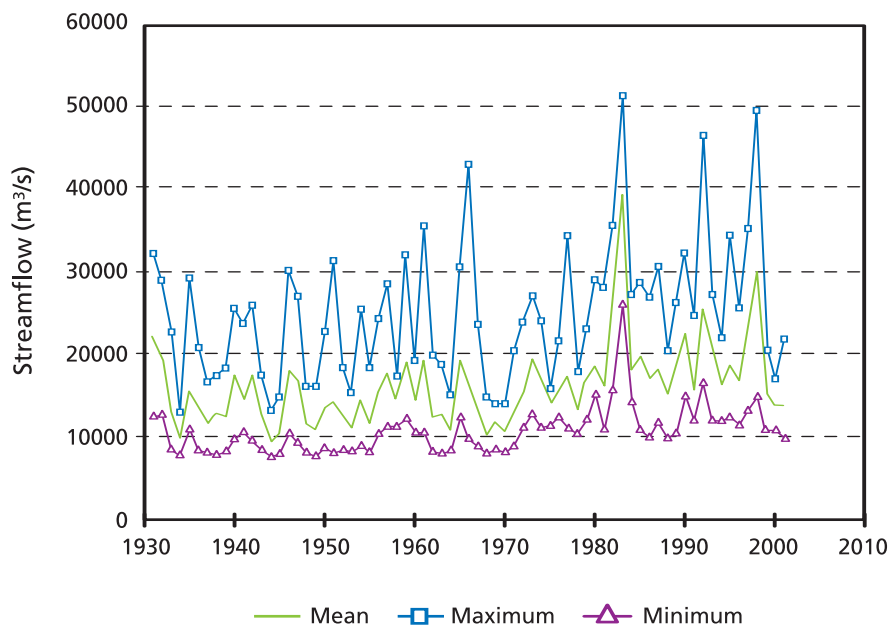


**Fig. 6.2.** Yearly maximums, minimums and mean of the mean monthly flows of the Paraná River in the section Paraná-Santa Fe for the period 1931-2001.

[Jaime and Menéndez 2002]

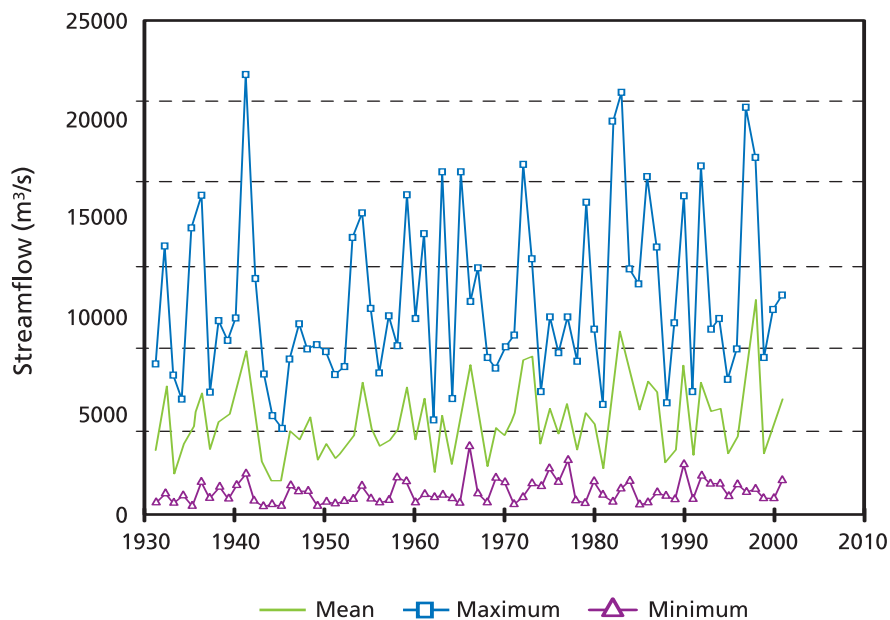


**Fig. 6.3.** Annual maximums, minimums and mean of the mean monthly flows of the Uruguay River in Concordia for the period 1931-2001.

[Jaime and Menéndez 2002]

In the case of the Paraná River the relative increase of mean minimum and maximum flows is similar to that of the mean flow, indicating an increase in the amplitude (that is, greater variability), while for the Uruguay River such amplitude has remained practically invariable (Jaime and Menéndez 2002).

Figure 6.4 shows the evolution of the monthly mean flows of the three main rivers of the basin, including the mean flow of the La Plata River, for most of twentieth century. From simple observation, the interannual and interdecadal variability of the streamflow is inferred. In particular, the increase observed in the second half of the century.

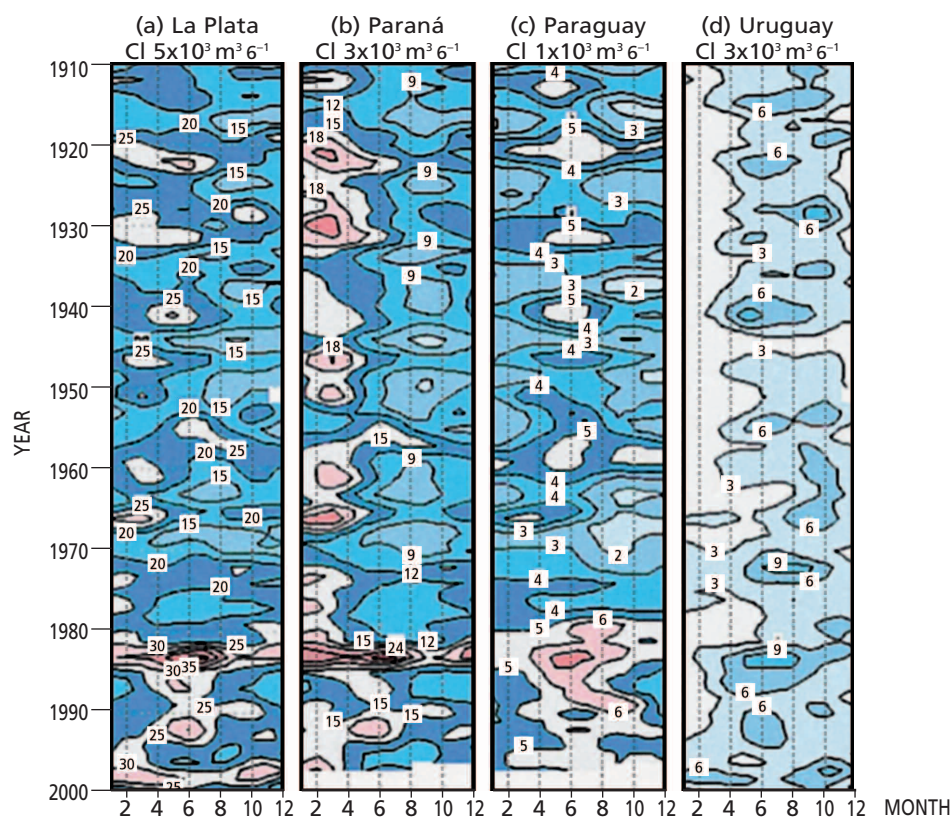
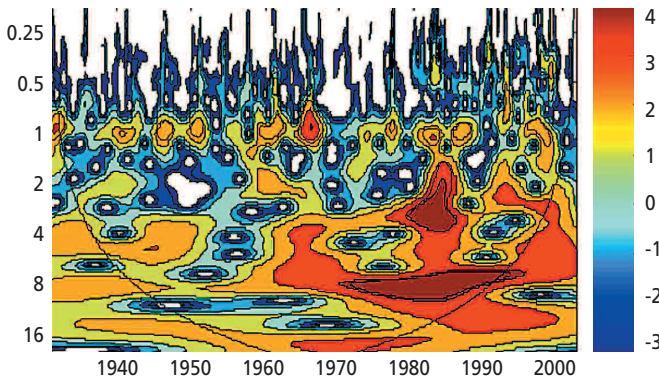


Fig. 6.4. Evolution of the mean monthly flows.

Figures 6.5 and 6.6 show the power spectra of the series of monthly mean flows of the Paraná and Uruguay rivers, respectively, obtained by means of the wavelet technique (Jaime and Menéndez 2002). The years of the period of analysis are shown in abscissas, and in the ordinate axes, the periods of the spectral components. The level curves represent a measure of the energy (amplitude) of those components. It is observed that in the Paraná river, the components of around 8-year

period from beginning of the 1970 decade have been noticeably activated; to a lesser extent have those around 4 years. Notice that 8 years are, exactly, the mean time among marked peaks (Fig. 6.2): 1966, 1977, 1983, 1992, and 1998. On the other hand, in the Uruguay River, only the components of around 4 years of period was enhanced, although less noticeable than in the Paraná River. It is interesting to note that these are periods compatible with those associated to El Niño phenomenon whose influence on the regime of precipitations of the region has already been repeatedly reported (see below).



**Fig. 6.5.** Wavelet power spectrum of the Paraná River for the period 1931-2001. [Jaime and Menéndez 2002].

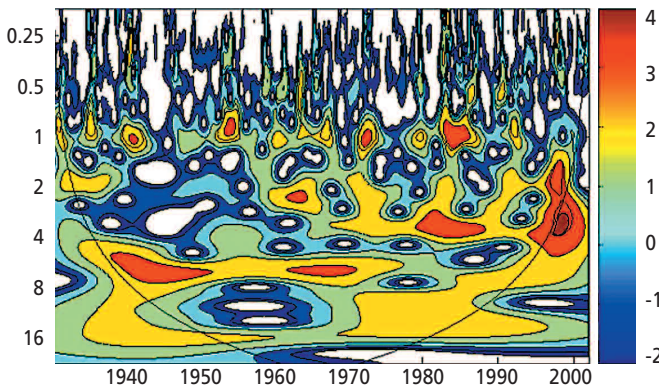


**Fig. 6.6.** Wavelet power spectrum of the Uruguay River for the period 1931-2001. [Jaime and Menéndez 2002].

In order to complete the scenario of streamflows trend changes in the La Plata basin, in *figure 6.7* it is presented the annual mean flow of other tributaries. In each case, the mean flow is indicated for the complete period with available information (red line) and the linear trend calculated starting from 1970 (green line), when there are available data. It is observed that the Bermejo, Paraguay, Iguazú, Paraná and Uruguay rivers show positive trends in their streamflow from 1970, while the Pilcomayo River presents a trend to higher annual flows between 1960 and 1990 and from there on, a negative trend.

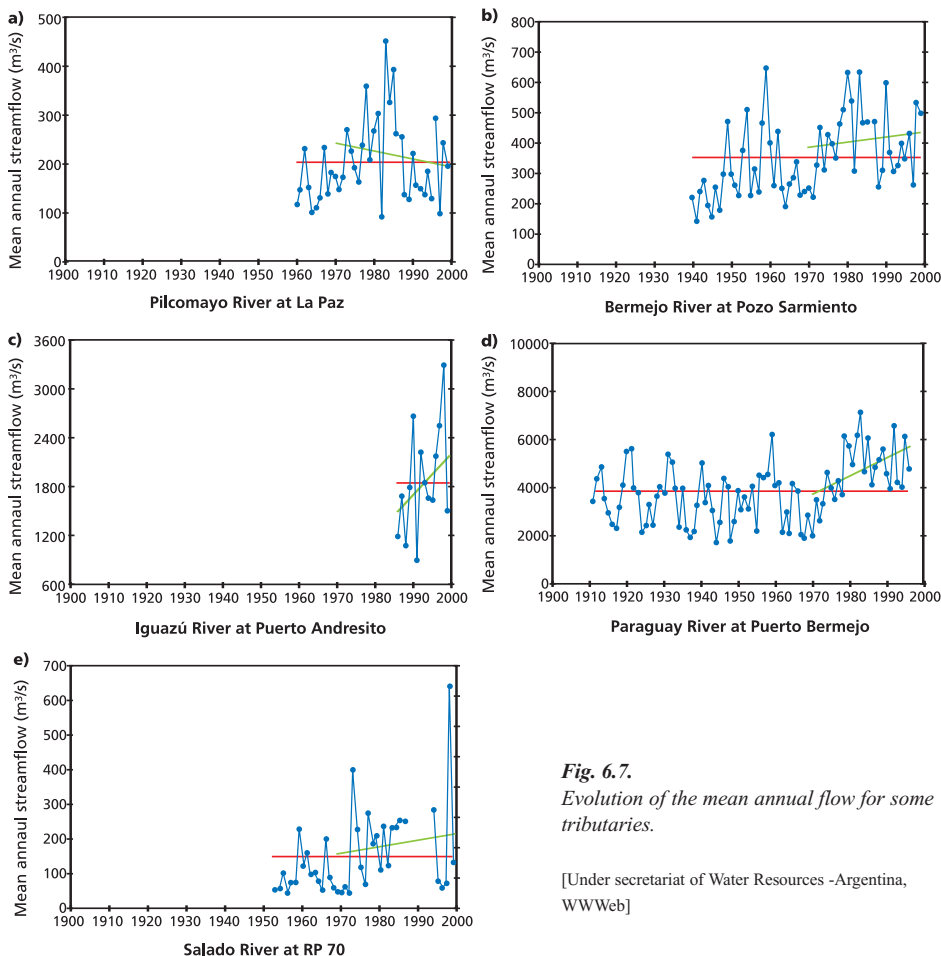


**Fig. 6.7.**  
 Evolution of the mean annual flow for some tributaries.

[Under secretariat of Water Resources -Argentina, WWWeb]

### 6.3. Extreme hydrological events (EHE)

Extreme hydrological events (EHE) in the La Plata basin are great phenomena that produce significant consequences on the surrounding areas of the water courses.

In order to illustrate the extraordinary effects of the great discharges, a series of images and pictures are presented. In *figure 6.8* is shown an image corresponding to the 1983 the Paraná River flood, which not only had the particularity of being one of the most intense of last century, but also the most long-lasting, what caused the Delta of the Paraná to lose its buffer capacity and get flooded almost up to its mouth (*Fig. 6.9*). *Figure 6.10* shows an image of the 1998 Paraná flood at its peak moment. Both floods were associated to intense El Niño phenomena (Mega Niño).

**Fig. 6.8.** Satellite image of the Paraná flood in March 1983.

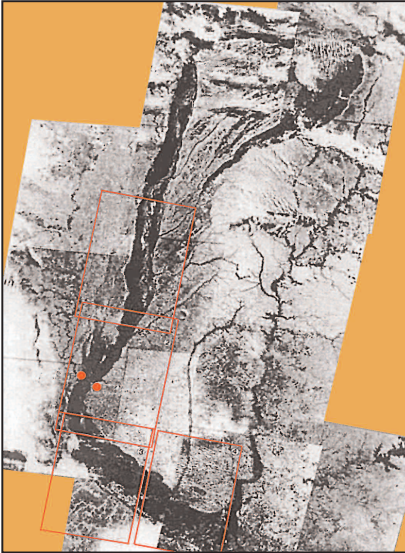
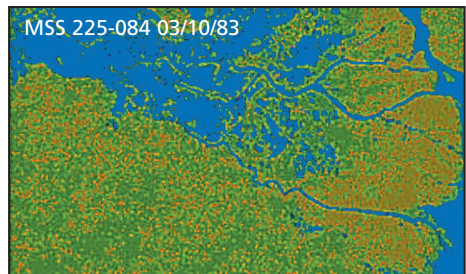
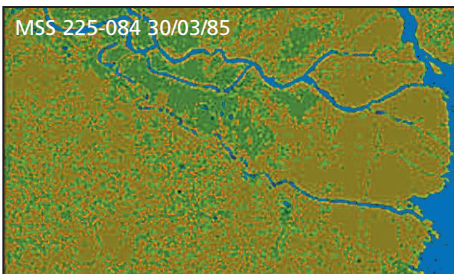
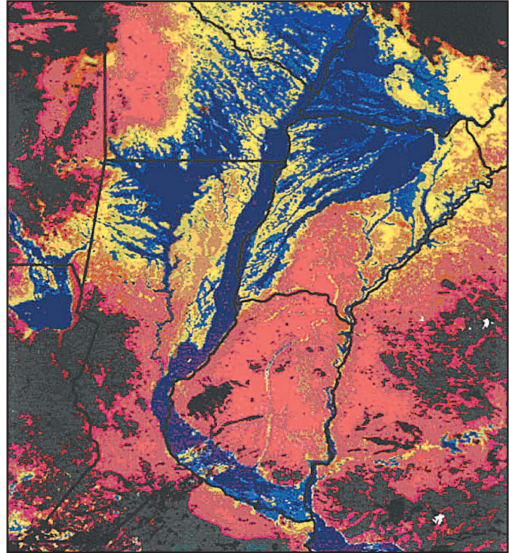


**Fig. 6.10.** Satellite image of the May 5, 1998 Paraná flood.



SATELLITE IMAGES

Water Wetlands

**Fig. 6.9.** General image of the 1983 flood in the Paraná Delta.

In *table 6.1* it is presented a list of the 10 largest discharges and ebbs of the Paraná River of the period 1902-2004, in function of their daily peak flow. It is observed that 80% of the maximums occur from 1966 on, while all the minimums were previous to 1950. In the Paraguay River, two thirds of the 16 largest discharge of the twenty century in Asunción took place during the last fourth of the century. This deviation toward the occurrence in the last fourth of the century is more evident the larger the considered discharges were, since out of the more intense 5, 4 were after 1975 (Barros et al. 2004). In the Uruguay River, out of the 16 larger daily peaks from 1950, none took place before 1970 and only 2 before 1975 (Camilloni and Caffera 2003). All this illustrates the noticeable impact that the regional climatic change has caused in the intensity and frequency of the floods in the flood valleys of the main rivers of the La Plata basin.

Rivers and plain lagoons with relatively small or narrow basins respond quickly to large precipitations concentrated on one or few days. In the case of the Salado del Norte River (Argentina), during April 2003 several days with intense precipitations occurred; in particular, in the days 23 and 24 at least two Mesoscale Convective Systems (MCS) produced more than 300 mm in less than two days in towns as distant as the north of Santa Fe and the east of Entre Ríos. This provoked the catastrophic flood of the city of Santa Fe. The MCS events have given place to frequent floods in the last two decades in the west, northwest and centre of the Province of Buenos Aires (Argentina), starting with that of 1982 and culminating with the October 2001 case. In the south of the Province of Santa Fe similar situations are seen, even with water transfers between basins, like it is the case of the significant flood of the Picasa lagoon. In Corrientes the system of lagoons and wetlands of Iberá grew notably in surface from the 1960 decade, causing big losses to the owners of the flooded fields. Recently, after a year of drought, the lagoons retreated considerably.

*Table 6.1* Ranking of annual extreme discharges and ebbs of the Paraná River based on its daily peak flow.

Major discharges		Ebbs	
Year	Flow (m <sup>3</sup> /s)	Year	Flow (m <sup>3</sup> /s)
1905	56025	1944	7703
1992	54925	1916	7756
1983	53992	1925	7765
1998	52308	1934	7765
1966	48602	1911	7774
1982	48025	1924	7783
1929	41964	1938	7783
1997	41570	1949	7783
1990	41048	1910	7792
1977	40918	1913	7801

*Table 6.1.* Ranking of annual extreme discharges and ebbs of the Paraná River based on its daily peak flow.

The most important floods in the Paraguayan territory happened during June 1997 (with an area flooded of 31400 ha). An event of similar happened during November 1998, flooding 29400 has. This covered a third of the total area of grassland and palm tree savannah in the vicinity of the Paraguay River (approximately 90000 has area). The extension of these habitats suggests that, in exceptional cases, all the area could be flooded. The flooded minimum area was in November 1999, with 6870 has. It is interesting to notice that only one month later (December 1999) the flooded area had almost increased 4 times, to 22600 has, which illustrates the speed of the changes in the local regime.

To characterize the intensity of the EHE of the Paraná and Uruguay rivers, Jaime and Menéndez (2002) established as criterion to take the excess (for floods) or defect (for ebbs) flow (monthly mean) with respect to of each of floods waters and ebbs thresholds, respectively. To define these thresholds an analysis of frequency of occurrence of extreme events was made and were chosen those corresponding to a 4 year recurrence, representative of El Niño's periodicity. But the three hydrological periods identified by García and Vargas (1998) were distinguished: mean up to 1943, dry up to 1970 and humid up to 2001, so thresholds values are different for each one of them. These values are shown in *table 6.2* (Jaime and Menéndez 2002).

*Table 6.2* Thresholds of floods and ebbs events for Paraná and Uruguay rivers in  $m^3/s$  (Jaime and Menéndez 2002).

**Table 6.2.** Thresholds of floods and ebbs events for Paraná and Uruguay rivers in  $m^3/s$

Río	Umbral	1931-43	1944-70	1970-2001
Paraná	Floods	27800	28500	32000
Paraná	Ebbs	8200	8250	11000
Uruguay	Floods	13700	12000	17300
Uruguay	Ebbs	600	600	850

[Jaime and Menéndez 2002]

*Figures 6.11* and *6.12* show the results for the Paraná and Uruguay rivers, respectively, identifying the month of occurrence. For the Paraná River (*Fig. 6.11*) it is observed that from 1970 on, not only larger floods have occurred, but also relatively more intense ebbs. This indicates an increase of the variability mentioned in the previous section. For this period, the intensity of the larger floods of the Paraná River were between 15 and 20 thousand  $m^3/s$  while that of the ebbs were between 500 and 1000  $m^3/s$ , with a singular negative peak of 2000  $m^3/s$  in December 1971.

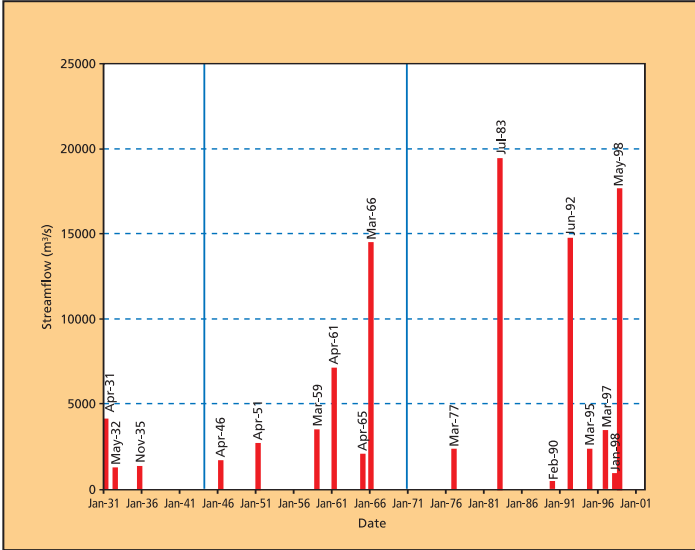


**Fig. 6.11.**  
Intensity of the EHE for the Paraná River in the period 1931-2001, (a) floods, (b) ebbs.

[Jaime and Menéndez 2002]

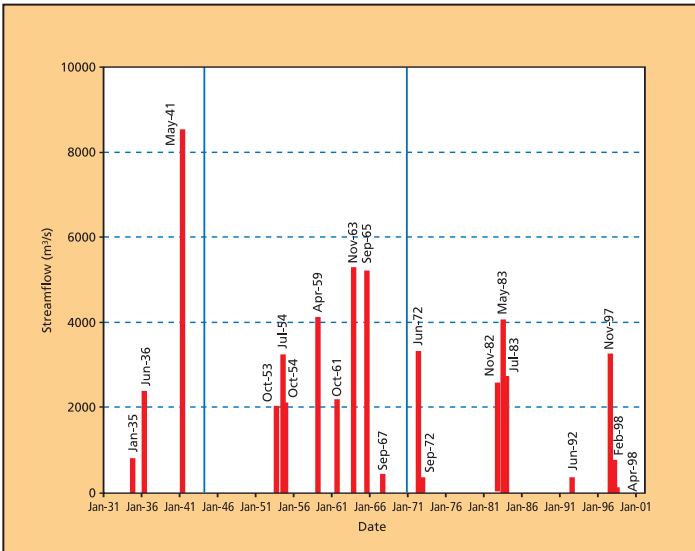


**Fig. 6.12.**  
Intensity of the EHE for the Uruguay River in the period 1931-2001, (a) floods, (b) ebbs.

[Jaime and Menéndez 2002]

On the other hand, in the case of the Uruguay River (Fig. 6.12), there are not so significant variations in the intensity of the EHE. Except for the peak of May 1941, that surpassed 8000 m<sup>3</sup>/s, the intensity of the largest discharges is within the range from 3000 to 5000 m<sup>3</sup>/s, being even observed a light decrease for the period after 1970 with respect to those of 1950-1970. The most intense ebbs of the period after 1970 do show a remarkable increase regarding the immediately previous period, although with similar values to the ones registered until around 1950. The range of intensity of the current ebbs is in the range from 200 to 300 m<sup>3</sup>/s, with a peak like in the Paraná River in December 1971 that reached more than 350 m<sup>3</sup>/s.

#### **6.4. Relationship between precipitations and EHE**

Camilloni and Barros (2003) studied the relationship between the precipitations and extreme discharges of the Paraná River. They determined that the extreme peaks at Corrientes usually originate in the central and south areas of the High Paraná River basin, especially in the central area. Also, they established that the contribution of the north area of the high basin of the Paraná is not only generally small, but rather, sometimes negative.

A similar study for the Uruguay River was carried out by Camilloni and Caffera (2003). Daily extreme flows during the warm season are related to intense rains in the upper basin, particularly in the period from 9 to 12 days before the maximum of flow takes place in Salto Grande. On the other hand, the daily extreme flows during the cold season are due mostly to intensive rains over and close upstream of Santo Grande in two separate periods: from 9 to 12 and from 1 to 4 days before the date of the flow peak at the Salto Grande station. From these results, it comes out that floods at the lower Uruguay River can be predicted by hydrological forecasts during warm season, while meteorological forecasts are needed for the cold season.

An interesting additional result of the study of Camilloni and Caffera (2003) is that around 50% of largest discharges of the Uruguay River can be the result of the precipitation increment due to the convergence of fluxes of humidity in the region of the South America Low Level Jet (SALLJ). Also, they observe that the frequency of occurrence of the SALLJ causing large discharges is slightly higher in the cold season than in the warm one.

For the Paraguay River, Barros et al. (2004) found that the origin of largest discharge peaks are in the high and middle Paraguay River basin, and that its occurrence doesn't depend on the volume of water stored in the Pantanal. Additionally, they verified that the contribution of the Pantanal does not correlate considerably with the contribution of the high and middle basins. They explain that the situation is different for annual ordinary discharges, since the annual peak of June takes place because the slow contribution of the Pantanal, loaded with the precipitations of the Summer, on top of the contribution of the high and middle basins of the Paraguay River caused by the Autumn precipitations. Besides, the decrease of flow from June to February is due, in Winter, to the small precipitation and, in Spring and Summer, to the great evaporation.

#### **6.5. Relation between El Niño and EHE**

In the work by Camilloni and Barros (2003) about the Paraná River is shown that two thirds of the major monthly peaks (and of the largest contributions from

the central area of the high basin of the Paraná) happened during El Niño events, and that none happened during the La Niña phase. Those maximum peaks took place in Spring 0 (0 indicates the onset year of El Niño event) or in Autumn + (+ indicates the year following the onset of El Niño event). The largest peaks took place during the Autumn +, when SST anomalies in El Niño 3 persisted until May +. Also, whenever the anomalies in El Niño 3 persisted until Autumn +, there were important discharges in the Paraná River. The third remaining part of the maximum peaks happened during the Spring or the Summer of neutral periods.

In the case of the Uruguay River, Camilloni and Caffera (2003) explain that its basin is part of a region with a strong precipitation signal during the ENSO warm phase, when in general, the largest monthly discharges take place, associated most of the times to extreme daily peaks. They establish that the most intense anomalies in monthly discharges happen mostly during El Niño's warm phases that seem to induce extensive positive rainfall anomalies in the region.

Barros et al. (2004) show that two third of the maximum peaks of the Paraguay River in Asunción occur during the ENSO warm phase, and that El Niño's signal is particularly clear for the peaks that happen during Autumn +. The third remaining part of the maximum peaks happens indistinctly during La Niña or neutral phases. In these cases an average consistent meteorological pattern in the south Pacific is observed from April until August that, eventually, would allow a precipitation forecast.

## **References**

- Barros, V., L. Chamorro, G. Coronel and J. Baez 2004: The major discharge events in the Paraguay River: Magnitudes, source regions, and climate forcings. *J Hydrometeorology* 2004 Vol 5, 1061-1070
- Camilloni, I.A. and V. R. Barros 2003: Extreme discharge events in the Paraná River and their climate forcing. *J. of Hydrology*, 278, 94-106.
- \_\_\_\_\_ and R. M. Caffera 2003: The largest floods in the Uruguay river and their climate forcing, enviado al *J. of Hydrometeor.*
- García, N. and W. Vargas 1998: The temporal climatic variability en the Río de la Plata basin displayed by the river discharges, *Climate Change*, 38, 359-379.
- Jaime, P. and A. N. Menéndez 2002: Análisis del Régimen Hidrológico de los Ríos Paraná y Uruguay, Informe INA-LHA 05-216-02, Comitente: Proyecto Freplata.
- Subsecretaría de Recursos Hídricos-Argentina. WWWeb.  
[www.mecon.gov.ar/hidricos/mapashidricos/mapageneral.htm](http://www.mecon.gov.ar/hidricos/mapashidricos/mapageneral.htm)

## REAL EVAPORATION TRENDS

*Julián Báez<sup>1</sup>*

<sup>1</sup> Servicio Meteorológico, Paraguay.

### ABSTRACT

Trends of real evapotranspiration (ETR) in the center and west of the La Plata basin were estimated using a simple model of water balance. For this study, three regions were identified, West of Argentina and Paraguay with stations Santiago del Estero and Mariscal Estigarribia; the region along the Paraguay River and the Argentine Litoral with data from stations at Puerto Casado, Concepción, Asunción, Santa Fe and Junín; and Eastern Paraguay with stations at Encarnación and Ciudad del Este. Monthly ETR was calculated from the potential evapotranspiration (ETP), obtained from the Thornthwaite's approach, precipitation (P) and water soil capacity (W) that was assumed constant at 100 mm.

The annual precipitation and ETR trends are positive in all the localities analyzed, while this is also true for annual temperature, except in Mariscal Estigarribia, Paraguay, where its trend is negative. The greater trend in ETR is found in Mariscal Estigarribia with 6 mm/ year, followed by Ciudad del Este, also in Paraguay, con 4.32 mm/ year. The lower trends in the ETR are in Concepción, Paraguay con 0.41 mm/ year and Junín, Argentina, with 0.83 mm/ year. With the exception of Mariscal Estigarribia, in the West of Paraguay, it seems that the greater trends in the ETR were in the East of Paraguay and in the Argentine Litoral.

The precipitation and ETR trends seem almost similar all over the West of the La Plata basin and in the North of Paraguay. In the rest of the analyzed region, since precipitation considerably exceeds ETP, the trends of ETR are lower than those of precipitation, giving place to trends of the same sign as in precipitation in the runoff and consequently in the streamflows.

## 7.1. Introduction

Several authors, Barros and Doyle (1996); Barros, Castañeda and Doyle (2000a) and more recently Liebmann et al. (2004) have shown a clear positive trend of the rainfall in the La Plata basin, especially in its central region that includes the West and North-East of Argentina, Paraguay and South of Brazil. This rainfall increase must directly influence the water balance of the basin, for what it is to be expected an increase in the runoff and to a lesser degree in the real evapotranspiration (RET), see chapter 5.

In the United States, Walter et al. (2004) found positive trends of the real evapotranspiration in most of the country. They employed precipitation information and assuming that the balance among rainfall, runoff and evapotranspiración dominates the water balance in the soil at annual time scale.

Assuming that the other terms of hydric balance, such as the underground losses and the net storage are void or very small for one year or longer time scales, then a single model that relates rainfall, the potential evapotranspiration and the water storage in the soil can be applied in order to calculate the actual evapotranspiration.

This chapter shows the results of the analysis of the actual evaporation calculated with observed data of rainfall and temperatures of nine meteorological stations of Argentina and Paraguay, using the serial hydric balance simplified model.

## 7.2. Data

Data used for the analysis correspond to daily series of rainfall and maximum and minimum temperatures of 6 (six) meteorological stations of Paraguay and 3 (three) stations of Argentina, whose details are shown in *table 7.1*.

## 7.3. Methodology

The methodology used for the RET calculation is based on a single model of hydric balance of the soil that relates monthly rainfall, monthly potential evapotranspiration (PET) and the field capacity of the soil. The model determines the monthly PET for Thornthwaite's method (Thornthwaite 1948) which uses as input information, the monthly mean temperature (resulting from the average of the maximum and minimum temperatures) and the local latitude.

This model of the water balance assumes the following simplifications:

- a. Neither the lateral nor the vertical movements of water are considered;
- b. Precipitation is the only input;
- c. The stock of water in the soil for a one month period is fully available for the following month, with no regards of the amount.

**Table 7.1.** Stations and data periods.

Nº	Station	Southern latitude	West longitude	Record period
1	Mariscal Estigarribia	22° 02'	60° 37'	1968-1999
2	Puerto Casado	22° 17'	57° 56'	1964-1999
3	Concepción	23° 25'	57° 18'	1960-1999
4	Asunción	25° 15'	57° 31'	1960-1999
5	Ciudad del Este	25° 32'	54° 36'	1966-1999
6	Encarnación	27° 20'	55° 50'	1951-1999
7	Santiago del Estero	64° 18'	27° 46'	1965-2001
8	Santa Fe	31° 36'	60° 42'	1960-2001
9	Junín	34° 33'	60° 55'	1959-2001

**Fig. 7.1.** Geographic location of the stations.

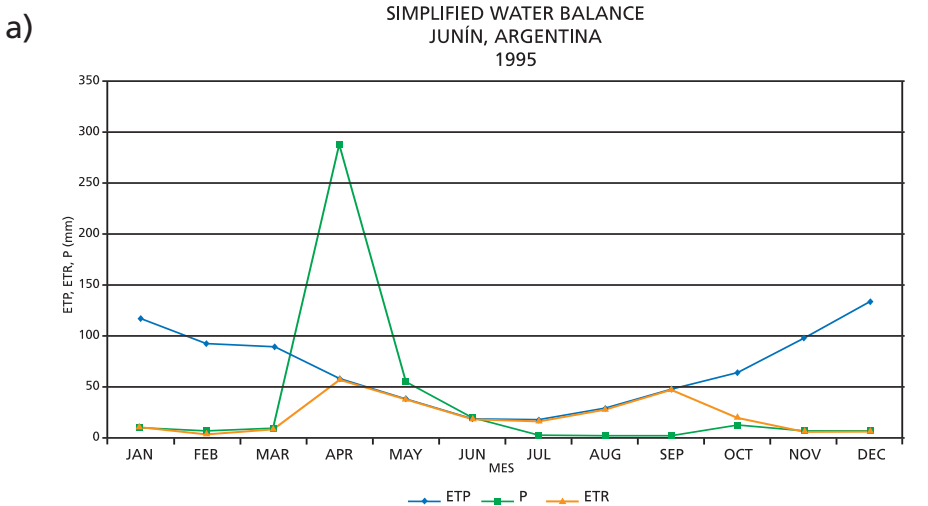
The water balance model calculates the RET and losses or gains of water in the soil, in a serial manner for every month since the beginning of the data series. Input data are monthly precipitation and potential evapotranspiration (PET). Although it is a strong simplification, the maximum water capacity ( $W$ ) was assumed at 100 mm for the whole region.

Depending on the Precipitation ( $P$ ) and the Potential Evapotranspiration (PET) values, two situations are considered:

a)  $PET > P_i$ ; then the water “availability” is estimated as  $P_i + W_{i-1}$ . If the water availability is enough,  $RET_i = PET_i$ . If not,  $RET_i = P_i + W_{i-1}$  and the difference  $RET_i - PET_i$  is saved as a deficit. In this case, either the atmosphere or the vegetable cover can only spend what entered as precipitation plus the quantity that they can take from the soil, which had been stored before. This can happen only up to the moment when the humidity content in the soil turns to zero. Once arrived this point, the  $RET_i$  acquires the precipitation value for that month and the difference  $RET_i - ETP_i$  is saved as the new deficit.

b)  $PET < P_i$ ; in this case there is water enough, so the  $RET_i$  acquires the  $PET$  value for that month, and the difference between the precipitation and  $RET (P - ETR_i)$  will storage in the soil adding to the former value:  $W_i = W_{i-1} + (P - RET_i)$ . This happens up to the moment when the soil humidity content reaches its maximum value, which in this case was defined as 100 mm. Once arrived that moment, the difference  $P - RET_i$  is saved as an excess.

Figure 7.2 shows an example of the application of this methodology for one particular year.



b)

	JAN	FEB	MAR	APR	MAY	JUN	JUL	AUG	SEP	OCT	NOV	DEC	ANNUAL
Corr ETP	116,5	92,5	89,9	57,4	38,8	19,3	18,2	28,5	47,6	63,6	97,5	134	803,8
P	9,3	5,4	9,4	287,3	55	19,4	2,3	0,5	1,2	11,1	6,2	6,9	414,0
ETR	9,3	5,4	9,4	57,4	38,8	19,3	18,2	28,5	47,6	20,8	6,2	6,9	267,8
Deficit	107,2	87,1	80,5	0,0	0,0	0,0	0,0	0,0	0,0	42,8	91,3	127,1	536,0
Storage	0	0,0	0,0	100,0	100,0	100,0	84,1	56,1	9,7	0,0	0,0	0,0	
Runoff	0,0	0,0	0,0	129,9	16,2	0,1	0,0	0,0	0,0	0,0	0,0	0,0	146,2

Fig. 7.2. (a) Example of the results of the model of water balance for a particular year at Junín, Argentina and (b) numeric results.

## 7.4. Results

Interannual RET results are presented for the period of available data. Figures of annual temperature RET and precipitation along with linear trends are shown in the following sub-sections. Results are organized in three geographical areas: West of Argentina and Paraguay; Paraguay River and littoral of Argentina and East of Paraguay.

### 7.4.1. West of Argentina and Paraguay

This is the region of the La Plata basin, west of the Paraguay- Paraná axes where the runoff is very small and the contributions to the larger rivers are the lowest of the whole basin. In this region the positive trend of the precipitation and of the RET is more evident than in the mean annual temperature. In the case of the Santiago del Estero location, Argentina, the mean temperature trend is of just  $0.017^{\circ}\text{C}/\text{year}$ , while both the rainfall and the RET trend is of the order of  $2\text{ mm}/\text{year}$ , see *figure 7.3 (a, b, c)*.

On the other hand, at Mariscal Estigarribia, Paraguay, the mean temperature trend is slightly negative, of the order of  $-0.015^{\circ}\text{C}/\text{year}$ , being the only analyzed location with negative trend. Notwithstanding, precipitation and RET have very high linear trend values,  $10.7\text{ mm}/\text{year}$  and  $6\text{ mm}/\text{year}$ , respectively.

In this semiarid region, where precipitation barely overpasses the RET (PET is most of the time larger than both, precipitation and RET), an increase in rainfall produces similar increases in the RET. Although this may not be true for each year because of temperature fluctuations, it is however confirmed in the long-term trends.

### 7.4.2. Río Paraguay and Littoral of Argentina

These localities are in the central axes of the La Plata basin, more precisely over the Paraguay and Paraná rivers, with the exception of Junín that however is at the same western longitude.

In the localities of Northern Paraguay, in the high basin of the Paraguay River and in the southern part of the Pantanal basin, there are positive trends in the mean temperature, both in Puerto Casado and in Concepción. Trends in the RET are also positive in both localities, although with a larger magnitude in Puerto Casado, with values of the order of  $3\text{ mm}/\text{year}$  as compared with the  $0.4\text{ mm}/\text{year}$  in Concepción. The precipitation trends have the same order of magnitude than the RET of both localities.

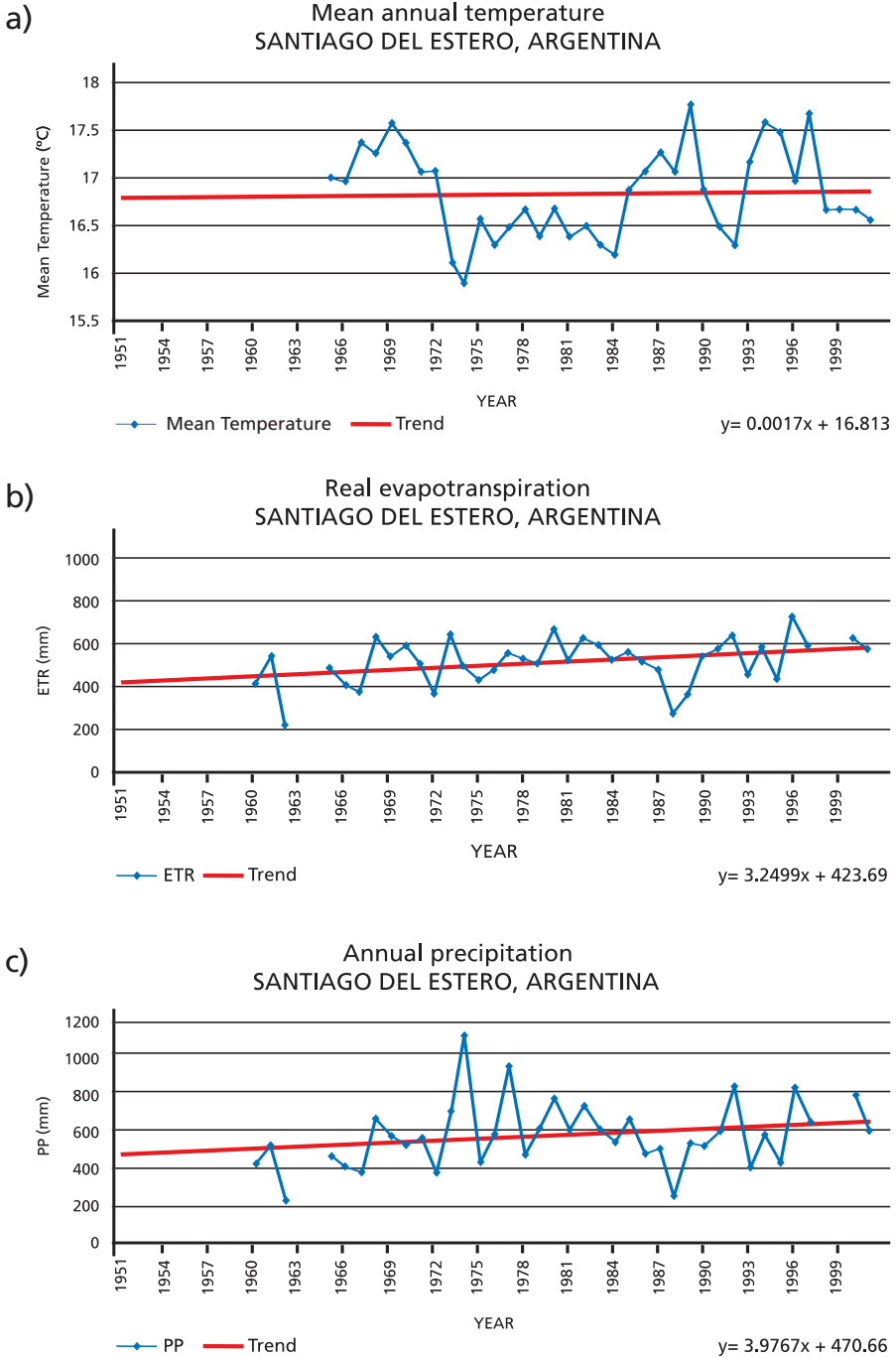


**Fig. 7.3.** (a) Trend of the mean annual temperature of Santiago del Estero, Argentina; (b) Idem of ETR; (c) Idem of precipitation.

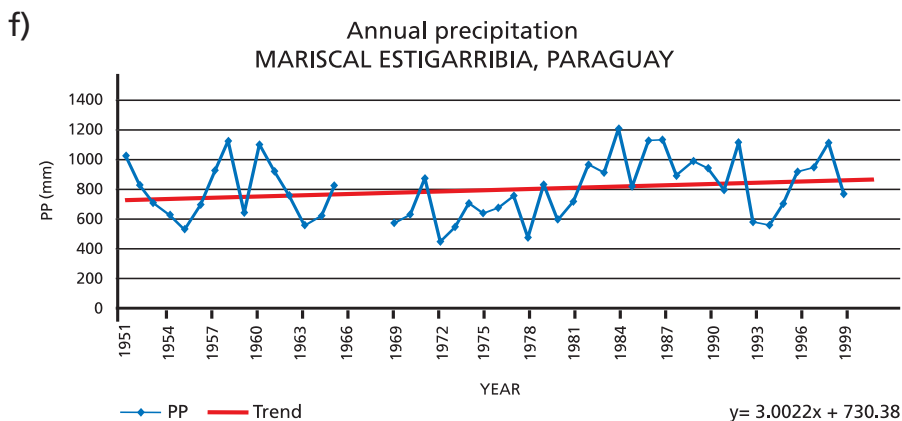
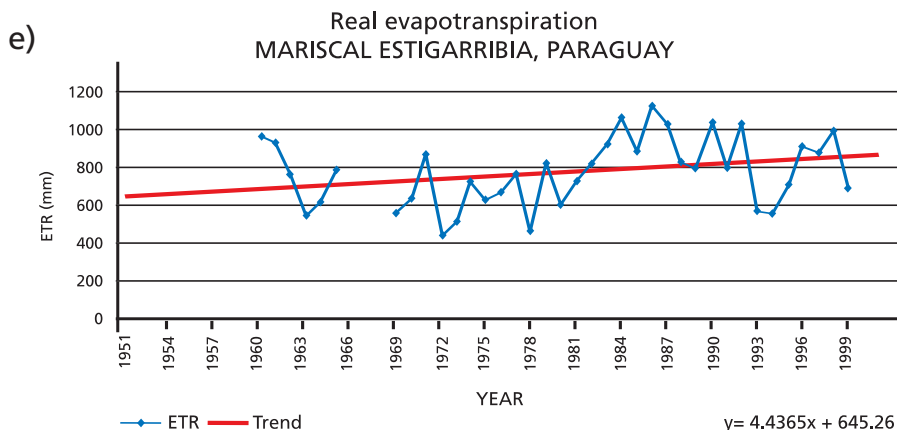
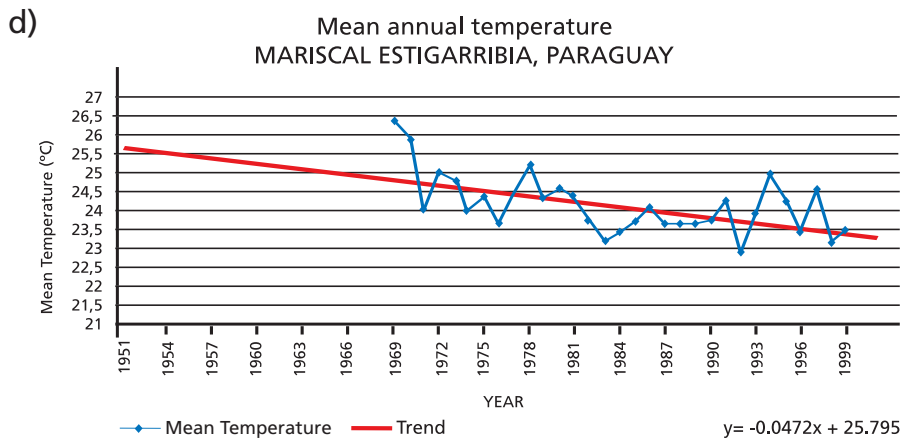


Fig. 7.3. (d) as a) for Mariscal Estigarribia; (e) Idem of ETR y (f) Idem of precipitation.

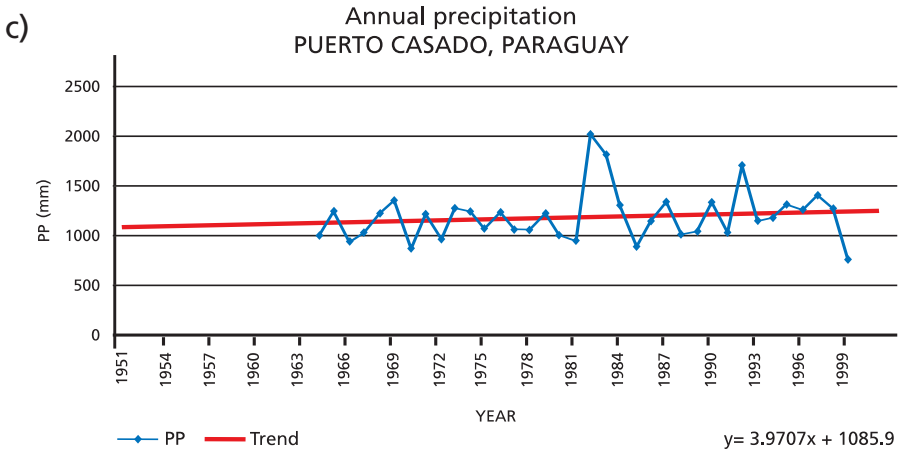
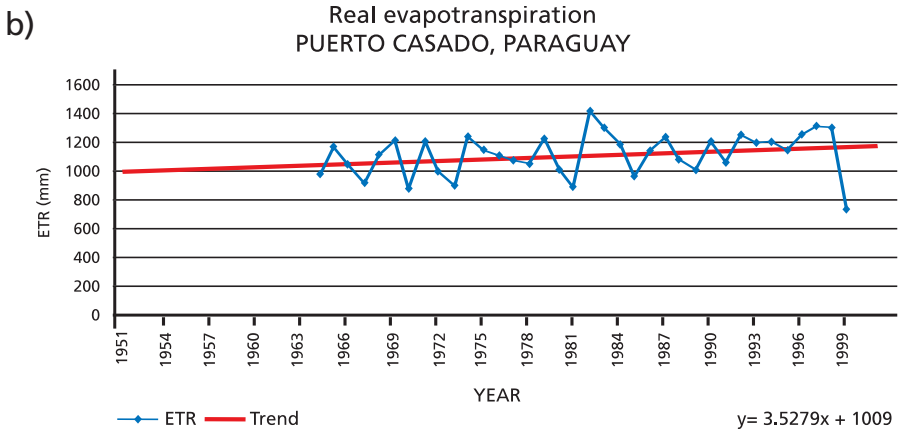
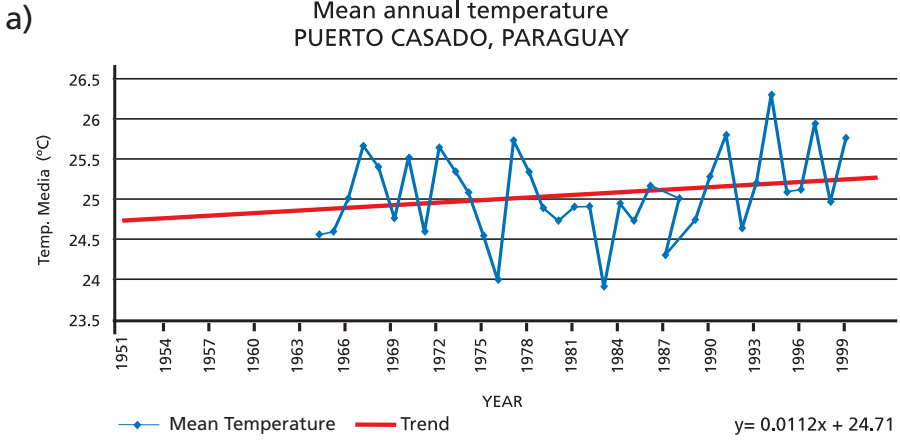


Fig. 7.4 (a, b, c). As Fig. 7.3 but for Puerto Casado and Concepción, in Paraguay.

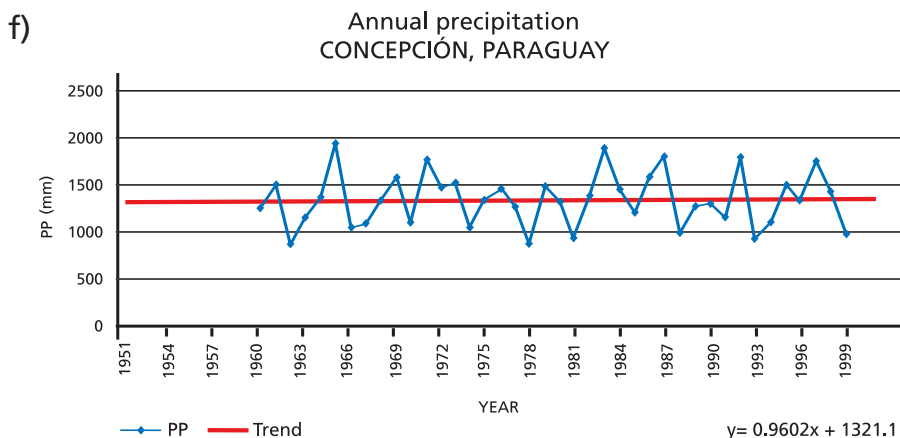
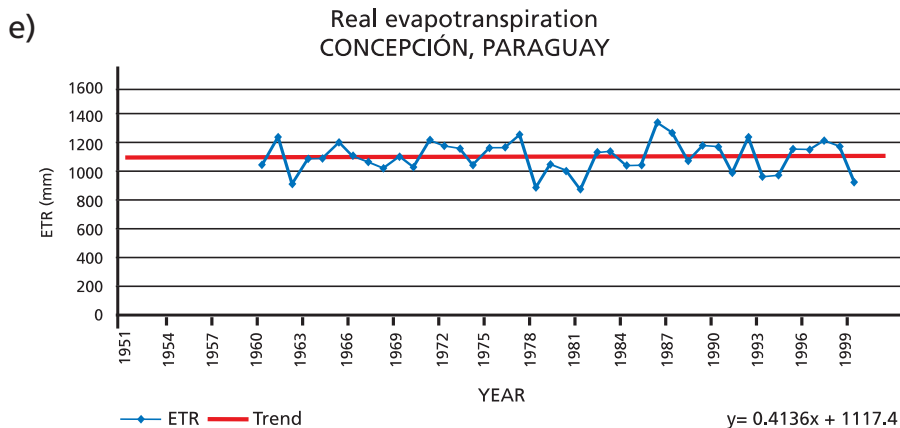
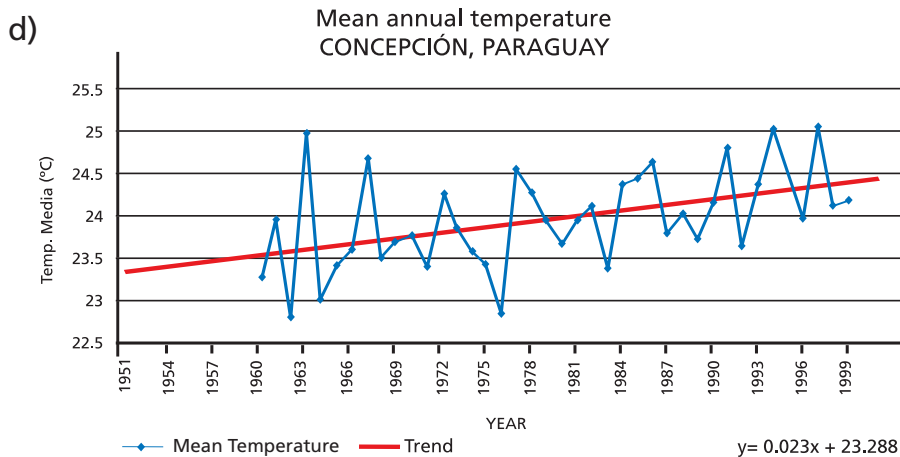


Fig. 7.4 (d, e, f). As Fig. 7.3 but for Puerto Casado and Concepción, in Paraguay.

The positive trends of the mean temperature in Asunción, Paraguay and Santa Fe, Argentina, are of the same order of magnitude,  $0.01^{\circ}\text{C}/\text{year}$ . Positive trends are also observed in the RET and the precipitation of both localities. The RET trend in Asunción has a magnitude of  $2.6 \text{ mm}/\text{year}$ , while in Santa Fe is  $2.1 \text{ mm}/\text{year}$ . The precipitation trends for both localities also have a higher magnitude, between 4 and  $5 \text{ mm}/\text{year}$ . These trends can be visualized in more detail in *figure 7.5*.

The Argentina locality of Junín shows a mean temperature trend of the order of  $0.01^{\circ}\text{C}$ , while the RET trend is only  $0.8 \text{ mm}/\text{year}$ , being one of the lower positive trend among the analyzed localities. Precipitation, though, presents a  $3.9 \text{ mm}/\text{year}$  positive trend, comparable to Santa Fe.

In the north of the central fringe of the basin, namely in Puerto Casado and Concepción, though precipitation is more abundant than in the western region, temperature is very high because of the low latitude. Consequently, the RET is quite close to precipitation. Therefore, as in the western region, trends in precipitation are similar to those of the RET. This situation changes towards the South, where as the temperature decreases, the RET is a considerable lower fraction of the rainfall, and precipitation trends only reflects partially in the RET trends, thus giving rise to greater excesses and eventually larger runoffs.

#### 7.4.3. East of Paraguay

The cities of Encarnación and Ciudad del Este, Paraguay, are located in the basin of the Paraná River, where important precipitation positive trends have been found (Liebmann et al. 2004) that were also verified with the trends of the Paraná River and of its tributaries streamflows (Berbery and Barros 2002). Temperature, RET and precipitation trends are positive in both localities. However, the magnitude of the temperature trend in Encarnación is very low, of the order of  $0.005^{\circ}\text{C}/\text{year}$ , while in Ciudad del Este is  $0.04^{\circ}\text{C}/\text{year}$ .

Regarding the ETR the difference in the magnitude of the trends is of the order of 100%. Thus, while in Encarnación the ETR has a trend of  $2.5 \text{ mm}/\text{year}$ , in Ciudad del Este is of  $4.3 \text{ mm}/\text{year}$ . The precipitation trend shows very different values. In Encarnación it is of  $4.9 \text{ mm}/\text{year}$ , when in Ciudad del Este reaches  $12.2 \text{ mm}/\text{year}$ .

The hydrological conditions in this region are such that there is a considerable excess of precipitation over evaporation, which implies that trends in the first one, considerably exceeds those of the second, since evaporation is in general not restricted by the lack of water in the soil. Thus, the positive trends in the precipitation are converted in larger runoffs and streamflows, as it was observed.

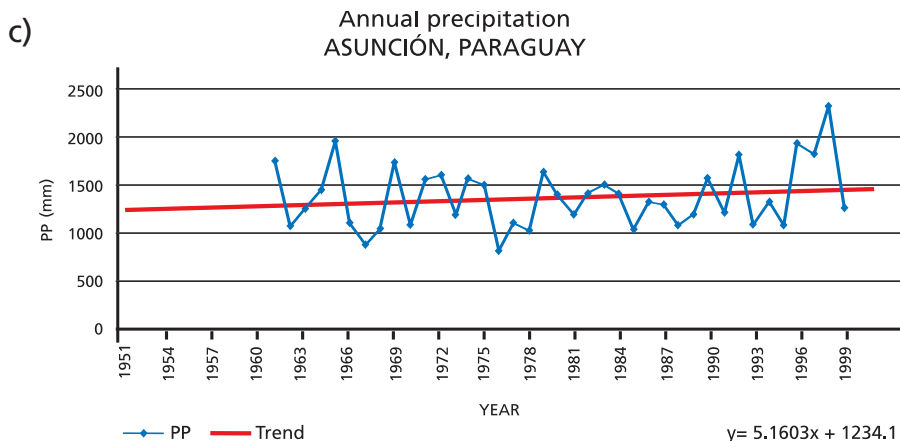
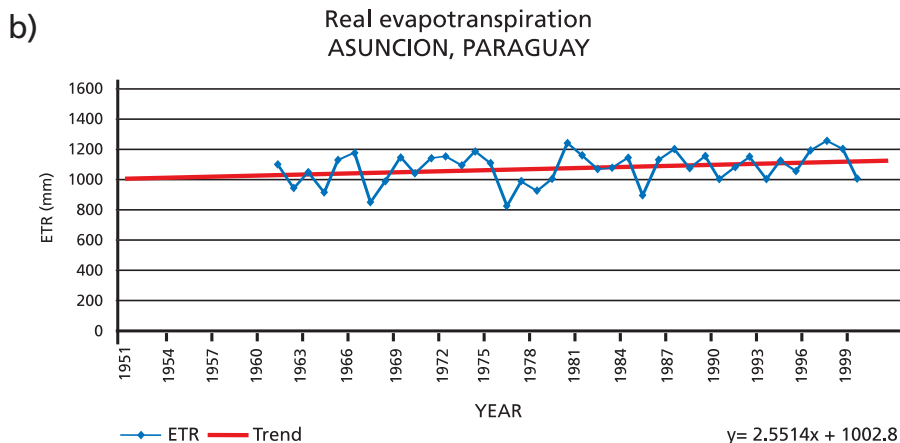
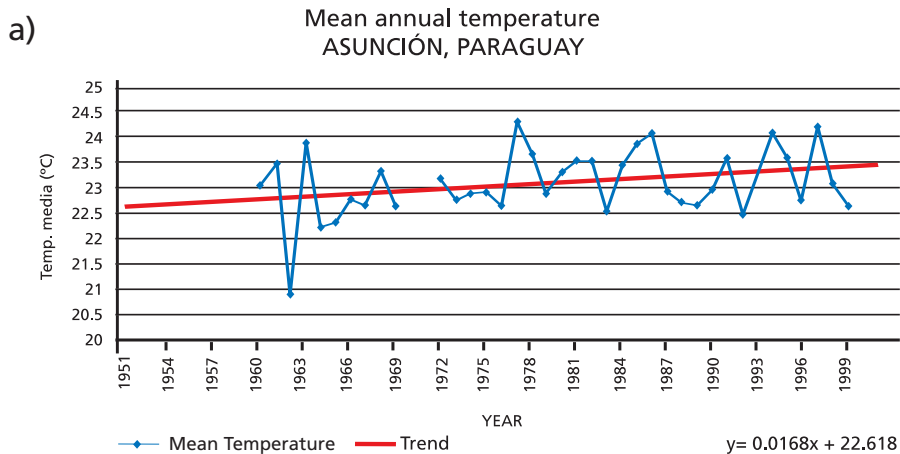


Fig. 7.5 (a, b, c). As Fig. 7.3 but for Asunción, Paraguay and Santa Fe and Junín, Argentina.

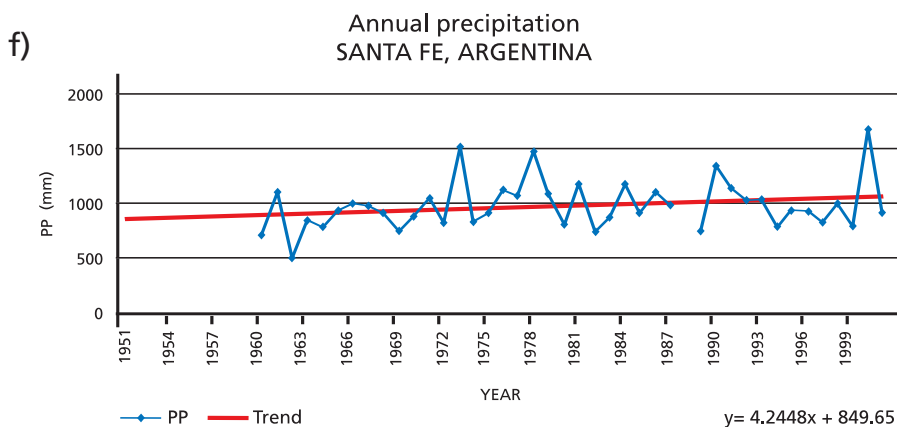
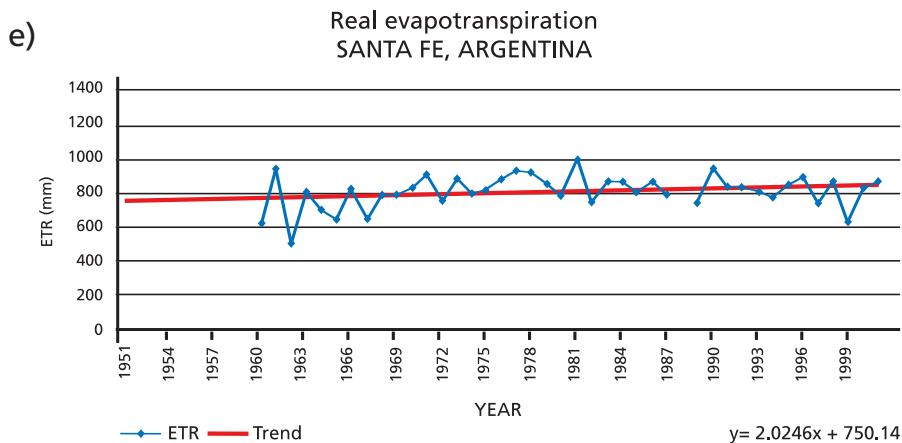
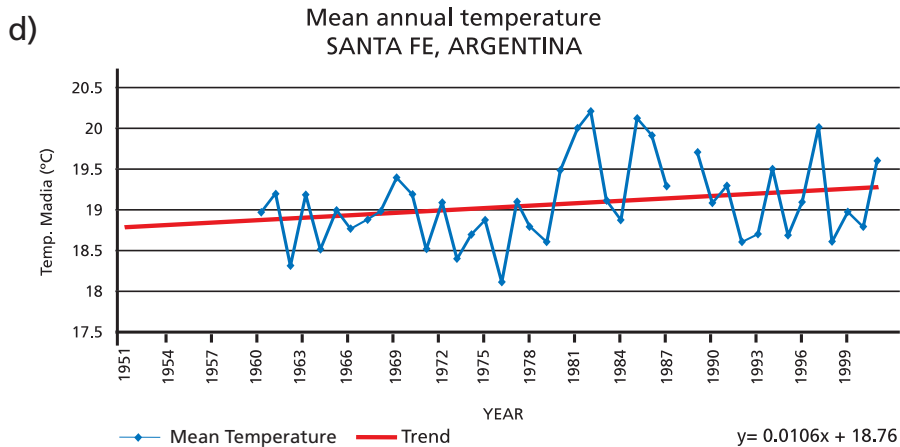


Fig. 7.5 (d, e, f). As Fig. 7.3 but for Asunción, Paraguay and Santa Fe and Junín, Argentina.

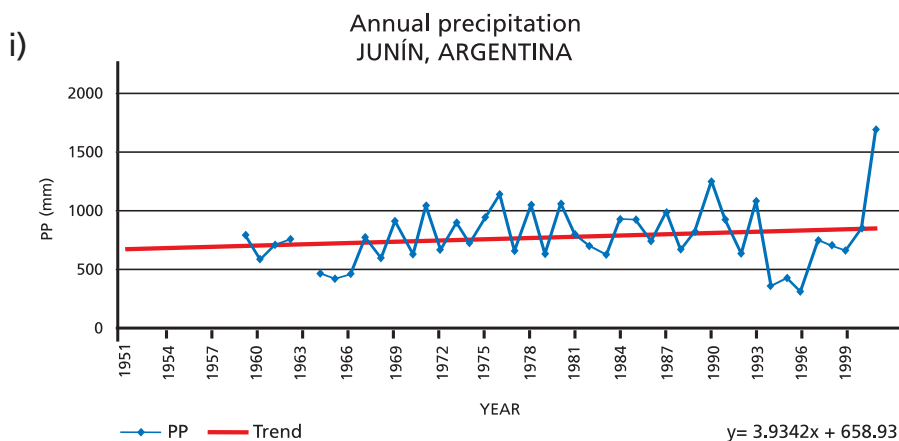
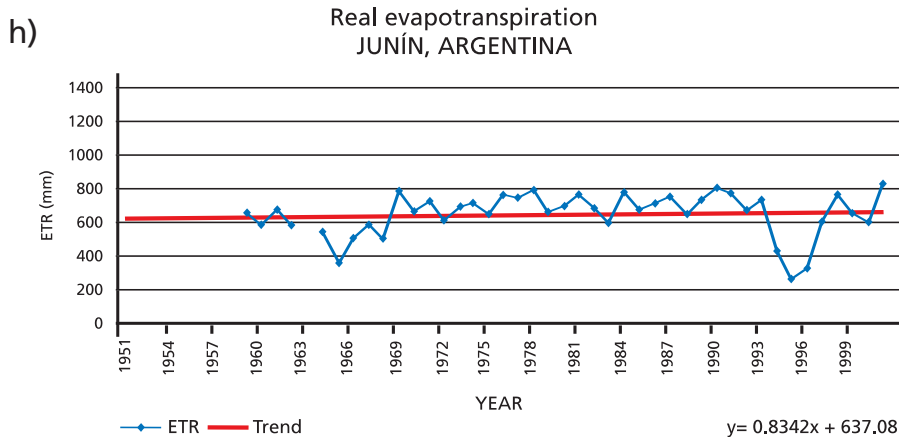
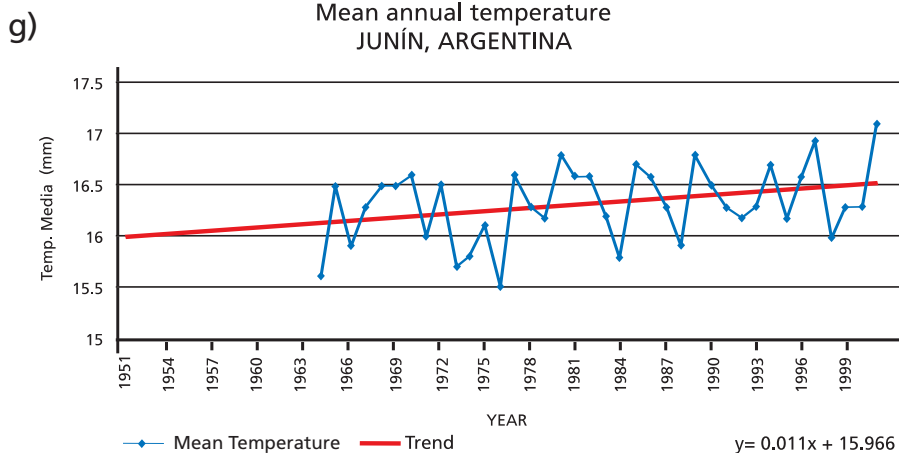


Fig. 7.5 (g, h, i). As Fig. 7.3 but for Asunción, Paraguay and Santa Fe and Junín, Argentina.

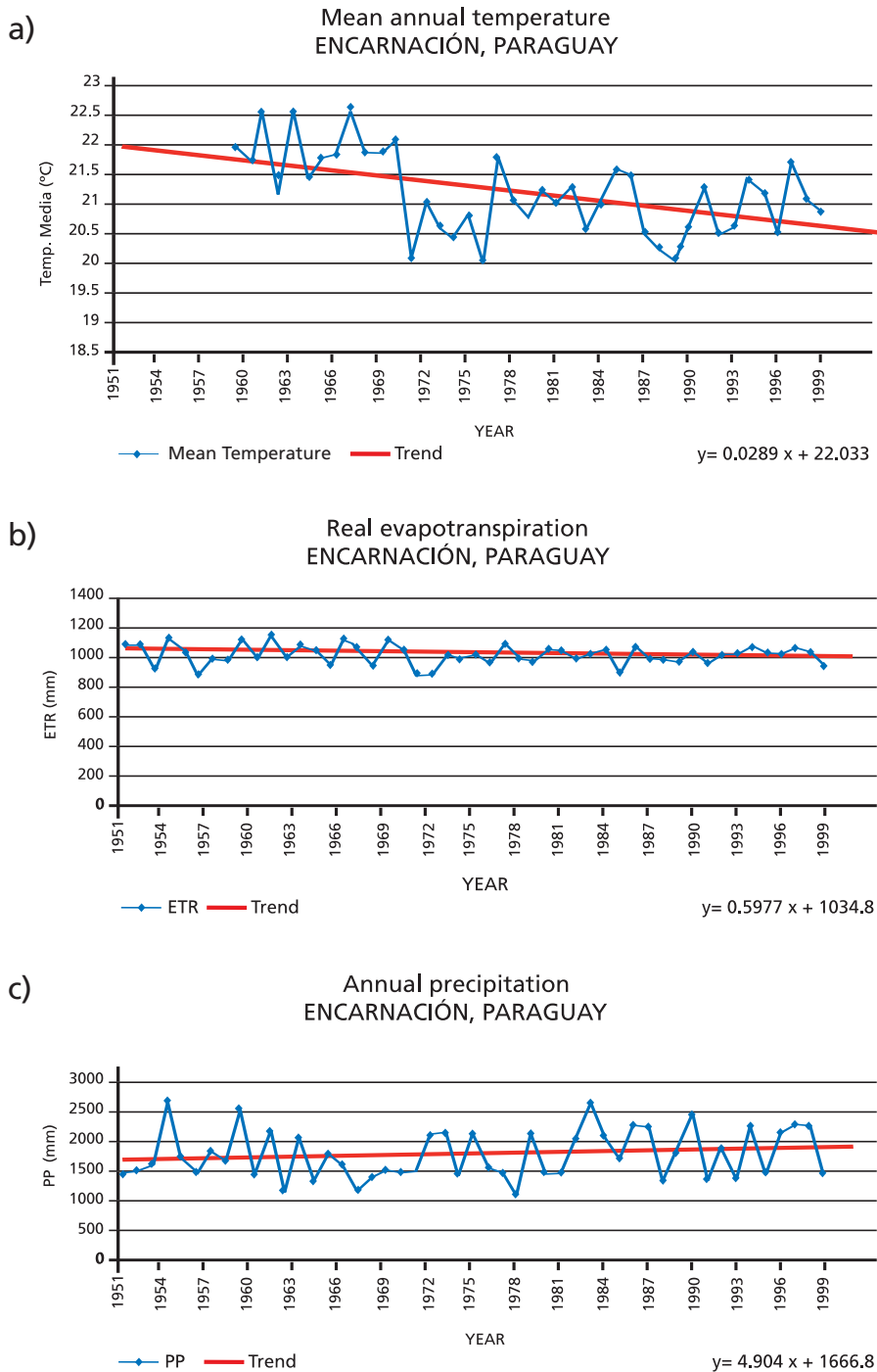


Fig. 7.6 (a, b, c). As Fig. 7.3, but for Encarnación and Ciudad del Este, Paraguay.

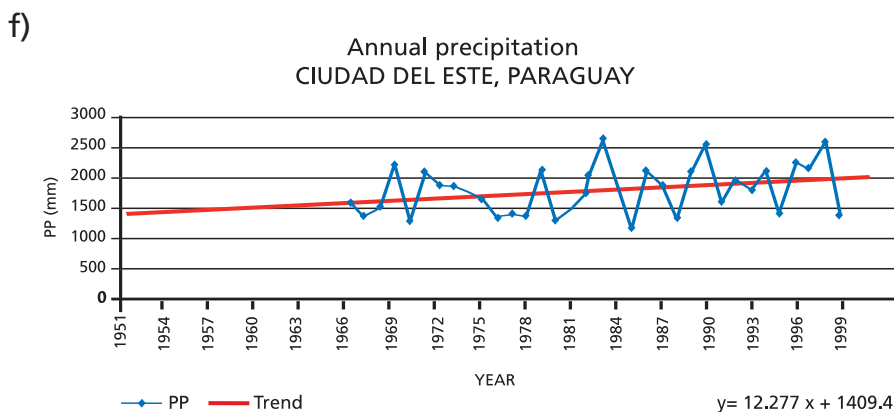
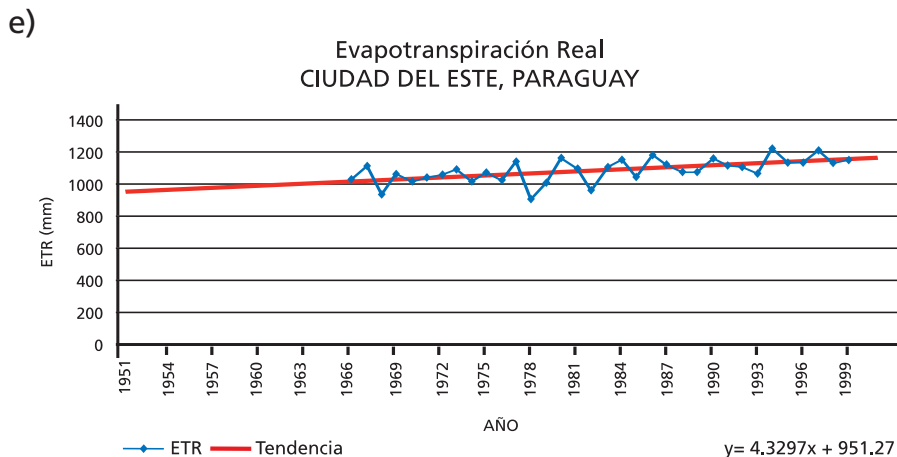
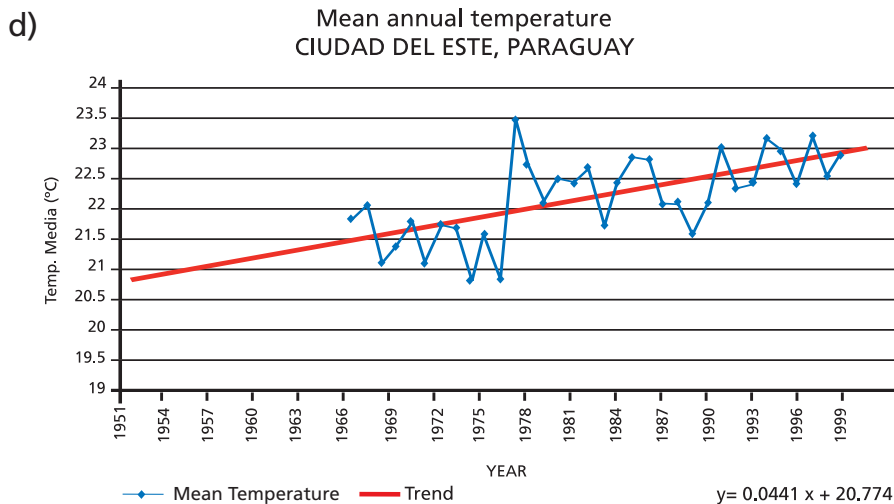


Fig. 7.6 (d, e, f). As Fig. 7.3, but for Encarnación and Ciudad del Este, Paraguay.

## 7.5. Discussion and final comments

This methodology has several limitations, especially associated with the PET calculation and the assumption that the soil has a uniform field capacity of 100 mm. Besides, the RET is punctual (for each station) and not regional. Even with this limitation, the large features of the balance between precipitation and ETR can be assessed. Most of the series studied show positive trends in the RET with values that range from 2 to 6 mm/year, and only the localities of Junín, Argentina and Concepción in Paraguay, has positive trends lower than 1 mm/year, *Table 7.2*.

*Table 7.2. Summary of Temperature, ETR and Precipitation trends.*

N°	Station	Trends		
		Temperature °C/year	ETR mm/year	Precipitation mm/year
1	Mariscal Estigarribia	-0.015	6.00	10.71
2	Puerto Casado	0.011	3.52	3.97
3	Concepción	0.023	0.41	0.96
4	Asunción	0.016	2.55	5.16
5	Ciudad del Este	0.044	4.32	12.27
6	Encarnación	0.005	2.51	4.59
7	Santiago del Estero	0.001	2.24	2.08
8	Santa Fe	0.010	2.14	4.45
9	Junín	0.011	0.83	3.93

The larger magnitudes of the ETR trends are observed in Ciudad del Este and Mariscal Estigarribia, Paraguay, in that order.

In general terms, trends in precipitation and RET seem almost similar in the West of the basin and in the North of Paraguay. In the rest of the La Plata basin, as the precipitation considerable exceeds the RET, trends in the last one seems to be smaller than those of precipitation, thus, given rise to streamflows trends.

## References

- Barros, V. and M. Doyle 1996: Precipitation trends in Southern South America to the east of the Andes. Center for Ocean-Land-Atmosphere Studies. Report N° 26. Editors J. L. Kinter III and E. K. Schneider. pp. 76-80
- \_\_\_\_\_, M. E. Castañeda and M. E. Doyle 2000a: Recent precipitation trends in Southern South America east of the Andes: an indication of climatic variability. Southern Hemisphere paleo - and neoclimates. Eds.: P. P. Smolka, W. Volkheimer. Springer-Verlag Berlin Heidelberg New York, 187-206.

- Berbery, E. H. and V. R. Barros 2002: The hydrologic cycle of the La Plata basin in South America. *J. Hydrometeor.*, 3, 630-645.
- Liebmann, B., C. Vera, L. Carvalho, I. Camilloni, V. Barros, M. Hoerling and D. Allured 2004: An Observed Trend in Central South American Precipitation. *J. Climate*, 17, 4357-4367.
- Thornthwaite, C. W. 1948: An approach toward a rational classification of climate. *Geographical Review*, 38, 55-94.
- Walter, M. T., D. Wilks, Y. Parlange and R. Shneider 2004: Increasing Evapotranspiration from the Conterminous United States. *J. Hydrometeor.*, 5, 405-408.

## THE MAIN SERVICES AND PROBLEMS OF WATER RESOURCES

*Lucas Chamorro<sup>1</sup>*

<sup>1</sup> Universidad de Asunción, Paraguay.

### ABSTRACT

The water, as resource, is already under pressure in certain zones of the La Plata Basin as a consequence of the growing demand. The main problems of the basin are discussed, that is, the floods and the vulnerability of some ecosystems, particularly wetlands. It is also examined the provision of drinking water and the urban drainage, the agricultural use and the hydropower generation. The regional dependence of the hydropower is discussed as well as some aspects of the large dams. It is discussed what climatic changes associated to global change can affect negatively the availability of the water resources, damaging different sectors as the provision of drinking water, the generation of energy and the river transportation.

## **8.1. Introduction**

According to long term scenarios, tropical region would be the most affected by Climatic Change. Likewise, developing countries will be the most affected due to their scarce financial resources, deficient markets and the predominance of farming activities among other factors.

In the La Plata basin, the water resource is already under the pressure in certain zones and sectors as a result of the increasing demand. It might happen that climatic changes associated to global change could affect negatively water resources availability, affecting different sectors such as drinkable water supply, energy generation and fluvial navigation.

People in the La Plata basin suffer the impact of adverse weather and its physical consequences (riverside floods, sudden and localized floods, intense precipitation, landslides, alluviums, droughts, waves of cold and hot weather, etc.) They are also affected by indirect effects through the impact to other sector, such as water supply, energy distribution, transport, agriculture, sanitary services, etc. Thresholds beyond which impacts increase rapidly are unique for each local situation and depend on the degree of adaptation response (systems and procedure for monitoring and alert, as well as procedures for traffic enrouting, flexible welfare systems, emergency systems, etc. (IPCC 1996, SIE GT II, Section 12.2.)). The above mentioned impacts become generally more severe when they add to an unhealthy environment, lack of water supply or sewage service, restricted access to transport, to communications and to a decent habitat. Some precarious settlements around big cities, have many hundreds of thousands persons living these negative conditions for public health, which are enhanced by extreme climate situations.

Climatic Change can affect human activities in many ways. Economical sector can be affected by changes in their productive capacity (for instance, in farming, cattle rising or fishing) or by changes in the market demand of the goods and services they produce. The importance of this impact will depend on the sector being rural -which in general means that depends on one or two resources- or urban, in which case, in general, not always, there is a wider set of alternative resources. Climatic effects will also depend on the adaptation capacity of the affected sector.

Some aspects of physical infrastructure, including energy distribution and transmission, buildings, urban services, transport systems and specific industries such as agro industries, tourism and construction can be directly affected. For example, the buildings and the infrastructure in zones of plain rivers could be affected by changes in the frequency and intensity of coastal and riverside floods; the demand of urban energy can increase or diminish as result of the change in the balance between in-house warming and cooling; and the tourism can be affected by the changes in the temperatures of each season and in the intensities and duration of rainfall. The concentration of population and the infrastructure in urban zones

puts in risk large number of persons and physical assets of great value. Nevertheless, the risk is reduced if there are also economies of great scale and access to services together with an infrastructure well administered. When the latter factors combine with prevention measures, risks derived from climatic change can diminish considerably.

People can be directly affected by extreme climate events, causing health damage, or even migrations. The climatic extreme episodes can modify the rates of death, injuries or diseases. For example, the health condition can improve as result of less exposure to cold, or deteriorate as result of a major stress due to heat waves. The displacements of population caused by climate changes can affect the size and the characteristics of the population of the urban settlements, which in turn modifies the demand of services. The problems are slightly different in the biggest cities (for example, those of more than one million inhabitants) that in small villages. It is more likely than the first ones be places of final establishment for immigrants from rural zones or smaller settlements or even from other countries. In the poor settlements that surround major and middle size cities in development continue there are several dangers for both health and environment that might be enhanced by global warming. Nevertheless, big cities have in general a greater influence on national resources, and therefore, smaller settlements can actually be the more vulnerable.

To reduce social vulnerability to water resource stresses driven by Climate Change (floods and droughts) it is required the action of a wide range of stakeholders, including city administrators, community organizations, planners, farming and health sectors and disaster managers, as well as representatives and institutions of the water sector. A very important element in this adaptation process is climate information.

## **8.2. Main problems**

### *8.2.1. Floods*

From the effects produced by floods, arises the perception of risk, which in turn is composed by a social environmental dimension (vulnerability) and a hydrological dimension (natural threat). According with the frequency, duration and intensity with which this phenomenon takes place, impacts in a certain area, with a dynamic boundary of effects in both natural and not natural habitats. Their characteristic in time is the recurrence and those of severe and extreme magnitude leave their marks in the geomorphology.

According with data compiled by Munich Reinsurance, there was a peak record of natural disasters at a worldwide scale between 1997 and 1998. Damages caused by climatic events amounted to US\$ 92 trillions and 32000 dead people.

Floods are not events as dramatic as hurricanes or earthquakes, but they are the most lethal phenomena since, before the Indic Ocean tsunami, 40% of the victims of disasters are produced by them. They result in humanitarian catastrophes because great part of the world population lives in the coasts and banks of rivers and estuaries.

In the regions of abrupt topography, many hundreds of thousands persons live in poor settlements located in unstable hillsides, especially vulnerable to intense rainfalls. In the last decades hundreds of persons died or were seriously wounded and thousands lost their homes due to the collapse of areas in Rio de Janeiro, Sao Paulo and Santos (Commission of Health and Environment of the WHO 1992).

Slums that surround the big cities of the region are installed sometimes in the drainage valleys of rivers or superficial currents, whose flood frequency has increased as consequence of the climate trends (chapters 5 and 6). For example, copious rains, from the beginning of January 2004 and for more than one month, poured over regions of the Northeast, South, centre, West and Southeast of Brazil, provoking land slides and floods and causing the death of 84 persons, whereas more than 40000 lost their homes and other 63000 decided their self evacuation. In addition, there were damages due to energy supply cuts, destruction of the infrastructure of entire neighbourhoods, bridges and roads. The situation affected 338 municipalities of 15 states of Brazil and the economic losses, only assessing the destroyed housing, reached near 34 million dollars.

In Paraguay, the floods of the Paraguay River cause millionaire losses, affecting thousands of persons, destroying houses, public buildings, roads, cattle and farms. A preliminary estimate indicates that more than 60000 persons were damaged in the 1982/83 floods. Another relatively precise record carried out by the Committee of National Emergency (CEN) of Paraguay estimated in more than 70000 persons those who resulted affected by floods of the Paraguay River and its tributaries in 1992. In the 1997 and 1998 floods, the affected people were near 25000 in Asuncion (principal urban centre of Paraguay) and more than 80000 in the rest of the country.

In Argentina, the damages of the 1983 flood reached a total of approximately 965 millions of American dollars. These figures only amount the losses due to direct damages suffered by the cattle rising, agriculture and infrastructure (Aisiks 1984).

A great part of the economic and social damages including lives losses produced by the floods in the La Plata basin are due to the occupation of currently floodable areas in the flood valleys of the rivers. This occupation was done before, but in some cases after the pronounced climatic regional change that began in the 1970 decade (Chapter 5), which has increased the frequency of floods (Chapter 6). Land planning policies are required to face this current situation as well as the eventual threats of even greater floods in the future.

### *8.2.2. Environment and ecosystem vulnerabilities*

The quantity and the quality of water have a direct relation and constitute a very important factor for the biological diversity. Therefore, changes in the water quality or its absence can cause negative impacts on biodiversity.

As an example, the potential problems in the biodiversity of Paraguay will be discussed here. It includes numerous species of mammals, birds, fish, invertebrates, plants and planktonic microorganisms that are distributed in a wide scale of terrestrial, aquatic and marshy environments. Gamarra de Fox et al. (1997) estimate that in this country there are 1228 species of vertebrates among mammals, birds, reptiles, amphibians and fish of which 50% would have conservation problems. It is considered that 29 species of flora and forty of fauna are in danger of extinction.

The marshlands are particularly sensitive to the changes of the hydrology, especially to the systems of shallow lagoons, which are strongly influenced by the environmental conditions and by local climate changes. Since wetlands, reservoirs and creeks are almost dry during extreme ebbs, the wild fauna dies, emigrates, or develops other survival responses, being the fish, carpinchos (great South American rodent), crocodiles (caymans) and herons among other species the most affected by the lack of water. For example, the crocodiles is one of the key species of commercial value of the Esteros del Iberá (wetlands of the Iberá). The crocodiles are very territorial and tend to nest in very similar places year after year, for what their nesting and survival are strongly dependent on water depth (Loureriro da Silva et al. 2003).

In the case of the ichthyic fauna, if at the very moment of reproduction the hydrometric levels are high enough, the juveniles enter and develop in the flood valleys of the rivers, where they find shelter and food. On the contrary if during the reproductive phase hydrometric levels are low, the juveniles would not have the possibility of getting into the above mentioned zones, and as a consequence it is very likely for this set of offsprings will not prosper. This happens especially in the migrating species such as sábalo, surubi, bogas, gilded, bagres and therefore, the variability and seasonality of the streamflows is of crucial importance for the population of these species.

Under the Climatic Change scenario of increase of the variability of the rainfall and therefore of the river flows, the effects on biodiversity and in the number of subjects of important species of economic value would be significant. This scenario is probable as will be discussed for the case of the navigation.

### 8.3. Main services of water resources

#### 8.3.1. Water supply and urban drainage

Water availability below 1000 m<sup>3</sup>/ per capita /year, characterizes a water stress scenario. At a regional level, all of the countries of the La Plata basin are over this value. Even though South America has the 28% of the global water resources, there is a great spatial and temporal (interannual and within the year) variability, and therefore, there are events of water stress.

Consumption uses of the countries of the La Plata basin are presented in *table 8.1* in percentages of the total. It can be seen that in all the countries, farming is the sector with the highest consumption of water.

*Table 8.1. Use of water per sector in %, 1999.*

Country	Residential	Industrial	Farming
Argentina	9	18	73
Bolivia	10	5	85
Brazil	22	19	59
Paraguay	15	7	78
Uruguay	6	3	91

[GWP 2000]

In some large cities, water utilities and their distribution systems are not enough for the extraordinary demand during extreme droughts. In these circumstances, water utilities have to operate beyond their technical margins because their water intakes are compromised for the reduced water flow level. Thus, palliative measures such as massive perforation of new underground wells are taken, which in turn cause a substantial reduction of phreatic levels.

Large supply problems take place at the headwaters of basins where large urban concentrations exist, such as Sao Paulo, Curitiba and Campo Grande in Brazil. For example at the beginning of October 2003, the water rationing in Great Sao Paulo affected 440 thousand inhabitants. The Pedro Beicht dam, the only one of the system, had to provide 1110 l/s and it was only producing 100 l/s . The capacity of the reservoir was draining off at a rate of 0.4% per day, which led to the lowest volume (7.6%) since its operation started in 1916. In the year 2000, it had reached another low (14.6%) but not as serious level, (source Folha de São Paulo). Likewise, water supply was unavailable in several parts of the city and surroundings of Ciudad del Este affecting 50 thousand residents during April 2004. Because of a severe drought, the República Lake that was the water pumping source reached very low levels (source Diário ABC).

There are similar problems in different areas, such as in the Uruguay River basin (Ibicuí basin), where there are conflicts during dry seasons between the urban water supply and the irrigation of rice. But in most of the La Plata basin, water availability is not a problem, with the exception of the before mentioned cities and in the western semi arid region where precipitation is scarce.

Growing urban population in the region has generated difficulties in the water supply both in terms of quantity and quality. In most of cities pipeline water service and sewage services are not available for all residents. In the metropolitan area of Buenos Aires, an important percentage of the population obtains water from wells, some of which have serious levels of pollution, derived from industrial residues and mainly because of precarious sanitary systems, consisting of black wells (wells for faecal matter) (De Filippi et al. 1994; González 1990). This situation improved substantially with the extension of the water pipeline system during the first half of the 1990 decade, but still now, many people remains without this service.

In those areas, such as the ones mentioned in the previous paragraphs, which already experiment difficult situations in the water supply, present a huge potential vulnerability to Climatic Change, since an eventual reduction of the resource would drive to a very expensive adaptation.

The strong urban population growth with the consequent increase of impermeable areas, associated with the higher frequency of intense (see Chapter 5) rainfalls produces significant increases of urban floods, since the old rain drainage systems are under dimensioned. The situation worsens even more in those combined systems, when pipes also carry sewage liquids or have clandestine connections. The overflow of this type of systems produces serious inconveniences. In such circumstances the curves Intensity Duration Frequency of rainfalls, which are tools for the design of hydraulic works, especially for the calculation of overflow pipes and outlets, become outdated, what makes necessary to adequate them to the current climatic conditions.

### *8.3.2. Agriculture*

The agriculture is an activity highly dependent on climatic factors, whose changes and variability can affect productivity. Adaptation conditions of agriculture to climate changes can be variable, becoming more or less vulnerable, depending on the different climatic scenarios. (De Lima et al. 2001). Main annual crops in the La Plata basin are soybean, rice, sunflower, wheat and maize. Rice represents the major consumer of water, since it is cultivated by the system of flooding. This system of cropping uses around 15000 m<sup>3</sup>/ha /year, which represents the domestic consumption of 800 persons. Currently this crop extends over the south of Paraguay and in Brazil in the basin of the tributaries of river Uruguay, Ibicuí and Quarai. The

last one is part of the border between Brazil and Uruguay. *Table 8.2* presents a summary of the areas devoted to agriculture in the countries of the La Plata basin. It can be observed that irrigation is limited to the 4.6% of the potentially agricultural soils.

**Table 8.2.** Farming areas in thousands of hectares.

[CEPAL 2003]

Country	Agricultural Soil 2000	Permanent Crops 2000	Irrigated Area 2000	Rice 2001	Corn 2001	Soy bean 2001	Wheat 2001
Argentina	25.000	2.200	1.561	151	2.745	10.318	7.108
Bolivia	1.944	262	132	149	306	556	110
Brazil	53.200	12.000	1.910	2.147	12.355	13.935	1.702
Paraguay	2.290	88	67	27	353	1.209	171
Uruguay	1.300	40	180	154	57	11	128
Total	83.734	14.590	3.850	2.628	15.816	26.029	9.219
% of agricultural area		17,4	4,6	3,1	18,9	31,1	11,0

Long droughts strongly affect the agricultural sector, both in the commercial crops and in the subsistence farming. The lack of water or the reduction of its quality and the lack of grass lead to losses of weight in the cattle, milk productivity reduction or even to animal deaths.

The vulnerability of the agriculture to Climate Change has been a matter of concern of numerous studies in the region and in the world. However, there are at least two reasons to assume that, unless the change led to extreme scenarios as permanent flood or very important reduction of the soil moisture because of temperature rise or less precipitations, the adjustment to the Climatic Change would be very rapid. The first one is that being an activity of annual cycle, producers are able to adapt rapidly and in autonomous way to the progressive but relatively slow climate changes. An example of fast autonomous adaptation is the extension of the agricultural frontier that accompanied the positive rainfall trends in Argentina (Chapter5). The second reason is that current development of biotechnology is so formidable that surely it will be able to overcome many of the problems caused by climatic adverse trends (Barros 2004).

### 8.3.3. Energy

#### a. Hydroelectric dependence

Worldwide, the big hydroelectric dams provide 10% of the total generation of electricity in 113 countries. They contribute to more than 20% of this generation in 91 countries and in more than 50% in 63 countries. Almost all the above mentioned are developing countries or from the ex-Soviet Union.

Many of the countries dependent on the hydroelectricity are already experiencing energetic shortage in periods of drought. The countries that have suffered blackouts and energy rationing due to the droughts in the recent years, include Albania, Argentina, Brazil, Chile, Colombia, Ecuador, Ghana, Guatemala, India, Kenya, Peru, Sri Lanka, Tadjikistan, Vietnam, Zambia and Zimbabwe. Regions of Norway and USA have also experienced problems in the supply of energy due to low levels of water in the dams.

In several of these countries that already highly depend on hydroelectricity, the construction of new hydroelectric facilities is being planned, as in the case of the countries of the La Plata basin. There is a need to satisfy the increasing demand and in addition, the relation between installed power and maximum demand is currently relatively small for a situation where most of the stock is hydraulic and therefore capable of great variability due to climatic reasons. The power installed in the countries of the La Plata basin in the year 2000 was reaching 97800 MW, of which 76% was hydraulic power. On the other hand the installed power was only 1.34 times higher than the maximum demand, mainly due to the weight of Brazil within the countries of the basin, both in the installed power and in the maximum demand, *Table 8.3*. This low relation puts in crisis the whole supply in cases of long droughts and is one of the factors that make necessary the expansion of the installed power.

*Table 8.3. Structure of the MERCOSUR markets. Offer and Demand of year 2000.*

COUNTRY	Installed Power				Maximum Demand	
	Hydro (MW)	Thermal (MW)	Total (MW)	% Hydro	MW	Ratio InstP./ Max. Dem.
Argentina	8.926	11.785	20.711	43%	13.754	1,51
Bolivia	336	629	965	35%	645	1,50
Brazil	56.262	9.929	66.191	85%	56.000	1,20
Paraguay	7.840	0	7.840	100%	1.120	7,00
Uruguay	1.534	563	2.097	73%	1.463	1,43
Total	74.898	22.906	97.804	76%	72.982	1,34

Source: CIER Magazine N° 43

The production of hydraulic power is influenced by precipitation variability. The changes of streamflows to take place as a consequence of the Global Climatic Change, will be able to either favour or hinder the generation of hydraulic power depending not only on how is the total generation affected but also its seasonal variation in relation with the demand of electricity. In case changes were unfavourable, the vulnerability of the electrical sector will depend to a great extent on the percentage of hydroelectric generation. Therefore, the electric power generation in the La Plata basin is potentially highly vulnerable to the Climatic Change being from this point of view one of the regions of the world of greater vulnerability.

The vulnerability to the climatic variability and eventually to Climate Change can increase in the future since only a fraction of the technically exploitable potential of hydroelectric energy in the countries of the La Plata basin is being used. Therefore, the region would be in conditions to increase the installed hydraulic power during this century to satisfy the increasing demands, even if the climate change led to some reductions in the energy generation in certain dams.

#### *b. Large hydroelectric utilities*

The need to diminish the vulnerability of the society to Climate Change is increasingly receiving the attention of governments and international agencies. It is likely that the most serious consequence of global warming for human beings will not be the warmer climate, but the changes in the pattern of the hydrology. At global scale, unprecedented changes are already being perceived, such as a major frequency and intensity of extreme floods and droughts. It is likely that this situation will become even worse in the future.

The droughts bring many economic and social prejudices, especially in countries with great dependence of the agriculture. The impact of droughts in the hydroelectric generation can also cause economic costs, in moments in which the economy is already affected by the low production of food and the reduction of exports. The generation could be reduced substantially and in some cases the reservoirs could reach extreme low levels like in Itaipú in 1999 and in Salto Grande in 2004.

The big hydroelectric plants are being built assuming that the past hydrological behaviours can be used to predict the future energy production, the volume of the floods that should threaten the safety of the dams, the design of the alert programs. Sometimes these assumptions were exceeded because their designers have estimated climatic and hydrological scenarios, which are different from what are currently being observed. This happens as consequence of assuming that the meteorological and climatic conditions do not change so that the statistical conditions of the past will be repeated in the future. The least than can be said about this premise is that it is no longer acceptable. Even with the uncertainties to predict the future

(chapters 12 and 13), because of the global warming, it cannot be discarded extremes that will probably overcome all the historical records in the future. Consequently, designers of the large hydroelectric factories should take into account Climate Change. They should a priori consider larger margins of safety so that the dams should have a greater aptitude in order to face floods in a sure manner and be environmentally compatible. Likewise, the designs for the production of energy should include the possibility of extreme droughts. It is clear that these greater safety margins would increase costs, but surely they would reduce both the socioeconomic and environmental risks, and therefore they would facilitate the viability of the projects. A more sophisticated alternative is to try to reduce the future uncertainty by a proper use of climate scenarios and other tools like the ones discussed in chapters 12 to 15.

### *c. Dams sedimentation*

The World Bank has calculated that, every year, 0.5-1% of the global reservoir capacity is lost due to sedimentation. This means that 240-480 new dams should be added every year only to support the global reservoir capacity. The increasing volume of sediments in a reservoir will eventually either hinder seriously or hamper completely the functioning of the hydroelectric plant.

There are technologies capable of reducing the level of sedimentation in reservoirs and dredging the sediments already deposited in the above mentioned reservoirs. These technologies, anyway, have serious limitations due to different reasons. They are only good for specific types of dams, are in some cases prohibitively expensive and eventually reduce the capacity of the dam to generate energy.

A great part of the sediments are transported normally during the periods of flood. As global warming is being accompanied of a major frequency of large rainfalls, it is expected a greater intensity and frequency of floods, therefore increasing the charges of sediments. On the other hand, the changes in the vegetation in the basin due to the climatic change might complicate the efforts to predict the future levels of sedimentation.

### *8.3.4. Fluvial navigation*

The Paraguay- Paraná fluvial system is a commercial strategic hydro way that connects the interior of South America with the deep water ports in the low section of the Paraná River and in the La Plata River. With more than 3300 km length from its nascent in Cáceres Brazil up to the final end in the La Plata River, the Hydroway will provide access and will serve as important transport artery for large areas of

Argentina, Bolivia, Brazil, Uruguay and Paraguay, when the improvements of the navigation conditions were undertaken and concluded.

During atypical ebbs, in the upper Paraguay, the navigation of crafts of major fret (5 to 7 feet of brace) is precluded due to the risks of running aground in banks of sand or rock outcrops. Ebbs cause direct losses to the ship owners, for not transported freights are of the order of 8 million dollars, which is about 50% of the income during normal conditions.

The ebbs reduce the movement of goods and persons, raising the costs of freights, which, for example in Paraguay, affects the global economy of the country due to the fact that more than 50% of the import and exportation is transported by the Paraguay River. This forces multimillionaires expenditures in dredging and complementary signposting in order to support the minimal navigability of the principal water courses and the accesses to the principal ports. The dredging to facilitate the navigation and the access to the ports is a permanent activity also in Argentina in the Paraná and the La Plata rivers.

One of the possible scenarios of the Climate Change is the increase of the variability of rainfall and therefore in the river flow as it is already happening (Chapter 6). In such scenario, the costs to maintaining the Paraguay - Paraná navigation will increase.

## **References**

- Aisisks, E. G. 1984: La gran crecida del río Paraná. Organización Techint, Boletín Informativo, Pág. 45.
- Barros, V. 2004: El Cambio Climático Global. Ed. Libros del Zorzal. Buenos Aires, 172 pp.
- CEPAL, 2003: Anuario estadístico da América Latina y Caribe. CEPAL.
- CIER Magazine 2003: Comisión de Integración Energética Regional. Abril -Mayo -Junio, 43.
- Colecciones de flora y fauna del Museo Nacional de Historia Natural del Paraguay. MNHNP-DPNVS - SSERNMA - MAG. Asunción. 573pp.
- De Filippi y coautores 1994: Los residuos sólidos urbanos en ciudades pequeñas y medianas. Seminario de gestión municipal de los residuos urbanos. La Plata, Provincia de Buenos Aires, Instituto de Estudios e Investigaciones sobre el Medio Ambiente, IEIMA, Buenos Aires, 51-62.
- De Lima M.A. 2001: Mudancas Climáticas Globais e a Agropecuaria Brasileira, Pág.9.
- Folha de São Paulo, quinta-feira, 9 de octubre de 2003. Brasil.
- Gamarra de Fox, I. y A. J. Martin 1997: Mastozoología, en Romero Martínez, O.
- González, N. 1990: La Contaminación del agua. Política ambiental y gestión municipal. Instituto de Estudios e Investigaciones sobre el Medio Ambiente, Buenos Aires, Argentina.
- GWP 2000: Agua para el Siglo XXI: de la Visión a la Acción para América der Sur. SAMTAC. South American Technical Advisee Comité. GWP.

- IPCC 1996: Climate Change 1995: Impacts, Adaptations, and Mitigation of Climate Change: Scientific-Technical Analyses. Contribution of Working Group II to the Second Assessment Report of the Intergovernmental Panel on Climate Change [Watson, R.T., M.C. Zinyowera, and R.H. Moss (eds.)]. Cambridge University Press, Cambridge, United Kingdom and New York, NY, USA, 880 pp.
- Loureriro da Silva, J. A., M. de Castro and D. Justo 2003: El Manejo Sustentable de los Recursos de Humedales en el Mercosur. Buenos Aires , Argentina, pp 185
- WHO 1992: Our Planet, Our Health. World Health Organization, Geneva, Switzerland.

## GLOBAL CLIMATIC CHANGE

*Vicente Barros<sup>1</sup>*

<sup>1</sup> CIMA/CONICET. Universidad de Buenos Aires.

### ABSTRACT

This chapter is intended to introduce a synthetic view of the Climate Change issue for readers not acquainted with the subject. The possible causes of general climate changes are briefly addressed to identify those acting in the same scale of the human interference with climate, namely one to three centuries. The greenhouse effect is described, as well as the greenhouse gases and the human activities responsible for their emissions.

The augment of the human-caused emissions and of the global temperature trends during the industrial period are addressed, as well as other trends of the climate system that are consistent with the global warming process and are indicative that this warming was, at least partly, caused by human activities.

Climate projections for the twentieth century and their potential impacts over some of the human and natural systems are described. It is concluded that due to the intrinsic slow answer of both the climate system to its driving forces, and of the socioeconomic system to fast action, part of the Climate Change is and will be unavoidable taking place during the first half of the century. Therefore, adaptation to Climate Change is required at the same time that more effective measures to control greenhouse emission to avoid more important damages during the second half of the century.

## **9.1. Introduction**

The emissions of greenhouse gases (GHG) resulting from certain activities have been the main cause of the unusual heating of the planet during the last 150 years, this process that continues is known as Climatic Change. Actually, it is a global warming of the planet that also involves an important climatic change not only in temperature but also in the other climatic variables such as precipitation, winds and humidity.

## **9.2. Causes of climatic changes**

The changes in the Earth climate were and are produced by diverse natural processes that affect the climatic system or some of its components. In order to conclude that the trend to the global warming is due to human activity, it has been necessary to discard or at least to measure the effect of these processes.

The variations of the Earth orbit around the sun have induced important climatic changes in the past. However, these changes are very slow and significantly influence the climate, only after thousands years. The undergoing process of global warming is a process that started not before two centuries ago. Therefore, the changes in the terrestrial orbit must be disregarded as its possible cause, which in any case at present astronomic circumstances would drive to a cooling of the planet.

For the same reason, the geological processes that modify the geography of the Earth have to be disregarded. The drift of the continents, the raising and destruction of the mountain chains modify not only local but also global climate. These processes and the concurrent climatic changes that they originate are very slow and only important at a million year timescale.

Other possible natural causes of climatic change that could have an effect in the scale of time from decades to centuries are the variations of the solar radiation and of the volcanic activity, but they have not been as important as to explain the observed warming. Although solar radiation has been increasing in the last two centuries, its contribution to the warming from the beginning of the industrial period has been six times lower than that of the CHG.

Volcanic activity produces explosions that when, due to its intensity, injects gases into the stratosphere, they remains in it for several years. This material increases the reflection of the solar light, thus contributing to the cooling of the planet. The absence of eruptions of this type in the first half of the twentieth century contributed to the warming in this period in a similar magnitude to the increase of the solar radiation.

The dynamics of the climatic system like that of other complex systems might generate changes in its equilibrium statistical conditions without being forced by any external cause. This is called internal variability. Using global climate models, it is possible to discard with great probability, that the internal variability had generated the global observed trend, since in simulations of the climate for thousands of years, these models do not reproduce trends of the global temperature during periods of 100 years, so pronounced as the current trend of the last century.

The change of the chemical composition of the atmosphere, when it affects the so called greenhouse gases is another of the causes of climatic changes. From the beginning of the industrial period the concentration of these gases has been altered by the emission of human origin.

The emission of soot and other particles, as well as of sulphates and nitrates originated in human activities increases the formation of aerosols. These emissions add to the natural ones and are a potential source of both global and regional climatic changes. A direct effect of the aerosols is to reflect the solar light to the outer space contributing to the cooling, although in the case of soot they can have a greenhouse effect. Besides, they alter the process of formation of the clouds and their duration. About their effect on global climate there is still a great uncertainty. Anyway, whereas the emission of aerosols of human origin grows in a linear way, those of GHG are growing exponentially, and thus, the relative effect will be losing importance with time at worldwide scale. This topic will be approached in more detail in chapter 10.

### **9.3. Solar and terrestrial radiation**

All the bodies emit and absorb the electromagnetic radiation in a different way according to their temperature. In general, emissions are very close to those of a black body and proportional to the fourth power of the absolute temperature (Stefan-Boltzman law). For each temperature, emissions are practically within a certain range of wave lengths according to the law deduced by Planck. The maximum of the emission varies with the temperature so that the warm bodies emit in a shorter wave length than cold ones.

The Earth receives energy from the sun in the form of electromagnetic radiation. This radiation coming from a body with high temperature (about  $6000^{\circ}\text{K}$ ) is of very short wave length, passing through the atmosphere with little absorption. A part of it is reflected to outer space by the clouds, the atmosphere itself and the terrestrial surface and the rest is absorbed in the surface of the planet. In turn the terrestrial surface, the atmosphere and the clouds emit electromagnetic radiation with a longer wave length since they are at much lower temperatures, 200 a  $300^{\circ}\text{K}$ .

## **9.4. Greenhouse effect**

The atmosphere is not transparent to terrestrial radiation as it is to large part of the solar radiation. Most of this radiation is absorbed, except in a determined band of wave length called radiation window because through it escapes to space the terrestrial radiation. The transparency of the atmosphere to solar radiation and its opaqueness to terrestrial radiation causes the mean temperature of the planet to be higher (approximately 30°C) than the one it would have in case of lacking the atmosphere. This natural action of the atmosphere is called greenhouse effect. This effect is being intensified now by the increase in the concentrations of GHG.

The atmosphere is composed mostly by nitrogen and oxygen, but also in minor measure by other gases. Among these, water vapour (H<sub>2</sub>O), carbon dioxide (CO<sub>2</sub>), methane (CH<sub>4</sub>) and nitrous oxide (N<sub>2</sub>O) are greenhouse gases since they absorb part of the outgoing radiation in the band of wave lengths of the window of radiation. In colloquial and illustrative terms it is said that the increase of the concentration of these gases is closing the radiation window. Thus, when the concentration of these gases increases, the radiation leaving to outer space is reduced and global warming is produced, since temperature increases until the outgoing radiation balance again the solar radiation absorbed in the planet.

## **9.5. Greenhouse gases (GHG.)**

The human activities cannot yet directly modify the concentration of water vapour in the atmosphere, because this gas is regulated by the temperature that determines its removal through the processes of condensation and freezing in the clouds. On the other hand, there are clear evidences that anthropogenic emission of the other GHG has modified their atmospheric concentrations. Following the industrial revolution, due to the burning of fossil fuels (coal, oil and natural gas) for the production of energy, a large quantity of CO<sub>2</sub> has been liberated to the atmosphere and the same happened with the emission of other gases by other human activities.

The emissions of carbon dioxide, originated in the combustion of fossil hydrocarbons, had an exponential growth since the beginning of the industrial period and on top of that there are emissions of this gas due to deforestation, which nowadays are three or four times smaller than the first ones. Part of carbon dioxide is being captured by the oceans, by the biosphere and through it, by the soils, but almost half is being accumulated in the atmosphere. Due to it, an increase of its concentrations of about 30% has taken place in the last 150 years. In the same period, the methane concentration in the atmosphere increased 150% and the nitrous oxide concentration has risen by 16%.

The GHG concentration alterations the atmosphere produced by their emission last in the average from about 15 years in case of methane, to 100-150 years

in the carbon dioxide and nitrous oxide cases. There are other artificial CHG., luckily of very low emission, for which are estimated times of permanency in the atmosphere before their destruction that go from 40 years up to several thousands of years according to the chemical substance.

The long permanence of the GHG emissions in the atmosphere causes these emissions to have a cumulative effect. Due to the fact that the time of permanency of the CO<sub>2</sub> and N<sub>2</sub>O emissions is superior to 100 years, in the hypothetical case that these emissions were reduced to zero, the atmosphere would continue with concentrations over those of the pre industrial period for a long time, returning only after approximately two centuries to their initial values. It is necessary to add to it that the calorific capacity of the climatic system is enormous, particularly because of the oceanic component. Hence, the thermal balance of the climatic system with GHG new concentrations is only reached approximately 50 years after these are modified.

The combined effect of the GHG long permanency in the atmosphere together with the delay of the temperatures of the climatic system to adjust to the new GHG concentrations has two implications of significant political content. The changes that have already taken place in climate and those to happen in the next decades are mainly a result of past emissions, for which developed countries are fundamentally responsible. However, the present emissions will determine the future climate, and consequently, the climate of the second half of the century will depend critically on the emissions pace during the next decades to come.

## **9.6. Global warming during the industrial period**

The average temperature of the planet's surface increased between 0.6 and 0.7°C during the last 150 years, *Fig. 9.1*. The trend and the fluctuation pattern are similar in both hemispheres. There is no doubt about the global warming since, even though there can be queries on these global trends because of possible modifications of the environment of the meteorological stations over the years, there is, however, a number of other indicators of the climatic system that are consistent with this trend. There is a general retreat of the glaciers and the temperature of the sea surface warmed up at least in 0.6°C. This warming included practically the whole mixed layer, which thickness varies from 50 m or less in the tropical zones up to 700 m in high latitudes. The calorific capacity of this sea layer is at least 35 times superior to that of the atmosphere, which shows the formidable accumulation of heat that is going on in the planet. Also, there is an acceleration of the hydrological cycle, which is consistent with the global warming. Since 1950, the night temperature increased more rapidly than the diurnal one, which is indicative that the increase in the temperature is due to the greenhouse effect. All of these indications, together with some other coincide to indicate that there has been a global

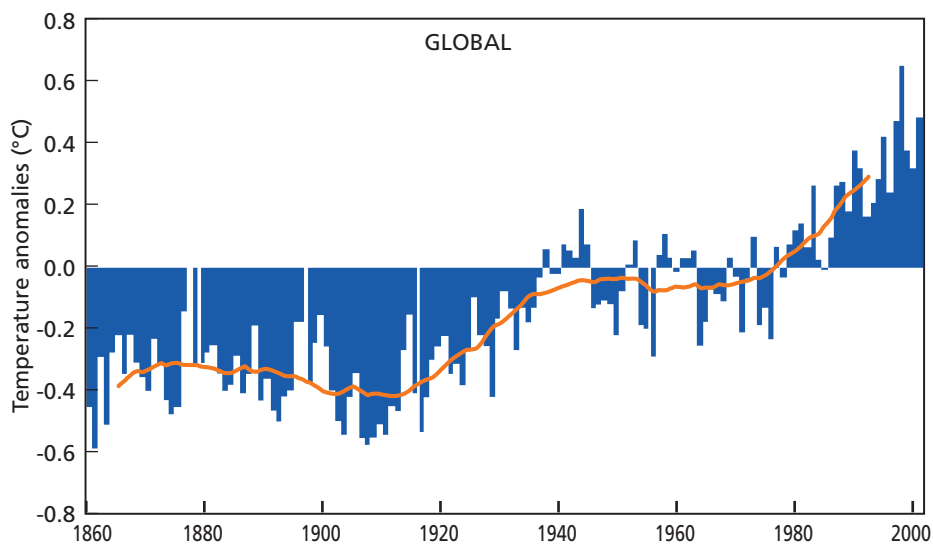


*Fig. 9.1. Anomaly of the mean annual surface temperature with respect 1961-1990 average. Solid line represents a 21-year moving average.*

warming, especially in the last 30 years, with the fingerprint of the GHG increase of concentrations including, as paradoxical as it may seem, the cooling of the stratosphere in more than  $0.5^{\circ}\text{C}$  since 1980.

On the other hand, a paleo-climatic reconstruction (*Fig. 9.2*) indicates that a change as intense as the current one does not have precedents in the last 1000 years, which would contribute to discard that it has been originated by natural variability.

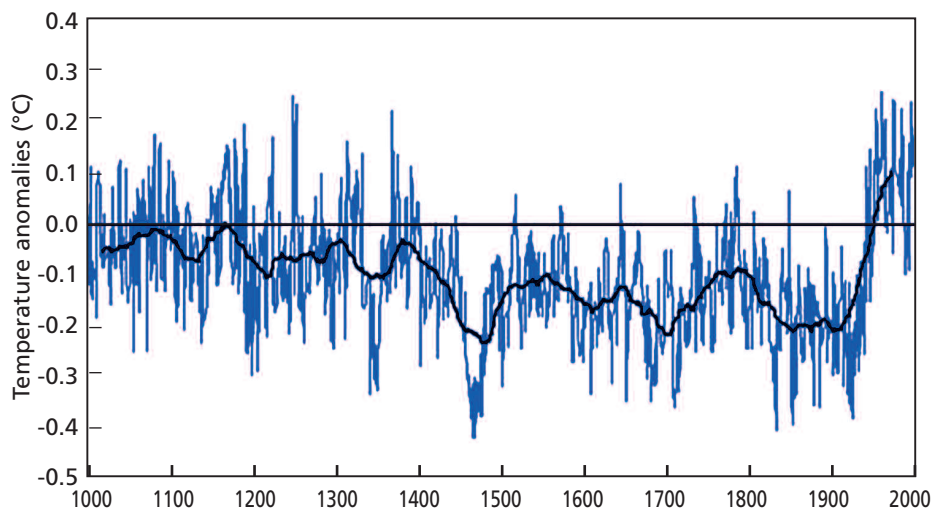


*Fig. 9.2. Anomaly of the mean annual temperature of the Northern Hemisphere with respect 1900-1950 average. The thick line is the mobile average of 51 years.*

[Based on paleo-climatic data taken from Mann and others, 1999]

On the base of these and other facts, the Inter-governmental Panel for the Climatic Change (IPCC 2001a) in its report of the year 2001 has concluded that the trend to warming observed in the twentieth century has an important component of human origin.

### **9.7. The climate in the twenty first century**

The evolution of the emission of GHG in the future will depend on numerous factors whose prediction is quite complex. They are the economic and demographic growth, the technological changes and even the development towards a society with more or less equity. Finally, but not less important, it will depend of the collective answers of the humanity to reduce or at least to diminish the rate of growth of the emission.

Since all these factors are very difficult to foresee, the only possibility is to build possible socioeconomic scenarios of the future. The building and characteristics of these scenarios are discussed in chapter 13. The different scenarios suppose dissimilar levels of economic activity that imply in turn different emissions scenarios. It is possible to build as many emission scenarios as arise from the combinations of the driven factors of the level of economic activity and of its characteristics, without certainty on which will be the one really happening. However, for a given scenario of GHG emissions throughout time, it will be a corresponding scenario of concentration evolution of these gases.

The effect of GHG concentrations in the climate is studied with the help of global climate models (GCM) that simulate the climatic system in almost all its complexity. These models represent the physical processes of the sea, the atmosphere, the soil and the cryosphere, and simulate its evolution using huge computers. In chapter 11, they are described in more detail. Only the most sophisticated GCM have been capable of reproducing, forced by the observed evolution of GHG concentrations, the global climate global changes observed during the industrial period. This generates certain confidence in their capacity to simulate the global changes of the future climate.

The different GCM project different values of the global temperature, still under the same socio-economic scenarios. Nevertheless, they all give the same qualitative response, important warming throughout the twenty first century for any of the socioeconomic scenarios.

The GCM are a reliable methodology to assess climate changes at global scale, but they still have a limited capacity to simulate the climate at regional scale, understanding for such the one that goes from a locality up to a continent. Although the different models are consistent among one another in terms of their predictions

at a global scale, they show notable differences at a regional scale, particularly in the simulations of the current fields of rainfall and of their future prediction. This is an important limiting factor at the moment of evaluating the impacts of the climatic change.

This is in turn also a great limitation to estimate the vulnerability to the climatic change, since it is to be expected that most of the ecological, economic and social impacts will be at regional or local scale. However, the models are consistent in the prediction of some aspects that, though of global character, will emerge in many regions. For example, an increase of the intensity of the hydrologic cycle is expected with more intense rainfalls, though in some regions the opposite could happen. It is estimated that there will be a major frequency and intensity of the intense precipitations (IPCC 2001b) and in consequence of the phenomena associated with them, what is already happening in several regions of the planet. In chapter 5 it has been seen that it is already occurring in the La Plata basin.

As a consequence of the oceans thermal expansion and to a lower degree due to the melting of glaciers and continental mantles of ice, it is estimated that the mean sea level will increase. As a result, by the 2100 it would be about 60 cm over its current level. This global effect will be felt with few variants on all the coasts of the planet, but severe problems can be anticipated in those relatively low as it is the case of the deltas and estuaries and in the insular states of the Caribbean and Polynesia, causing huge socioeconomic losses and migrations.

Another global impact that will display uniformly at regional scale is the fertilization of a great part of the biosphere with the consequent ecological change. Part of the vegetation has a type of photosynthesis in which the carbon dioxide is a limiting factor, thus, CO<sub>2</sub> increase favours its growth. Other vegetables, on the other hand, do not change their level of photosynthesis depending on the concentration of the carbon dioxide. The augment of the concentration of this gas can alter the ecological balance favouring the expansion of the first type of vegetables at the expense of the second one. Much more serious will be the effects of the regional climatic changes on the ecosystems. These can turn out to be very critical in the isolated systems such as mountains or marshlands where it might come to the massive extinction of many species and ecosystems. Something similar would happen with almost all the ecological systems since the human use of the space has led to their fragmentation and isolation.

Some studies suggest that even in the cases in which the continuity of the ecosystems is not geographically limited, the speed of the climatic change would be two or three times greater to the one at which many species could displace. Because of that, it is growing the idea that if a drastic GHG emission reduction and their elimination do not take place within the next 50 years, the ecological catastrophe to come will not have precedents since the mankind appeared in the planet.

In the food production, no great difficulties are foreseen at a global scale, but they surely will occur in some regions. The productivity losses in certain areas, principally tropical and subtropical, would be compensated by increases in other regions, particularly in middle and high latitudes. Nevertheless, the expected rapid advances in biotechnology would allow a rapid adaptation to the new climatic conditions in almost the whole world.

Finally, there exists consensus regarding the impact to be major in every sense in developing countries since they lack knowledge, the organization and the material resources to anticipate and to adapt to Climatic Change.

### **9.8. The Climatic Change is already unavoidable: mitigation and adaptation**

When the warming potential of GHG emissions is calculated according with the different human activities, 48% corresponds to energy, mainly due to the burning of fossil fuels. 24% corresponds to the emission of chlorofluorocarbons. 13% is attributed to deforestation, particularly in the Amazon and Borneo. A 9% is accountable to the agricultural sector, due to the bovine cattle and rice cultivation with flooding, which is the principal source of food for half of the world population. The remaining 6% is a consequence of the managing of organic residues and of some few industrial processes. Regarding the emission of the chlorofluorocarbons and of other substances that damage the ozone layer, there are reductions in force agreed by the Montreal Protocol. Therefore, the energetic sector contributes with two thirds of the warming potential of the remaining emissions.

Any attempt to seriously mitigate the Climatic Change must include a drastic reduction (of the order of 50%) of the burning of fossil fuels and in the future, its elimination. As fossil fuels are the principal source of energy (more than 80% of the world total), this would not be possible at once without causing an economic catastrophe in the world. Besides, the substitution of a primary source of energy is a process shown by the historical experience to take, at least, several decades. Hence, a substantial substitution of the hydrocarbons as energy source does not seem to be feasible in a horizon ranging from 10 to 20 years.

Apart from this inertia in the socioeconomic system, as aforementioned, GHG concentrations remain for long time in the atmosphere and the thermal adjustment of the climate system to them is also slow. Consequently, the temperature will increase in the next decades in any of the possible scenarios. This implies that in spite of the little or much that would be achieved to diminish the GHG emissions, the Climatic Change in the next decades and its consequences are already inevitable. Indeed, no significant differences until the year 2040 among the different scenarios can be appreciated (*Table 13.2* in chapter 12).

In view of the unavailability of the climatic change during the twenty first century, it is not only being considered the mitigation of the climatic change, but the adaptation to it. The optimum adaptation would be one that could be planned in advance and not the one occurring after changes appear. However, in many cases this is still impossible given the lack of credible scenarios at regional scale. Anyhow, the use of climate scenarios allows in certain cases to minimize the potential risks without major costs. Especially it is always advisable the utilization of options that in any case are good options in the current climate conditions (non regret options).

The international concern about Climatic Change lead to the United Nations Framework Convention on Climatic Change (UNFCCC) signed in 1992 in Rio de Janeiro and within its system, to the Kyoto's Protocol in 1997. Both instruments constitute the first steps towards a collective and progressive solution for the mitigation of this serious problem. The Kyoto's Protocol compromises a modest reduction of the developed countries' emission during the next year. However, these reductions should be very much larger if what is intended is to stop or at least reduce the speed of the global warming by the second half of the century.

The adaptation to the already unavoidable part of the climatic change is an imperious need, but by no means, it should be understood as an alternative to the process of mitigation, since if this process is not deepened, the outcome during the second half of the century can be catastrophic.

## **References**

- Barros, V. 2004: *El Cambio Climático Global*. Libros del Zorzal, Buenos Aires, 172 pp.
- IPCC 2001a: *Climate Change 2001: The Scientific Basis*. Cambridge University Press, USA, 881 pp.
- IPCC 2001b: *Impacts, Adaptation and Vulnerability*. Cambridge University Press, USA, 1031 pp.
- Mann, M. E., R. S. Bradley and M. K. Hughes 1999: Northern Hemisphere temperatures during the past millennium: inferences, uncertainties and limitations, *Geophys. Res. Lett.*, 26, pp. 759-762.

## BACKGROUND ON OTHER REGIONAL ASPECTS: LAND USE CHANGE, AEROSOLS AND TRACE GASES

*Pedro Leite da Silva Dias<sup>1</sup>*

<sup>1</sup> Instituto de Astronomia, Geofísica e Ciências Atmosféricas, USP, São Paulo, Brasil.

### ABSTRACT

Recent studies on the impact of land use change in the climate have explored the role of realistic patterns of deforestation and the results indicate that an increase of precipitation may be observed if clearing is partial, although a decrease of the order of 25% is typical if total conversion to pasture is assumed. Several recent dynamic vegetation simulations have reported the savanization process of the Amazon in global change scenarios with significant impacts in the South American continent.

The impact of biomass burning has also been shown to extend the impacts away from the burning areas. In particular, it has been reported that aerosols produced by biomass burning in the Amazon, Central Brazil and Bolivia may have an impact in the precipitation in the La Plata Basin caused by the radiative impact of the airborne aerosols. Impact of mega cities in the regional climate has also been explored. The impact on the precipitation variability and on the occurrence of extremes has been detected in some cases such as the increase in the frequency of occurrence of days with total precipitation exceeding some high thresholds.

## **10.1 Introduction**

Relevant examples of the complexity of the interactions of the non-linear relations of the Climate System have been detected in S. America in the context of the effect of biomass burning aerosols and land use. Land use change is associated with ecosystems changes and it is known that ecosystems have an impact on the concentration of gases in the atmosphere both as a source and as a sink for many atmospheric constituents including the greenhouse gases. Changes in land use and ecosystems also impact the water flow (hydrology), the energy balance (reflection and absorption of solar radiation), and air circulation (surface properties and aerodynamics). Biomass burning is a major and sometimes unique source of several gases that affect climate and air quality. It is a common and natural phenomenon (Haberle and Maslin, 1999; Liu and Colinvaux, 1988, Martin et al. 1992) in many savanna areas such as the Cerrado in central South America and also in some higher latitude forests, as well as being a common land management practice. Reasons for biomass burning include deforestation, shifting cultivation, grazing in savannas, clearing agricultural residue, and fuel wood.

Changes in physical properties of surface can modify the fluxes of water (hydrological cycle) and energy (solar radiation, radiative forcing, heat exchange) that can have significant climate impacts at the local regional scale, affecting air circulation, precipitation patterns and temperatures. The impacts are highly dependent of the geographical location and season and quite often the mean global impact is very small and therefore difficult to be detected in global averages. However, locally, the effects associated with land use change of regional changes in the atmospheric composition may be very important. The main physical processes impacting regional climate change through changes in land use and atmospheric chemical composition are:

- a) Surface albedo (fraction of solar radiation reflected back into the atmosphere). Surface albedo depends on the vegetation cover, and is lower in a forested landscape than in open land or agriculture.
- b) Evapotranspiration. The transport of water from the plants to the atmosphere directly impacts the hydrological cycle, radiative forcing (indirectly via clouds), and energy budgets. It is controlled by vegetation rooting depth, leaf area and soil moisture.
- c) Aerodynamic roughness of surfaces. The surface of the landscape affects the circulation of air passing over it and thus also influences evapotranspiration and energy fluxes.
- d) Aerosols. Aerosols directly influence the radiative balance of the atmosphere with positive and negative feedbacks. Some aerosols are highly reflective and therefore decrease the solar energy available at the surface, having a cooling

effect. Others are more effective in terms of absorbing solar radiation thus heating the atmosphere. But aerosols also impact the cloud formation and structure since they act as cloud condensation nuclei. Soil dust can also influence the regional climate through the wind erosion.

- e) Trace gases. Vegetation emits Volatile Organic Compounds (VOC) that have a great influence on atmospheric chemistry, hydrology and climate through the production of tropospheric O<sub>3</sub>, production of organic aerosols, cloud condensation nuclei and acid rain formation. Land use change may have a significant impact of the emission of VOC's because of the associated changes in the vegetation.

## **10.2 Regional effects of biomass burning**

Biomass burning is certainly the major source of atmospheric aerosols in South America away from the main cities (Artaxo et al. 1990; Echalar et al. 1998). Carbonaceous aerosols of many forms, besides their radiative forcing also cause respiratory problems. The main sources are fossil fuel and biomass burning, and oxidation of VOCs. Natural biogenic aerosols also exist in the atmosphere and are formed from plant debris (cuticular waxes, leaf fragments, etc.) organic matter, and microbial particles (bacteria, fungi, viruses, algae, pollen, spores, etc.) as discussed in Artaxo et al. (2003). Representative measurements of the various organic carbon species in aerosols and the differentiation between black and organic carbon still require improvement but there has been substantial progress in estimating the regional impact in South America. Substantial progress has been made in recent years with regard to the emissions factors i.e. the amount of aerosol emitted per amount of biomass burned based on controlled experiments (Procópio et al. 2004).

Modelling studies have indicated the potential impact of biomass burning on the precipitation (Moreira et al. 2004). Several recent studies have indicated that the prevailing atmospheric circulation transports a significant amount of aerosols from the biomass burning areas in the tropical region to higher latitudes in South America (Freitas et al 1996, 2004, 2005). Under certain meteorological conditions, in general associated with the presence of a strong northerly low level jet along the Andes or a strong low level north westerly flow, the aerosol plume, produced by biomass burning in the southern Amazon, travels towards Paraguay, northern Argentina and Southern/Southeastern Brazil.

Greenhouse gases are also emitted during fires. The main emissions are: CO<sub>2</sub>, CO (a quarter of all sources), CH<sub>4</sub> (5 to 10% of all sources), nitric oxide, ammonia, NO and VOCs. Significant amounts of methyl chloride (CH<sub>3</sub>Cl) and methyl bromide (CH<sub>3</sub>Br) are emitted, both of which react with stratospheric ozone. Many of the nitrogen and carbon-containing compounds emitted are chemically reactive and are precursors of tropospheric ozone, and the interannual trends and seasonal cycle

of tropospheric ozone concentrations correspond to the seasonal cycle and extent of biomass burning in tropical South America (Kaufman, 1998).

Tropospheric ozone associated with biomass burning is an important greenhouse gas and modifies atmospheric chemistry though its impact on the radical OH that affects the atmospheric cleansing capacity and it has an indirect effect on the greenhouse gas concentration. Photochemical production of ozone is tied to the abundance of pollutants from sources such as biomass burning, and urban pollution. Ecosystems have a significant interaction with the tropospheric ozone. Some vegetation emissions play an important role in cleansing the atmosphere of tropospheric ozone but may also increase the concentration through photochemical reactions associated the VOC's emitted by vegetation Tropospheric measurement of ozone concentration in S. America have been showing significant concentration in rural areas, away from main urban centers and have been attributed to biomass burning (Andreae et al. 1988; Kirschhoff et al. 1988).

During the peak of the burning season in central South America the number of particles in the air goes up an order of magnitude from the values during the rest of the year (Martins et al 1998). Solar radiation and in particular the Photosynthetically Active Radiation (PAR) reaching the surface is reduced by about 10-30% reducing surface temperature and light available for plant growth (Schafer et al. 2002). The effect of this on vegetation is not well established (Gu et al. 2004). A dynamical vegetation model was successfully coupled to the mesoscale atmospheric model with the biomass burning aerosols emission module. It has been shown that the non-linear effects associated to the interaction between the aerosols, radiation and vegetation are responsible for significant changes in the vegetation properties and the precipitation regime in the transition season between the dry and wet periods in southwestern Amazonia. A preliminary report was presented by Moreira et al. (2004).

However particulate matter containing black carbon and greenhouse gases absorb radiation causing warming. The combination of a cooler surface (by a couple of degrees) for lack of solar radiation and a warmer boundary layer due to absorption increases the thermal stability and reduces the chances of cloud formation, thus reducing the possibility of rainfall. Freitas et al. (2004) have indicated the possibility of rainfall decrease in the La Plata Basin as a response to the radiative effect of the aerosol load transported from biomass burning the Cerrado and Amazon regions. An individual case studied by Freitas et al. (2004) during the transition period from the dry to the wet season in central South America (September) suggests a reduction of precipitation of the order of 10-15% in Southern Brazil/Uruguay in a particular event.

The beginning of the South American Monsoon System is characterized by the transition of a very polluted to a clear atmosphere, due to biomass burning. Biogenic aerosol and aerosol produced by biomass burning have a direct role on the

surface and troposphere energy budget due to their capacity to scatter and absorb solar radiation (Artaxo et al, 1990). These aerosols can also impact atmospheric thermodynamic stability as much as they tend to cool the surface (by scattering radiation that would otherwise be absorbed at the surface) and by warming atmospheric layers above by absorption.

Recent model and observational results have indicated that the aerosol plume produced by biomass burning at the end of the dry season is transported to the south and may interact with frontal systems thus indicating a possible impact on the precipitation regime (Andreae et al., 2004; Freitas et al. 2004, 2005) through the radiative effect of the aerosols. From a purely observational point of view, Fu and Li (2004) have found some evidence that biomass burning aerosols might be influencing the rainfall distribution in the beginning of the wet season, based on comparisons between observed data and ECMWF precipitation estimates based on the reanalysis (because the reanalysis does not include the radiative effect of the biomass burning aerosols).

Rainfall can be further reduced due to the effect of aerosols as cloud condensation nuclei in warm clouds - they compete for the available water vapor, reducing the size of cloud droplets that remain in suspension in the air and do not fall as rain. Reduction in rainfall is a positive feedback effect making further fires more likely. This effect is particularly important in the Amazon basin (Rosenfeld et al. 2004) and it has not been explored in other regions downwind of the main biomass burning areas.

## **10.3 Land Use Change**

Various studies of observational or model generated data have quantified the statistical correlations between precipitation and land surface parameters (Dirmeyer, 2001; Koster et al, 2001; 2002; Reale and Dirmeyer, 2002; Reale et al, 2002; Koster et al, 2003; Koster and Suarez, 2004). Kalnay and Cai (2003), Kalnay et al (2004) have pioneered a new approach to separating surface temperature changes forced by changing boundary conditions from those expected from constant boundary conditions and observed atmospheric temperatures.

### *10.3.1 Deforestation*

The change in vegetation from forest to pasture or crop has a direct effect on surface albedo (increase) and roughness (decrease) and evaporation (decrease). Trees have deeper roots and sustain the evaporation for longer periods of time than the alternative vegetation. Therefore, the annual cycle of evapotranspiration in tropical forests

has been shown to be rather flat even in areas where the dry season is very well defined (Salati, 1987; Gash and Nobre, 1997; Werth and Avissar, 2004). A possible feedback between soil moisture and the monsoon activity over tropical S. America has been discussed by Grimm (2003) thus making a plausible case for the interaction between deforestation and precipitation changes through soil moisture processes.

The impact of deforestation in the tropical areas is somewhat different in the wet and dry seasons (Avissar et al. 2002). In the dry season, the non-forested areas become hot and dry. Relevant impacts occur in deforested regions in a scale of a few hundred of kilometres in width surrounded by forest. A local circulation develops from forest to non forest areas during day time leading to convergence of air in the non forest area inducing vertical motion which enhances cloudiness. Also, a drier surface leads to enhanced thermal turbulence which favours formation of clouds. During the dry season, shallow clouds are seen in visible satellite imagery, as a result. The shallow clouds would produce showers in clean conditions (see above the biomass burning issues). During the wet season, evaporation in forest and pasture are about the same but the darker forest reflects less radiation. The excess radiation over forest goes into heating and generates more thermal turbulence which favours the formation of clouds and rainfall. In the wet season it rains more over forest than over non forested areas.

Some observational evidence of the impact of deforestation is available. During the dry season, Cutrim et al (1995) showed that the preferred regions of formation for shallow cumulus clouds are deforested areas and over elevated terrain. Fisch et al (1999) and Fisch and Nobre (1999) show significant differences in the evolution and structure of the planetary boundary layer (PBL) between the dry and the wet season, indicating that the height of the mixed layer over extensive pastures is large in the dry season but decreases in the wet season; while over forest, the height of the mixed layer has basically little seasonal variation. It was found that there are more shallow clouds over deforested areas during the afternoon, and less deep convection at night during the dry season and that convection is stronger at night over deforested areas during the wet season. In conclusion, there is more precipitation over deforested areas in the wet season and less in the dry season and therefore increased seasonality. This conclusion is coherent with a northward shift of the equatorial-tropical transition zone.

The effects of deforestation on the regional climate have been studied through modelling techniques. Nobre et al (1991) showed that a complete replacement of forest by pasture in the Amazon Basin would lead to a local increase in temperature and decrease in precipitation. Several other studies have been published more recently, under scenarios of total deforestation in the Amazon and in general they point out to a reduction of the order of 20-30% in the regional precipitation and warming of the order of 2-3 oC (Silva Dias and Marengo, 1999, Nobre et al. 2002). These vegetation-climate modelling experiments have usually tested the effects of

radical changes in vegetation, such as the complete replacement of forest with cattle pasture, and have run the GCM to equilibrium following the implementation of this vegetation change. Using a set of simulations produced with the NASA Goddard Institute for Space Studies (GISS) general circulation model (GCM), Werth and Avissar (2002) find that the deforestation of the Amazon basin affects very significantly the hydroclimatology of the basin. Moreover, they find that this deforestation also affects the hydroclimatology of other locations on earth, including a significant reduction of precipitation in North America. In general, the further away from the tropics, the weaker the teleconnected signals. Teleconnection studies (Grimm and Silva Dias 1995) have indicated the possibility of significant remote impact (e.g. Europe) from anomalous precipitation in the region of the South Atlantic Convergence Zone but small effect associated with the anomalous heating in the Amazon region.

Model work on the impact of more realistic patterns of deforestation, with patches of the order of few hundred km to a few tens of km have been reported. Silva Dias and Regnier (1995) and Souza et al. (2000) show that local circulation impose a low level mass and moisture convergence over the pasture of enough magnitude to explain local cumulus cloud formation. Baida Roy and Avissar (2002) and Silva Dias et al. (2002) investigated the impact of deforestation at the microscale and the mesoscale on the formation of convective clouds during the dry season. Using simulations produced with the Regional Atmospheric Modelling System (RAMS) supported with satellite images, they find that deforested areas (pasture) trigger cloud formation. They also emphasize that synoptic flow advects the clouds away from their original location but does not eliminate them. In a follow up study, Weaver et al. (2002) and Baida et al (2003) investigated the various parameters, in addition to land-surface characteristics, that affect the development of mesoscale circulation generating clouds as a result of landscape heterogeneity. They find that model configuration (e.g., grid size, nudging strength, among others) can have an impact as important as that of the landscape heterogeneity.

New developments in dynamic vegetation schemes and coupled climate-carbon models (Cox et al., 2000; Betts et al 2004, and Huntingford et al. 2004) have shown that the physiological forcing of stomatal closure can contribute 20% to the rainfall reduction in the Amazon associated with rising atmospheric CO<sub>2</sub> levels. The forest die-back exerts two positive feedbacks on the precipitation reduction: (1) a biogeophysical feedback through reduced forest cover suppressing of local evaporative water recycling, and (2) a biogeochemical feedback through the release of CO<sub>2</sub> contributing to an accelerated global warming (Betts et al. 2004).

The forest die-back exerts two positive feedbacks on the precipitation reduction: (1) a biogeophysical feedback through reduced forest cover suppressing of local evaporative water recycling, and (2) a biogeochemical feedback through the release of CO<sub>2</sub> contributing to an accelerated global warming (Betts et al. 2004).

Considering the non-linear interaction between the atmosphere and vegetation through the sensible, latent and momentum transfer, radiation and that, in the long time scales, climate exerts the main control on vegetation and that the biome type influences climate, it is possible to conceive the existence of multiple equilibrium of the climate/vegetation system. Oyama and Nobre (2003) coupled a dynamical biome model to the global climate model of Center for Weather Forecasting and Climate Research in Brazil in order to study the equilibrium solutions. They have shown the possibility of two stable solutions for the particular case of the biomes of South America: the first stable solution provides a biome distribution similar to the observed in the present; the second solution is characterized the savannah in the eastern Amazon and semi-desert in the Northeast region of Brazil and the Atlantic Forest domain extended to the Central region of Brazil (Nobre et al. Oyama, 2004).

Nevertheless, it is still unclear the influence of land surface variations in explaining the slightly positive rainfall trends documented in southern Amazonia since the middle 1970's (Marengo 2004) and the significant positive trends detected in rainfall and streamflow over the subtropical portion of the La Plata Basin (Liebmann et al. 2002). Strong correlation with the SST anomalies in the Pacific and Atlantic oceans is usually detected and therefore a direct signal between deforestation and precipitation changes in the long term is not evident. More recent results have suggested different trajectories of the precipitation reduction as a function of deforestations (Avisar et al. 2002). *Figure 10.1* (an adaptation of Figure 1 of Avisar et al., 2002) suggests three different patterns, among many possible speculated options. One option suggests an increase in precipitation as a result of partial deforestation maybe due to the mesoscale circulations triggered by the deforestation as in Silva Dias et al. (2002).

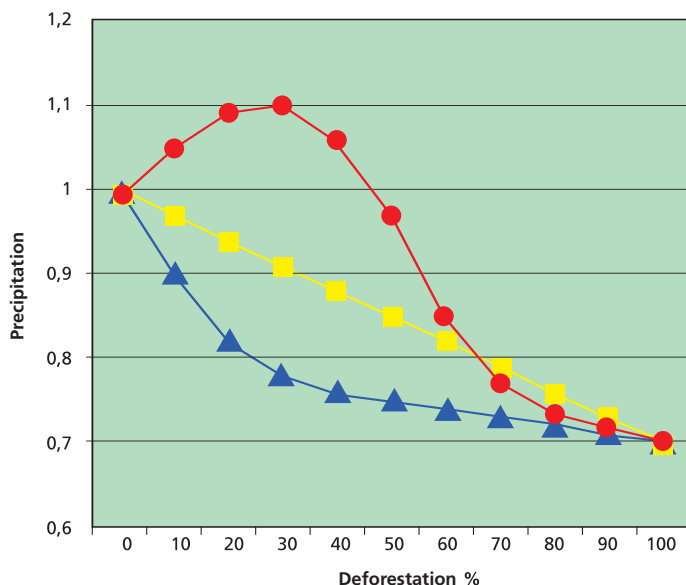


**Fig. 10.1.** Conceptual impact of deforestation in precipitation. The lines indicate results of three different models among many possible.

### *10.3.2 Urban effects*

Some features related with the urbanization effect over urban heat island (UHI) development have been clearly demonstrated over large urban areas in the La Plata Basin. In particular, observational studies in the Metropolitan Area of São Paulo (MASP) have indicated statistically significant impacts of the urbanization. Xavier et al. (1994) suggest a possible relationship between precipitation in São Paulo and the heat island effect. With increasing minimum temperature during the night, the probability of saturation during the night decreases. Furthermore, pollution increases the number of cloud condensation nuclei (CCN). The available water vapour is distributed among a larger number of CCN's which tend to remain in suspension in view of their smaller size and resulting decrease in the droplet fall velocity. Thus, the number of days with precipitation below 2mm has gradually decreased during the XX century. For intense precipitation (daily accumulation greater than 30mm), the effect is reversed: the increased thermal instability and the plausible effect associated with increased number of ice nuclei (associated with the urban pollution) tend to increase the probability of heavy precipitation. More recent results by Freitas and Silva Dias (2004) separate the radiative effect of the urban aerosol plume and the heat island forcing. It is shown that the radiative effect of the aerosols is significantly large, comparable to the thermodynamical forcing of the surface thermal forcing associated with the heat island effect

Although changes in the MASP climate have been attributed to the surface forcing and air pollution impact in cloud microphysics, remote effects associated with long term changes in the SST patterns can also be responsible for the observed changes. A diagnosis of the winter climatology cold temperature extremes in the Metropolitan Area of São Paulo (MASP) is presented in Goncalves et al. (2002). The diagnosis is based on temperature data at the Meteorological Station of Parque Estadual das Fontes do Ipiranga (IAG/USP) from 1950 to 2000. The persistence of synoptical and climatological patterns has been studied through principal component (PC) analysis and the results are compared to monthly anomalies in sea surface temperature (SST) of the Eastern Pacific and South Atlantic. The extreme cold air temperatures, on monthly bases, have shown no significant change since 1950. On the other hand, the mean monthly air temperatures have shown a slight warming trend, in agreement to the South Atlantic Ocean warming trend. The PC indicates significant loadings of two SST anomaly types: the cold anomaly of the South Atlantic Ocean, and the warm anomaly of the Southern Brazilian coast. The latter could also be responsible for some extreme cold events (for daily minimum temperatures) in the MASP, also presenting dominant westerly wind direction (SW to NW). Both the cold events and the westerly wind direction were evidenced in such winters as 1953, 1975, 1978, 1981 and 1994. On the other hand, the cold mean monthly temperatures are highly correlated to a broad cold pool anomaly in the South Atlantic near 25 to 35°S and 15 to 55°W. Thus, SST anomalies in the South Atlantic Ocean have a dominant effect on the S. Paulo winter temperature climatology.

SST anomalies also have influence on thunderstorm formation when associated with urban heat island effects. Freitas and Silva Dias (2004), throughout numerical simulations and factor separation analysis, showed that urban heat island positively contributed to the total precipitation during a severe thunderstorm episode occurred in February 01, 2003 in the Metropolitan Area of São Paulo (MASP) and that this contribution is dependent on SST, with distinct responses to its increasing or decreasing. With an increase of 2 °C in the observed SST the UHI can cause an increase of 28 % in the total accumulated precipitation in the grid domain. The same temperature increase in a situation that the SST is 2 °C colder results in an increase of 14 % only. In some areas of the studied domain the UHI contribution can cause an increase of the order of 100 %.

Thunderstorm formation and pollution dispersion can be also affected by the interactions between UHI and the sea breeze. Freitas et al (2005) showed that the complex interaction of these two circulations can be described in the following way. First, the urban heat island forms a strong convergence zone in the center of the city and thereby accelerates the sea breeze front toward the center of the city. The presence of the urban region increases the sea breeze front propagation mean speed by about 0.32 ms<sup>-1</sup>. Second, the sea breeze front stalls over the center of the city for about two hours, as the urban heat island eventually decelerates the sea breeze front propagation. This situation can contribute to the transport of humidity and pollutants to higher levels of the atmosphere.

## References

- Andreae, M.O., E.V. Browell, M.Garstang, G.L. Gregory, R.C.Harriss,G.F.Hill, D.J.Jacob,M.C.Pereira, G.W.Sachse, A.W.Setzer, P.L. Silva Dias, R.W.Talbot, A.L.Torres and S.C.Wofsy, 1988: Biomass burning emissions and associated haze layers in Amazonia. *J. Geophys.Res.*,Vol. 93,pp. 1509-1527.
- Andreae, M.O., D. Rosenfeld, P. Artaxo, A. A. Costa, G. P. Frank, K. M. Longo and M. A. F. Silva-Dias, Smoking rain clouds over the Amazon, 2004: *Science*, Vol 303, 1342-1345.
- Artaxo, P., Maenhaut, W., Storms, H. and Van Grieken, R.,1990: Aerosol characteristics and sources for the Amazon Basin during the wet season. *Journal of Geophysical Research* 95, 16971-16985.
- Artaxo, P., T. M. Pauliquevis and L. L. Lara, 2003: Dry and wet deposition in Amazonia: from natural biogenic aerosols to biomass burning impacts. *International Global Atmospheric Chemistry Project - Newsletter*, 27, 12-16.
- Avissar, R., Silva Dias, P. L.; Silva Dias, M. A. F. and Nobre, C.,2002: The Large-Scale Biosphere-Atmosphere Experiment in Amazonia (LBA): Insights and future research needs. *J. Geophys. Res.* 107, D20, LBA, pp. 54.1-54.6.
- Baidya, R.S. and R. Avissar, 2002: Impact of land use/land cover change on regional hydrometeorology in Amazonia. *Journal of Geophysical Research (Atmospheres)*, Volume 107, Issue D20, pp. LBA 4-1, CiteID 8037, DOI 10.1029/2000JD000266 (JGRD Homepage).

- Betts, R., Cox, P., Collins, M., Harris, P., Huntingford, C. and Jones, C., 2004: The role of ecosystem-atmosphere interactions in simulated Amazonian precipitation decrease and forest dieback under global change warming. *Theoretical and Applied Climatology*, Volume 78, Numbers 1-3, 1434-4483 (Online).
- Cox, P.M, R.Betts, C.D. Jones, S.A.Spall and I.J. Totterdell, 2000: Acceleration of global warming due to carbon-cycle feedbacks in a coupled climate model. *Nature* 408, 184 - 187 (09 November 2000); doi:10.1038/35041539.
- Cutrim, E., D. Martin and R. Rabin, 1995: Enhancement of cumulus clouds over deforested lands in Amazonia. *Bull. Amer. Met. Soc.*, 76, 1801-1805.
- Echalar, F., Artaxo, P., Martins, J.V., Yamasoe, M., Gerab, F. Maenhaut, W. and Holben, B., 1998: Long-term monitoring of atmospheric aerosols in the Amazon Basin: Source identification and apportionment. *Journal of Geophysical Research* 103, 31849-31864.
- Fisch, G. F. and Nobre, C. A., 1999: Carbon dioxide measurements in the nocturnal boundary layer over Amazonian Tropical Forest Carbon pools and dynamics in tropical ecosystem. *Advances In Soil Sciences*, v. 1, p. 5-7.
- Fisch, G. F. ; Culf, A. D. ; Malhi, Y. ; Nobre, C. A. and Nobre, A. D., 1999: Carbon dioxide measurements in the nocturnal boundary layer over Amazonian forest. In: Lal, R; Stewart, B. (Org.). *Global climate change and tropical ecosystem*, , p. 301-403.
- Freitas, E.D. and Silva Dias, P. L, 2005: Some effects of urban áreas in the generation of the heat island. Submitted to the *Revista Brasileira de Meteorologia*.
- Freitas, S. R., K. M. Longo, M.A.F.Silva Dias and P. Artaxo, 1996: Numerical modeling of air mass trajectories from the biomass burning areas of the Amazon Basin. *Anaes da Academia Brasileira de Ciências*,v.68, (Supl 1), 193-206.
- Freitas S.R., K.M. Longo, M.A.F.Silva Dias, P.L. Silva Dias, F.S. Recuero, R. Chatfield, E. Prins, P. Artaxo, G.Grell and F.S. Recuero, 2004: Monitoring the Transport of Biomass Burning Emissions in South America. *Environmental Fluid Mechanics*, 5, 135-167.
- Gash, J. and Nobre, C. A., 1997: Climatic effects of Amazonian deforestation: some results from ABRACOS. *Bulletin of the American Meteorological Society*, v. 78, n. 5, p. 823-830.
- Gonçalves, F.L.T., P.L. Silva Dias and G.P. Araújo, 2002: Climatological analysis of wintertime extreme low temperatures in São Paulo City, Brazil: impact of sea-surface temperature anomalies. *International Journal of Climatology*, Volume 22, Issue 12, 1511-1526.
- Grimm, A. M. and P. L. Silva Dias, 1995: Analysis of tropical-extratropical interactions with influence functions of a barotropic model. *J. Atmos. Sci*, 52, 20, 3538-3555.
- Grimm, A.M, 2003: The El Niño Impact on the Summer Monsoon in Brazil: Regional Processes versus Remote Influences. *J. Climate*,16, 263-280.
- Haberle, S.H. and Maslin, M.A., 1999 Late Quaternary Vegetation and Climate Change in the Amazon Basin Based on a 50,000 Year Pollen Record from the Amazon Fan, ODP Site 932. *Quaternary Research*, 51, 27-38..
- Huntingford, C., P. Harris, N. Gedney, P. Cox , R. Betts, J. Marengo, and J. Gash, 2004: Using a GCM analogue model to investigate the potential for Amazonian forest dieback. *Theoretical and Applied Climatology* Volume 78, Numbers 1-3 , 1434-4483.
- Liebmann, B ; Marengo J. A., 2002: The Seasonality and Interannual Variability of Rainfall in the Brazilian Amazon Basin. *Journal of Climate*, Boston, v. 14, p. 4308-4318.
- Kirchhoff, V. W. J. H., E. Marinho, P. L. Silva Dias, R. V. Calheiros, A. R. Volpe 1991: O<sub>3</sub> and CO from burning sugar cane. *Nature*, London, 339, pg. 264.

- Liu K. B. and Colinvaux, P.A., 1988: A 5200-year history of Amazon rain forest. *Journal of Biogeography*, 15, 231-248.
- Marengo J. A., 2004: Interdecadal variability and trends in rainfall in the Amazon basin. *Theoretical And Applied Climatology*, United Kingdom, UK, v. 78, n. 1-3, p. 79-96.
- Moreira, D.S., P.L.Silva Dias and A.Beltran, 2004: Dry to Wet Transition Simulation with Dynamic Vegetation. III LBA International Conference, Brasília Brazil, July 2004. Paper 45.10-P.
- Martin, L.; Absy, M.L.; Flexor, J.M.; Fournier, M.; Mouguiart, P; Siferdine, A. and Turcq, B.J., 1992 : Enregistrement de conditions de type El Nino, en Amerique du Sud, au cours des 7000 dernieres annees. *C. R. Acad. Sci. Paris*. t. 315. 97-102.
- Martins, J. V., P. Artaxo, C. Lioussé, J. S. Reid, P. V. Hobbs and Y. J. Kaufman, 1998: Effects of black carbon content, particle size and mixing on light absorption by aerosol particles from biomass burning in Brazil. *Journal of Geophysical Research* 103, 32041-32050.
- Nobre, C. A., Sellers, P. and Shukla, J., 1991 :. Regional Climate Change And Amazonian Deforestation Model. *Journal of Climate*, v. 4, n. 10, p. 957-988.
- Nobre, C. A. and Oyama, M. D., 2004: A simple potential vegetation model for coupling with the Simple Biosphere Model (SIB). *Revista Brasileira de Meteorologia*, v. 19, n. 2, p. 203-216
- Nobre, C. A., Artaxo, Silva Dias, M. A. F., Victoria, R. L., Nobre, A. D. and Krug, T., 2002: The Amazon basin and land-cover change: a future in the balance?. In: *Global Change - The IGBP Series*. (Org.). Vegetation, water, humans and the climate. New York, v. 26, p. 137-141.
- Oyama, M. D. and Nobre, C. A., 2003: A new climate-vegetation equilibrium state for Tropical South America. *Geophysical Research Letters*, EUA, v. 30, n. 23, p. 5-1-5-4.
- Procópio, A. S., P. Artaxo, Y. J. Kaufman, L. A. Remer, J. S. Schafer and B. N. Holben, 2004: Multiyear analysis of amazonian biomass burning smoke radiative forcing of climate. *Geophysical Research Letters*, 31, 3, L03108 - L03112, doi:10.1029/2003GL018646.
- Salati, E., 1987: The forest and the hydrological cycle, In Dickinson R.E. eds. *The Geophysiology of Amazonia*, Wiley, New York., 273-296.
- Schafer, J. ; Holben, B. ; Eck, T. ; Yamasoe, M. A. and Artaxo, P. , 2002: Atmospheric effects on insolation in the Brazilian Amazon: Observed modification of solar radiation by clouds and smoke and derived single scattering albedo of fire aerosols. *Journal of Geophysical Research*, EUA, v. 107, p. 41-1-41-15.
- Silva Dias, M. A. F. and P. Regnier 1995. Simulation of mesoscale circulation in deforested areas of Rondonia in the dry season. In *Amazon Deforestation and Climate*, eds. J.C.H. Gash, C.A. Nobre, J.M. Roberts and R. Victória. John Wiley & Sons, Chichester, UK, p. 531-548.
- Silva Dias, P.L. and J. Marengo, 1999: Águas Doces do Brasil: Águas Atmosféricas, Capital Ecológico, Uso e Conservação. Editado por A.Rebouças, B. Braga e J. Tundizi. Instituto de Estudos Avançados e Academia Brasileira de Ciências, pp 65-115.
- Silva Dias, M. A. F., S. Rutledge , P. Kabat, P.L. Silva Dias, C. Nobre, G. Fisch, A.J. Dolman, E. Zipser, M. Garstang, A. Manzi, J. D. Fuentes, H. Rocha, J.Marengo, A. Plana-Fattori, L. Sá, R. Alvalá, M. O. Andreae, P. Artaxo, R. Gielow and L. Gatti, 2002a: Clouds and rain processes in a biosphere atmosphere interaction context, *J. Geophys. Res.* 107, D20, LBA, pp. 46.1- 46.23.
- Silva Dias , M.A.F., W. Petersen, P. Silva Dias, R. Cifelli, A. K. Betts A. M. Gomes, G. F. Fisch, M. A. Lima, M. Longo (IC ), M. A. Antonio and R. I. Albrecht, 2002b: A case study of the organization of convection into precipitating convective lines in the Southwest Amazon, *J. Geophys. Res.* 107, D20, LBA, pp. 39.1- 39.20.

- Souza, E. P., N. O. Rennó and M.A.F. Silva Dias, 2000: Convective circulations induced by surface heterogeneities. *Journal of Atmospheric Sciences*, 57, 2915-2922.
- Xavier, T.M.B.S , A.F.S.Xavier and M.A.F.Silva Dias, 1994: Evolução da Precipitação Diária num Ambiente urbano: O Caso da Cidade de São Paulo. *Rev. Brasileira de Meteorologia*, Vol. 9, 44- 53.
- Werth, D. and R. Avissar, 2002. The local and global effects of Amazon deforestation, *J. Geophys. Res.*, 107, 8087, doi:10.1029/2001JD000717.
- Werth, D. and R. Avissar, 2004. The regional Evapotranspiration of the Amazon. *J. Hydromet.*, 5, 100-109.

## GLOBAL CLIMATE MODELS

*Tércio Ambrizzi<sup>1</sup>*

<sup>1</sup> Universidade de São Paulo, Brasil.

### ABSTRACT

The purpose of this chapter is to provide an overview of the development and use of three-dimensional computational models of the global climate system, including its four main components: atmosphere, oceans, land and marine ice. In this description, it will be assumed that the reader has only a vague idea about climate models and it will be provided a basic understanding of what the models are trying to simulate, of how they are built, what has them managed to simulate and how they are used for evaluative purposes and predictions. After a short introduction, a brief description of an Atmospheric General Circulation Model will be given (MCG) and it will be discussed its use for Climatic Change studies and the uncertainties of these studies.

## 11.1. Introduction

A large number of climate change experiments using Global Climate Models (GCMs) have been completed in recent years, both equilibrium and transient experiments, and both experiments forced with changes in greenhouse gas concentrations alone and those forced with greenhouse gas and sulphate aerosol changes. A number of parallel experiments have also been completed using high resolution Regional Climate Models. Results from a considerable number of these experiments have been used in climate change impacts and adaptation assessments. It is not always easy, however, to know which experiment has been used in an impacts study, nor how the particular modelling results fit into the larger population of GCMs climate change experiments.

Comprehensive climate models are based on physical laws represented by mathematical equations that are solved using a three-dimensional grid over the globe. For climate simulation, the major components of the climate system must be represented in sub-models (atmosphere, ocean, land, surface, cryosphere and biosphere), along with the process that go on within and between them. Global climate models in which the atmosphere and ocean components have been coupled together are also known as Atmosphere-Ocean General Circulation models (AOGCMs). Most results to be presented in this report are derived this kind of models.

Climate models have developed over the past few decades as computing power has increased. During that time, models of the main components, atmosphere, land, ocean and sea ice have been developed separately and then gradually integrated. This coupling of the various components is a difficult process. Most recently, sulphur cycle components have been incorporated to represent the emissions of sulphur and how they are oxidized to form aerosol particles. Currently in progress, in a few models, is the coupling of the land carbon cycle and the ocean carbon cycle (IPCC 2001). The atmospheric chemistry component is currently modelled outside the main climate model. The ultimate aim is to model as much as possible of the whole of the Earth's climate system so that all the components can interact and, thus, the predictions of climate change will continuously take into account the effect of feedbacks among components. *Figure 11.1*, obtained from the Intergovernmental Panel on Climate Change report from 2001 (IPCC 2001), shows the past, present and possible future evolution of climate models.

In summary, from the description above, one can see that the GCMs can be very complex, however, can we grasp how do they work? In the next section, some basic ideas about these models will be addressed.

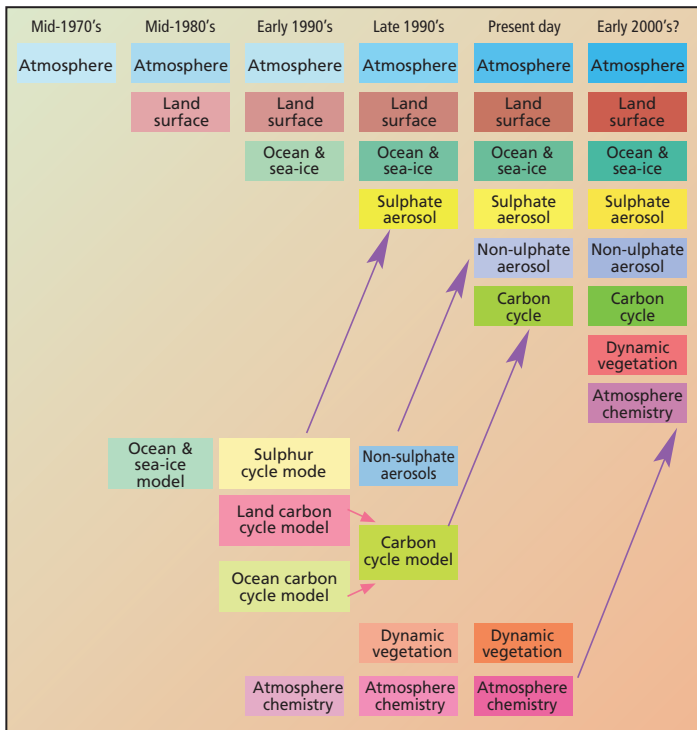


**Fig. 11.1.** Development of climate models over the last 25 years showing how the different components were first developed separately and later coupled into comprehensive climate models.

## 11. 2. Atmospheric General Circulation Models (AGCMs)

Zero-, one- and two-dimensional climate models present a qualitative picture of how the atmospheric climate system works. However, these models either neglect various processes that are known to be important in the atmosphere, or they use simple mathematical representations for these atmospheric process. The representation of these processes is called parameterization. In order to accurately account for the general motions of the atmosphere requires the solution of a complete set of equations. The solution of these equations on the sphere, given realistic boundary conditions, defines the AGCM (Trenberth 1993).

An AGCM to be implemented requires: a numerical solution technique, algorithms for the various physical parameterizations, and boundary data sets for predetermined vertical and horizontal resolutions. The solution of the system of equations (called primitive) and parameterizations proceeds is outlined in *figure 11.2*. Assuming initial data are available for the prognostic variables, the model calculates initial fluxes for use in the planetary boundary layer (PBL) and surface components of the model. These, along with the thermodynamic and moisture profiles at each gridpoint, are used to test whether the atmospheric column is stable or unstable. If unstable, a convection parameterization is used to determine the convective heating and moistening terms. Otherwise, if saturated, the stable condensa-

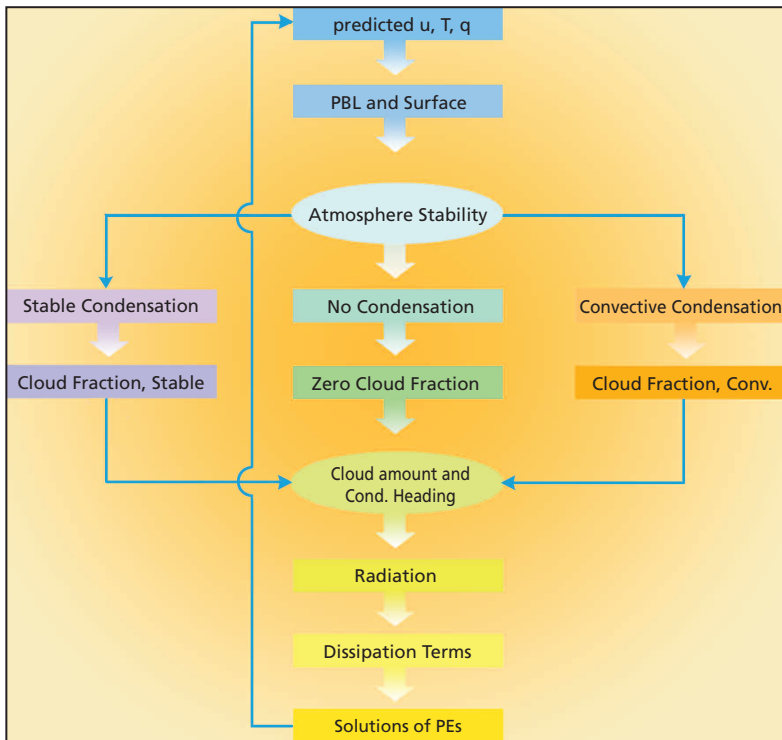


**Fig. 11.2.**  
Diagram of the  
procedures  
employed in an  
AGCM.

[Adapted from  
Kiehl 1993]

tion process is invoked. Based on the type of condensation process, cloud fractions are assigned to model layers. Condensational heating and cloud amounts are stored for further use for the radiation process. Radiative fluxes and heating rates are then calculated based on the thermal, moisture and cloud profiles in the atmosphere. Mechanical dissipation terms are then determined. At this point all forcing and dissipative terms of the primitive equations are available, and a numerical solution technique (e.g., Hack 1993) is applied to obtain new values for the prognostic variables. Note that *figure 11.2* only shows one of the ways that the sequence of the model physics could be calculated.

The number of iterations of the above procedure is usually determined by the problem under consideration, which in turn is governed by time scales inherent to the various physical processes. The time length of the AGCM integration can go from a few days for weather forecast, to a few months for climate prediction, or even thousand of years for climate change projections.

Usually the boundary conditions to be specified in a climate system model are: sea surface temperature, surface albedo (which is determined by the surface vegetation), distribution of sea ice, ozone mixing ration and other climatologic observations. A summary of the most frequent prescribed boundary data used by the AGCMs is presented in *table 11.1*.

**Table 11.1.** Boundary data sets required for an AGCM.

Source: CIER Magazine N° 43

Boundary Data	Parameterization	Dimensions
Sea Surface Temperature	Radiation and PBL	Lat, Lon and Time
Surface type (land, ocean, ...)	Surface temperature	Lat, Lon
Surface roughness length	Surface	Lat, Lon
Land hydrology	Surface	Lat, Lon
Surface albedos	Radiation	Lat, Lon
Ozone mixing ration	Radiation	Lat, Lon
Orography	Dynamics	Lat, Lon
Subgrid variance of orography	Gravity wave drag	Lat, Lon

One of the most challenging aspects of modeling the climate system is the treatment of nonresolvable physical processes, otherwise known as parameterization. Atmospheric processes operate over a very wide range of time and space scales. Because of computational cost, however, numerical integrations of the governing meteorological equations explicitly resolve only the primary energetic and phenomenological scales of motion. Nevertheless, there are significant interactions between the explicitly resolved large-scale flow and the truncated scales of motion which must be accounted for in some way. Parameterization techniques seek to express the statistical contribution of these nonresolvable processes to the time evolution of the explicitly resolved motions. At the same time, the contributions of these nonresolvable motions are diagnosed as functions of the large-scale fields. As observed from the *table 11.1*, there are many physical parameterizations employed by AGCMs and the continued success of atmospheric modeling depends on improving these various parameterizations.

The treatment of the water budget is the most difficult component of the parameterization problem. Convective scale motions (e.g., motions on the order of several km) are responsible for most of the phase change and associated precipitation occurring in the atmosphere. These processes occur well below the resolvable scales of motion in a GCM, but represent a very large, and often dominant, local energy source/sink in the climate system. The effect of convective motions on the evolution of the thermal, moisture and even dynamical properties in the model atmosphere must be parameterized. Since the meteorological term for convective clouds is cumulus, in the atmospheric modeling community it is also called cumulus parameterization. These parameterizations are, in general, for deep convective clouds that occur in regions of moisture convergence. Over the years, several deep convective parameterizations have been developed for AGCMs. Like many parameterizations, the unresolved properties must be linked to the large scale model variables, see for instance Kiehl (1993) for a detailed description of the method and examples.

Examples of other physical processes that must be parameterized are the transfer of long wave and shortwave radiation in the atmosphere, surface energy exchanges, atmospheric boundary layer process, vertical and horizontal diffusion processes, etc. Certain parameterized process can be treated completely independently from all other nonresolvable processes. Other processes tend to be more tightly coupled with each other (e.g., planetary boundary layer, convection, cloud formation, and radiative transfer).

### **11.3. AGCMs uncertainties and their use for climate change studies**

The confidence in future scenarios obtained in model results relies on the ability of the models in representing the present climate. Results of the present climate simulation by several models were discussed in Gates et al. (1999) for the Atmospheric Model Intercomparison Project (AMIP). The largest errors of the ensemble mean were found in the cloudiness and 200 hPa temperature and the smallest errors were identified in the surface air temperature. Global hydrological processes for the AMIP results were discussed in Lau et al. (1996) comparing results from 29 models. Although there was large variability among models, the ensemble mean results of all models were very close to the observations. The ensemble of the models overestimated the rainfall in the tropics and underestimated it in the extratropics.

The MCGs have been increasing their complexity to represent in an increasingly suitable manner the physical processes of the climatic system. Though they cannot still represent all of the processes and certain difficulties specially related to the interaction between the radiation and the aerosols exist, their capacity to represent the current climate has been improving, offering an increasing reliability on future projections. The results of these models developed by institutes with high scientific and computer capacity are available through the web page of the Distribution Data Centre (DDC) of the IPCC ([www.dkrz.de/ipcc/ddc/html/SRES/SRES\\_all.html](http://www.dkrz.de/ipcc/ddc/html/SRES/SRES_all.html)). Another set of information comes from a simulation of 50 years made by the CPTEC used for the analysis of the current climatology. *Table 11.2* lists the models and organizations responsible for each of them as well as the period with available information.

In Fact, the confidence in the ability of models such as AGCMs or AOGCMs to project future climates is increased by the ability of several models to reproduce warming trends in the 20th century surface air temperature when driven by the observed increase of greenhouse gases and sulphate aerosols. This is illustrated in *figure 11.3*. This figure shows three independent simulations with the same greenhouse gas plus aerosol forcing and slightly different initial conditions and a control run with initial conditions of the levels of atmospheric CO<sub>2</sub> referred to as pre-industrial era.

**Table 11.2.** MCG with available information through DDC.

Model	Institution	Current Period	Future Period
HADCM3	Hadley Centre for Climate Prediction and Research (Reino Unido)	1950-1999	
CSIRO-mk2	Australia's Commonwealth Scientific and Industrial Research Organization (Australia)	1961-1999	1961-2100
ECHAM4/OPYC3	Max Planck Institute für Meteorologie (Alemania)	1990-1999	1990-2100
GFDL-R30	Geophysical Fluid Dynamics Laboratory (Estados Unidos)	1961-1999	1961-2100
NCAR-PCM	National Centre for Atmospheric Research (Estados Unidos)	1981-1999	1981-2100
CCCma	Canadian Center for Climate Modeling and Analysis (Canadá)	1950-1999	1950-2100
CPTEC/COLA	Centro de Previsão de Tempo e Estudos Climáticos	1950-1999	In development

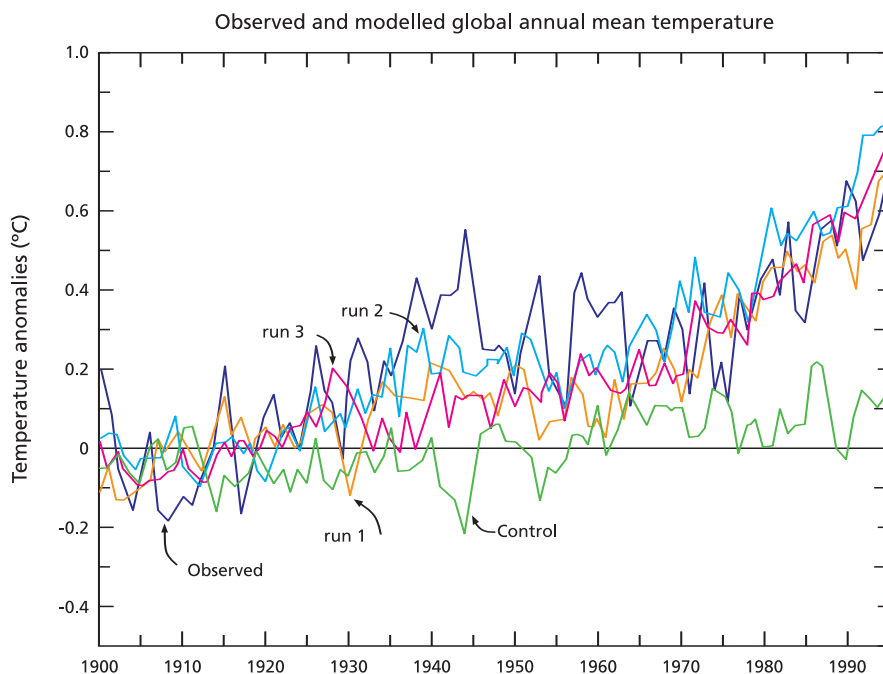


**Fig. 11.3.** Observed and modelled global annual mean temperature anomalies ( $^{\circ}\text{C}$ ) relative to the average of the observations over the period 1900 to 1930. The control and three independent simulations with the same greenhouse gas plus aerosol forcing and slightly different initial conditions are shown from an AOGCM. The three greenhouse gas plus aerosol simulations are labelled 'run 1', 'run 2', and 'run 3' respectively.

[Adapted from IPCC 2001]

The last shows a trend much lower than the observed but also positive. This can be explained because some studies suggest that there were additional forcings like solar and volcanic aerosols variability. The observed temperature anomaly along the century was also plotted. As can be seen, in general, there is a reasonable adjustment between the model and the observations with regard to long term trends, but the model does represent in an adequate manner the interannual variability. This is because of the intrinsically unpredictable character of the natural variability of the climatic system and according to this, no matter how perfect the models could be, the interannual variability in the long term will never be able to be well simulated. Meanwhile it is to be noticed that the trend of increase represented by the model follows the observed trend. Some further results of climate change simulation can be seen in the Chapter 12 and 13.

Model intercomparison studies, such as those discussed above, provide valuable information on the differences between GCM projections and the reasons for these differences. However, the range of differences between GCM results is unlikely to be indicative of the full range of uncertainties about future climate. Three main sources of uncertainty can be identified:

1. Uncertainties in future greenhouse gas and aerosol emissions. The IS92 and provisional SRES emissions scenarios described in Chapter 12 exemplify these uncertainties, with each scenario implying different levels of atmospheric composition and hence of radiative forcing.
2. Uncertainties in global climate sensitivity, due to differences in the way physical processes and feedbacks are simulated in different models. This means that some GCMs simulate greater mean global warming per unit of radiative forcing than others.
3. Uncertainties in regional climate changes, which are apparent from the differences in regional estimates of climate change by different GCMs for the same, mean global warming.

While the results of GCM experiments probably capture a large part of the uncertainty ranges in 2 and 3, they certainly cannot describe the range of uncertainty due to emissions described in 1. Due to constraints of time and resources, only a limited number of GCM experiments can be conducted. In addition, many experiments have been specifically designed to be directly comparable with other models, to aid model development, and their assumed forcing is very similar. Most early GCM experiments were for a hypothetical  $2 \times \text{CO}_2$  equilibrium case. The AOGCM outputs in the DDC are for transient forcing approximating to a 1% increase in equivalent  $\text{CO}_2$  per year (close to the IS92a emissions scenario). One set of runs for an IS92d emissions scenario (approximately a 0.5%/year increase) is also included from the HadCM2 model. Some alternative emissions scenarios have also been used in experiments with the GFDL model assuming 0.25, 0.5, 1, 2, and 4%/year increases (Kattenberg et al. 1996), but these are not included in the DDC.

Although changes in weather and climate extremes are important to society in general, it is only recently that evidence for changes we have observed until now has been able to be compared to similar changes that we see in model simulations for future climate (see Chapter 12). Despite of the global models have improved over time, they still have limitations that affect the simulation of extreme events because of the insufficient spatial resolution and of simulation errors, and because parameterizations that must represent processes that cannot yet be included explicitly in the models, particularly dealing with clouds and precipitation, are not adequate to represent this extreme events (Meehl et al. 2000).

There is no general agreement yet among models concerning future changes in mid-latitude storms (intensity, frequency and variability), though there are now a number of studies that have looked at such possible changes and some show fewer weak but greater numbers of deeper mid-latitude lows, meaning a reduced total number of cyclones, which agree with some observational studies (e.g., Pezza and Ambrizzi 2003 and references therein). Due to the limitations of spatial resolution in current AOGCMs, climate models do not provide any direct information at present regarding lightening, hail, and tornadoes. These limitations are particularly important over the La Plata basin, once that a large percentage of its precipitation comes from MCCs and mid-latitude front systems. If the models are not able to include such systems, they will certainly have problems to correctly simulate the rainfall amount over the region.

## References

- Gates, W. L., J. S. Boyle, C. Convey, G. G. Dease, C. M. Doutriaux, R. S. Drach, M. Fiorino, P. J. Gleckler, J. J. Hnilo, S. M. Marlais, T. J. Phillips, G. L. Potter, B. D. Santer, K. R. Sperber, K. E. Taylor and D. N. Williams 1999: An overview of the results of the atmospheric model intercomparison project (AMIP I). *Bull. Amer. Meteor. Soc.*, 80, 29-55.
- Hack, J. J. 1993: Climate Sytem simulation: basic numerical and computational concepts. In *Climate System Modeling*, K.E. Trenberth editor, Cambridge University Press, 283-318.
- Intergovernmental Panel on Climate Change 2001: *Climate Change 2001: The Scientific Basis*. Cambridge University Press, 881pp.
- Kattenberg, A., F. Giorgi, H. Hrassl, G. A. Meehl, J. F. B. Mitchell, R. J. Stouffer, T. Tokioka, A. J. Weaver and T. M. L. Wigley 1996: In: *Climate Change 1995: The Science of Climate Change*. Contribution of Working Group I to the Second Assessment Report of the Intergovernmental Panel on Climate Change [Houghton, J.T., L.G. Meira Filho, B.A. Callander, N. Harris, A.Kattenberg, and K. Maskell (Eds). Cambridge University Press, Cambridge, United Kingdom and New York, NY, USA, 572pp.
- Kiehl, J. T. 1993: Atmospheric general circulation modeling. In *Climate System Modeling*, K.E. Trenberth editor, Cambridge University Press, 319-369.

- Meehl, G. A., F. Zwiers, J. Evans, T. Knutson, L. Mearns and P. Whetton 2000: Trends in extreme weather and climate events: issues related to modeling extremes in projections of future climate change. *Bull. Amer. Meteor. Soc.*, 81, 427-436.
- Lau, K. M., J. H. Kim and Y. Sud 1996: Intercomparison of Hydrologic processes in AMIP GCMs. *Bull. Amer. Meteor. Soc.*, 77, 2209-2227.
- Pezza, A. B. and T. Ambrizzi 2003: Variability of Southern Hemisphere cyclone and anticyclone behaviour: further analysis. *J. Climate*, 17, 1075-1083
- Trenberth, K. E. 1993: *Climate System Modeling*. Cambridge University Press, 788pp.

## CLIMATE SCENARIOS

*Inés Camilloni<sup>1</sup>, Iracema Fonseca de Albuquerque Cavalcanti<sup>2</sup> and Tércio Ambrizzi<sup>3</sup>*

<sup>1</sup> Universidad de Buenos Aires/CONICET, ARGENTINA.

<sup>2</sup> Centro de Previsão de Tempo e Estudos Climáticos/  
Instituto Nacional de Pesquisas Espaciais, Brasil.

<sup>3</sup> Universidade de São Paulo, Brasil.

### ABSTRACT

Socio-economic variables and also some of the variables that drive climate may change in the future in many different ways, being impossible to predict which will be the actual one. Future climate scenarios are to be constructed according to certain hypothesis about future human activities that alter the composition of the atmosphere and as a consequence the global climate. This chapter describes the different available methodologies for preparing future climate scenarios; in particular, the advantages and disadvantages of global climate models are introduced. Scenarios of climate change at global scale for the period 2071-2100 with regard to 1961-90 baseline for surface temperature, precipitation and sea level pressure provided by an ensemble of global models are presented.

## 12.1. Introduction

Climate scenarios are representations about the future, consistent with assumptions on future greenhouse gases (GHG) emissions and other pollutants and with the scientific updated knowledge about the effect that the increase in the concentration of these gases will have on the global climate. Hence, they describe how given certain future human activities, the composition of the atmosphere and consequently global climate are expected to change. Therefore, climate scenarios are a guide on how climate could be in the upcoming decades, according to a set of assumptions that include: future trends on energy demand, GHG emissions, changes in the land use and approximations to the physical laws that rule the behavior of the climatic system over long periods of time. It is important to bear in mind that the uncertainty that surrounds these assumptions is large and will determine the range of possible scenarios. With this information, it is intended to estimate how both natural systems and human activities will be affected.

The election of climate scenarios for the evaluation of impacts is important since the extreme scenarios may produce extreme impacts while more moderate scenarios probably show more modest impacts. In consequence, the election of scenarios can be controversial unless the uncertainties inherent to future projections are adequately specified in the impact analyses.

The scenarios of emissions, based on assumptions about possible social and economic evolutions of the world, feed the projections of the GHG concentrations. They were made by request of the Intergovernmental Panel for Climate Change (IPCC) and constitute the base upon most scenarios for future climate were made.

## 12.2. Criteria for the selection of regional climate scenarios

For climate scenarios to be useful for the assessment of impact and decision making it is advisable that their elaboration comply with five basic criteria:

*Consistency with global projections:* When the scenarios are not developed from global scenarios, they must be consistent with the wide range of global warming projections based on the increase of GHG concentrations. This range varies between 1.4° and 5.8°C (IPCC 2001).

*Physical plausibility:* They should be physically plausible; this means that they must not violate basic physical laws. Therefore, changes in a region must be consistent with those in other regions and globally. In addition, the combination of changes in different variables (which frequently are correlated with one another) must be physically consistent.

*Applicability in impact assessments:* They must describe changes in the adequate variables, as well as in the spatial and temporal scales, that allows for impact assessment. For example, several impact models can require entry data of certain variables such as precipitation, solar radiation, temperature, humidity and wind speed at spatial scales that may range from global to local along with time scales varying from annual averages to daily or hourly values.

*Representativity:* Must be representative of the potential range of future regional climate changes.

*Accessibility:* They must be straightforward to obtain, interpret and apply for impact assessments.

### **12.3. Techniques for developing climate scenarios**

Climate scenarios can be classified in three main types: Synthetic, analogue and based on outputs from global climate models (GCMs).

#### *12.3.1. Synthetic scenarios*

They are built in such a way that certain climatic variables are changed in an arbitrary but realistic amount, frequently according to a qualitative interpretation of the climate model simulations for a region. For example, magnitudes of future change can be represented through +1°, 2°, 3° and 4°C rise regarding the baseline temperature, and changes in ±5, 10, 15 and 20% regarding the baseline precipitation.

The major disadvantage of the synthetic scenarios is their arbitrary nature. Frequently they present a realistic set of changes that are physically possible, in general representing uniform adjustments in space and time that are inconsistent among variables. Likewise, some scenarios can be inconsistent with the range of uncertainty of global changes. However, this limitation can be overcome when the selection of synthetic scenarios is guided by information provided by GCMs.

#### *12.3.2. Analogue scenarios*

They are constructed by the identification of climatic regimes observed in a certain region or period, which may resemble the future climate. These records can be obtained both from the past of a same region (temporal analogue) or from another region, which currently has the climate that is presumed would be at the time of the scenario in the region of interest (spatial analogue).

*a. Temporal analogue scenarios*

Temporal analogues make use of climatic information from the past as an analogue of a possible future climate. These analogue scenarios are of two types: paleoclimatic based on information from geological records and analogue scenarios selected from instrumental historic records usually from last century. Both methods were used to identify periods when the temperature at a global or regional scales was warmer than at present. Other climatic characteristics during these warm periods (e.g., rainfall, wind speed, etc.) if available, are then combined with the temperature patterns in order to define the climate scenario. This way, a set of observational data that define a physically feasible climate is available.

The paleoclimatic analogues are based on reconstructions of past climate from fossil evidences such as plant or animal remains and sedimentary deposits. In particular, three periods received special attention: the mid-Holocene (5000-6000 years before present) with northern hemisphere temperature estimated in 1°C warmer than today, the Last Interglacial (125000 years before present) approximately 2°C warmer than present and the Pliocene (3-4 millions years before present) about 3°- 4°C warmer.

The major disadvantage of using temporal analogues for climate scenarios is that changes in past climates were unlikely caused by the increase of GHG concentrations. Paleoclimatic changes were likely caused by variations in the Earth's orbit around the Sun. This implies that apart from a global forcing similar to GHG, there was a latitudinal differentiated forcing. In the same way, changes observed during the instrumental period, like the 1930 decade drought in North America, were likely related to changes in the atmospheric circulation due to the natural climate variability at decadal scale, and therefore, cannot be extended to scenarios of permanent change due to GHG emissions.

*b. Spatial analogue scenarios*

Spatial analogues are regions that at present have a climate analogous to the study region in the future. This approach has strong restrictions since frequently there is a lack of correspondence among other climatic and non-climatic features of both regions.

*12.3.3. Scenarios from global climate models outputs*

GCMs represent physical processes in the atmosphere, oceans, cryosphere and the land surface and constitute the most reliable tool for simulating the response

of the global climate system to the increase of GHG concentrations. Likewise, high resolution models nested in the boundary conditions provided by the GCMs have the potential to provide geographically and physically consistent estimates of regional climate change.

The limitations of use of GCMs outputs for impact assessments can be summarized as:

- I) The large computing resources needed to undertake GCM simulations and store their outputs, which restricts the range of experiments capable to be carried out.
- II) The coarse spatial resolution compared to the scale of many impact assessments
- III) The difficulty to distinguish an anthropogenic signal from the noise of natural internal model variability
- IV) The difference in the climatic response among the different models.

## **12.4. Development of other scenarios**

Independently if in future climate changes will take place, there will be modifications in the socio-economic and environmental conditions. Therefore in the preparation of future scenarios is necessary to make projections about the way these factors will change.

### *12.4.1. Socio-economic scenarios*

The most important cause of the rapid changes observed in the atmospheric composition is the human economic activity, which produces GHG and aerosol emissions and changes in the land cover and land use. The socio-economic scenarios developed by the IPCC in its last report and called SRES Scenarios include projections up to year 2100 and although they are frequently called “emissions scenarios”, they contain a wide variety of socio-economic assumptions.

The following terminology is used in reference of these scenarios:

- **Storyline:** It consists of a narrative description of a scenario (or family of scenarios) with emphasis in the main characteristics and dynamics of the scenario.
- **Scenario:** projections of a potential future, based on the quantification of a storyline
- **Scenario family:** one or more scenarios with the same demographic, politico-societal, economic and technological storyline.

The IPCC has proposed four scenarios families: The storylines of each of these families describes a demographic, politico-societal, economical and techno-

logical future. Within each family one or more scenarios consider the global energy, the industry and other developments together with their implications in terms of GHG and other pollutant emissions. Although the storylines do not contain explicit climate change policy measures, there are some examples of indirect mitigation actions in some scenarios.

The four marker scenarios called A1, A2, B1 and B2, combine two sets of divergent trends: one set varying between strong economic values and strong environmental values and the other set between increasing globalization and increasing regionalization (Fig. 12.1). The storylines can be described as follows:

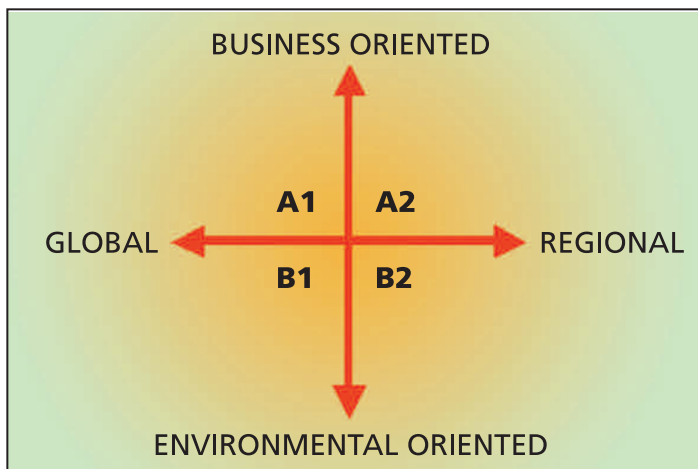


*Fig. 12.1.*  
Dimensions involved in  
the four scenarios of  
SRES emissions  
proposed by the IPCC.

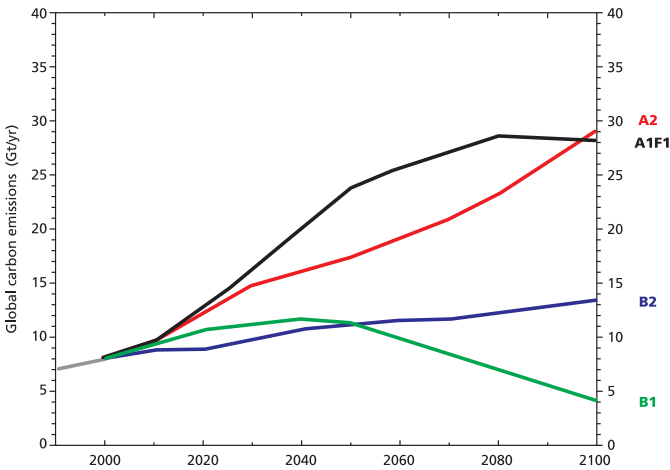
*A1:* Assumes a future world with a rapid economic growth, low population growth and a rapid introduction of new and more efficient technology. Main characteristics include an economic and cultural convergence and capacity building, with a substantial reduction in regional differences in per capita income. In a world of these characteristics, population looks for a personal well being rather than environmental quality.

*A2:* Assumes a well differentiated world in which regional cultural identities are preserved with emphasis on family values and local traditions, high population growth and different economic development, although high in the global average.

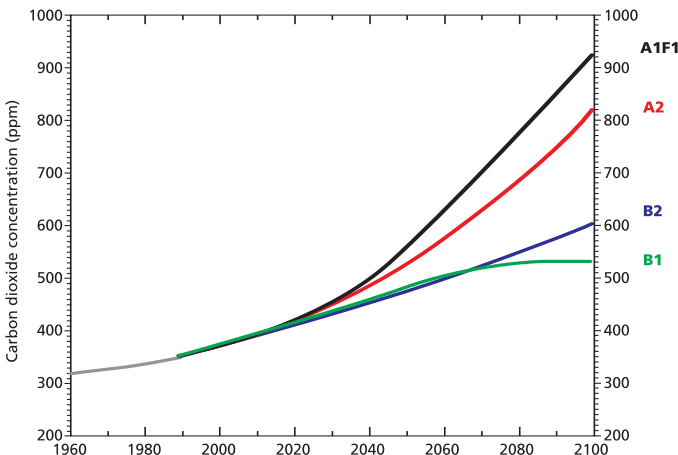
*B1:* Assumes a convergent world with rapid changes in economic structures and introduction of clean technologies. The emphasis is on global solutions to environmental and social sustainability, including efforts for rapid technology development, “dematerialization” of the economy and improving social equality.

**B2:** Assumes a world with emphasis on local solutions to economic, social and environmental sustainability. The world remains heterogeneous with less rapid and more diverse technological change, but with strong emphasis on local initiatives and social innovations in order to find local rather than global solutions. These solutions consider environment as a main concern.

The way that these socio-economic scenarios are considered in the GCM simulations is through the emission scenarios of each one of the gases, which are converted to concentration scenarios according the life times of these gases in the atmosphere. *Figure 12.2a* shows the carbon global emissions corresponding to four different scenarios for the period 2000-2100 and *figure 12.2b* shows the corresponding carbon dioxide concentrations.



a)



b)

**Fig. 12.2.** Global emissions of carbon for four different scenarios (a) and concentrations of carbon dioxide (b) for the period 2000-2100.

[IPCC, 2001]

### 12.4.2. Sea level rise scenarios

One of the projected impacts in the context of global warming is the sea level rise. Both the thermal expansion of the sea water as well as the melting of the ice sheets and glaciers contribute to this phenomenon. In addition, local conditions such as descents in coastal lands, tectonic movements, changes in the oceanic circulation, tides and storms must also be considered in the elaboration of scenarios of future sea level change. *Figure 12.3* shows different scenarios of sea level change that show between 0.25-0.45 m for the period 1900-2100 (IPCC 2001). If adding the uncertainties between the models this range increases to 0.20-0.70 m, and if all uncertainties are considered to 0.10-0.90 m.

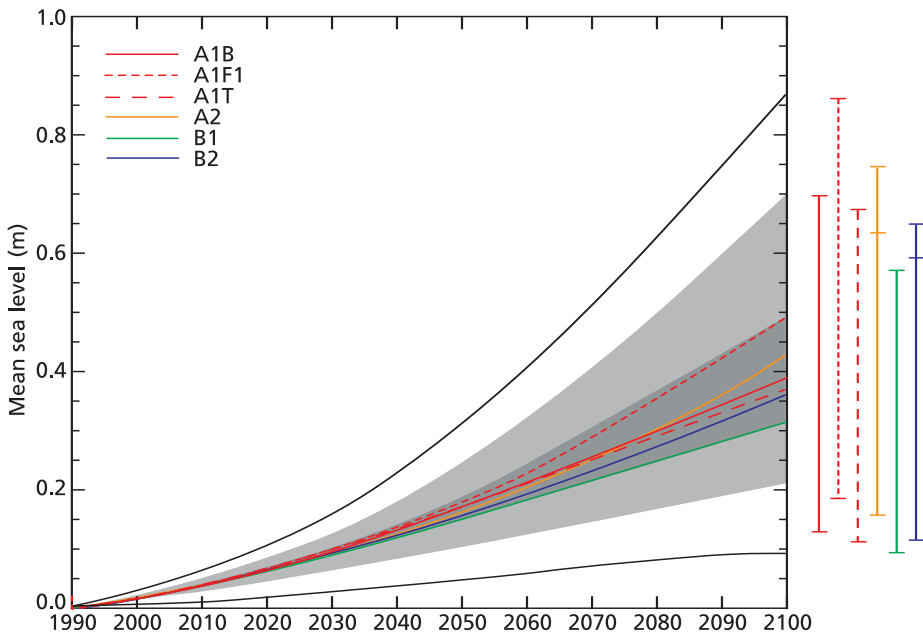


**Fig. 12.3.** Scenarios of sea level rise for the period 1990-2100.

[IPCC, 2001]

## 12.5. Validation of GCMs outputs for the current period

GCMs have been increasing their complexity to represent in an increasingly adequate manner the physical processes involved in the climate system. Even though they are not still capable of representing the totality of processes and have certain difficulties, like the interaction between radiation and aerosols, their capacity to represent current climate has been progressing and therefore the reliability of their future projections is growing.

The reliability of future climate scenarios obtained from GCMs is based on their ability to represent current climate and its variability. Gates et al. (1999) presents results of some simulations on current climate made in the context of the Atmospheric Model Intercomparison Project (AMIP). The largest errors correspond to cloud cover and temperature at 200 hPa, while the lowest ones are in the surface temperature. The outputs related to the global hydrological processes within the AMIP project were analyzed by Lau et al. (1996) from the analysis of 29 GCMs. Although it is observed a great variability among the different models, when considering an ensemble of them, the result is very close to the observations showing an overestimation in the tropical precipitation and an underestimation in the extra-tropics.

Results of GCMs developed by a group of institutes with high scientific and computer capability are available through the web page of the Data Distribution Centre (DDC) of the IPCC ([www.dkrz.de/ipcc/ddc/html/SRES/SRES\\_all.html](http://www.dkrz.de/ipcc/ddc/html/SRES/SRES_all.html)). *Table 12.1* shows a list of models and the institutions that developed them. Their validation for the climate of Southeastern South America is presented in Chapter 13.

*Table 12.1. GCM with information available through the DDC.*

Model	Institution	Current period	Future period
HADCM3	Hadley Centre for Climate Prediction and Research (Reino Unido)	1950-1999	2000-2100
CSIRO-mk2	Australia's Commonwealth Scientific and Industrial Research Organization (Australia)	1961-1999	2000-2100
ECHAM4/OPYC3	Max Planck Institute für Meteorologie (Alemania)	1990-1999	2000-2100
GFDL-R30	Geophysical Fluid Dynamics Laboratory (Estados Unidos)	1961-1999	2000-2100
NCAR-PCM	National Centre for Atmospheric Research (Estados Unidos)	1981-1999	2000-2100
CCCma	Canadian Center for Climate Modeling and Analysis (Canadá)	1950-1999	2000-2100

## 12.6. Climate change scenarios from GCMs

In the previous section, the difficulties of the GCMs to represent current climate were mentioned. This imposes limitations on the reliability of the scenarios of future climate. Likewise, it is necessary to validate the GCMs outputs at a regional level before using them in the preparation of scenarios. A way to elaborate climate change scenarios based on GCMs despite of errors that they show in the representation of current climate consists of preparing scenarios of differences between what is foreseen by GCMs for the future and its representation for the current baseline climate. This way, it is obtained a spatial distribution of the change in climate variables based exclusively on one GCM results.

### 12.6.1. Baseline scenarios

It is convenient to define a baseline scenario or observed climate with regard to which the changes in the different climate scenarios can be referred. The election of this baseline or reference period is frequently determined by the availability of climatic information. Most of the impact assessment studies aim to determine the effects of the change with respect to current conditions, and so they used recent base periods such as 1961-90. It is important to have in mind that no matter whatever the baseline period is, there are differences between climatic averages based on long periods of time (for instance, 100 years) and those considering shorter sub-periods. Moreover, different 30-years periods show differences in regional annual mean temperatures of  $\pm 0.5^{\circ}\text{C}$  and of  $\pm 15\%$  in annual precipitation (Hulme and New 1997; Visser et. al. 2000). Thus small regional changes in future climate scenarios cannot be consider significant.

### 12.6.2. Global scenarios

Scenario A2 proposed by the IPCC implies that in less than a century, carbon dioxide concentrations will reach more than three times pre-industrial levels, methane concentration will be more than 5 times and those of nitrous oxide will almost double. It is important to highlight that these values have never been reached at least in the last 20 millions years.

For year 2060, GCM project an increase of the global surface temperature of 1.3 to  $2.5^{\circ}\text{C}$  depending on the socio-economic scenario, with higher warming at high latitudes and in winter. This warming would not be uniform; in the continental areas of the northern hemisphere there would be regions where temperature would raise more than  $8^{\circ}\text{C}$ . *Table 12.2* shows mean projections of temperature rise for different decades up to 2100 with respect to the period 1961-90 for different scenarios. Beyond that date the increase of the temperatures could be much higher, critically depending on the future evolution of the GHG emissions.

**Table 12.2.** Increase in the surface mean global temperature ( $^{\circ}\text{C}$ ) for different socio-economic scenarios.

	SCENARIOS			
	A1	A2	B1	B2
2000	0,15	0,15	0,15	0,15
2020	0,50	0,50	0,50	0,60
2040	1,20	1,00	0,90	1,10
2060	2,50	1,80	1,30	1,60
2100	4,50	3,80	2,00	2,70

From *Table 12.2* it comes out that there would not be much difference between scenarios up to year 2040. That is, no matter what the emission scenario would be, climate changes up to that date would already be determined. However, the different options about emissions would be highly critical in the determination of the climate for the rest of the century.

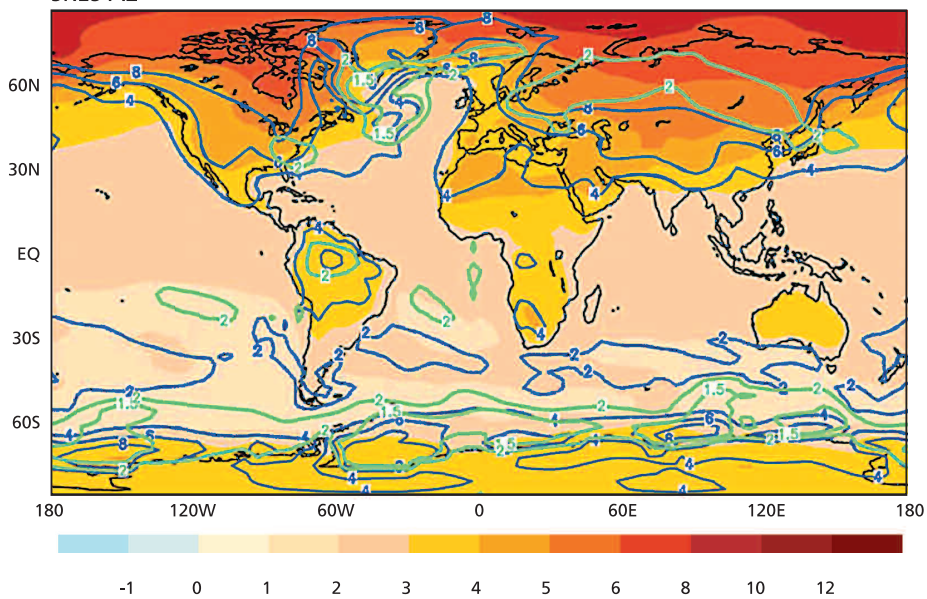
GCM projections indicate that the continental areas will warm faster and than oceans; the temperature increase of the air in the North Atlantic and in the areas around the Pole in the Antarctic Ocean will be less than in the world average. Likewise, there will be lower daily amplitude in temperature in many regions since minimum temperature will rise more than the maximum. Projections indicate a decrease of the snow and of ice cover in the northern hemisphere. It is important to highlight that many of these changes concur with trends detected in the observations.

With a set of results from a multi-model GCM ensemble, considering different scenarios of GHG emissions, it is estimated the average climatic change over the ensemble and its degree of uncertainty. *Figure 12.4* shows the annual mean changes of the surface temperature and their variation range (standard deviation) for the period 2071-2100 with respect to 1961-90 for scenarios A2 and B2. The features of the geographic response are similar for both scenarios but the amplitude of the climatic change patterns is lower for the simulations corresponding to scenario B2 than in the A2. The relationship between mean change and standard deviation increases to lower latitudes while at high latitudes next to the Antarctic continent has a minimum.

*Figure 12.5* shows the relative change in the mean of all models precipitation, which reveals a general increase in the tropics and the mid and high latitudes, and a reduction over most of the sub-tropical belts. The areas of decreased precipitation show a high inter-model variability and therefore little consistency among models, while at the tropics the change can exceed the standard deviation by a factor of 2. This is particularly evident over the central and eastern tropical Pacific where the El Niño-like surface temperature warming is associated with an eastward shift of positive precipitation anomalies. The A2 and B2 scenario experiments exhibit a relatively large increase in precipitation over the Sahara and Arabia, but with large inter-model variability. This is partly an artifact of using percentage change rather than absolute values, since in these regions the annual precipitation total is very small. In particular, over South America, it is also interesting to notice that the North and Northeast Brazil show negative precipitation anomalies in the future projection while the Southeast of the South America and particularly over the La Plata basin, the rainfall tends to increase.

In the case of the sea level pressure between the period 2071-2100 relative to 1961-90 (*Fig. 12.6*), the most relevant feature resulting of the ensemble of different models is the reduction of the pressure in high latitudes and the increase in mean latitudes. On the other hand, several studies on the southern hemisphere show that

## a) SRES A2



## b) SRES B2

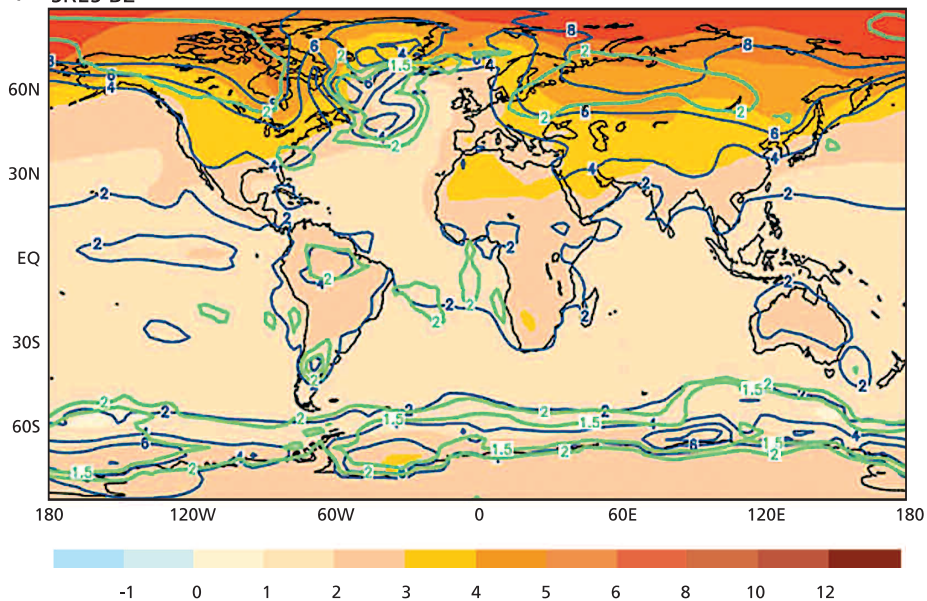
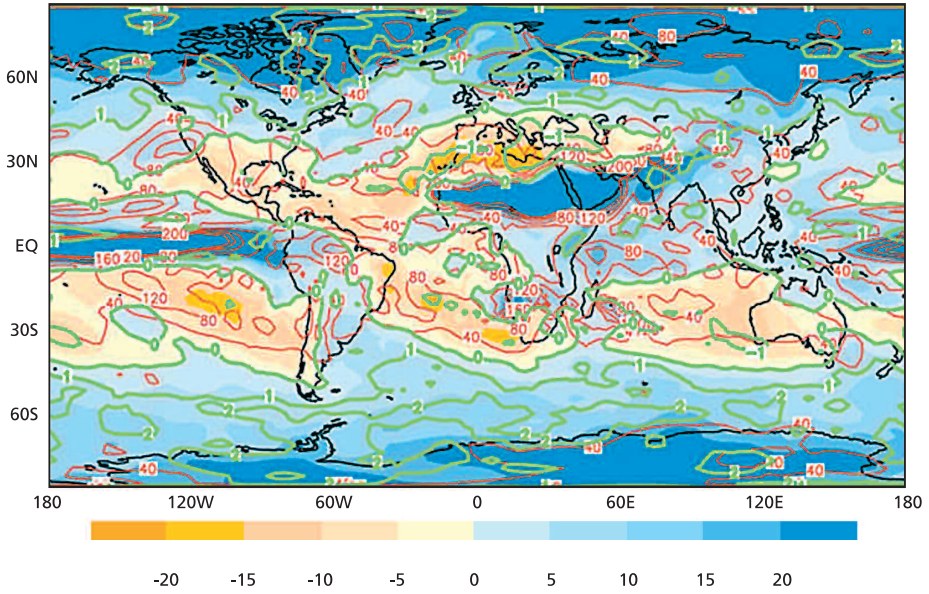


**Fig. 12.4.** The multi-model ensemble annual mean change of the temperature (colour shading), its range (thin blue lines) (Unit: °C) and the multi-model standard deviation (solid green lines, absolute values) for (a) the SRES scenario A2 and (b) the SRES scenario B2. Both SRES scenarios show the period 2071 to 2100 relative to the period 1961 to 1990.

[IPCC 2001]

## a) SRES A2



## b) SRES B2

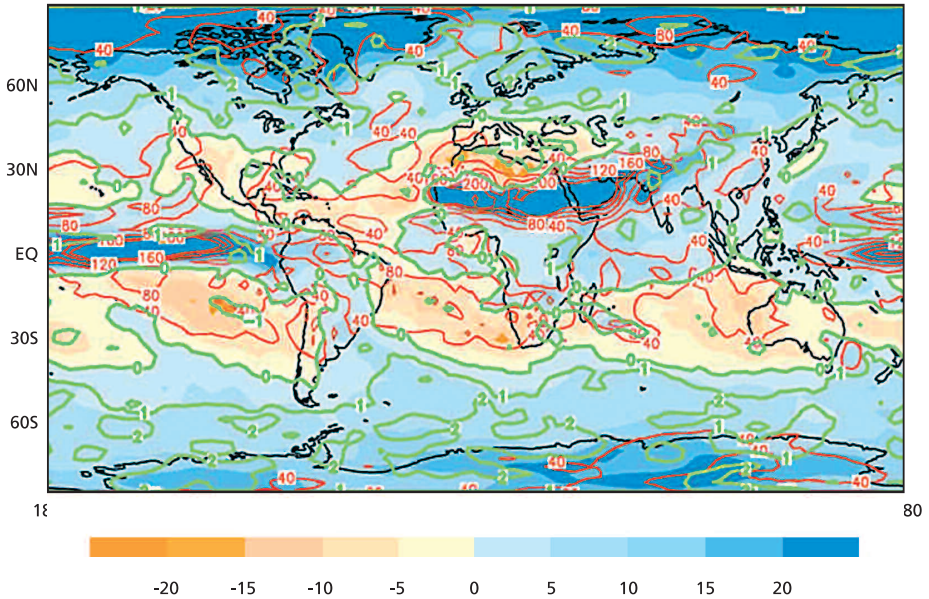
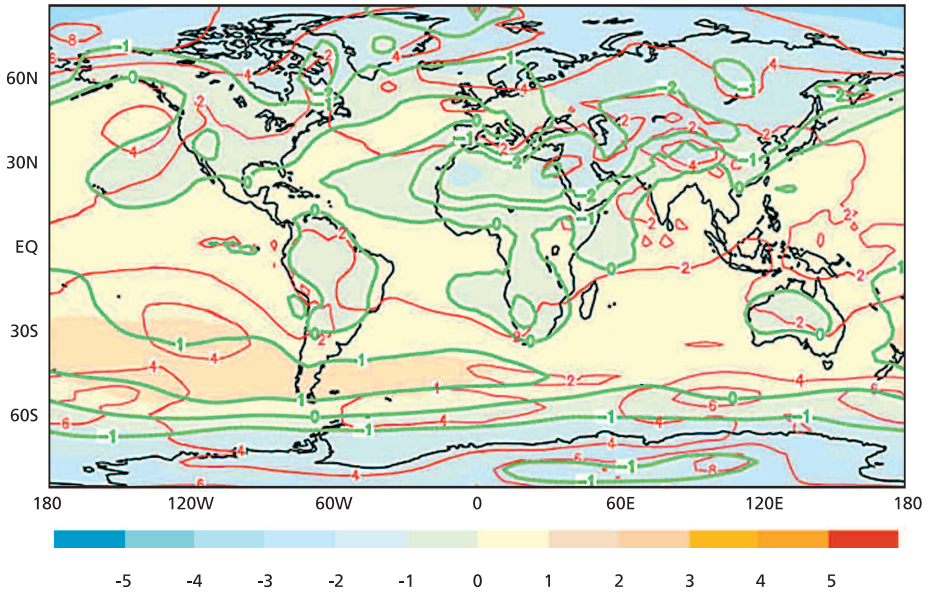


**Fig. 12.5.** The multi-model ensemble annual mean change of the precipitation (colour shading), its range (thin red lines) (Unit: %) and the multi-model mean change divided by the multi-model standard deviation (solid green lines, absolute values) for (a) the SRES scenario A2 and (b) the SRES scenario B2. Both SRES-scenarios show the period 2071 to 2100 relative to the period 1961 to 1990.

[IPCC 2001]

## a) SRES A2



## b) SRES B2

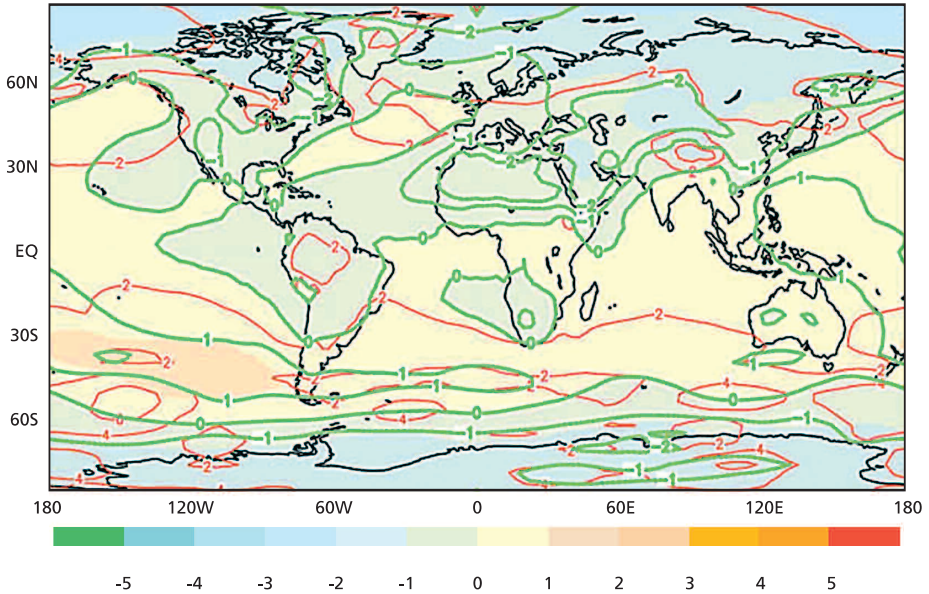


**Fig. 12.6.** The multi-model ensemble annual mean change of the sea level pressure (colour shading), its range (thin red lines) (Unit: hPa) and the multi-model mean change divided by the multi-model standard deviation (solid green lines, absolute values) for (a) the SRES scenario A2 and (b) the SRES scenario B2. Both SRES-scenarios show the period 2071 to 2100 relative to the period 1961 to 1990.

[IPCC 2001]

this would be related to a combination of changes in the gradients of the surface temperature and of those of the middle troposphere (Räisänen 1997; Fyfe et al. 1999; Kushner et al. 2001). Likewise, over extensive regions of high latitudes of both hemispheres, the signal of mean change overcomes the one of the standard deviation indicating a consistency in the response to the different models.

Table 12.3 shows evaluations about the degree of reliability on the changes observed in the last half of XX century and those projected for XXI in extreme climatic events (IPCC 2003). This evaluation resulted from the analysis of observations and results provided by GCMs. Some extreme phenomena at spatial and/or small temporal scale such as storms, tornadoes, hail events and electric discharges are not included since they are not represented by the GCMs.

**Table 12.3.** Evaluations about the degree of confidence in the observed and projected changes in climate extremes (IPCC 2003).

Degree of confidence in the observed changes (second half of XX century)	Climate changes	Degree of confidence in the projected changes (during XXI century)
Likely	Higher maximum temperatures and more heat in almost all land regions	Very likely
Very likely	Higher minimum temperatures, less cold and frosty days in almost all the land regions	Very likely
Very likely	Lower amplitude in daily temperature in most of the land regions	Very likely
Likely in many regions	Rise in the index of heat in land regions	Very likely in most of the regions
Likely in many middle and high land regions of the northern hemisphere	More episodes of intense precipitation	Very likely in many regions
Likely in some regions	Higher Summer continental dryness and drought related risk	Likely in most of the interior continental regions of middle latitudes
Not observed in the scarce available analyses	Increase of maximum intensities of tropical cyclones winds	Likely in some areas
Insufficient data to make an evaluation	Increase of maximum and mean intensities of precipitations of tropical cyclones	Likely in some areas

## References

- Fyfe, J. C., G. J. Boer and G. M. Flato 1999: The Arctic and Antarctic oscillations and their projected changes under global warming. *Geophys. Res. Lett.*, 26, 1601-1604.
- Gates, W. L., J. S. Boyle, C. Convey, G. G. Dease, C. C. Doutriaux, R. S. Drach, M. Fiorino, P. J. Gleckler, J. J. Hnilo, S. M. Marlais, T. J. Phillips, G. L. Potter, B.D. Santer, K.R. Sperber, K.E. Taylor and D.N. Williams 1999: An overview of the results of the atmospheric model intercomparison project (AMIP I). *Bull. Amer. Meteor. Soc.*, 80, 29-55.
- Hulme, M. and M. New 1997: The dependence of large-scale precipitation climatologies on temporal and spatial gauge sampling. *J. Climate*, 10, 1099-1113.
- IPCC 2001: *Climate Change 2001: The Scientific Basis*. Cambridge University Press, USA, 881 pp.
- IPCC 2003: *Cambio Climático 2001. Informe de síntesis*. Grupo Intergubernamental de expertos sobre el Cambio Climático, 207 pp.
- Kushner, P. J., I. M. Held and T. L. Delworth 2001: Southern hemisphere atmospheric circulation response to global warming. *J. Climate*, 14, 2238-2249.
- Lau, K.M., J.H. Kim, Y. Sud 1996: Intercomparison of Hydrologic processes in AMIP GCMs. *Bull. Amer. Meteor. Soc.*, 77, 2209-2227.
- Räisänen, J. 1997: Objective comparison of patterns of CO<sub>2</sub>-induced climate change in coupled GCM experiments. *Clim. Dyn.*, 13, 197-221.
- Visser, H., R. J. M Folkert, J. Hoekstra and J. J. de Wolff 2000: Identifying key sources of uncertainty in climate change projections. *Climatic Change*, 45, 421-457.

## REGIONAL CLIMATIC SCENARIOS

*Iracema Fonseca de Albuquerque Cavalcanti<sup>1</sup>, Inés Camilloni<sup>2</sup> and Tércio Ambrizzi<sup>3</sup>*

<sup>1</sup> Centro de Previsão de Tempo e Estudos Climáticos/  
Instituto Nacional de Pesquisas Espaciais, Brasil

<sup>2</sup> CIMA/CONICET, Universidad de Buenos Aires.

<sup>3</sup> Universidade de São Paulo, Brasil.

### ABSTRACT

Results of global circulation models are used to analyse climate change in a regional context. Validation of GCM results for mean precipitation and temperature of the La Plata Basin region and future scenarios for the region obtained from several models and experiments are presented. In the validation analysis, the Hadley Centre model presented smaller systematic errors than the other GCMs analysed. The CPTEC/COLA AGCM had also small errors although both models have an underestimation of precipitation over the region. The future scenarios from several different models are consistent in the results, showing an increase of precipitation over the La Plata basin. The precipitation increase occurs in several experiments of the A2 and B2 scenarios and also when a constant percent CO<sub>2</sub> increase is considered. Results of global results suggest that the mechanism for this regional increase is related to the increase of convection in the East Pacific, in a similar pattern of an El Niño episode. Concerning the air temperature near the surface (2 m), there is also an increase simulated by the models. When interpreting these scenarios for future applications, an uncertainty range must be considered, due to the fact that models are not perfect and may contain errors.

## 13.1. Introduction

Scenarios of changes in the future climate of the La Plata basin are an important issue to be developed by the scientific community and transferred to several sectors of the economy, such as agriculture, water resources, hydroelectric power, construction, tourism and others. Changes in precipitation, temperature and wind regimes, frequency of storms, frequency of dry or wet days, extreme weather conditions, are features that can have strong social influence. Simulations of the future climate can give an idea of these changes based on the physical mechanisms of global warming due to the increase of greenhouse gases. Other changes as deforestation, increase of aerosols and changes in the ozone layer can also be included in the models to investigate their influence on future climate.

The use of Global Circulation Models (GCMs) for the climate change scenarios development allows assessing global impacts of changes, mainly in greenhouse gases, but also of other processes. To investigate regional changes in the atmospheric variables and conditions, other methods can be considered that will be presented in section 13.2. It is already known that climate simulations using different models can display different global and regional results (Lau et al. 1996; Gates et al. 1999). Then, all the results from several models can be taken into account to evaluate the uncertainty around the average model ensemble.

## 13.2. Regional climatic scenarios

Outputs provided by GCMs in general do not have enough spatial resolution to be applied in regional evaluations of climatic change impacts. Hence, several methods have been developed in order to generate regional scenarios based on GCMs but with a smaller resolution than the model. This procedure is called “downscaling”. Next are described the different “downscaling” available methods.

### *13.2.1. Direct use of GCM outputs*

The simpler method is to use the outputs provided by GCMs at the closest to the study area grid point. In this method the analysis is made considering the global outputs in a specific region. However, this method presents little reliability due to the low spatial resolution of the GCMs.

### *13.2.2. Interpolation of GCM outputs*

The easiest way to make a “downscaling” is by interpolating GCM results with the grid points closest to the location or area of interest. The problem with this method is that introduces a false geographical accuracy.

### 13.2.3. Statistical downscaling

The most sophisticated downscaling techniques calculate changes at a sub-grid level according to climatic statistics or great scale circulation parameters. Some approaches use statistical relations between the large scale surface climate and local climate or between data at higher levels of the atmosphere and the local surface climate. When these methods are applied on GCM's daily level data, it is possible to obtain daily climatic models for specific areas or locations. Statistical downscaling is far less demanding computationally than other methods such as the dynamic downscaling through numeric models. Notwithstanding, they require a great deal of observational data to establish the statistical relations for current climate and are based on the assumption that the observed statistical relationships will continue to hold, even with different climate forcings in the future, that will be invariant with time. Another problem with daily downscaling is that in many regions, GCMs do not reproduce adequately interdiurnal variations.

### 13.2.4. High resolution experiments

Another method of obtaining more localized estimations of future climate is performing experiments with numeric models over the region of interest. This can be done in different ways:

- Performing experiments with higher resolution GCMs but for different “temporal cuts” for a limited amount of years,
- Running a GCM with variably resolution over the planet in such a way that the maximum resolution be over the interest region
- By using a different model, but with higher resolution over a limited area (LAM), using the GCM outputs as boundary conditions for the LAM, that is to say through the nesting of an LAM in a GCM.

These methods for obtaining estimations at sub-grid level can reach to a 20 km resolution, and differently from GCM, are capable of taking into account important local forcings such as coverage of soil and topography. Besides, even though they have the advantage of having better physical basis than the statistical downscaling, they present a high computational demand. However, it must we mentioned that the LAM use does not solve all of the problems of the GCM scenarios. This is in part because they keep non perfect physical parameterizations and in part because they transfer errors from GCMs such as the underestimation of the interdiurnal variability in certain regions.

In the present analysis, the method described in 13.2.1 is used to discuss the model results over the La Plata basin region and South America, and the method 13.2.4 will be used in experiments mentioned in section 13.5.

### 13.3 Regional validation of GCMs for South America

In order to have confidence in the GCMs future scenarios, it is necessary that these models satisfactorily represent current climate. It is important to know how the model results compare with observations in a regional scale. Among the difficulties faced in the utilization of these model outputs is that not all of them represent adequately the current climate in the whole range of climate variables. The percentages of the observed annual rainfall given by four different GCMs for the current period are shown in *figure 13.1*. Observed precipitation data were taken from Delaware University (Willmott and Matura 2001). All the models grossly underestimate the annual precipitation in part of the Pampas region, the Argentine Mesopotamia, Uruguay and South of Brazil. Therefore, they cannot be used directly and it is necessary to consider some additional methodologies to estimate future scenarios of this variable. One of them is to assume that differences between future and current precipitation fields are approximately similar in both the GCM and the real climate. In the case of HadCM3 model, which presents the lower differences between observed precipitation and the model's estimation, this underestimation in the Pampas region is of approximately 360 millimetres, which represents up to a 30% below the observed value. In the North of Argentina, Uruguay and South of Brazil, this underestimation is even larger. Difficulties to estimate the rainfall in the

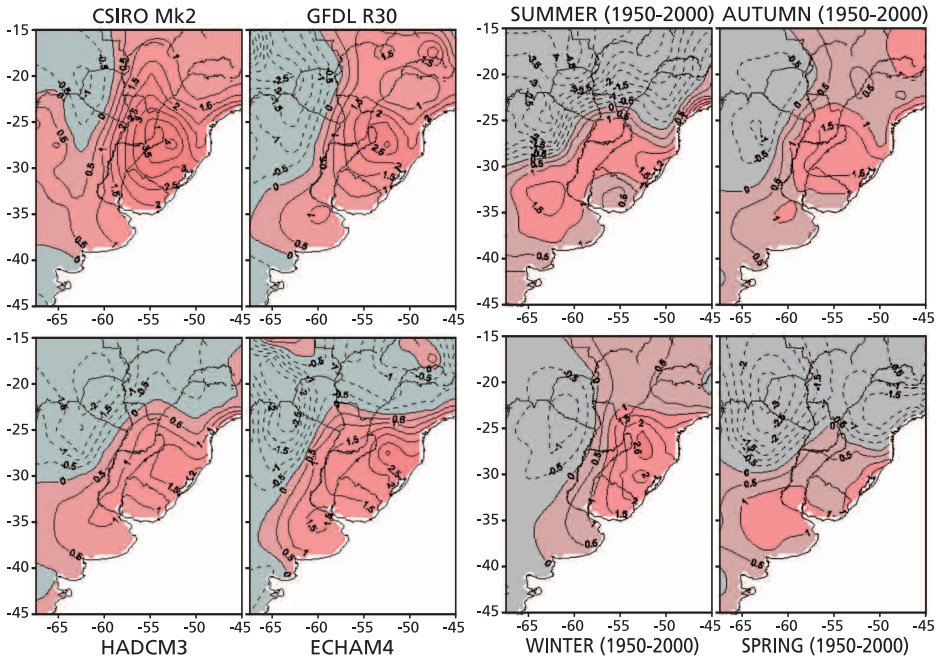


**Fig. 13.1**  
Difference (mm/day) between annual precipitation observed and estimated by four MCGs.

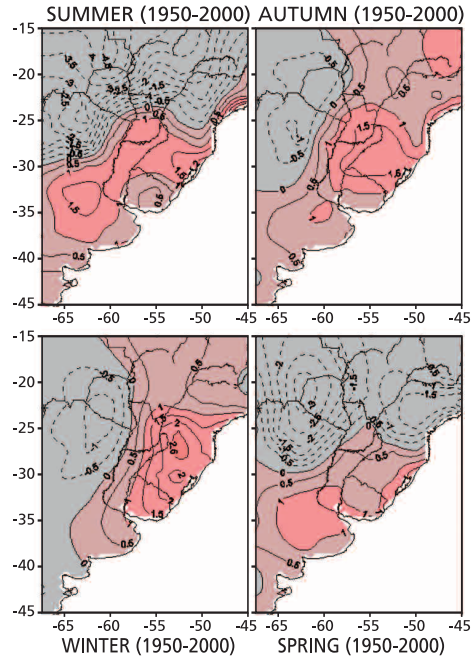


**Fig. 13.2**  
Difference (mm/day) between seasonal observed precipitation and the one estimated by the HADCM3 model.

La Plata basin are also considerable in the seasonal values. The differences of the observed and the estimated by the HadCM3 model precipitation for all four seasons are shown in *figure 13.2*. In all cases, precipitation is underestimated by the model for the Humid Papas, Mesopotamia, Uruguay and South of Brazil. During autumn and winter, the underestimation extends to the North and is larger.

Other results from seasonal climate simulation using the CPTEC/COLA AGCM, for the period 1982-1991 are discussed in Cavalcanti et al. (2002). Seasonal climatological features of the high and low levels flow observed over South America were reproduced by the ensemble of nine members. However there was an overestimation of precipitation in the southern sector of the South American convergence zone (SACZ) and an underestimation in the Amazon region and southern part of southeaster South America. These features can be seen in *figure 13.3*. The underestimation over the La Plata basin occurs in all seasons but with less intensity during the spring. Despite the large dispersion among members of the ensemble over southern Brazil-Uruguay, the model captures quite well the extremes of the observed interannual rainfall variability (*Fig. 13.4*), especially the above normal values observed in Winter of 1983 and the drought conditions in the Winter of 1989 (Marengo et al. 2003).

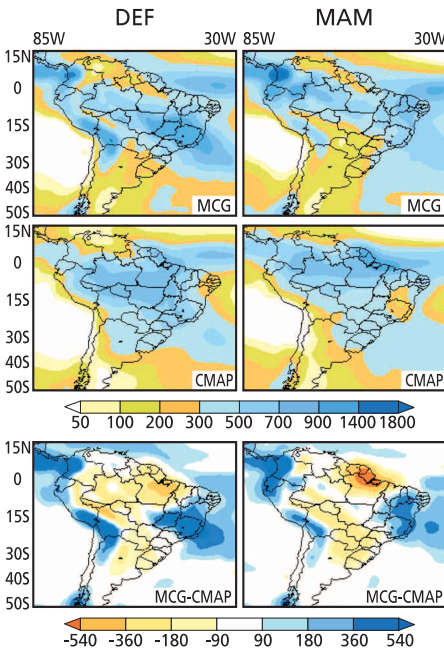


Fig. 13.3 a.

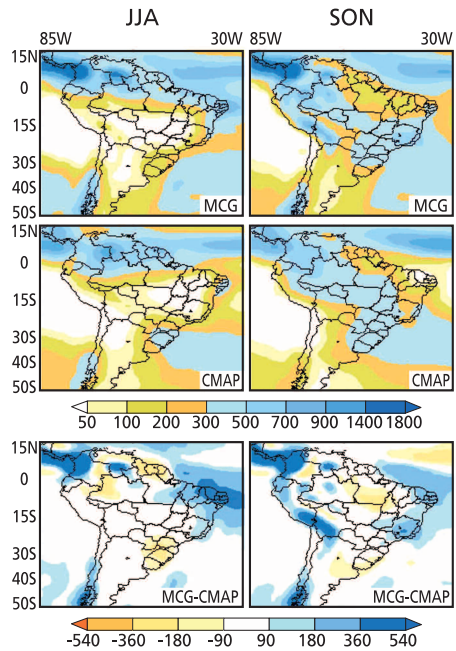
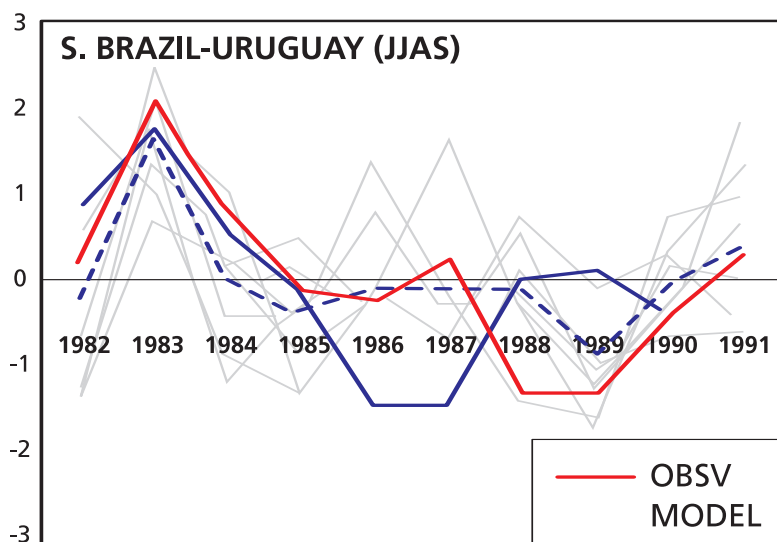


Fig. 13.3 b.

Fig. 13.3: CPTEC/COLA and CMAP Seasonal Climatological Precipitation (mm), and systematic errors (a) (DJF and MAM), (b) (JJA and SON).



**Fig. 13.4.** Precipitation anomaly over South Brazil and Uruguay from nine integrations (CPTEC/COLA AGCM) and CMAP, in JJAS.

[Source: Marengo et al 2003]

Correlations between CPTEC/COLA AGCM results and observation precipitation anomalies are presented in *figure 13.5*. There are high correlation values over northern and northeastern South America and some areas over the La Plata basin region with values above 60% in summer, autumn and spring, increasing the confidence on the model results during these seasons.

Differences between surface mean annual temperatures of the NCEP/NCAR reanalyses (Kalnay et al. 1996) and those of four GCMs indicate that models tend to overestimate the temperature in most of Buenos Aires province, Northeast of Argentina, Uruguay and South of Brazil and underestimate it in a longitudinal strip centred approximately at 62.5°W. The model that best represents the mean annual temperature of this region is HadCM3 that overestimates temperature between 0° and 1.5°C.

## 13.4. Regional scenarios for the La Plata basin

### 13.4.1. Hadley Centre GCM

Using the Hadley Centre GCM outputs for the emission scenarios A2 and B2, the differences between projected precipitation for the decades 2020, 2050 and 2080 and the reference period (1961-1990), are in *figures 13.6* and *13.7*. Results

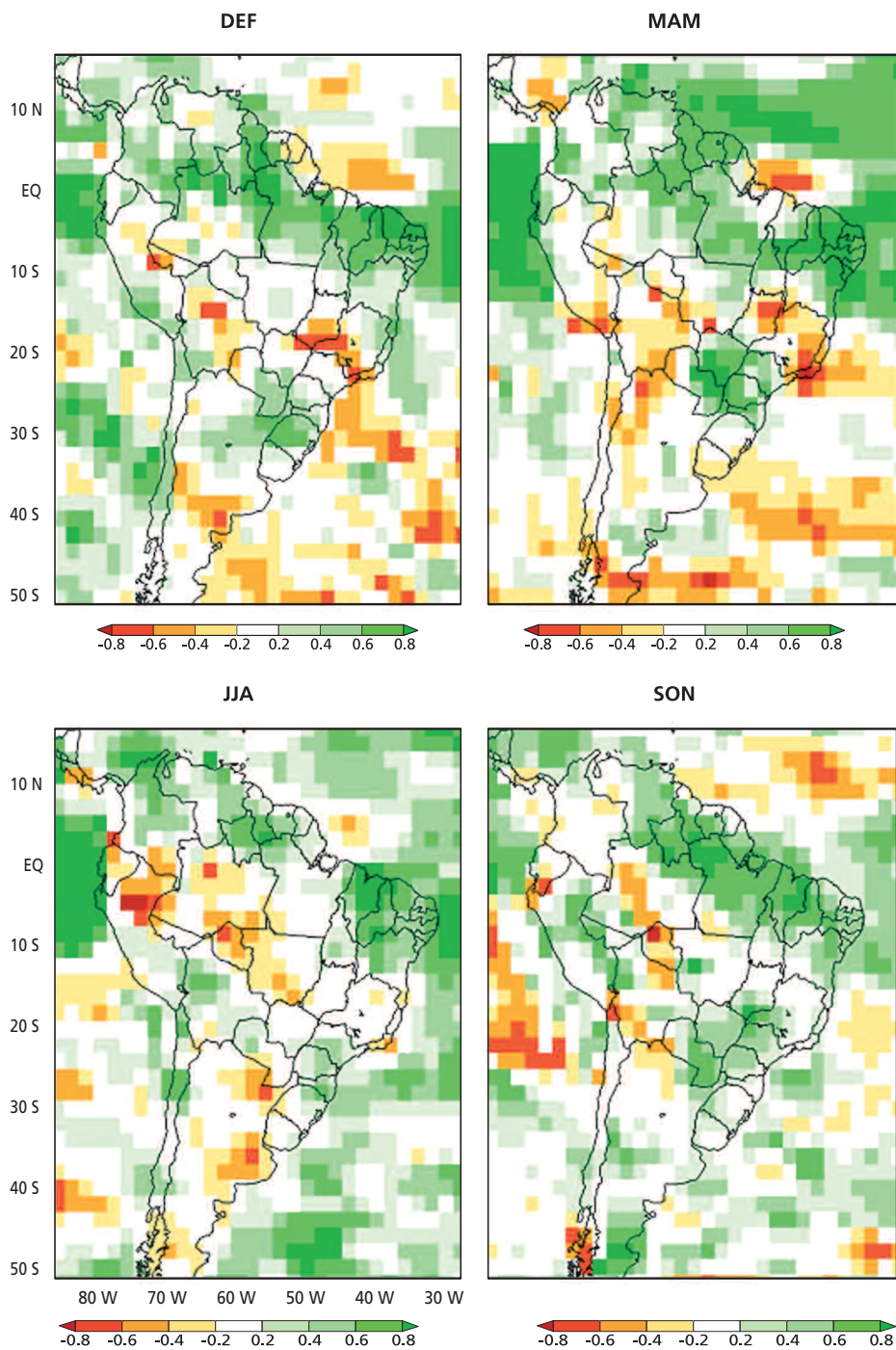


**Fig. 13.5.** Anomaly correlations between CPTEC/COLA AGCM (10 years) and CMAP.

[Source: Marengo et al 2003]

show a positive trend in most of centre-North of Argentina, Uruguay and South of Brazil, and in the southernmost part of Argentina. This increase is higher in scenario A2 than in B2. Likewise, it is observed a remarkable negative trend in the rainfall over the central region of Chile, Cuyo, Neuquén, West of Rio Negro and Chubut. Temperature differences are shown in *figure 13.8* and *13.9*.

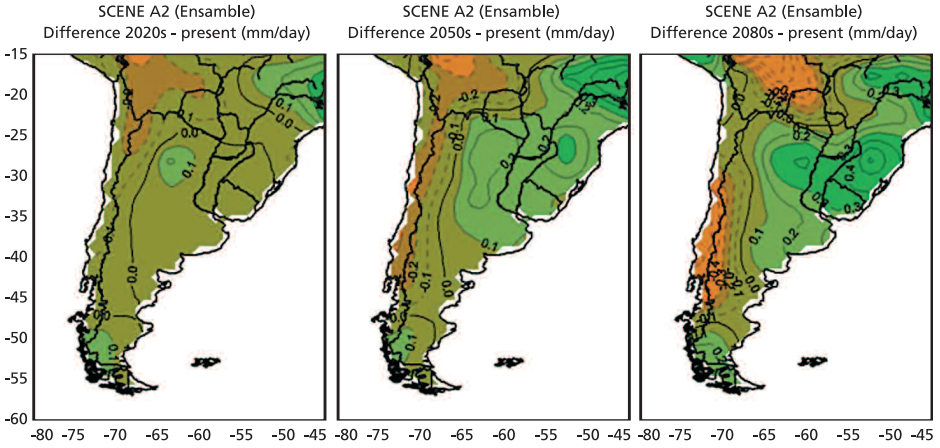


*Fig. 13.6. Scenarios of precipitation differences (mm/day) according to the HADCM3 model between decades 2020, 2050 and 2080 and present time (1961-90) for A2 scenario.*

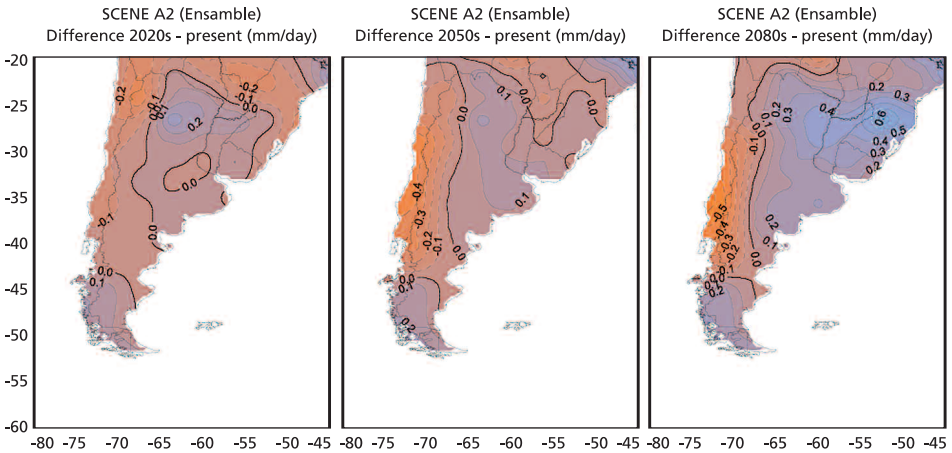


*Fig. 13.7. Scenarios of precipitation differences (mm/day) according to the HADCM3 model between decades 2020, 2050 and 2080 and present time (1961-90) for B2 scenario.*

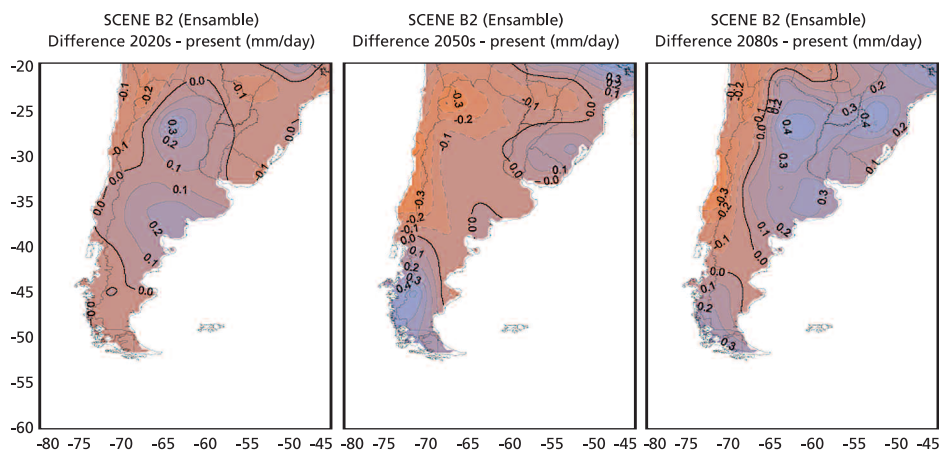


Fig. 13.8. Scenarios of temperature differences ( $^{\circ}\text{C}$ ) according to the HADCM3 model between decades 2020, 2050 and 2080 and present time (1961-90) for A2 scenario.

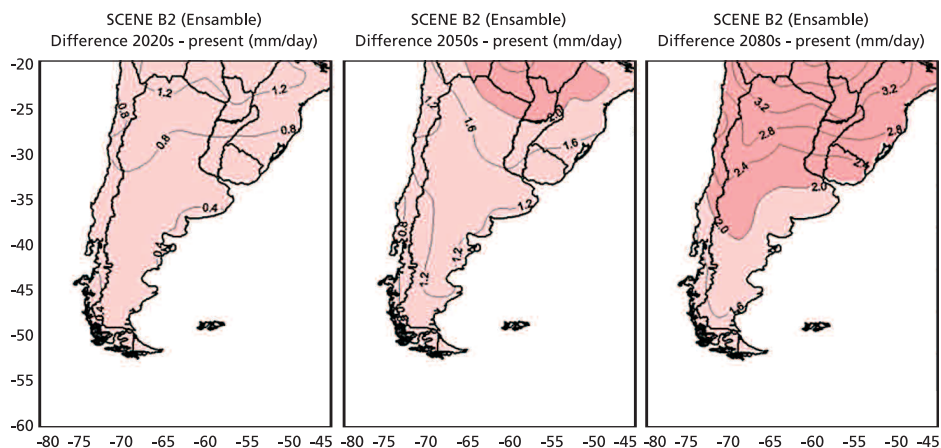


Fig. 13.9. Scenarios of temperature differences ( $^{\circ}\text{C}$ ) according to the HADCM3 model between decades 2020, 2050 and 2080 and present time (1961-90) for B2 scenario.

### 13.4.2. Regional features in other Climate Change experiments

Fourteen modelling groups from different institutions are preparing model simulations of climate change scenarios and the results will be available to the scientific community for diagnostic analysis. These analyses will be part of the IPCC Fourth Assessment Report and they have been organized by the Working Group Climate Simulation Panel. The objective is to have a diverse set of climate change scenarios and a few sets with high resolution ( $\sim 150$  km), a variety of fields, monthly, daily and 3 hourly timescale. The experiments refer to following conditions:

- Pre-industrial: run without anthropogenic forcing
- Present: run of 1990-2000
- The climate of twenty century
- The baseline climate change experiment: constant CO<sub>2</sub> concentration of year 2000.
- The SRES (Special Report on Emissions Scenarios) A2 experiment
- The 720 ppm stabilization experiment (SRES A1B)
- The 550 ppm stabilization experiment (SRES B1)
- A 1%/year CO<sub>2</sub> increase experiment (to doubling)
- A 1%/year CO<sub>2</sub> increase experiment (to quadrupling)

Preliminary analysis, for South America, of two experiments obtained from the GFDL coupled ocean-atmospheric model (CM2.0) are shown in *figures 13.10* to 13.12. It follows a brief discussion of the three of these experiments.

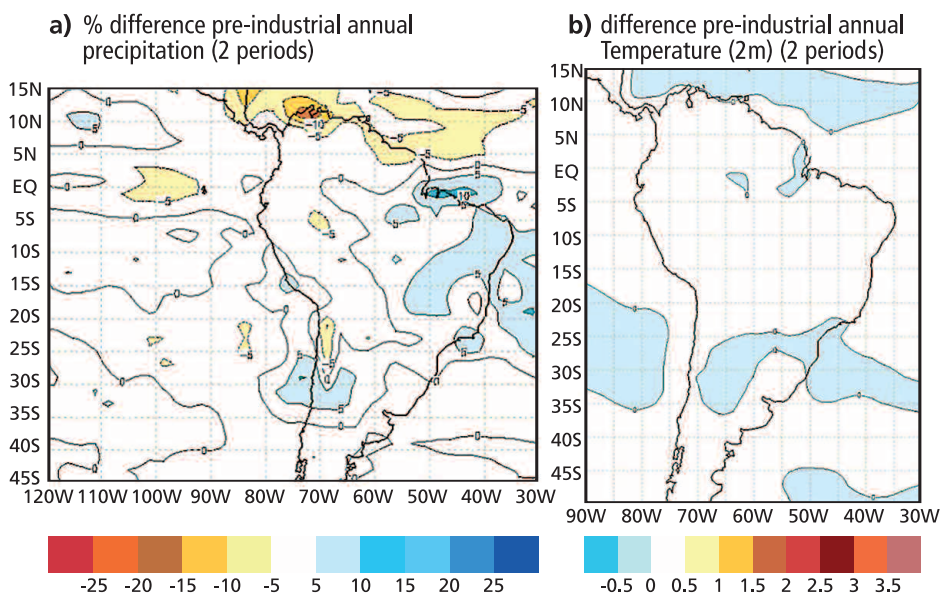


**Fig. 13.10.** Difference between two periods (year 71 to year 280) and (year 11 to year 70) of pre-industrial run (a) Precipitation (%); (b) Temperature (°C).

*a. Pre-industrial experiment:*

Initial conditions for this experiment were derived from a multi-step process. First, an atmosphere plus land surface model was started with forcing agents at levels representative of the late 20th century. Second, the spun up atmosphere plus land surface model was coupled to an ocean plus sea ice model. Initial conditions for sea ice, ocean potential temperature and salinity were derived from late 20th century observations. Forcing agents consistent with year 1860 were applied to the coupled model which was integrated for a ~300 year adjustment period. Year 1 experiment data begins at the end of this adjustment period. The forcing agents representative of conditions of 1860 include the well-mixed greenhouse gases (CO<sub>2</sub>, CH<sub>4</sub>, N<sub>2</sub>O), tropospheric and stratospheric O<sub>3</sub>, tropospheric sulphates, black and organic carbon, dust, sea salt, solar irradiance, and the distribution of land cover types.

In the pre-industrial run with no anthropogenic forcing, we can consider the variations due to the climate natural variability. *Figure 13.10a* shows the percentage of annual climatological precipitation, between two periods (year 11 to year 70) and (year 71 to year 280). It is seen very small differences over South America and almost no change over the La Plata basin. Low values are also seen over the tropical Pacific and Atlantic. There are not changes in the temperature field of the two periods (*Fig. 13.10b*).

*b. 1% increase in CO<sub>2</sub> up to doubling.*

The initial data correspond to 1 January of year 1 of the 1860 control model experiment, which had CO<sub>2</sub> concentration of 286.05 ppm. The increase rate is 1%/year up to year 70 (when the CO<sub>2</sub> = 2 X initial CO<sub>2</sub>). Then, this concentration (572.10 ppm) is held constant from year 71 to year 280. For the entire 280-year duration of the experiment, all non-CO<sub>2</sub> forcing agents (CH<sub>4</sub>, N<sub>2</sub>O, halons, tropospheric and stratospheric O<sub>3</sub>, tropospheric sulphates, black and organic carbon, dust, sea salt, solar irradiance, and the distribution of land cover types) were held constant at values representative of year 1860.

Considering the annual mean of the same two periods discussed in the previous analysis of the pre-industrial run, the impact of the CO<sub>2</sub> increase on the South America precipitation and nearby oceans is seen in *figure 13.11*. In the southern sector of the La Plata basin there is a maximum of 20% increase in precipitation, and in the northern sector of the basin, a maximum reduction of 10% precipitation. In the northern sector the annual mean reflects the behaviour of the summer rainy season. It is noticed the impact on the SACZ and Northeast Brazil, with less precipitation in the second period near the coast and more precipitation over western Amazonia region. There are large differences over tropical Pacific (increased precipitation) that affects the Peruvian coast, and Southwest Pacific (reduced precipitation) that affects Chile.

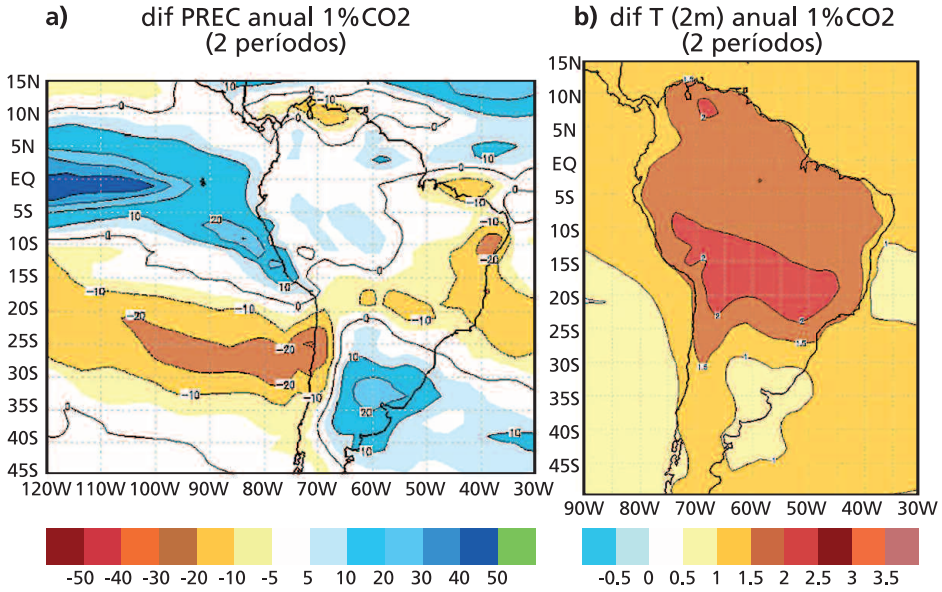


**Fig. 13.11.** Difference between period I (year 71 to year 280) and period II (year 11 to year 70) of 1% CO<sub>2</sub> increase experiment. (a) Mean annual precipitation (%); (b) Mean annual temperature (°C).

Taking the difference of results (total period annual mean) between the 1% CO<sub>2</sub> increase experiment and the pre-industrial experiment, the configuration is similar to that in the previous analysis. In that case the difference was performed between a period of constant high CO<sub>2</sub> value and a period of increasing concentration. *Figure 13.12* illustrates the impact. The differences are larger in the Pacific and Atlantic ITCZ regions; there is an increase of precipitation over the southern sector of the La Plata basin and part of the Amazon region, and a reduction over the SACZ area. The patterns are similar to other model results.

### c. Climate of twenty century

This experiment is running from 1861 to 2000, and contains all anthropogenic forcings during the period. The objective of this experiment is to establish one of the controls run to compare with future climates. The difference of this run with the 1% CO<sub>2</sub> increase experiment is shown in *figure 13.13*. Results are similar to the previous comparisons, with increased precipitation over the La Plata basin and increased temperature mainly over central South America.

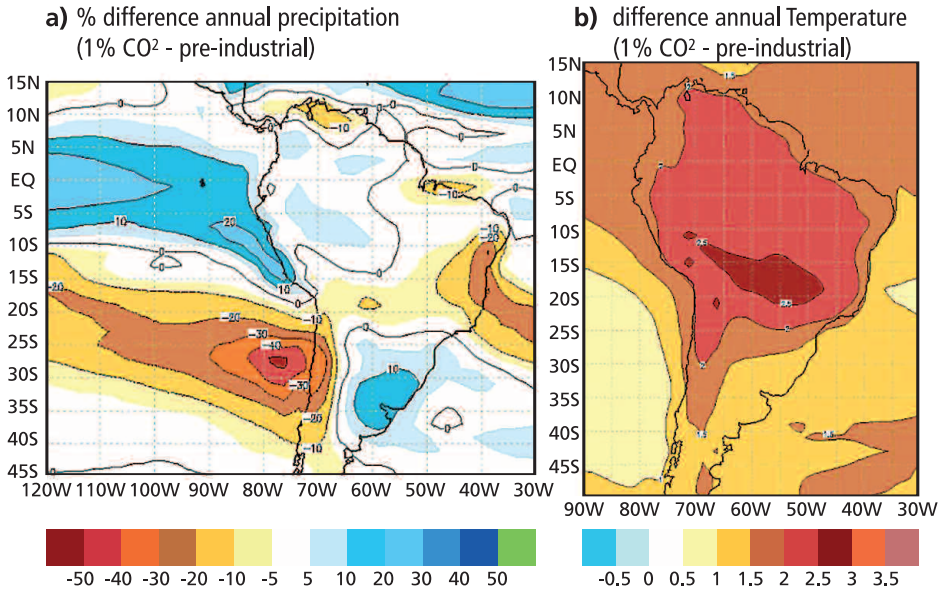


Fig. 13.12. Difference between 1% CO<sub>2</sub> increase experiment and pre-industrial experiment (year 11 to year 280) (a) Mean annual precipitation (%); (b) Mean annual temperature (°C).

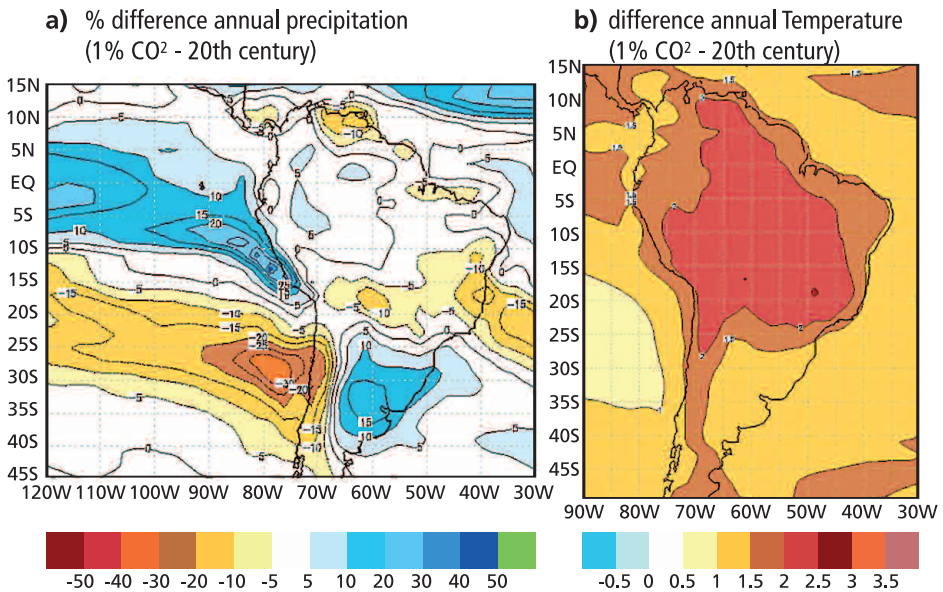


Fig. 13.13. Difference between 1%CO<sub>2</sub> increase experiment and 20th century experiment. (a) Mean annual precipitation (%); (b) Mean annual temperature (°C).

### 13.4.3. Hadley Centre and ECHAM GCM

Results from two other models (see *table 12.1* for model details), for the southern hemisphere winter and summer seasons and different periods are presented in *figure 13.14*. This figure shows the ECHAM4 and HadCM3 model simulations for the A2 scenarios averaged for the periods 2050 and 2080 and for the December-January-February (DJF) and June-July-August (JJA) periods. The ECHAM4 results indicate that independently of the period (*Figs. 13.14a* and *13.14c*), the precipitation patterns during the austral Summer show a positive anomaly over the Southeast South America and negative ones over the Northeast Brazil. During the Winter (*Figs. 13.14b* and *13.14d*), the negative anomalies seem to move towards the North of South America, while the excess of rainfall is confined to the South of Brazil. The HadCM3 model shows similar characteristics but with some important differences. For the austral summer, there is a noticeable change in the precipitation anomaly amplitudes between 2050 and 2080, being much larger in the last one (*Figs. 13.14e* and *13.14g*). It is worthy noting that the maximum values occur around the SACZ, which is to the North of the ECHAM4 results. Large amplitudes of negative precipitation anomalies over the North of South America are observed during the winter (*Figs. 13.14f* and *13.14h*). Again, the values are much stronger for the 2080 period (*Fig. 13.14h*), and positive anomaly values are basically observed in the South of South America.

## 13.5. Future plans of CPTEC/INPE in climate change modelling

Different improvements are currently been planned at CPTEC concerning climate change experiments. Some of them are related to the integrations of CPTEC models, and others will use dataset provided by other centres. CPTEC/COLA AGCM will be integrated to simulate the future climate, considering the increase of CO<sub>2</sub> and also simulating the past climate considering the observed CO<sub>2</sub> variation. Aspects of atmospheric and land components of the hydrological cycle over the La Plata basin will be analysed in the model results comparing the past and future climate. Experiments considering gradual Amazonia deforestation are also been planned with the global model. Aerosol increase and a chemical module that can consider the carbon cycle is a need for future implementations. In this module is expected the inclusion of other greenhouse gases as CH<sub>4</sub> and N<sub>2</sub>O. Improvements in convection and radiation parameterization schemes of the CPTEC/COLA model are in progress, as well as the inclusion of a new vegetation field and soil moisture provided by a hydrological model.

Climate change simulations planned at CPTEC will be the integration of the regional Eta model to do a downscaling, taking as lateral boundary conditions results of a simulation with the Hadley Centre Coupled GCM for the year 2070 to

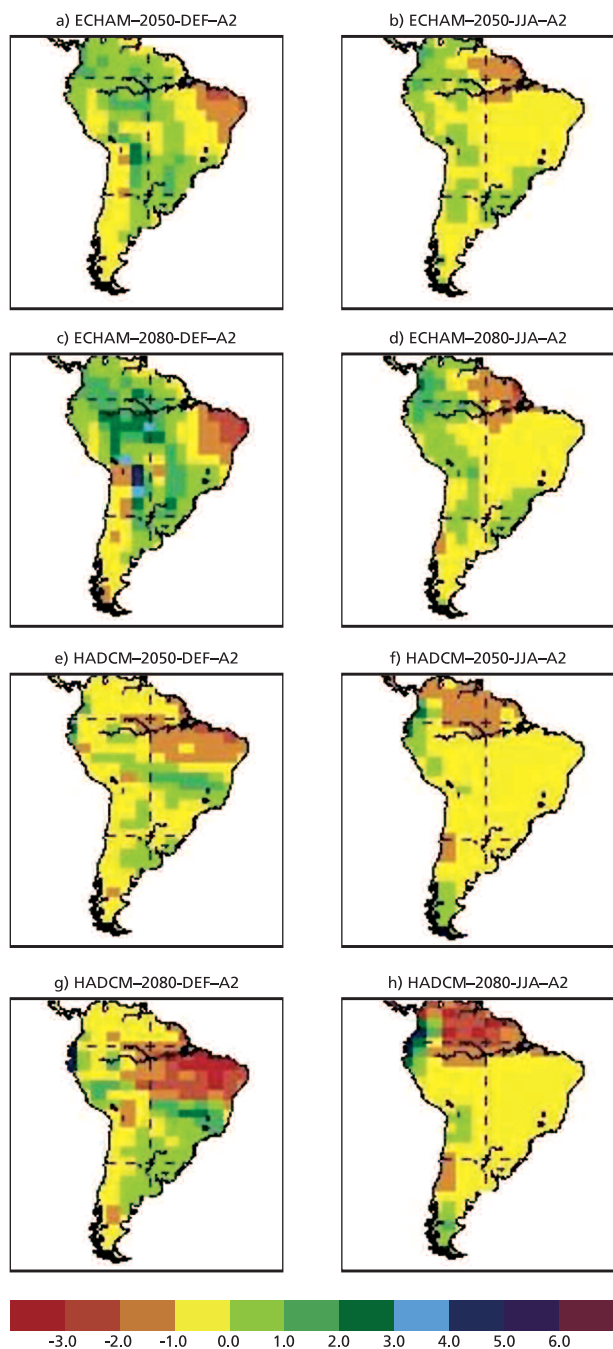


**Fig. 13.14.** ECHAM4 and HadCM3 A2 scenarios precipitation anomaly fields (mm/day) over South America for the periods DJF and JJA, and 2050s and 2080s relative to the 1961-90. The scale bar is at the bottom. [Source: IPCC-DDC]

2100. The results will be four daily data that will be used to analyse the variability in several scales, from changes in the annual means to the diurnal cycle. This activity is already in progress and analysis of model results are expected in the next few months. The resolution in the regional integrations is 40 km, and it is expected a more detailed spatial structure of the precipitation distribution, when compared to the global models. The control dataset will be the past climatology (1961-1990) of the ETA model using the Hadley Centre lateral boundary conditions. Similar experiments were being done in the Centre for Climate and Ocean Research (CIMA) with the MM5 model.

Another dataset available for diagnostics are climate change simulations from the Global coupled Hadley Centre model (monthly and daily) and results from the IPCC/WG1 project, already mentioned. CPTEC and CIMA are contributing to this project with proposals to do diagnostic analysis over South America on the South America Monsoon System, Hydrological cycle over the La Plata Basin, interaction tropics/extratropics and teleconnections related to anomalies over the continent. Some experiments are already available, such as: GFDL\_CM2.0, GISS\_AOM, NCAR\_PCM1, and some results were reported in section 13.4.3. Results from these analysis are expected to be included in the Fourth IPCC Report of Climate Change, namely changes at the surface, at upper levels, in the circulation, changes in the tropics, subtropics and extratropics, changes in extreme events, changes in snow and ice, changes in oceanic variables and sea level, coupling between climate change and biogeochemistry, seasonal to interannual prediction of climate change, projection of regional and global climate change and scenarios, and other related topics.

*The authors acknowledge the international modeling groups for providing their data for analysis, the Program for Climate Model Diagnosis and Intercomparison (PCMDI) for collecting and archiving the model data, the JSC/CLIVAR Working Group on Coupled Modeling (WGCM) and their Coupled Model Intercomparison Project (CMIP) and Climate Simulation Panel for organizing the model data analysis activity, and the IPCC WG1 TSU for technical support through the IPCC Data Archive at Lawrence Livermore National Laboratory, supported by the Office of Science, U.S. Department of Energy.*

## References

- Cavalcanti, I. F. A. , J. A. Marengo, P. Satyamurty, C. A. Nobre, I. Trosnikov, J. P. Bonatti, A. O. Manzi, T. Tarasova, L. P. Pezzi, C. D'Almeida, G. Sampaio, C. C. Castro, M. B. Sanches, H. Camargo 2002: Global climatological features in a simulation using CPTEC/COLA AGCM. *J. Climate*, 15, 2965-2988.
- Gates, W. L. and Coauthors 1999: An overview of the results of the Atmospheric Model Intercomparison Project (AMIP). *Bull. Amer. Meteor. Soc.*, 80, 29-55.

- Kalnay, E. and Coauthors 1996: The NCEP/NCAR 40-year reanalysis project. *Bull. Amer. Meteor. Soc.*, 77, 437-471.
- Lau, K. M., J. H. Kim and Y. Sud 1996: Intercomparison of Hydrologic processes in AMIP GCMs. *Bull. Amer. Meteor. Soc.*, 77, 2209-2227.
- Marengo, J. A., I. F. A. Cavalcanti, P. Satyamurty, I. Troniskov, C. A. Nobre, J. P. Bonatti, H. Camargo, G. Sampaio, M. B. Sanches, A. O. Manzi, C. C. Castro, C. Dálmeida, L. P. Pezzi and L. Candido 2003: Assessment of regional seasonal rainfall predictability using the CPTEC/COLA atmospheric GCM. *Clim. Dynam.*, 21, 459-475.
- Willmott, C. J. and C. K. Matura 2001: Terrestrial air temperature and precipitation: monthly and annual time series (1950-99). Version 1.02. (Available at <http://climate.geog.udel.edu/~climate/>).

## LOW-FREQUENCY VARIABILITY

*Mary T. Kayano<sup>1</sup> and Rita V. Andreoli<sup>1</sup>*

<sup>1</sup> Instituto Nacional de Pesquisas Espaciais, São José dos Campos, SP, Brasil.

### ABSTRACT

This chapter re-examines El Niño/Southern Oscillation (ENSO) related rainfall anomaly patterns in southern South America over the La Plata basin during the 1912-1999 period. Global associated anomaly patterns of the sea surface temperature and the sea level pressure for this same period are also re-examined. Monthly composites of the variables are obtained for El Niño and La Niña events separately. These composites are also stratified accordingly to the phases of the Pacific decadal oscillation (PDO). The composites show quite robust (weak) and well defined (noisy) spatial structure when the ENSO and the PDO phenomena are in the same (opposite) phase. So, the present analysis provides strong indications that the non-linear aspects of the climate relative to the PDO phases and to the ENSO phases should be taken into account for both climate monitoring and forecasting purposes, in particular for the La Plata basin climate.

### **14.1. Background on low frequency variability**

It is well known that the Tropical Pacific is dominated by a single mode of interannual climate variability, which reflects in the ocean-atmosphere coupling expressed by El Niño/Southern Oscillation (ENSO) phenomenon. Interannual climate variations in many parts of the globe are closely related to this mode. However, the Pacific climate contains another mode (or modes) of variability similar to the ENSO, but varying in a decadal to multi-decadal scale. Among these modes a recurring anomalous mode of the ocean-atmosphere system in the Pacific with dominant multi-decadal sign in the North Pacific has been known since the end of the 1980s (Nitta and Yamada 1989; Trenberth 1990; Trenberth and Hurrell 1994; Tanimoto et al. 1993; Latif and Barnett 1994; Mantua et al. 1997; Minobe 1997, 1999; Enfield and Mestas-Nuñez 1999). This mode shows significant climate teleconnections and it is commonly referred to as the Pacific (inter-) Decadal Oscillation (PDO) mode (Mantua et al. 1997; Zhang et al. 1997).

The high PDO phase or the warm PDO regime (WPDO) features anomalously cold surface waters in the western and central North Pacific and warmer than normal surface waters in the central and eastern Tropical Pacific and along the West coast of Americas (e.g., Zhang et al. 1997; Mantua et al. 1997; Zhang et al. 1998; Enfield and Mestas-Nuñez 1999). The low PDO phase or the cold PDO regime (CPDO) features nearly reversed patterns. The inter-decadal variability of the ocean-atmosphere system in the North Pacific determines the duration of the PDO regimes, which were cold during the 1900-1924 and 1947-1976 periods and warm during the 1925-1946 period and from 1977 to mid-1990s (Mantua et al. 1997).

Mantua et al. (1997) suggested that the PDO constitutes the background of the interannual ENSO variability. In agreement, several authors showed that PDO modulates El Niño (EN) and La Niña (LN) effects in certain regions of the globe (Gershunov and Barnett 1998; McCabe and Dettinger 1999; Gutzler et al. 2002; Krishnan and Sugi 2003). Gershunov and Barnett (1998) found that EN- (LN-) related dry/wet (wet/dry) conditions over the northwestern/southwestern North America tends to be strong and more consistent during the WPDO (CPDO) regime.

Since the PDO regimes last about 20-30 years, the information on the ENSO effects stratified accordingly to the PDO phases may have a potential use to improve the climate forecasting. So, this section revises the ENSO-related rainfall anomaly patterns over southern South America, but taking into account the PDO phases. The associated anomaly patterns for the sea surface temperature (SST) and sea level pressure (SLP) will also be obtained and discussed.

## 14.2. Data analysis

The data used consist of monthly gridded SST and SLP values and monthly precipitation series at rainfall stations and grid points in the South American sector between 10° and 40°S. Although rainfall analyses are done for this sector, the focus will be on the southern South America (SSA) which is limited between 20° and 40°S. SST data are the extended reconstructed SST at 2° by 2° latitude-longitude resolution grid for the 1854-2000 period (Smith and Reynolds 2003). SLP data are at 5° by 5° latitude-longitude resolution grid for the 1871- 1994 period and were obtained from the British Atmospheric Data Centre at the webpage <http://www.badc.rl.ac.uk/>.

A total of 373 monthly rainfall series in the South American sector between 10° and 40°S were obtained from several sources. The Brazilian series are obtained from: The Instituto Nacional de Meteorologia and the Agência Nacional de Energia Elétrica. The series in the other countries of SSA are extracted from a monthly precipitation 'gu23wld0098.dat' (version 1.0) dataset for global land areas gridded at 2.5° by 3.75° latitude-longitude resolution grid for the period 1900-1998 (Hulme 1992, 1994; Hulme et al. 1998). This dataset was constructed by Dr. Mike Hulme at the Climatic Research Unit, University of East Anglia, Norwich, UK. Only rainfall series spanning for at least a 30 years of the precipitation base period ranging from 1912 to 1999 were used. These data are checked for errors. Monthly values higher than 2000 mm and suspicious values (detected by visual inspections of the series) are replaced by a missing data code.

ENSO extreme years are determined using the Trenberth's (1997) criterion for the Niño-3 SST index, which is defined as the 5-month running mean of the averaged SST anomalies in the area bounded at 6°N, 6°S, 150°W and 90°W. SST anomalies used in the computation of this index are departures from the 1854-2000 base period means. An EN (a LN) event is identified when the Niño-3 SST index exceeds 0.5°C (is less than -0.5°C) for at least six consecutive months. *Table 14.1* lists the onset years of EN and LN events identified during the 1912-1999 period. PDO phases are identified using Mantua et al. (1997) PDO index. So, the WPDO

*Table 14.1. The onset years of the ENSO extremes during the warm and cold PDO regimes.*

ENSO Phase	WPDO	CPDO
El Niño	1925, 1930, 1939, 1940, 1941, 1976, 1979, 1982, 1986, 1987, 1991, 1994, 1997	1914, 1918, 1951, 1957, 1963, 1965, 1968, 1969, 1972
La Niña	1933, 1938, 1942, 1985, 1988	1916, 1917, 1922, 1924, 1949, 1950, 1954, 1955, 1967, 1970, 1973, 1975

regime occurred during the periods of 1925-1946 and 1977-1999 and the CPDO regime occurred during the periods of 1912-1924 and 1947-1976.

ENSO-related monthly anomaly patterns for the rainfall, SST and SLP are obtained using the composite technique. The SST composites are done in the 60°N-30°S band and the SLP composites are done in the 20°N-80°S band. The anomalies for all variables are relative to monthly means of the years that exclude (from the 1912-1999 period) the onset years of the ENSO extremes for the months from July to December and the following years for the months from January to June. So, monthly means are obtained from 49 years of the 1912-1999 period with close to normal conditions relative to ENSO phenomenon. Monthly anomalies are computed for the SST and SLP time series at each grid point. Monthly precipitation anomaly time series are standardized by the standard deviation of the anomaly time series.

Monthly mean anomalies of precipitation, SST and SLP for EN and LN years stratified according to the PDO phases are calculated separately. These composites are obtained for each month of the period from September<sup>(0)</sup> to August<sup>(+)</sup> for rainfall anomalies, every other month of this same period for the SST anomalies and for each month of the period from October<sup>(0)</sup> to March<sup>(+)</sup> for SLP. The symbols <sup>(0)</sup> and <sup>(+)</sup> after the month refer to the onset and the following years of the ENSO extremes, respectively. The statistical significance of the composites is assessed assuming that the number of degrees of freedom is the number of events and using the Student-t tests (Press et al. 1986). The confidence level of 95% is used.

### 14.3. Precipitation patterns

The sequential EN-related monthly mean precipitation anomaly patterns for the WPDO regime shows a robust feature in SSA during the period from October<sup>(0)</sup> to February<sup>(+)</sup> (*Fig. 14.1*). Significant anomalies are observed in southern Brazil and in central Chile (positive) and in small areas to the North (negative) in October<sup>(0)</sup>. Gradually, the positive anomalies intensify and expand, occupying most of SSA in December<sup>(0)</sup>. At this time, the negative anomalies intensify and extend over southern Peru and over eastern Brazil. Significant positive anomalies remain over northeastern Argentina and Paraguay, whereas the rest of the study domain shows non-significant anomalies in January<sup>(+)</sup>. This configuration is modified in such a way that significant positive anomalies are noted in central and eastern Argentina, and opposite sign anomalies are found in southern Peru, Bolivia, northern Chile, and northern and northwestern Argentina during February<sup>(+)</sup>. Although the magnitude of the anomalies is quite small in March<sup>(+)</sup>, significant positive anomalies are reestablished in southern Brazil and in part of southeastern Brazil in April<sup>(+)</sup>. These anomalies weaken and remain in a small area of southern Brazil in May<sup>(+)</sup>. The precipitation anomaly patterns for the subsequent months are quite disorganized without a robust structure.

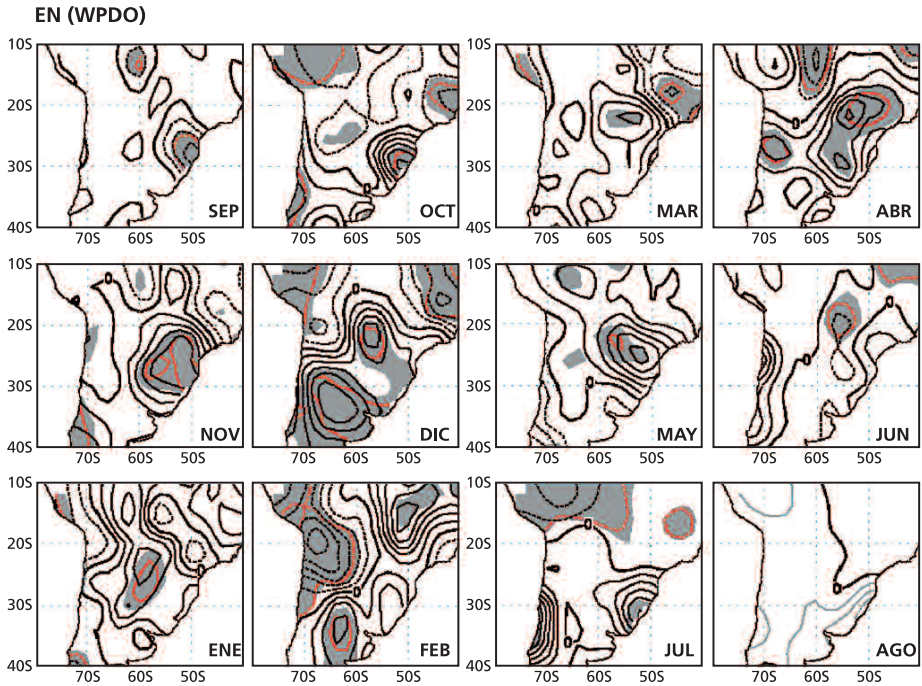


**Fig. 14.1.** Monthly El Niño-related mean standardized rainfall anomalies for the WPDO regime. Contour interval is 0.2 standard deviation, with negative (positive) contours being dashed (continuous). Shading encompasses values which are significant at the 90% confidence level. Red contours encompass values which are significant at the 95% confidence level.

The sequence of the monthly mean rainfall anomaly patterns of EN composites for the CPDO regime (Fig. 14.2) shows less robust feature than that of EN composites for the WPDO regime (Fig. 14.1). In fact, the areas with significant positive anomalies remain to the South of 30°S and for only three months of the sequence (November<sup>(0)</sup>, December<sup>(0)</sup> and March<sup>(+)</sup>). It seems that the significant negative anomalies in southern Peru, in northern Chile and in northern Bolivia show consistent evolving features during the period from October<sup>(0)</sup> to April<sup>(+)</sup>. EN-related precipitation anomalies for the CPDO regime show quite small magnitudes in the subsequent months.

The monthly mean rainfall anomaly patterns of LN composite for the WPDO regime feature well organized structures, in particular in SSA, during the period from October<sup>(0)</sup> to February<sup>(+)</sup> (Fig. 14.3). Consistent with LN events, negative rainfall anomalies are established in most of the study domain by October<sup>(0)</sup>. A robust structure with significant negative rainfall anomalies occupying a large area in the central and eastern SSA is conspicuous in November<sup>(0)</sup>. These anomalies weaken but remain well organized during the following three months being significant in most of SSA in December<sup>(0)</sup>, in a small area centred at (60°W; 25°S) in January<sup>(+)</sup>, and in most of SSA area South of 30°S in February<sup>(+)</sup>. LN-related rainfall anomalies in SSA present small magnitudes during the period from March<sup>(+)</sup> to August<sup>(+)</sup>.

EN (CPDO)

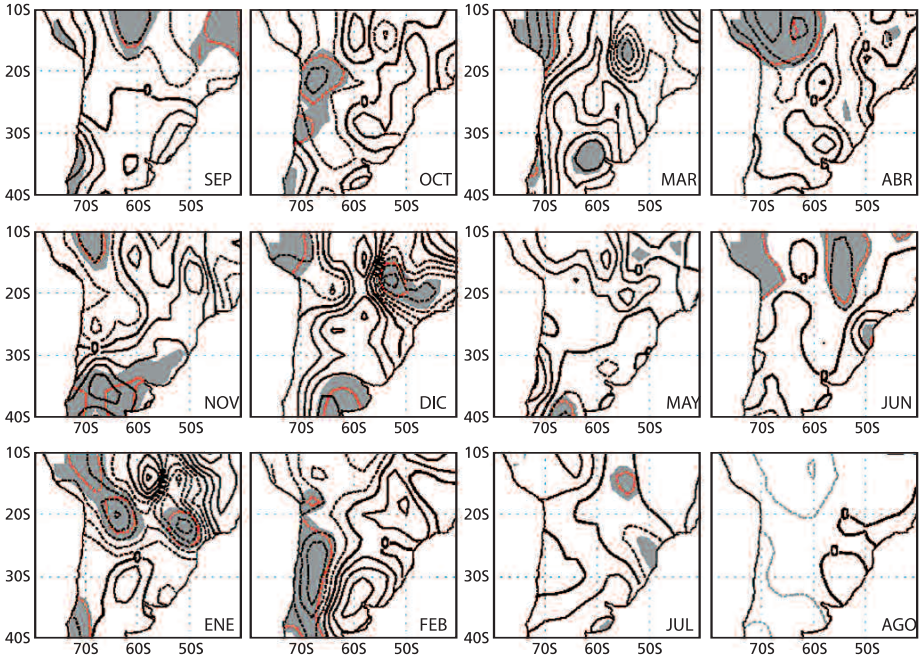


Fig. 14.2. As Fig. 14.1, except for CPDO regime.

LN (WPDO)

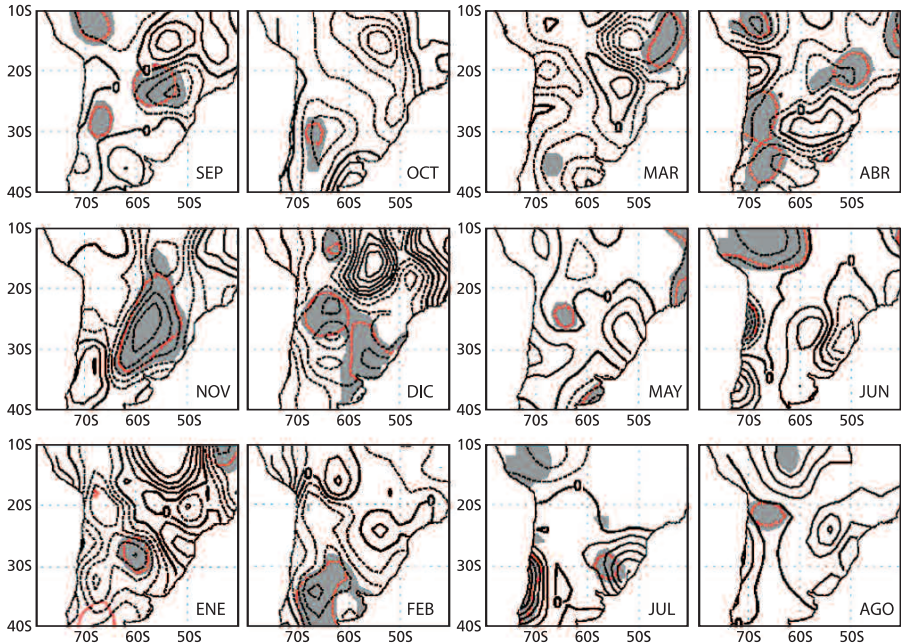


Fig. 14.3. Monthly La Niña-related mean standardized rainfall anomalies for the WPDO regime. Display is the same as that in figure 15.1.

Similar to LN rainfall composites for the WPDO regime, the corresponding composites for the CPDO regime show well organized and robust structures in SSA during the period from October<sup>(0)</sup> to February<sup>(+)</sup> (Fig. 14.4). Nevertheless, in this case, significant negative rainfall anomalies are located slightly to the South of those for the previous analysis. Negative rainfall anomalies for CPDO regime occupy most of the study domain by October<sup>(0)</sup>. These anomalies intensify yielding significant values extending over southern Brazil, Uruguay, Paraguay, southern Bolivia and eastern Argentina in November<sup>(0)</sup>. The negative anomalies remain relatively strong and occupy most of SSA South of 25°S by December<sup>(0)</sup>. The negative anomalies weaken and are limited to western central Argentina in January<sup>(+)</sup>. At this time, significant rainfall anomalies are noted in southern Peru (positive) and in eastern Brazil (negative). Significant anomalies are found in the eastern central Argentina (positive) and in a small area in central Chile (negative) in February<sup>(+)</sup>. Significant positive rainfall anomalies are noted only in a small area of the western central Brazil in March<sup>(+)</sup>. Significant negative rainfall anomalies are established in the southern Uruguay and in the eastern central Argentina in April<sup>(+)</sup>. LN-related rainfall anomaly patterns for the CPDO regime present quite small magnitude anomalies for the remaining subsequent months.

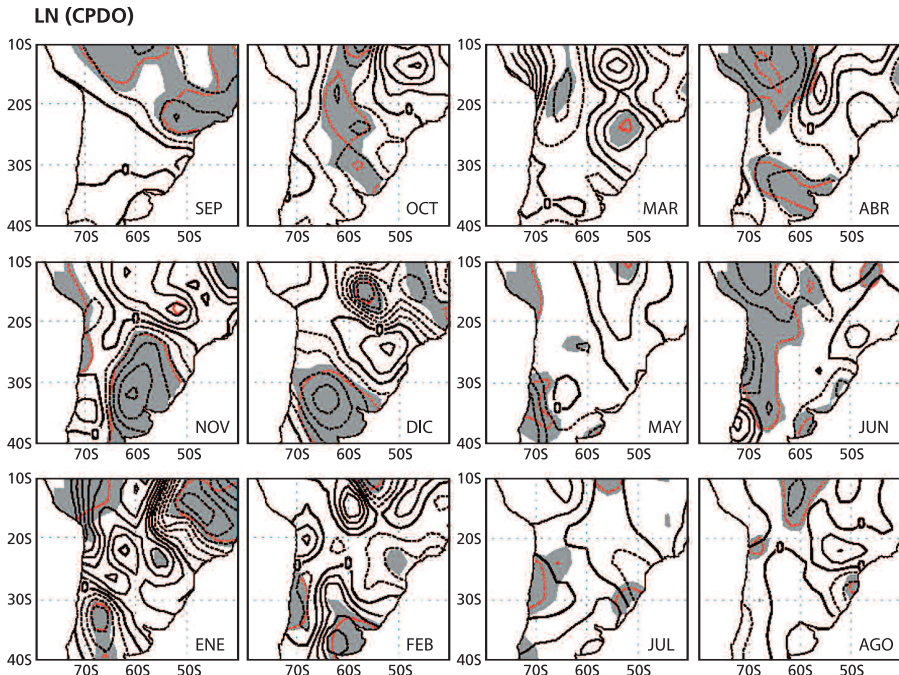
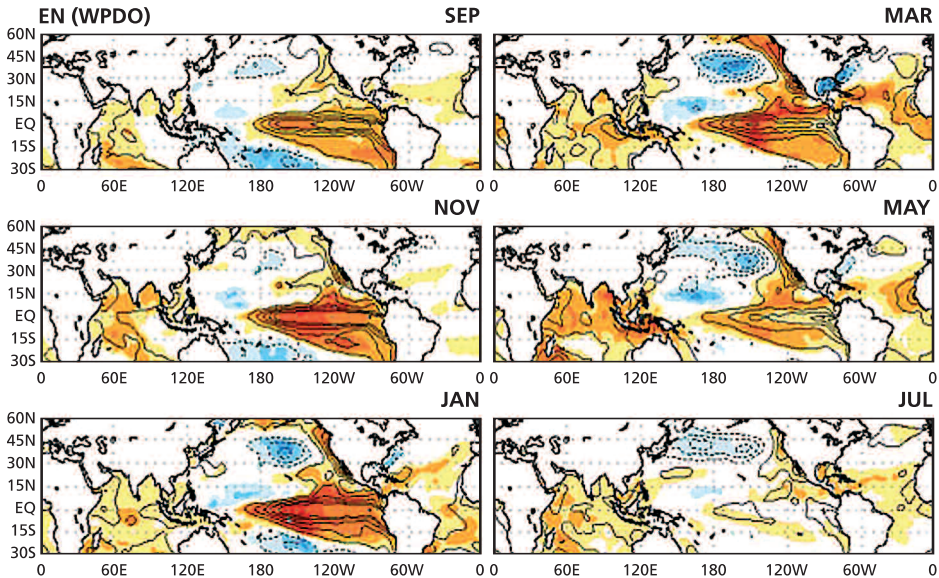


Fig. 14.4. As Fig. 14.3, except for CPDO regime.

## 14.4. SST composites

The sequential EN-related SST anomaly composites for the WPDO regime (Fig. 14.5) show significant positive SST anomalies over the central and eastern equatorial Pacific and along the West coast of the United States and significant negative anomalies in the North Pacific for the period from September<sup>(0)</sup> to May<sup>(+)</sup>. This pattern is similar to that associated with the PDO (Zhang et al. 1997). It is worthwhile noting that the negative centre in the North Pacific intensifies from November<sup>(0)</sup> to January<sup>(+)</sup>, and remains quite strong until July<sup>(+)</sup>. On the other hand, EN-related significant positive SST anomalies for the CPDO regime (Fig. 14.6) are confined to central and eastern equatorial Pacific. In this case, the positive anomalies remain quite strong until January<sup>(+)</sup>, when they start to weaken to almost disappear in May<sup>(+)</sup>. So, ENSO-like SST anomaly structure lasts longer for EN years of the WPDO regime than for EN years of the CPDO regime. This result is consistent with the reestablishment of positive rainfall anomalies in the southern and southeastern Brazil in April<sup>(+)</sup> and in the southeastern Brazil in May<sup>(+)</sup> for EN years of the WPDO and with very small rainfall anomalies in these same areas and months for EN years of the CPDO regime.



**Fig. 14.5.** Monthly El Niño-related mean SST anomalies for the WPDO regime for the indicated months. Contour interval is  $0.3^{\circ}\text{C}$ , with negative (positive) contours being dashed (continuous). Light to dark blue (yellow to red) shading encompasses negative (positive) values which are significant at the 95% confidence level. The zero contours have been omitted.

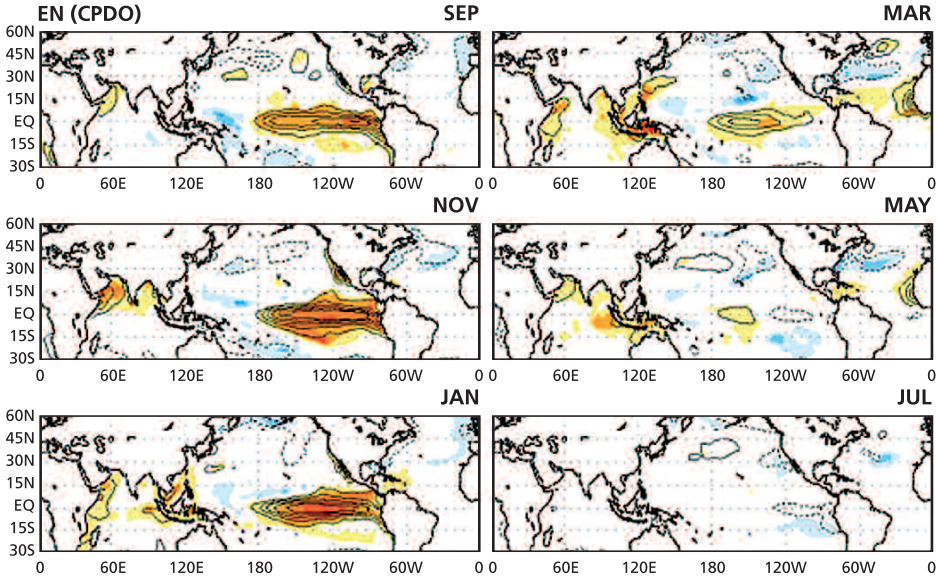


Fig. 14.6. As Fig. 14.5, except for CPDO regime.

The sequential LN-related SST anomaly composites for the WPDO regime (Fig. 14.7) show significant negative SST anomalies confined to central and eastern equatorial Pacific. These anomalies remain quite strong until January<sup>(+)</sup>, whereas they weaken considerably in March<sup>(+)</sup>. However, this pattern weakens further

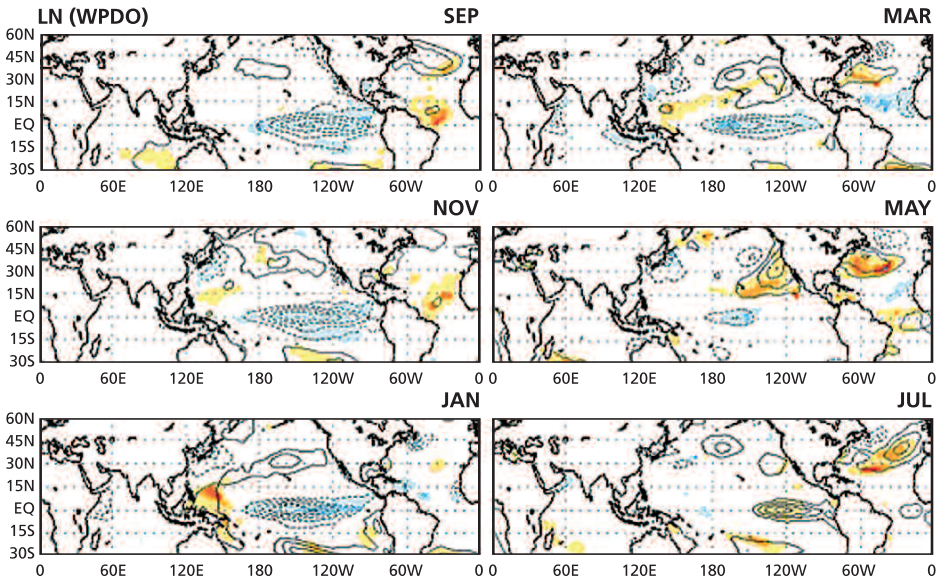
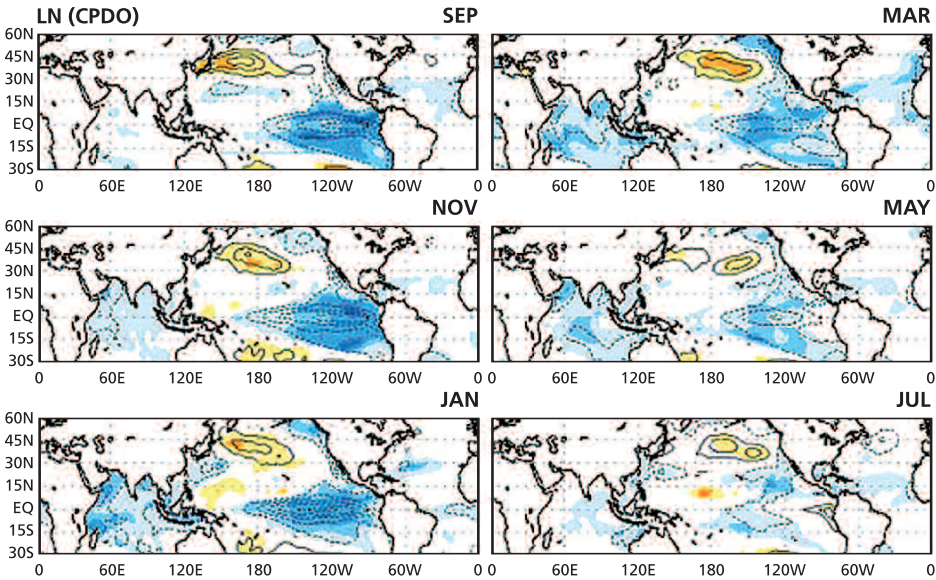


Fig. 14.7. Monthly La Niña-related mean SST anomalies for the WPDO regime for the indicated months. Display is the same as that in figure 14.5.

during the subsequent months to establish an opposite sign pattern in July<sup>(+)</sup>. LN-related SST anomaly patterns for the CPDO regime (*Fig. 14.8*) feature significant negative SST anomalies in the central and eastern equatorial Pacific and along the West coast of the United States and significant positive anomalies in the North Pacific during the period from September<sup>(0)</sup> to May<sup>(+)</sup>. This pattern resembles that one associated with the PDO (Zhang et al. 1997). The positive centre in the North Pacific keeps almost the same intensity and moves from the western North Pacific to the central North Pacific from September<sup>(0)</sup> to July<sup>(+)</sup>.



*Fig. 14.8.* As *Fig. 14.7*, except for CPDO regime.

### 14.5. SLP composites

Since ENSO-related SLP patterns show considerable monthly variations, the analyses for this parameter are done for the period from October<sup>(0)</sup> to March<sup>(+)</sup>, when ENSO-related rainfall patterns present the largest anomalies. EN-related SLP patterns for the WPDO regime show the largest anomalies in the tropics with the negative values in the central and eastern Tropical Pacific and the positive values prevailing in the Australasian and/or in the Atlantic/African regions (*Fig. 14.9*). The areas with the largest anomalies which take part in the East-West pressure balance are centred, in latitude, at the equator. Consequently, these areas define an anomalous Walker circulation in the equatorial vertical zonal plane. Although the longitudinal location and the intensity of the anomalous Walker circulation vary monthly, it is strong and well established in the Australasian-Pacific sector during most months of the period from October<sup>(0)</sup> to March<sup>(+)</sup>.

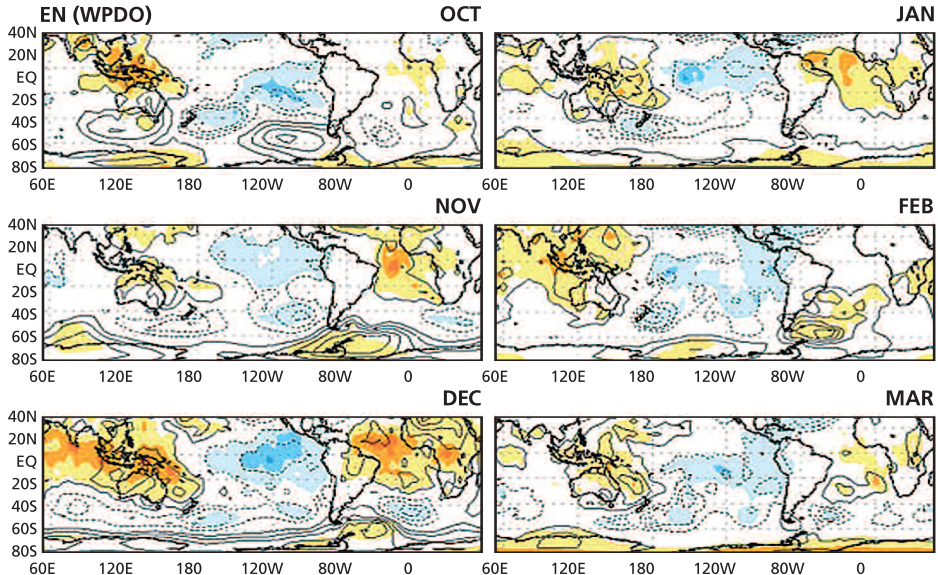


**Fig. 14.9.** Monthly El Niño-related mean SLP anomalies for the WPDO regime for the indicated months. Contour interval is 0.5 hPa, with negative (positive) contours being dashed (continuous). Light to dark blue (yellow to red) shading encompasses negative (positive) values which are significant at the 95% confidence level. The zero contours have been omitted.

On the other hand, EN-related SLP patterns for the CPDO regime show dominant positive anomalies in the Australasian region and quite small negative anomalies in the central and eastern Tropical Pacific (Fig. 14.10). So, the associated anomalous Walker circulation is relatively weaker than for the previous case. Similarly, LN-related SLP anomaly patterns for the WPDO regime feature positive anomalies in the central and eastern equatorial Pacific and negative anomalies in the Australasian region (Fig. 14.11). These anomalies show quite small magnitudes, that indicates almost normal Walker circulation.

LN-related SLP composites for the CPDO show significant anomalies in the tropics with the positive values in the central and eastern Tropical Pacific and the negative values over the Australasian and/or the Atlantic/African regions (Fig. 14.12). It is interesting to note that the areas with the largest anomalies in the Australasian-Pacific sector which take part in the East-West pressure balance are neither centred at the equator nor located at the same latitude. In fact, the negative area in the Australasian region has a variable latitudinal location. It is between the equator and 20°S from October<sup>(0)</sup> to December<sup>(0)</sup> and in March<sup>(+)</sup>, approximately in the equator in January<sup>(+)</sup>, and between the equator and 20°N in February<sup>(+)</sup>. On the other hand, the positive area in the central eastern Pacific is located between 20° and 40°S approximately in the southeastern side of the South Pacific Convergence Zone (SPCZ) in most months of the period from October<sup>(0)</sup> to March<sup>(+)</sup>. This result implies that considerable variations might occur in the convective activity along the SPCZ during LN years of the CPDO regime.

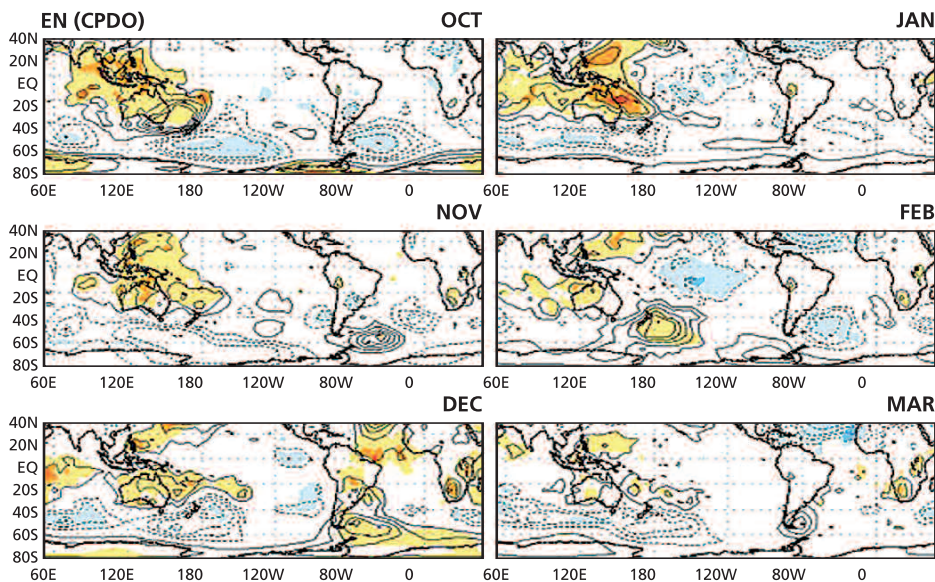


Fig. 14.10. As Fig. 14.9, except for CPDO regime.

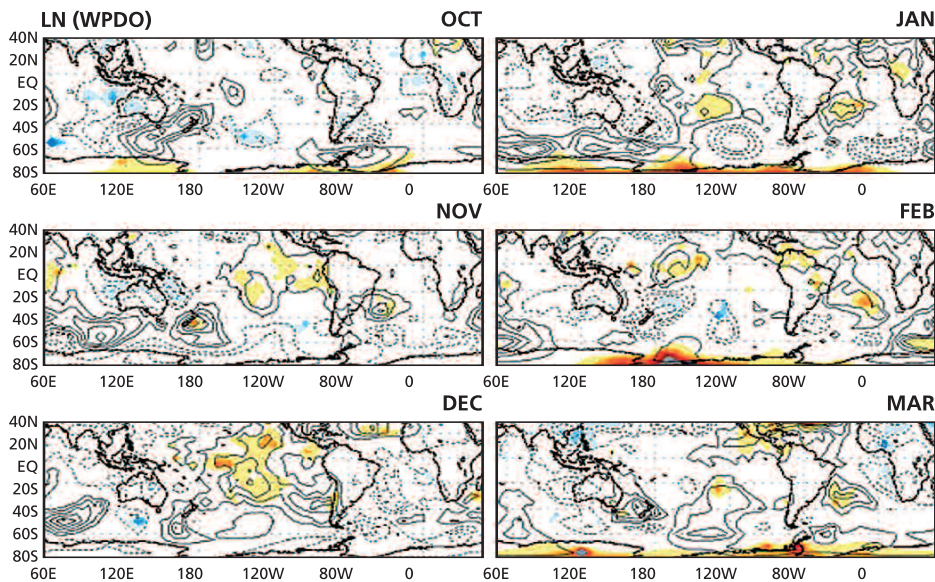


Fig. 14.11. Monthly La Niña-related mean SLP anomalies for the WPDO regime for the indicated months. Display is the same as that in figure 14.9.

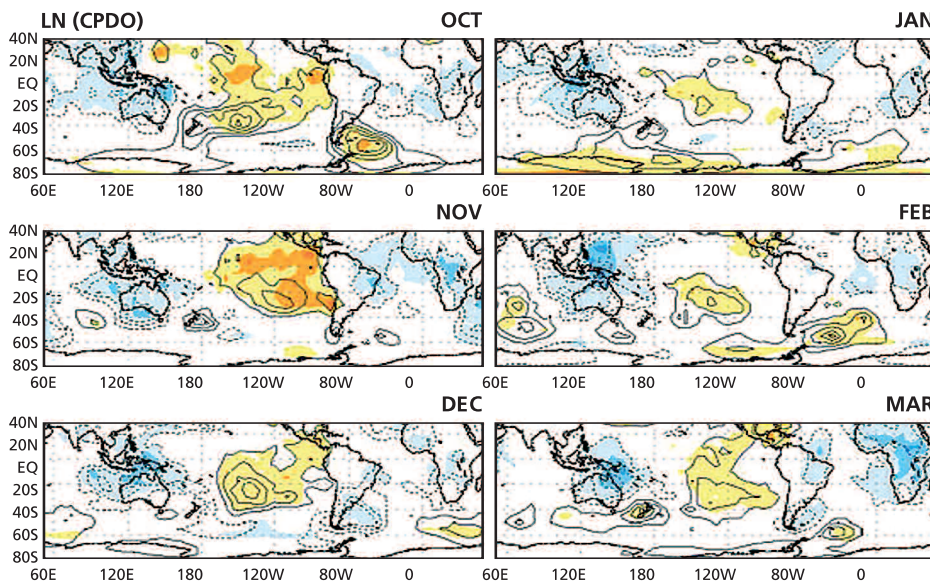


Fig. 14.12. As Fig. 14.11, except for CPDO regime.

## 14.6. Conclusions

Concerning the estimation of future hydro-meteorological conditions, Robertson et al. (2001) analyzed the decadal fluctuations of the streamflow for the Paraná River at Corrientes during the 1904–1997 period and provided indications that these fluctuations may be partially predictable. They isolated the oscillatory components with periods of 8 years and 17 years and constructed autoregressive predictive models for each component. Their prediction based upon the 8 year and the 17 year oscillatory components, including data up to the austral summer of 1999, suggested increased probability of below-average flows until 2006. Thus, they found a high probability of drought occurrence in the region of the La Plata River basin during the period from 2002 to 2006. However, it is worth noting that their results are based on near-cyclic components (with periods of 8 and 17 years) of the streamflow for the Paraná River and do not take into account the non-linear component of this parameter relative to the PDO phases. So, the present analysis provides another view of the interannual climate variability in the La Plata River basin, which takes into account the non-linear aspects of the climate in the region relative to the PDO phases and to the ENSO phases.

Comparisons between ENSO-related anomaly patterns of SSA rainfall, SST and SLP for the WPDO and CPDO regimes show important differences which represent the non-linear components of these composites relative to the PDO phases (for a given ENSO phase) and relative to ENSO phases (for a given PDO phase).

In general, these patterns show robust (weak) and quite well (noisy) spatial structure for the composites in which the ENSO and the PDO are in the same (opposite) phase for austral summer and autumn seasons. So, the WPDO (CPDO) background modulates the ENSO-effects in SSA rainfall, enhancing EN (LN) and weakening LN (EN), during austral summer and autumn months. The connection of the PDO phases and ENSO-related rainfall anomalies in SSA is similar to the PDO modulations of ENSO signals in the rainfall in the Northwest/southwest United States analyzed by Gershunov and Barnett (1998). The differences of EN-related rainfall composites in SSA between the WPDO and CPDO regimes might be explained comparing the corresponding SST composites. The SST composites for the WPDO (CPDO) regime resemble the SST anomaly pattern associated with EN conditions in the equatorial eastern Pacific and cold (warm) conditions in the subtropical south-central Pacific defined by Barros and Silvestri (2002) and Vera et al. (2004). So, a possible explanation for the differences in EN rainfall composites in SSA for the WPDO and the CPDO phases lies in the circulation anomalies characterizing differences in EN response in the South Pacific as shown by Vera et al. (2004).

Another important aspect shown in the present analysis consists of the non-linear components of the composites relative to the ENSO phases for a given PDO phase. It is worthwhile mentioning that the ENSO-related precipitation anomaly patterns with positive (negative) values in SSA for EN (LN) events documented in previous studies (Walker 1928; Caviades 1973; Hastenrath and Heller 1977; Kousky et al. 1984; Ropelewski and Halpert 1987, 1989; Aceituno 1988; Kayano et al. 1988; Kiladis and Diaz 1989; Kayano 2003; Grimm 2003) represent in fact the linear component of ENSO-effects in SSA rainfall. In order to take into account the non-linear component of the ENSO-effects in SSA rainfall, EN and LN composites should be considered separately. The sequences of monthly rainfall of the ENSO composites for SSA rainfall in *figures 14.1 to 14.4* might provide guidance for future climate monitoring and forecasting purposes for this region.

Another aspect that should be also taken into account for these purposes is the phase of the PDO. Concerning to this, several studies have suggested that the PDO shifted back into the cold regime in the late 1990 (Hare and Mantua 2000; Schwing and Moore 2000; Landscheidt 2001). If the PDO is now in a cold regime, EN-related and LN-related composites for the CPDO phase (*Figs. 14.2 and 14.4*) are more appropriate guides to estimate future hydro-meteorological conditions in SSA, while the cold regime lasts.

The authors were partially supported by the Conselho Nacional de Desenvolvimento Científico and Tecnológico of Brazil. Thanks are due to the UK Meteorological Office (UKMO) for the provision of the sea level pressure data used in this paper. Thanks are also due to Dr. Mike Hulme for the provision of the 'gu23wld0098.dat' (version 1.0) constructed at the Climatic Research Unit, University of East Anglia, Norwich, UK.

## References

- Aceituno, P. 1988: On the functioning of the Southern Oscillation in the South American Sector. Part 1: surface climate. *Mon. Wea. Rev.*, 116, 505-524.
- Barros, V. R. and G. E. Silvestri 2002: The relation between sea surface temperature at the subtropical south-central Pacific and precipitation in southeastern South America. *J. Climate*, 15, 251-267.
- Caviedes, C. N. 1973: Secas and El Niño: two simultaneous climatological hazards in South America. *Proc. Assoc. Amer. Geograph.*, 5, 44-49.
- Enfield, D. B. and A. Mestas-Núñez 1999: Multiscale variabilities in global sea surface temperatures and their relationships with tropospheric climate patterns. *J. Climate*, 12, 2719-2733.
- Gershunov, A. and T. P. Barnett 1998: Interdecadal modulation of ENSO teleconnections. *Bull. Amer. Meteor. Soc.*, 79, 2715-2725.
- Grimm, A. M. 2003: The El Niño impact on the Summer monsoon in Brazil: regional processes versus remote influences. *J. Climate*, 16, 263-280.
- Gutzler, D. S., D. M. Kann and C. Thornbrugh 2002: Modulation of ENSO-based long-lead outlooks of southwestern U.S. Winter precipitation by the Pacific decadal oscillation. *Wea. Forecast.*, 17, 1163-1172.
- Hare, S. R. and N. J. Mantua 2000: Empirical evidence for North Pacific regime shifts in 1977 and 1989. *Prog. Oceanogr.*, 47, 103-146.
- Hastenrath, S. and L. Heller 1977: Dynamics of climatic hazards in Northeast Brazil. *Quart. J. Roy. Meteor. Soc.*, 103, 77-92.
- Hulme, M. A. 1992: 1951-80 global land precipitation climatology for the evaluation of General Circulation Models. *Climate Dyn.*, 7, 57-72.
- \_\_\_\_\_. 1994: Validation of large-scale precipitation fields in General Circulation Models. In *Global Precipitations and Climate Change*, eds. Desbois, M., and F. Desalmand, NATO ASI series, Springer-Verlag, Berlin, 466 pp.
- \_\_\_\_\_, T. J. Osborn and T. C. Johns 1998: Precipitation sensitivity to global warming: comparison of observations with HadCM2 simulations. *Geophys. Res. Lett.*, 25, 3379-3382.
- Kayano, M.T. 2003: A note on the precipitation anomalies in southern South America associated with ENSO variability in the Tropical Pacific. *Meteorol. Atmos. Phys.*, 84, 267-274.
- \_\_\_\_\_, V. B. Rao and A. D. Moura 1988: Tropical circulations and the associated rainfall anomalies during two contrasting years. *J. Climatol.*, 8, 477-488.
- Kiladis, G. and H. F. Diaz 1989: Global climatic anomalies associated with extremes in the Southern Oscillation. *J. Climate*, 2, 1069-1090.
- Kousky, V. E., M.T. Kayano and I. F. A. Cavalcanti 1984: A review of the Southern Oscillation: oceanic-atmospheric circulation changes and related rainfall anomalies. *Tellus*, 36A, 490-504.
- Krishnan, R. and M. Sugi 2003: Pacific decadal oscillation and variability of the Indian Summer monsoon rainfall. *Climate Dyn.*, 21, 233-242.
- Landscheidt, T. 2001: Trends in Pacific decadal oscillation subjected to solar forcing. <http://www.john-daly.com/theodor/pdotrend.htm>.
- Latif, M. and T. P. Barnett 1994: Causes of decadal climate variability over the North Pacific and North America. *Science*, 266, 634-637.

- Mantua, N. J., S. R. Hare, Y. Zhang, J. M. Wallace and R. C. Francis 1997: A Pacific interdecadal climate oscillation with impacts on salmon production. *Bull. Amer. Meteor. Soc.*, 78, 1069-1079.
- McCabe, G. J. and M. D. Dettinger 1999: Decadal variations in the strength of ENSO teleconnections with precipitation in the western United States. *Int. J. Climatol.*, 19, 1399-1410.
- Minobe, S. A. 1997: 50-70 year climatic oscillation over the North Pacific and North America. *Geophys. Res. Lett.*, 24, 683-686.
- \_\_\_\_\_ 1999: Resonance in bidecadal and pentadecadal climate oscillations over the North Pacific: role in climatic regime shifts. *Geophys. Res. Lett.*, 26, 855-858.
- Nitta, T. and S. Yamada 1989: Recent warming of tropical sea surface temperature and its relationship to the Northern Hemisphere circulation. *J. Meteor. Soc. Japan*, 67, 375-383.
- Press, W. H., B. P. Flannery, S. A. Teukolsky and W.T. Vetterling 1986: *Numerical Recipes: The Art of Scientific Computing*. Cambridge University Press, Cambridge - NY, 818 pp.
- Robertson, A. W., C. R. Mechoso and N. B. Garcia 2001: Interannual prediction of the Paraná river. *Geophys. Res. Lett.*, 28, 4235-4238.
- Ropelewski, C.F. and M. S. Halpert 1987: Global and regional scale precipitation patterns associated with the El Niño/Southern Oscillation. *Mon. Wea. Rev.*, 115, 1606-1626.
- \_\_\_\_\_ and \_\_\_\_\_ 1989: Precipitation patterns associated with the high index phase of the Southern Oscillation. *J. Climate*, 2, 268-284.
- Schwing, F. and C. Moore 2000: A year without a Summer for California, or a harbinger of a climate shift? *EOS Trans., AGU*, 81, 304-305.
- Smith, T. M. and R. W. Reynolds 2003: Extended reconstruction of global sea surface temperatures based on COADS data (1854-1997). *J. Climate*, 16, 1495-1510.
- Tanimoto, Y., N. Iwasaka, K. Hanawa and Y. Toba 1993: Characteristic variations of sea surface temperature with multiple time scales in the North Pacific. *J. Climate*, 6, 1153-1160,
- Trenberth, K. E. 1990: Recent observed interdecadal climate changes in the Northern Hemisphere. *Bull. Amer. Meteor. Soc.*, 71, 988-993,
- \_\_\_\_\_ 1997: The definition of El Niño. *Bull. Amer. Meteor. Soc.*, 78, 2771-2777.
- \_\_\_\_\_ and J. W. Hurrell, 1994: Decadal atmospheric-ocean variations in the Pacific. *Climate Dyn.*, 9, 303-319.
- Vera C., G. E. Silvestri, V. R. Barros and A. Carril 2004: Differences in El Niño response over the Southern Hemisphere. *J. Climate*, 17, 1741-1753.
- Walker, G. T. 1928: *World Weather III*. *Mem. Roy. Meteor. Soc.*, 97-104.
- Zhang, Y., J. M. Wallace and D. Battisti 1997: ENSO-like interdecadal variability: 1900-93. *J. Climate*, 10, 1004-1020.
- \_\_\_\_\_, J. Norris and J. M. Wallace 1998: Seasonality of large-scale atmosphere-ocean interaction over the North Pacific. *J. Climate*, 11, 2473-2481.

## STATISTICAL ANALYSIS OF EXTREME EVENTS IN A NON-STATIONARY CONTEXT

*Robin Clarke<sup>1</sup>*

<sup>1</sup> Instituto de Pesquisas Hidráulicas, UFRGS, in Porto Alegre, RS Brazil.

### ABSTRACT

This chapter discusses aspects of the statistical analysis of trends in extremes of precipitation (typically maximum intensities, of different durations) and streamflow (typically annual maximum instantaneous discharges; annual maximum mean daily discharges). An important feature of such data is that they are unlikely to follow a Gaussian distribution, so that analyzing for trend using theory based on the Normal distribution (e.g., regression analysis) is no longer appropriate. Although non-parametric methods can be used to test for trend, they do not provide a means for estimating the probability of occurrence of extremes in future periods. The parametric methods described in this chapter deal with analyses of trend in annual maxima (e.g., annual maximum one-day rainfall), and in “peaks over a threshold” (POT) approach, in which a threshold event is selected, and all events larger than this threshold are included for analysis. Analytical techniques are illustrated with examples from the La Plata basin; adaptations are presented for cases where records are only partially complete, and the concept of return period in the presence of non-stationarity is discussed.

## **15.1. Introduction**

At a time when the possibility of climate change might be bringing about extreme events of increasing severity, good analytical procedures are required to detect the existence of trends in extreme values of hydrological variables, such as rainfall intensity and peak discharges; of meteorological variables such as extreme wind speeds, the frequency of hurricane occurrence, and the frequency and intensity of hail storms; and of oceanographic variables such as the magnitude and frequency of occurrence of large waves.

This section is concerned with some aspects in the statistical analysis of trends in extremes of precipitation (typically maximum intensities, of different durations) and streamflow (typically annual maximum instantaneous discharges; annual maximum mean daily discharges). Irrespective of the existence of trend, two approaches to the analysis of extremes are possible: (a) the “Block” method, in which a period is selected, commonly of one year's duration, and the maximum of a variable of interest (for example discharge) is selected from each block, thus giving rise to a series of annual events that are used to draw inferences about the distribution of extreme events, the presence or absence of trend, and - where no trend exists - on the return period of events of interest. (b) the “peaks over a threshold” (POT) approach, in which a threshold event is selected. In the case of flood discharges and rainfall intensities, all events (“peaks”) exceeding the threshold are used for analysis; the threshold event is taken as one which commonly gives about three or four peaks over the threshold, on average, in any year. This approach has the advantage that more data are included for analysis than in the “Block” method, a point of particular importance when records are of limited length (in the Block method, only one observation is used per year). This section discusses aspects of both the Block and POT methods. Both approaches are very fully described in the book by Coles (2001).

In the above paragraph, the account given of the POT method referred to peaks over a threshold because one of the principal applications has been in the analysis of flood frequencies. However in principle there is no theoretical reason why the selected events should not lie below the threshold, as when drought periods are of interest. Where used in flood frequency analysis, a possible limitation of the POT method in the particular context of large drainage basins of South America is that the annual hydrograph (that is, the plot of discharge against time) is smooth, typically showing just one well-defined maximum and one well-defined minimum. For basins of this kind, the peaks of the POT method are identical with the annual maxima of the Block approach, and the two methods are indistinguishable. However, the POT approach will still be useful for frequency analysis of runoff records from small basins which respond rapidly to rainfall, and where runoff records are short. An important requirement for the POT approach is that the “peaks” be independent of each other. This will not be the case where, for example, the peaks occur in “clusters”; if, for example, a threshold of 40mm were selected when analyzing a series of daily rainfall, one storm might perhaps give rise to two

or three consecutive days on which rainfall exceeded this threshold; it would then necessary to select, from this “cluster” of days, only the day on which the maximum rainfall occurred. If all days in the cluster were included for analysis, the peaks could not be considered as statistically independent. Independence between peaks can be obtained by choosing the threshold to be very high, but if the threshold is very high, the number of retained peaks will be small. The occurrence of “clumping” is, of course, much more evident when the “peak” events are low discharges below a threshold.

Independence between successive observations is also important when using the Block method. It is almost always assumed that the events that occur in successive years are statistically independent. This assumption is valid for the analysis of rainfall intensities of short duration, but it may be less appropriate for the analysis of droughts, which may extend from one hydrological year into the next. It may also be invalid for the analysis of flood discharges in large drainage basins with extensive storage in soils and aquifers, since above-average rainfall in one year will fill storage, which may then contribute to the peak discharge of the following year. Conversely, below-average rainfall in a given year will deplete the volume in storage, so that the recharge of storage by rainfall in the following year may result in a depletion of flood flow. This is a feature of flood peaks observed at Ladário on the Upper Paraguay, where there is a highly significant serial correlation (0.48) between peak flood levels in successive years. Thus, the assumptions commonly made in the frequency analysis of flood records need to be carefully checked, in the case of large drainage basins of South America. Serial correlation in hydrological variables such as mean annual discharge is likely to be more important than the correlation between annual maximum discharges, but since this report is concerned with extremes rather than mean values, this problem is not considered further. However it should be noted that there will be strong correlation between annual maximum rainfall intensities of different durations (the rainfall event giving annual maximum 5-minute and 10-minute intensities is likely to be the same); this will be important where it is required to give confidence regions for curves that relate rainfall intensity to rainfall duration, for different return periods.

## **15.2. Parametric and non-parametric methods for detecting trend in hydrological variables**

Where the Block approach is used, trends may be detected in records of extreme rainfall, or in records of extreme discharges, by either parametric or non-parametric methods. The Mann-Kendall test is perhaps the most well-known non-parametric test for trend in annual values of a hydrological variable, when it can be assumed to be independent from one year to the next; this and other non-parametric tests have the advantage that nothing need be assumed about either the form of probability distribution of the variable being analyzed, or the nature of the trend.

Parametric methods, on the other hand, require specific assumptions about the form of the underlying probability distribution of the data, and about the form (linear, curvilinear, etc.) of any trend that may exist. This might seem to be a disadvantage. However, by assuming a particular probability distribution (provided it is supported by the data!) it is possible to make inferences about the trend, such as setting limits to its magnitude, estimating the uncertainty of future values where the user is sufficiently courageous to extrapolate the trends for a few years ahead; and to test whether simpler or more complex probability distributions are needed to represent the data. Thus, despite the fact that they require more assumptions, parametric methods are generally held to offer a more flexible approach to the study of extremes, than non-parametric methods. The emphasis in the present report is therefore on parametric methods. There is now an extensive literature on such methods (see, for example, the book by Coles 2001, which lists software in S-Plus that can be downloaded); much material is also available from the internet (see, for example, the site [www.maths.lancs.ac.uk/~stephena/software.html](http://www.maths.lancs.ac.uk/~stephena/software.html)). There is also a journal (Extremes, published by Kuyper) specifically devoted to developments in the analysis of extreme values. The book by Coles (2001) has a chapter on the estimation of trends in the parameters of probability distributions, including the Block approach used with a Generalized Extreme Value (GEV) probability distribution, and the POT approach used with exceedances above the threshold represented by a Generalized Pareto distribution.

### 15.3. Example: Testing for trend in annual maximum one-hour rainfall at Porto Alegre, Brazil

Table 15.1 shows annual maximum one-hour rainfalls at Porto Alegre, Brazil, over the 23-year period 1975-1997. As an example, we fit a GEV distribution and test whether there is a time trend in the location parameter, although a look at the data suggests that this is unlikely. The cumulative probability function is

*Table 15.1. Annual maximum rainfall of one-hour duration, 1975-97, Porto Alegre, Brazil.*

Year	1975	1976	1977	1978	1979
P_01_hr	30.9	73.4	25.0	21.4	27.3
Year	1980	1981	1982	1983	1984
P_01_hr	33.0	81.2	28.9	25.1	45.6
Year	1985	1986	1987	1988	1989
P_01_hr	41.3	43.6	50.2	20.5	33.7
Year	1990	1991	1992	1993	1994
P_01_hr	43.6	34.0	47.2	33.8	26.8
Year	1995	1996	1997		
P_01_hr	56.2	32.1	22.7		

$$\begin{aligned}
 F(x) &= \exp(-[1 + \xi(x - \mu)/\sigma]^{-1/\xi}) & \xi \neq 0 \\
 &= \exp(-\exp(-(x - \mu)/\sigma)), & \xi = 0
 \end{aligned}$$

where the second form with  $\xi=0$  is the well-known Gumbel distribution. We wish to test whether the location parameter  $\mu$  changes over the 23-year period of record, and the simplest starting point is to assume that  $\mu$  changes linearly over the period of record: that is,  $\mu = \alpha + \beta t$ , where  $t$  is the time in years. Thus four parameters ( $\alpha, \beta, \sigma, \xi$ ) must be estimated from the 23 data values in *table 15.1*. The method of fitting is the method of Maximum Likelihood (denoted by ML: see explanation of the method given below), and it is desired to know whether the parameter  $\beta$  differs significantly from zero, which would indicate a time-trend. Use of a standard statistical package (GenStat©) gives the results shown in *table 15.2*.

**Table 15.2.** Results from fitting a GEV distribution, with time-trend in the location parameter  $\mu$ , to data of *table 15.1*.

Fitting Trend term: Year		
*** Estimates of GEV parameters ***		
estimate "s.e."		
Mu (Intercept)	30.09	3.190
Sigma	9.017	2.668
Eta	0.2765	0.3223
Slope(Year)	0.05857	0.3079
Maximum Log-Likelihood = -90.498		
Maximum value of GEV Distribution is Infinite (Eta >= 0)		
Significance Test that Eta = 0 (ie P_01_hr follows a Gumbel distribution)		
Likelihood Ratio test statistic: 2.029		
Chi-Squared Probability of test: 0.1544		

It is seen that the estimate of the slope parameter  $\beta$  is  $0.05857 \pm 0.3079$  (units: mm year<sup>-1</sup>, recalling that the data are one-hour annual maxima), so that the estimate is much smaller than its standard error. Thus there is no significant evidence that the location parameter  $\mu$  of the GEV distribution changed over the period 1975-97. It is also seen that the shape parameter  $\xi$  of the GEV distribution is estimated as  $0.2765 \pm 0.3223$ , so that this estimate too is less than its standard error and not significantly different from zero. This means that the simpler Gumbel form  $F(x) = \exp(-\exp(-(x - \mu)/\sigma))$ , with two parameters instead of three, can be used in further analyses, instead of the GEV distribution.

The example of the preceding paragraph explored whether the 23 annual observations showed a trend in time, but it is also possible (again using standard software) to test whether time-trends exist in the dispersion parameter  $\sigma$  and the

shape parameter  $\xi$  of the GEV distribution. In the case of the dispersion parameter, a trend would be explored using  $\sigma = \exp(\alpha + \beta t)$ , the exponential being used to ensure that the dispersion parameter is always non-negative. Also, instead of looking at trends where the parameters vary in time, it is also possible to use the same approach to determine whether other kinds of trend exist; for example, it might be of interest to test whether annual maximum one-hour rainfall is related in some way to the Southern Oscillation Index (SOI). In this case, SOI would take the place of the time variable  $t$  in the above example.

The method of Maximum Likelihood, used in the above example, underpins a very large part of estimation and hypothesis-testing procedures in parametric statistics, and it is not proposed here to re-present the theory that is already fully presented in many text-books. Briefly, given independent observations  $x_1, x_2, \dots, x_N$  of a random variable  $X$  with probability distribution  $f_X(x, \theta)$  where  $\theta$  is a parameter to be estimated, the likelihood function  $L(\theta, x_1, x_2, \dots, x_N)$  is the product  $f_X(x_1, \theta) f_X(x_2, \theta) \dots f_X(x_N, \theta)$ , and the ML estimate of  $\theta$  is the value that maximizes this function. The variance of the estimate of  $\theta$  is approximately  $-1/(\text{second derivative of } \log_e L \text{ with respect to } \theta)$ . ML estimates have desirable statistical properties which makes ML estimation the procedure of choice, when the distribution  $f_X(x, \theta)$  can be specified. The brief account given here assumes just one parameter  $\theta$ ; extension to the case of several parameters  $\theta = \{\theta_1, \theta_2, \dots\}$  is straightforward.

To determine whether the selected distribution (in this case, the GEV) is appropriate for the data being analyzed, diagnostic techniques are used which are also provided by the available software packages. *Figure 15.1*, known as a Q-Q plot, shows a plot of the order statistics of the Porto Alegre data (vertical axis) against the corresponding quantiles (“scores”) for a GEV distribution; if the GEV provides a good fit to data, the plotted points should lie close to a straight line. The degree of agreement between the points and a straight line is ascertained by looking at whether the plotted points lie within the 95% confidence band, which is also shown in *Fig. 15.1*. This shows that there is no reason to doubt that the GEV is appropriate for the data. Since, in the present example, there is no evidence of time-trend in the data, return periods can be calculated as shown in *Fig. 15.2*; the return period, in years, is shown on the horizontal axis, and the hourly rainfall for this return period is shown on the vertical axis. The 95% confidence limits, also plotted, show that there is considerable uncertainty in the calculated rainfalls.

#### 15.4. Example: POT procedure applied to fitting daily rainfalls at Ceres, Argentina

This example uses the 44-year record 1959-2002 of daily rainfall for Ceres, Argentina, supplied by the National Meteorological Service. The example uses a threshold of 100mm. Theory (e.g., Coles 2001) shows that the distribution of daily

Standardized Q-Q graphics (P\_01\_hr) for a GEV distribution

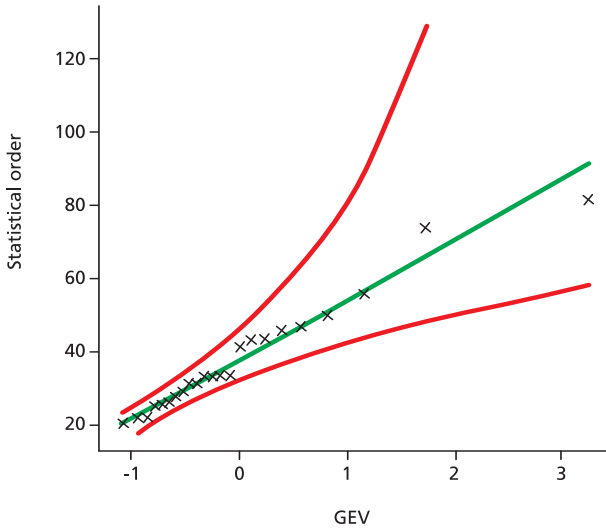


Fig. 15.1. Q-Q (“quantile-quantile”) plot for fitting a GEV distribution to annual maximum one-hour rainfall at Porto Alegre, Brazil (data shown in Table 15.1). Points lying near to a straight line shows that the GEV distribution is appropriate for the data. The figure also shows a 95% confidence band, within which the plotted points all lie (if points lay outside this band, the GEV distribution would be inappropriate).

Graphic of the return level for the standardized (P\_01\_hr)

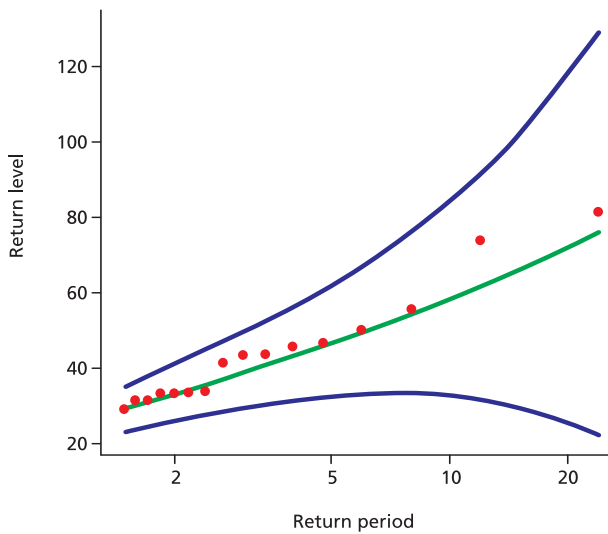


Fig. 15.2. Plot of return period in years (horizontal axis), with hourly rainfall, for the annual maximum one-hour rainfall at Porto Alegre, shown in Table 15.1.

rainfalls in excess of the threshold has a generalized Pareto distribution (GPD), closely related to the GEV distribution of the early example. The GPD has cumulative probability function

$$\begin{aligned}
 F(x) &= 1 - [1 + \xi (x - T)/\sigma]^{-1/\xi} & \xi \neq 0 \\
 &= 1 - \exp(-(x - T)/\sigma), & \xi = 0
 \end{aligned}$$

for  $x$  greater than the threshold value  $T=100$  mm. The form of  $F(x)$  for the case  $\xi = 0$  is the cumulative probability distribution for the exponential distribution, which has simpler form than GPD, requiring a single parameter instead of two. The output from fitting this distribution is given in *table 15.3*.

**Table 15.3.** GenStat™ output from fitting a GPD to daily rainfall data from Ceres, Argentina, 1944-2002, with threshold value 100 mm.

Threshold = 100		
Proportion > Threshold = 0.00143		
*** Estimates of GPareto parameters ***		
estimate "s.e."		
Sigma	13.56	6.055
Eta	0.2638	0.3443
Maximum Log-Likelihood = -89.026		
Maximum value of G. Pareto Distribution is Infinite (Eta >= 0)		
Significance Test that Eta = 0 (ie pp_1_d_a follows an Exponential distribution)		
Likelihood Ratio test statistic: 1.949		
Chi-Squared Probability of test: 0.1627		

The output of *table 15.3* shows that a proportion 0.00143 of daily rainfalls exceeded the threshold, or 23 events, since the 44-year record contained 16104 daily values. The ML estimates of the GPD parameters  $\sigma$ ,  $\xi$  ('Sigma', 'Eta') are  $13.56 \pm 6.055$  and  $0.2638 \pm 0.3443$ ; the value of the shape parameter  $\xi$  is less than its standard error, whilst a formal  $\chi^2$  test, shown at the end of *table 15.3*, shows that the probability of getting a value of  $\xi$  equal to or larger than this value is 0.1627, not sufficiently small for the hypothesis that  $\xi=0$  to be rejected. Thus, the simpler exponential distribution can be used to represent daily rainfall exceedances greater than 100 mm.

A next step might be to test whether there is a time trend in the number of occurrences of rainfalls in excess of 100mm. The number of occurrences in the 44 years 1959-2002 are 0,0,0,0,1,1,0,2,0,1,0,0,0,0,1,0,0,0,0,0,1,0,1,1,0,2,0,0,1,0,0,1,0,0,1,0,2,1,2,1,0,1,3. These 44 values are well fitted by a Poisson distribution with

parameter  $0.545 \pm 0.111$ , but there is a suggestion that occurrences of events greater than 100 mm are more frequent in later years. The model proposed is therefore that the number of occurrences per year,  $X$ , is a random variable having a Poisson distribution  $f(x) = \lambda^x \exp(-\lambda) / x!$ , where the expected value of  $X$  is a linear function of time, measured in years. A variable 'Years' is therefore defined with values from 1 to 44, with  $\lambda = \alpha + \beta \text{ Years}$ . This is a Generalized Linear Model (GLM) and the result of fitting it is shown in *table 15.4*.

**Table 15.4.** Output from fitting a GLM to number of occurrences of daily rainfall in excess of 100mm, over 44 years of record 1959-2002, to test for linear trend.

Regression Analysis					
Response variate: No					
Distribution: Poisson					
Link function: Identity					
Fitted terms: Constant, Year					
Summary of analysis					
mean deviance approx					
d.f.	deviance	deviance	ratio	chi	pr
Regression	1	4.22	4.223	4.22	0.040
Residual		42		42.55	1.013
Total		43		46.78	1.088
Dispersion parameter is fixed at 1.00					
Estimates of parameters					
Estimate	s.e.	t(*)	t	pr.	
Constant	0.182	0.173	1.05	0.292	
Year	0.01614	0.00819	1.97	0.049	

It is seen from the output that the trend coefficient  $\beta$  is estimated as  $0.01614 \pm 0.00819$ , a value about equal to twice its standard error. Using an approximate  $\chi^2$  test, the probability of obtaining an estimate of  $\beta$  as large as 0.016 or greater, simply by chance, is 0.04, quite a small value; if the conventional significance probability of 0.05 (5%) is adopted, the conclusion is that the Ceres record contains some evidence of trend in annual occurrences of daily rainfall greater than 100mm, although for this one site the evidence is not overwhelming.

In the above analysis, the test for trend was made after concluding that the GPD could be simplified to the exponential distribution. Strictly, it would be better to test for trend in the GPD itself; this is illustrated by Coles (2001, page 119) in an analysis of daily rainfall data to which a GPD is fitted, with a linear trend in log-scale parameter  $\sigma$  of the form.

$$\sigma(t) = \exp(\alpha + \beta t)$$

In the examples given above, the data were considered as annual extremes, but extension to the case of monthly data is straightforward as long as the monthly extremes can be taken to be uncorrelated. For example, monthly maximum rainfall intensities of one-hour duration could be modeled as a GEV distribution with time-variant parameters. One such model is

$$\mu(t) = \beta_0 + \beta_1 \cos(2\pi t/12) + \beta_2 \sin(2\pi t/12)$$

in which the sine and cosine terms allow for the possibility that monthly maximum one-hour rainfalls might vary seasonally throughout the year. Further harmonic terms, such as  $\cos(4\pi t/12)$ ,  $\sin(4\pi t/12)$ , might need to be included, if the simplest model  $\mu(t) = \beta_0 + \beta_1 \cos(2\pi t/12) + \beta_2 \sin(2\pi t/12)$  does not fit well (although the inclusion of the two additional harmonics would require the estimation of two additional parameters  $\beta_3, \beta_4$ ). If it is required to test whether a linear time-trend is superimposed upon the simplest harmonic model, exploration of models incorporating this trend would begin from the starting point

$$\mu(t) = \beta_0 + \beta_1 \cos(2\pi t/12) + \beta_2 \sin(2\pi t/12) + \alpha t$$

Also, just as in the case of the dispersion parameter  $\sigma(t)$ , an exponential was introduced to ensure that the parameter had non-negative values; functions other than the identity function can be used for the modeling of  $\mu(t)$ . Thus, in his analysis of rainfall extremes at 187 stations over the United States, Smith (2001) used a GEV model in which the parameters  $\sigma, \mu, \xi$  were expressed in terms of time as follows:

$$\mu_t = \mu_0 e^{v_t}, \quad \sigma_t = \sigma_0 e^{v_t}, \quad \xi_t = \xi_0$$

where  $\mu_0, \sigma_0, \xi_0$  are constants, and

$$v_t = \beta_1 t + \sum_{p=1}^p \{ \beta_{2p} \cos(\omega_p) + \beta_{2p+1} \sin(\omega_p) \}$$

The general form is  $h(\mu(t)) = \text{any function in which parameters occur linearly, with } h(\cdot) \text{ any known function}$ ; similar relationships can be used for the dispersion parameter  $\sigma(t)$  and the shape parameter  $\xi(t)$ . Perhaps fortunately, however, the shape parameter appears to stay fairly constant (note that it was constant in Smith's model, given above). Also, in the two examples given above which used rainfall data from Porto Alegre in Brazil and Ceres in Argentina, it can be seen that the two values of  $\xi$  were also similar: namely  $0.2765 \pm 0.3223$  at Porto Alegre in Brazil, and  $0.2638 \pm 0.3344$  at Ceres in Argentina.

The models for non-stationarity mentioned above for the parameters of probability distributions have all had parameters which describe linear variations; thus in  $\mu(t) = \alpha + \beta t$ , the parameters  $\alpha$  and  $\beta$  describe a linear variation, and the same is true of the harmonic model of the preceding paragraph. Even the model for non-stationarity in dispersion,  $\sigma(t) = \exp(\alpha + \beta t)$ , can be converted to a linear form by taking logarithms. Models with this in-built linearity will not be appropriate for modelling every kind of statistical non-stationarity in hydrological extremes, however. One instance requiring an alternative approach would be where consideration of the physical processes that give rise to the non-stationarity suggests that the change in (say) mean value will eventually achieve a stable value. For example, non-stationarity in annual maximum discharges recorded at a flow-gauging site may be a consequence of deforestation in upstream areas; deforestation might be expected to cause annual maximum discharges to fluctuate about a mean value that is higher than that the mean which existed before deforestation began, giving rise to a change in the form of a trend towards a “plateau”. If it were reasonable to assume that deforestation is the only influence driving the non-stationarity, a more complex model - perhaps a GEV in which the parameter  $\mu(t) = \alpha + \beta \exp(-k t)$  - could be appropriate. The three parameters  $\alpha$ ,  $\beta$  and  $k$ , (together with the GEV dispersion and shape parameters  $\sigma$  and  $\xi$ ) can be estimated by Maximum Likelihood, following the general procedure briefly outlined in Section 16.3 above. Excellent software packages are available (e.g., Matlab®) for such calculations.

## 15.5. Records with missing values

In records of rainfall intensity, it is quite common for years to be incomplete. This is not a problem if the POT approach is used, but causes difficulties for the Block method. To avoid rejection of years for which part of the record is missing, one approach is the following, assuming that there are  $N$  years of record, some of which are incomplete.

(I) Taking each month in turn, select the monthly maxima for all months that have no data missing. Thus for January, abstract the data from all years for which the January record is complete. (If  $r$  of the Januaries are incomplete, the number of monthly maxima for January will be  $N-r$ ). Repeat for each of the 12 months.

(II) Fit GEV distributions to each month in turn; denote the fitted cumulative probability distributions by  $F_1(x, \mu_1, \sigma_1, \xi_1) \dots F_{12}(x, \mu_{12}, \sigma_{12}, \xi_{12})$ .

(III) The cumulative probability distribution of the annual maximum intensity is then the product given by

$$F_{Annual}(x) = F_1(x, \mu_1, \sigma_1, \xi_1) \cdot F_2(x, \mu_2, \sigma_2, \xi_2) \dots F_{12}(x, \mu_{12}, \sigma_{12}, \xi_{12})$$

In the absence of trend, this product may be used to calculate the rainfall intensities of any given return period  $T$  years. Thus the point of the method is to utilize data for all those months that are complete, avoiding the need to sacrifice incomplete years. If trends in intensity over time are suspected, each of the 12 GEV distributions can be tested for trend in the way shown in the above text.

If the incomplete records are of mean daily discharge instead of rainfall intensity, other approaches are needed because (unlike rainfall intensity) it will not be appropriate to assume that monthly maximum mean daily discharges are statistically independent; in a drainage basin where there are long periods of recession, or long rising limbs to the hydrograph, monthly maximum discharges are likely to be correlated. A different approach to that suggested above is then required. One approach is to include, in the likelihood function  $L(\cdot)$ , allowance for the fact that in an incomplete year during which the maximum value observed was (say)  $x^*$ , the true maximum value for the whole year, if it had been observed, would be greater than or equal to  $x^*$ . Thus, if the incomplete year is the last of  $N$  years of record, the likelihood function becomes

$$L(\theta, x_1, x_2, \dots, x_{N-1}, x^*) = f_x(x_1, \theta) f_x(x_2, \theta) \dots f_x(x_{N-1}, \theta) [1 - F(x^*, \theta)]$$

which can be maximized to give the ML estimate of the parameter  $\theta$ . A disadvantage of this procedure is that it takes no account of the proportion of missing data within the year; an extension of the procedure due to D. A. Jones of the UK Centre for Ecology and Hydrology (personal communication) is as follows.

(I) Assume that in year  $j$ , a proportion  $p_j$  of the record is complete. Thus  $p_j = 1$  if no data are missing. Set the cumulative probability function for year  $j$  as  $G_j(x) = F(x)^{p_j}$  so that the probability density function for year  $j$  is  $g(x) = p_j f(x) F(x)^{p_j-1}$ . Three cases can then be distinguished.

(II) *Case 1:* All that is known for year  $j$  is that the value  $x^* = \{\text{maximum value in the fraction } p_j \text{ of the year}\}$ . Then the contribution to the log likelihood function  $\log_e L(\cdot)$  from that year is

$$\text{constant} + \log_e f(x^*) - (1-p_j) \log_e F(x^*)$$

(III) *Case 2:* It is known that  $x^* = \{\text{maximum value in the fraction } p_j \text{ of the year}\}$  and it is also known that the maximum value in the rest of the year is less than  $x^*$ . This would be the case where the known part of the record coincides with the period of the year with high flows, with flows in the missing part of the year much lower. Then the contribution to the log likelihood function  $\log_e L(\cdot)$  from that year is

$$\text{constant} + \log_e f(x^*)$$

(IV) *Case 3:* It is known that  $x^* = \{\text{maximum value in the fraction } p_j \text{ of the year}\}$  and it is also known that the maximum value in the rest of the year is greater

than  $x^*$  (although its value is unknown). This would be the case where the known part of the record coincides with the period of the year with low flows flows, with flows in the missing part of the year much higher. Then the contribution to the log likelihood function  $\log_e L(.)$  from that year is

$$[constant + \log_e f(x^*) - (1-p) \log_e F(x^*)] + \log_e \{1 - F(x^*)^{1-p}\}$$

In each of the three cases, the log of the likelihood function for those years that are complete has its usual form, only the incomplete years being modified as shown above. These modifications both incorporate the information about what proportion of the year is complete, and whether the true annual maximum in an incomplete year will lie in the period of observation, or in the part of the record which is missing.

## 15.6. Spatial trends

At the simplest level, the existence of spatial trends can be explored using the method given above for the analysis of time trends simply by substituting the time variable by one or more variables defining spatial position. Thus suppose that there are data from  $p$  sites, with  $N_j$  observations of annual maxima at site  $j$ ,  $j = 1 \dots p$ . Suppose that the GEV distribution to be fitted at site  $j$  has parameters  $\mu_j$ ,  $\sigma_j$ ,  $\xi_j$ . Then if  $E_j$ ,  $N_j$ ,  $A_j$  are the easting, northing and altitude of the  $j$ -th site, one model taking account of spatial relationships between the annual maxima at the  $p$  sites is

$$\mu_j = \beta_0 + \beta_1 E_j + \beta_2 N_j + \beta_3 A_j$$

The likelihood function  $L(.)$  for all  $p$  sites can be written down, and  $\log_e L(.)$  can be maximized with respect to the parameters  $\beta_0$ ,  $\beta_1$ ,  $\beta_2$ ,  $\beta_3$ ,  $\sigma_j$ ,  $\xi_j$  ( $j=1 \dots p$ ). Extensions of this model to explore the possibility of spatial trends in the parameters  $\sigma_j$  y  $\xi_j$  are also possible. Models of this kind have been described by Coles and Tawn (1991, 1996). It is possible that numerical difficulties might be encountered in practice. Assuming that the model can be fitted, Likelihood theory can be used to test hypotheses about the model parameters: for example, that all sites possess a single shape parameter  $\xi$ ; that the dispersion parameter  $\sigma$  does not vary from site to site; that Altitude does not contribute significantly to the spatial variability in  $\mu$  (equivalent to the hypothesis that  $\beta_3 = 0$ ). Estimates of the parameter  $\mu$  can be obtained for any ungauged site by substituting its spatial co-ordinates in the above expression for  $\mu$ .

A disadvantage of this approach is that it does not take account of the correlation that is likely to exist between annual extremes observed at sites which are geographically close to each other. Thus the annual maximum 1 hour rainfall intensities at sites one kilometer apart are likely to be more similar than those observed

at sites 100 km apart. To allow for this spatial correlation, more sophisticated models, analogous to the kriging models used where spatial data are Normally distributed, have been proposed by Casson and Coles (1999). These authors develop a spatial model that is also based on GEV distributions at each site, but with a spatial 'latent process' to describe the variability in  $\mu$  and other parameters, which are now regarded as random variables. The stochastic process used to model  $\mu(z)$ , where  $z$  is now used to describe the two or three spatial co-ordinates, is

$$h_{\mu} = (\mu(z)) = f_{\mu}(z; \beta_{\mu}) + S_{\mu}(z; \alpha_{\mu})$$

with similar expressions for  $\sigma(z)$  y  $\beta(z)$ . Fitting them requires the use of Monte Carlo Markov Chain (MCMC) iterative procedures, which are revolutionizing the potential for undertaking calculations in multi-dimensional space.

## **15.7. Methods based on L-moments**

The use of sample moments (mean, variance, coefficients of skewness and kurtosis) to provide statistical summaries of data sets is well known. In addition to their use as numerical summaries, these sample moments were also used in the past (before desk-top computers became widely available) to estimate the parameters of probability distributions, such as the GEV mentioned above; the mean, variance and skewness of the probability distribution to be fitted were simply equated to their values calculated from data, and the resulting equations were solved, by iterative methods when necessary, to give estimates of the distribution parameters. This estimation by the "Method of Moments" (MM) often avoided the numerical complexity of Maximum Likelihood (ML) estimation, but is theoretical inferior to ML estimation, for reasons presented in statistical texts. One of the reasons contributing to the inferiority of MM estimation is that the variance and skewness coefficients calculated from data are subject to large sampling errors.

As a better alternative to the use of sample moments, Hosking and his fellow-workers have proposed the use of probability-weighted moments, from which L-moments are calculated. These L-moments have more advantageous properties than variances and coefficients of asymmetry and kurtosis, and using them to fit probability distributions is often simpler than fitting by ML. There is now an extensive literature (Hosking et al. 1985; Hosking and Wallis 1997) on the use of L-moments in the analysis of hydrological extremes. The book by Hosking and Wallis (1997) in particular gives a very thorough account of the use of L-moments for regionalization of hydrological variables. The authors give methods for estimating GEV parameters (as well as the parameters of other distributions) by L-moments as an alternative to the more complex calculations required for the calculation of ML estimates. It is certainly true that L-moments can be calculated in some cases where ML estimation procedures fail, for example when the ML iterative calculations fail

to converge. However, Smith (2001) considers that the whole debate over L-moments has been a distraction from more important issues. The real potential for improving on standard extreme value techniques comes not in finding estimates which improve slightly on existing ones (Smith and others doubt whether the claims made for L-moment improvements over ML are justified) but in generalizing the methods to handle richer sources of data. Examples include taking suitable covariates into account, combining data from different series, and incorporating physical information such as that generated by atmospheric and ocean circulation models. Maximum likelihood methods, and the recent developments in Bayesian methods that have been made possible by the MCMC techniques referred to above, are very general techniques which may often be applied in a routine way to such problems, whereas specialized techniques such as L-moments are limited to the context for which they have been derived. Exploration of time-trends in hydrological processes, for example, is a straightforward application of standard ML methods, but has no obvious counterpart in L-moment procedures.

### **15.8. The concept of return period in the presence of time-trends**

The concept of *return period* is widely used in engineering design, and refers to the frequency with which a given characteristic (of rainfall, discharge, wind speed, wave height, etc) will occur, over a very long period extending into the indefinite future. The return period is commonly measured in years. In the absence of changing hydrological regime, an event with return period  $T$  years is also the event which may occur in any one particular year with probability  $1/T$ .

The reasoning given above as the basis of return period rested critically on the concept of stationarity: the concept that the record of measurements of rainfall observed in the past provides information about the structure of the random process which will continue unmodified into the indefinite future. Under the assumption of stationarity, it is entirely valid to calculate a value for the rainfall characteristic - whether it be annual total, annual maximum intensity, longest run of consecutive days without rain, or whatever - that will occur in the future, in the long run, with a frequency of once in  $10$  years, once in  $100$  years,...once in  $T$  years. Where, however, analysis of a rainfall record shows that trend exist, the assumption of stationarity is inappropriate. It is always possible that a trend detected in a relatively short period of record will prove, in the longer term, to be part of a longer-term fluctuation, so that what appears to be a trend in a 50-year record would, if observation were allowed to continue for say 500 years, appear as part of a longer-term pattern resulting perhaps from slowly-varying climate fluctuations. This is of little consolation, however, when decisions are required and must be based on the limited, apparently nonstationary data currently available. Until the future courses of atmospheric and oceanic processes that give rise to changes of climate can be predicted

into the future, estimating how often extreme events will occur in the future will remain a very difficult problem.

Where hydrologic regimes are changing, a different approach to quantifying the probability of occurrence of extreme events is required, which avoids reference to the long-term frequency of occurrence. Recall that, in the first paragraph of this section, an event with return period  $T$  years was defined as the event which may occur in any one year with probability  $1/T$ ; under changing hydrological regime, this probability is no longer constant, and to generalize the concept of return period it is necessary to describe how the probability is changing. Clarke (2003) has suggested the following series of steps by which statements about the future frequency of occurrence of hydrological events become possible, where time-trends are found to exist in records. *Step 1:* identify the extreme event which, if it occurred, would influence the choice of decision. This might be, for example, a particularly intense rainfall over a duration that would lead to severe flooding. Call the magnitude of this event  $x_{crit}$ ; several values of  $x_{crit}$  may be explored. *Step 2:* Assuming that the trend in regime exhibited in the available hydrologic records continues into the future at the rate hitherto observed, determine the probability distribution of the time to first occurrence of  $x_{crit}$ , the event selected at Step 1. *Step 3:* determine the probability of the extreme event  $x_{crit}$  occurring in the next  $t$  years, where  $t$  extends up to an acceptable (but limited: see discussion below) planning horizon. Clarke (2003) gave expressions for two cases: first, where trends have been detected in annual maximum rainfall intensity represented by a Gumbel distribution or, more generally, by a GEV distribution, with time-variant means; and second, where trends have been detected in rainfall records consisting of pairs of values  $(t, x_t)$ , where  $x_t$  is the magnitude of rainfall intensity exceeding some 'threshold' value  $x_{thresh}$ , and  $t$  is the time at which  $x_t > x_{crit} > x_{thresh}$  occurs. Thus, Clarke's suggestion, in the presence of trend, is to replace the concept of 'event with return period  $T$  years', by the concept 'the probability that a critical event, suitably defined, will occur at least once during the forthcoming limited period of  $S$  years, assuming that the observed trend in the record continues over this limited period at the same rate as that recently observed'.

In conclusion, changes in hydrological regime - whether as a consequence of climate change or of change in land-use - require the concept of return period to be redefined. If further evidence in support of climate change accumulates, this will have important consequences for the many kinds of civil engineering project which have long been designed according to principles based on the return level of events with  $T$ -year return period, estimated from data sequences that are realizations of stationary processes.

## **References**

- Clarke, R. T. 2003: Frequencies of Future Extreme Events Under Conditions of Changing Hydrologic Regime. *Geophys. Research. Letters*, 30, 3, 10.1029/2002GL016214.
- Coles, S. 2001: *An Introduction to Statistical Modeling of Extreme Values*. Springer.
- \_\_\_\_\_ and J. A. Tawn 1996: Modelling extremes of the areal rainfall process. *J. R. Statist. Soc. B* 58(2) 329-347.
- \_\_\_\_\_ and \_\_\_\_\_ 1991: Modelling extreme multivariate events. *J. Royal Stat. Soc.*, 53, 377-392.
- Casson, E. and S. Coles 1999: Spatial Regression Models for Extremes. *Extremes* 1:4 449-468.
- Hosking, J. R. M., J. R. Wallis and E. F. Wood 1985: Estimation of the generalized extreme value distribution by the method of probability weighted moments. *Technometrics* , 27, 251-61.
- \_\_\_\_\_ and J. R. Wallis 1997: *Regional Frequency Analysis*. Cambridge University Press.
- Smith R. L. 2001: *Environmental Statistics*. <http://www.stat.unc.edu/postcript/rs/envnotes.ps>

## CURRÍCULA OF THE AUTHORS

---

**Vicente Barros:** Doctor in Meteorology (University of Buenos Aires, 1973). Full professor in Climatology and Director of the Master in Environmental Sciences at the Faculty of Natural and Exact Sciences, University of Buenos Aires, Argentina. Senior investigator in the Center of Investigations of the Sea and the Atmosphere (CIMA/CONICET). Publications in scientific magazines with peer review: 55 papers on climatology, climatic changeability, wind power and atmospheric circulation. Other scientific publications (chapters in books, institutional reports, etc): 20. Coordinator of the National Report to the Conference of United Nations on Sustainable Development and Environment, Rio de Janeiro 1992,. Coordinator of the Background Report for the First National Communication to the United Nations Framework Convention on Climatic Change. National Director of the Project Greenhouse gases emissions inventory and studies of Climatic Change on vulnerability and Mitigation 1997-1998. Coordinator of the Revision of the First National Communication to the United Nations Framework Convention on Climatic Change, 1997. Contributing author in the Third Report of the Intergovernmental Panel on Climatic Change, Group 1, Chapter 12.

**Robin Clarke:** has degrees in mathematics and statistics from the universities of Oxford and Cambridge, and a DSc in hydrology from the University of Oxford. From 1970 to 1983 he was head of group of engineers, physicists and mathematicians developing models of how river basins respond to rainfall at the Institute of Hydrology, Wallingford; a particular responsibility was to predict how river basin behaviour was modified by changes in land use. In 1983 he was appointed Director of the Freshwater Biological Association, funded by the UK Natural Environment Research Council, and directed freshwater research and ecological studies of UK lakes and rivers. He took early retirement in 1988, and moved to Brazil for family reasons. Since 1988 he has been a visiting Professor at the Instituto de Pesquisas Hidráulicas, UFRGS, in Porto Alegre, RS Brazil. As well as his academic career, he has been a consultant at various times for international agencies including FAO, UNDP, UNESCO, IAEA, WMO and WHO.

**Pedro Leite da Silva Dias:** Bachelor degree in Applied Mathematics (Univ. of São Paulo/USP in 1974), MSc and PhD in Atmospheric Sciences by the Colorado State University in 1977 and 1979, respectively. Professor at the Institute Geophysics and Atmospheric Sciences - IAG/USP since 1975. Visiting researcher at NCAR and NCEP in the USA in several occasions. Senior researcher of the National Institute for Space Research (INPE) and head of CPTEC between 1988 and 1990. President of the Brazilian Meteorological Society between 1992 and 1994. Currently coordinates the

Environmental Area of the Institute of Advanced Studies of USP and the Laboratory MASTER/IAG/USP (regional weather and climate studies, training and operational products). About 70 papers, mostly in international journals, about 160 complete papers in national and international science events, about 35 MSc students and 15 PhD were advised in the career. Full member of the Brazilian Academy of Sciences.

**Tércio Ambrizzi:** MSc. in Meteorology (USP, Brazil, 1990). Ph.D. in Meteorology (University of Reading, England, 1993). Head of the Department of Atmospheric Sciences, IAG/USP for four years. Chief Editor of the Brazilian Journal of Meteorology for four years. PI and Co-PI in many national and international projects funded by different financial agencies (FAPESP, CNPq, IAI, etc). Lecturer and Scientist Researcher at the Department of Atmospheric Sciences since 1988. Areas of interest: Climate Dynamics, Numerical Modeling, Atmosphere General Circulation and Atmosphere Climate Variability.

**Rita V. Andreoli:** Her current position is Research Assistant at the Modeling and Development Division of the Center for Weather Prediction and Climate Studies of the National Institute Space Research (INPE). Lic. Physics (1990-1995) in the University of Rio Claro. M.S. in Meteorology (1996-1998) in the National Institute for Space Research. Ph. D. in Meteorology (1998-2002) in the National Institute for Space Research. Number of publications: 13 papers, 3 abstracts in congress annals.

**Hugo Ernesto Berbery:** graduated from the University of Buenos Aires as a Doctor in Meteorology in 1987. His research was on numerical modeling the effects of the Andes Mountains on the weather and climate of South America, for which he got an award at the 5th Argentine Congress of Meteorology. After receiving his Doctorate, Dr. Berbery spent three years at the University of Utah doing research on Southern Hemisphere teleconnections and tropical and extratropical interactions. In 1992 he joined the University of Maryland where he currently is a Research Associate Professor. His research interests are on regional climate variability and its linkages to the hydrologic cycle. He has written numerous articles in international journals discussing the role of the North American and South American Monsoon circulations, the hydrologic cycle, and land surface-atmosphere interactions. He is a member of several VAMOS/CLIVAR/WRCP scientific panels: the Hydroclimate of La Plata basin (PLATIN), the North American Monsoon Experiment (NAME) and the Monsoon Experiment of South America (MESA). He also participates in working groups that focus on the water and energy cycles of large basins.

**Rubén Mario Caffera:** Licentiate in Meteorology (University of Buenos Aires, Argentina, 1979). Third Cycle Master in Environmental Sciences, option in Agricultural Meteorology, Foundation Universitaire Luxembourgeoise (Arlon, Belgium, 1984). 31 years of professional activity in the Uruguayan National Weather Service. Consultant on Emergencies of Atmospheric and Climate origin, National Direction of Environment (Uruguay). Adjoint Professor of Meteorology at the Faculty of Sciences, of the University of the Republic (UdelaR). Invited Professor at the Faculty Technical College of the National University of Asunción.

**Inés Camilloni:** Licentiate in Meteorology (University of Buenos Aires, Argentina, 1987), Doctor in Atmospheric Sciences (University of Buenos Aires, Argentina, 1995). Assistant Professor in the Department of Atmospheric and Oceanic Sciences (University of Buenos Aires, Argentina, since 1987). Scientist researcher in Centro de Investigaciones del Mar y la Atmósfera (CONICET, Argentina, since 1998). Participation in several projects of climate variability and climate change in South America (IAI/PRO-SUR, AIACC, CONICET, UBA).

**Iracema Fonseca de Albuquerque Cavalcanti:** Ms in Meteorology (INPE, Brazil, 1982), PhD in Meteorology (Reading University, U.K, 1991). Working at CPTEC/INPE as scientist researcher since 1982. Lecturing Climate Dynamics in Meteorology Pos Graduation Course of INPE since 1992. Participation in several projects of Climate variability of South America (IAI/Prosur, MESA/VAMOS/CLIVAR, LLJ, CNPq, FAPESP).

**Genaro Coronel:** Master of Science (Physics) Profesor Titular del Departamento de Física e Investigador del Laboratorio LIAPA de la Facultad de Ciencias Exactas y Naturales de la Universidad Nacional de Asunción), Co-Investigador Principal del Proyecto CRN 055 que Estudiar la Variabilidad Climática Regional y sus Cambios, su Predicción e Impacto, en el Área del MERCOSUR. Participación en el Proyecto Piloto “Inundaciones en la Cuenca del Paraná-Plata: Impacto Socio-Económicos, Forzantes climáticos y Balance Hídrico en el suelo”. Últimos trabajos realizados en colaboración y sometidos a la Revistas Journal of Climate; “Trenes in total and extreme South American rainfall 1960-2000 and links with sea surface temperatura” y “Observed trenes in índices of daily temperatura extremes in South America 1960-2000”. “Comparative Study of UV-B Attenuation Observed during Dry and Wet Seasons in a South American Region”, presentado en el International Radiation Symposium 2004, August 23-28, 2004, Busan, South Korea. The Major Discharge Events in the Paraguay River: Magnitudes, Source Regions, and Climate Forcings, Journal of Hydrometeorology December 2004.

**Lucas Chamorro:** Civil Engineer and Topographer (FIUNA) with specialization in Hydrometeorology (Tel Aviv, Israel) and in Hydrologic Forecasts (Davis University of California USES), Surface Hydrology and Environment, Water Emergencies, Two-dimensional modeling in Hydrodynamics (Quebec - Canada), Hydrologic database (Central University of Venezuela). Professor of Hydrographic Basin Management and Probability and Statistics at the Faculty of Engineering of the University National Asunción, Invited Professor in Physics (University technical college of Valencia, Spain). Research and publications in Water Resources on the Plata Basin and other regions. Consultant of PNUD, CEPAL and FONPLATA.

**Maira Doyle:** Licentiate in Meteorology (University of Buenos Aires, 1994). Doctor Atmospheric Sciences (University of Buenos Aires, 2001). Lecturer at the Department of Atmospheric and Oceans Sciences (University of Buenos Aires), since 1999). Scientific researcher of the Center of Investigations of the Sea and the Atmosphere (CIMA/CONICET,). Participant in various projects on variability and Climate Change in South America ((IAI/PROSUR, AIACC, CONICET, UBA).

**Mary T. Kayano:** Current Position: Senior Researcher at the Modeling and Development Division of the Center for Weather Prediction and Climate Studies of the National Institute Space Research (INPE). B.S. Mathematics (1973-1976) University of Campinas. M.S. Meteorology (1977-1979) National Institute for Space Research. Ph. D. Meteorology (1980-1986) National Institute for Space Research. Number of publications: 50 papers, 22 abstracts in congress annals.

**Ángel Nicolás Menéndez:** Director of the Hydraulics. Computational Program of INA (National Institute of Water, Argentina). Associated professor. Faculty of Engineering of the UBA (University of Buenos Aires), Independent consultant in Hydraulics, Hydrology and Environmental Sustainability. Licentiate in Physics. Faculty of Natural and Exact Sciences of UBA. 1975. Ph.D. in Engineering Hydraulics. The University of Iowa, USES, 1983. Prize “Ing. Luis A. Huergo”. National Academy of Engineering, 1997. Prize to the Scientific, Professional, and Educational trajectory. Argentine Association of Computational Mechanics, 2002. Prize “Hilario Fernández Long” in Computational Mechanics. National Academy of Natural, Physical, and Exact Sciences, 2004.

Project:  
SGP II 057:

"Trends in the hydrological cycle of the Plata basin:  
Raising awareness and new tools for water management"  
of INSTITUTO INTERAMERICANO PARA EL CAMBIO GLOBAL (IAI)